Fundamental Controls on Kinetic Hydrate Inhibitor Performance and Polymer Removal from Produced Waters

Foroogh Tohidikaloorazy

Submitted for the degree of Doctor of Philosophy

Heriot-Watt University

School of Energy, Geoscience, Infrastructure and Society

April 2016

ABSTRACT

Gas hydrate formation is one of the major concerns in the oil and gas industry, posing considerable risks to production operation when it is not controlled. Gas hydrates are traditionally avoided by injecting thermodynamic inhibitors (THIs) such as methanol or MEG, however over the past two decades, in response to economic and HS&E concerns associated with THIs, low dosage "Kinetic Hydrate Inhibitors" (KHIs) have seen increasing use in the industry as an alternative. Although KHIs use is now quite widespread and can offer considerable CAPEX/OPEX benefits, their hydrate inhibition mechanisms are still relatively poorly understood.

In this thesis, a novel PVT phase behaviour/ crystal growth inhibition (CGI) method previously developed in-house has been used to study fundamental controls on KHI inhibition mechanisms in terms of gas and aqueous phase composition, pressure, polymer type and presence of other pipeline chemicals. Particular focus has been placed on gas composition, notably acid/sour gases, with results strongly suggesting that cage occupancy patterns play a crucial role in KHI inhibition performance as a function of pressure and presence of CO_2 and H_2S being a significant factor. In contrast, work on the effect of pH does not suggest pH reduction to be the main contributor to the observed behaviour in system containing CO_2/H_2S. In addition, extensive studies on KHI-THI mixtures for different KHI polymers in multi-component natural gas systems have revealed a potential synergistic effect of methanol up to a certain concentration, while proving a consistent 'top-up' effect for ethylene glycol, opening up options for novel combined KHI-THI inhibition strategies.

While KHIs are gaining particular interest, there is the issue of handling/disposal of produced waters with the potential of polymer fouling problems. To address this problem, robust evaluation of a recently developed solvent extraction based polymer removal method shows this to have significant promise. Results also suggest that presence of other pipeline chemicals will not affect the removal effectiveness significantly. Work has also been expanded to examine whether the treatment chemicals themselves might offer a novel means to create "water immiscible KHIs" for certain applications. Results indicate that such a KHI formulation can work well, even though the bulk of the polymer is not in the aqueous phase but in an immiscible organic chemical. The treatment chemical extraction method also opens up options for potential KHI recovery and re-use.

Dedicated to my husband ***Mohammad*** *for his love, support and encouragement; and to my beautiful baby girl* ***Parnian***

ACKNOWLEDGEMENTS

I would like to deeply thank my first supervisor Professor Bahman Tohidi for providing me the opportunity to do this research and also for his genuine technical and personal support throughout this work. His creativity and hard-work has always been an inspiration to me.

A very special thanks goes to Mr. Ross Anderson my second supervisor, whose knowledge, expertise and skills have guided me through this journey. He provided me with direction, technical advice and became more of a mentor and friend, than a supervisor.

I wish also to thank Dr. Rod Burgess, Dr. Antonin Chapoy and Dr. Jinhai Yang for the help and support they provided along the way. I am also grateful to all my friends and colleagues at the Institute of Petroleum Engineering and Hydrafact Ltd who made these years pleasant and memorable.

I greatly appreciate the examiners and reviewers of this thesis Dr. Ana Cameirao, Dr. Philippe Glénat and Dr. Robin Westacott for their precious time and valuable suggestions.

Additionally, I would like to thank the members of the mechanical and electrical workshop who were responsible for manufacture and maintenance of the experimental equipment designed and used as part of this study.

The project has been financed by grants by a Joint Industrial Project (JIP) conducted at the Institute of Petroleum Engineering, Heriot-Watt University. The JIP was supported by Petrobras, Baker Hughes, Statoil, Shell/NAM, NALCO Champion and Saudi Aramco and is gratefully acknowledged.

Last but not least, I would like to express my appreciation to my family for the support they provided me through my entire life and in particular, I must acknowledge my husband and best friend, Mohammad, without whose love, encouragement and help, I would not have finished this thesis.

ACADEMIC REGISTRY

Research Thesis Submission

Name*:*	FOROOGH TOHIDIKALOORAZY		
School/PGI:	School of Energy, Geoscience, Infrastructure and Society		
Version: *(i.e. First, Resubmission, Final)*	Final	Degree Sought (Award **and** Subject area)	PhD Petroleum Engineering

Declaration

In accordance with the appropriate regulations I hereby submit my thesis and I declare that:

1) the thesis embodies the results of my own work and has been composed by myself
2) where appropriate, I have made acknowledgement of the work of others and have made reference to work carried out in collaboration with other persons
3) the thesis is the correct version of the thesis for submission and is the same version as any electronic versions submitted*.
4) my thesis for the award referred to, deposited in the Heriot-Watt University Library, should be made available for loan or photocopying and be available via the Institutional Repository, subject to such conditions as the Librarian may require
5) I understand that as a student of the University I am required to abide by the Regulations of the University and to conform to its discipline.

* *Please note that it is the responsibility of the candidate to ensure that the correct version of the thesis is submitted.*

Signature of Candidate*:*		Date:	

Submission

Submitted By *(name in capitals):*	
Signature of Individual Submitting:	
Date Submitted:	

For Completion in the Student Service Centre (SSC)

Received in the SSC by *(name in capitals):*			
Method of Submission *(Handed in to SSC; posted through internal/external mail):*			
*E-thesis Submitted (**mandatory for final theses)***			
Signature:		Date:	

Table of Contents

LIST OF FIGURES

LIST OF TABLES

LIST OF ABBREVIATIONS

ΔP_h	Pressure change due to hydrate formation
ΔT_{s-I}	Subcooling from structure-I hydrate phase boundary
ΔT_{s-II}	Subcooling from structure-II hydrate phase boundary
ΔT	Subcooling from hydrate phase boundary
ΔT_{sub}	Subcooling from hydrate phase boundary
AA	Anti-Agglomerant
C1	Methane
C2	Ethane
C3	Propane
C_n	Carbon Number
CAPEX	Capital Expenditure
CGI	Crystal Growth Inhibition
CH_4	Methane
CI	Corrosion Inhibitor
CIR	Complete Inhibition Region
CO_2	Carbon dioxide
DSC	Differential Scanning Calorimeter
EGBE	Ethylene glycol butyl ether
EtOH	Ethanol
FO	Fractional Occupancy
FTIR	Fourier Transform Infrared Spectroscopy

G	Gas
GC	Gas Chromatography
H	Hydrate
HCL	Hydrochloric acid
HHI	Hybrid Hydrate Inhibition
HPLC	High Performance Liquid Chromatography
H_2S	Hydrogen sulphide
HSZ	Hydrate Stability Zone
KHI	Kinetic Hydrate Inhibitor
HMW	High Molecular Weight
L	Liquid
LDHI	Low Dosage Hydrate Inhibitor
LMW	Low Molecular Weight
M	Moderate (Growth Rate)
MEG	Mono Ethylene Glycol
MeOH	Methanol
MW	Molecular Weight
NaCl	Sodium Chloride
NG	Natural Gas
OPEX	Operating Expenditure
P	Pressure
PVCap	Poly-nVinylCaprolactam

PVP	Poly-n-VinylPyrrolidone
RGR	Rapid Growth Region
S	Slow (Growth Rate)
s-H	Structure-H hydrate
s-I	Structure-I hydrate
s-II	Structure-II hydrate
SDR	Slow Dissociation Region
SGR	Slow Growth Region
SI	Scale Inhibitor
SR	Shear Rate
SRK	Soave-Redlich-Kwong
T	Temperature
TF	Treatment Formula
TC	Treatment Chemical
TC7	1-heptanol
TC8	1-octanol
THI	Thermodynamic Hydrate Inhibitor
THF	Tetrahydrofuran
ti	Induction time
Vol	Volume
VS	Very Slow (Growth Rate)

CHAPTER 1 – INTRODUCTION

Ensuring a safe and uninterrupted fluid flow has become a major concern in recent years, as the oil and gas industry is moving toward deepwater exploration and long tiebacks. Fluid flow can be interrupted by formation of gas hydrates, wax, halite and asphaltenes thus leading to serious operational and economic problems. Preventing gas hydrate formation therefore reducing the risk of flow line, wellhead and pipeline blockages, is an important aspect of flow assurance to avoid production loss. Thermodynamic inhibitors (such as "Ethylene Glycol" and "Methanol") have been traditionally utilized to prevent gas hydrate formation. However, the required concentrations of inhibitor for more challenging conditions such as large subcoolings at deepwater exploration, high water cuts and long tiebacks, are likely to be relatively high. Such high concentrations can cause a considerable increase in Capital and Operating expenditures (CAPEX and OPEX).

Over the past two decades, due to the economic and Health, Safety and Environment (HS&E) concerns associated with thermodynamic inhibitors, the "Low Dosage Hydrate Inhibitors (LDHIs)" have gained considerable attention from industry as promising alternatives to thermodynamic inhibition. LDHIs are typically divided into two categories:

- Kinetic Hydrate Inhibitors (KHIs) which work by affecting hydrate nucleation and/or growth
- Anti-Agglomerants which allow hydrate formation but prevent them from agglomeration and thus plugging.

Kinetic Hydrate Inhibitors (KHIs) were among the first LDHIs utilised to control hydrate in oil and gas systems. The major benefit of them, like other LDHIs, is that the required dosage for hydrate prevention is typically only a few mass percent based on the water phase. They are now seeing increasing use in production operations due to giving considerable economic benefits.

1.1 Clathrate Hydrates

Gas hydrates, or clathrate hydrates, are ice-like crystalline compounds formed by the inclusion of low molecular diameter "guest" molecules (usually gases) inside hydrogen-bonded cavities formed by water molecules as "host" under favourable conditions of pressure and temperature. Although clathrates have similar properties to ice, they differ in that they may form at temperatures well above the ice point under elevated pressure conditions and can sometimes be as high as 30 °C (Kelland, 2006).

Common gas hydrates in the oil and gas industry are divided into three well-defined categories. Cubic structure I (sI) predominates in the earth's natural environment and contains small (0.4 - 0.55 nm) guests such as methane, ethane, carbon dioxide and hydrogen sulphide. Cubic structure II (sII) generally occurs with larger (0.6 - 0.7 nm) guests such as propane or iso-butane, but small molecules like nitrogen and hydrogen (d<0.4nm) can also form sII hydrates; and hexagonal structure H (sH) may occur but only with mixtures of both small and large (0.7-0.9nm) molecules like iso-pentane and neohexane(2,2 dimethylbutane) (Sloan, 2003; Sloan and Koh, 2008).

Structures I and II determination is the result of two decades of X-ray diffraction experiments by von Stackelberg and co-workers (von Stackelberg, 1949; von Stackelberg et al., 1954; von Stackelberg, 1956) as well as Claussen (Claussen, 1951a,b,c) and Pauling and Marsh (Pauling and Marsh, 1952). Discovery of structure H but only goes back to 1987 (Ripmeester et al., 1987). Figure 1.1 shows the three common hydrate unit crystal illustration and their geometry.

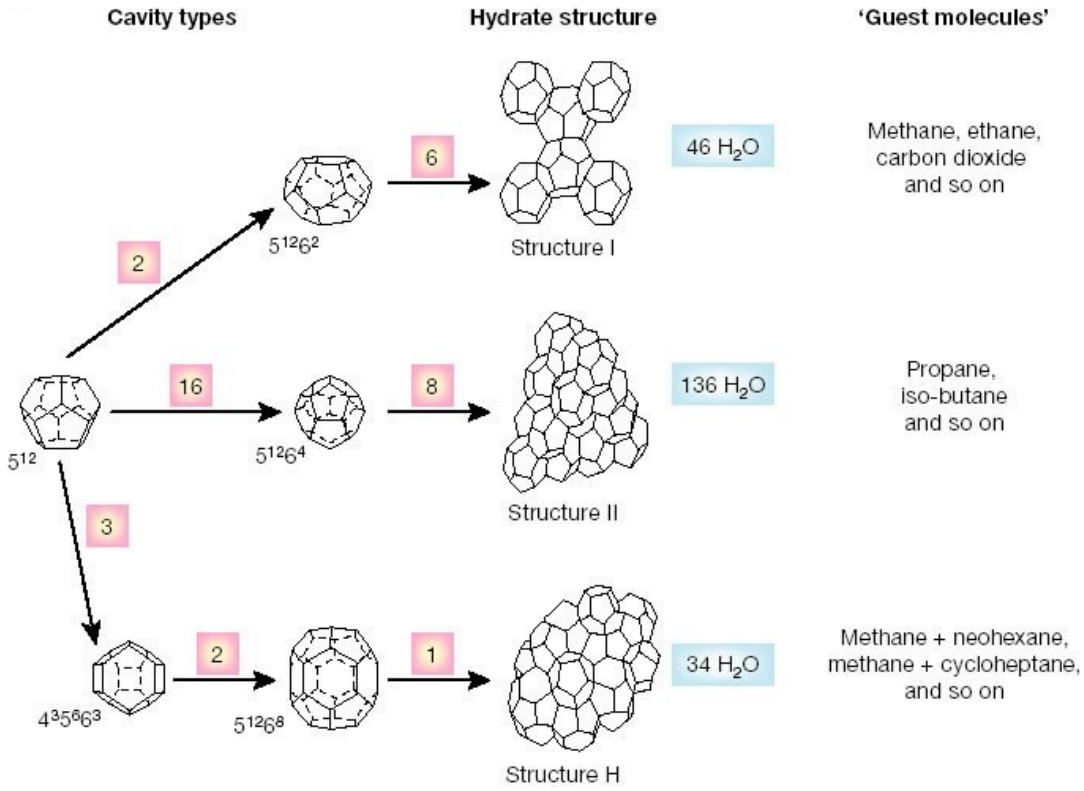

Figure 1.1 Three common hydrate unit crystals cavities and geometry (Sloan, 2003)

The properties of the three above mentioned crystal categories are summarized in Table 1.1. In both structures I and II, the basic block is the 5^{12} (pentagonal dodecahedral) cavity formed from hydrogen bonded water molecules. Within this cavity there are 12 faces of pentagonally bonded water molecules in which small guest molecules are enclathrated. In order to prevent the hydrogen bond strain and breakage, spaces between 5^{12} cavities are filled by other cavities with some hexagonal faces; $5^{12}6^2$ in structure I and $5^{12}6^4$ in structure II. The cages form basic repeating unit crystals with ratios of $2\times5^{12} + 6\times5^{12}6^2$ in sI and $16\times5^{12} + 8\times5^{12}6^4$ in sII. Likewise, structure H also has three 5^{12} small cavities but two other types of medium and large cavities. In this structure each crystal unit consists of $3\times4^35^66^3$ medium and $1\times5^{12}6^8$ large cavities in addition to the 5^{12} cavities (Sloan, 2003; Sloan and Koh, 2008).

Table 1.1 List of the properties of the three common hydrate unit crystals (Sloan, 2003)

Hydrate crystal structure	I		II		H		
Cavity	Small	Large	Small	Large	Small	Medium	Large
Description	5^{12}	$5^{12}6^2$	5^{12}	$5^{12}6^4$	5^{12}	$4^35^66^3$	$5^{12}6^8$
Number of cavities per unit cell	2	6	16	8	3	2	1
Average cavity radius(Å)	3.95	4.33	3.91	4.73	3.91†	4.06†	5.71†
Coordination number*	20	24	20	28	20	20	36
Number of waters per unit cell	46		136		34		

*Number of oxygens at the periphery of each cavity
†Estimates of structure H cavities from geometric models

Hydrates are solid clathrate compounds, which stabilise at certain pressure and temperature (depending on guest molecule). Low temperature and high pressure are generally favourable condition for hydrate formation; the exact conditions however depend on the composition of gas and liquid phase. Each hydrate forming system presents a hydrate stability zone and a hydrate free zone and the hydrate phase boundary between these two zones can be either experimentally measured or predicted. Due to the difficulties associated with experimental measurement and time-consuming nature of the procedures many predictive methods have been formulated for hydrate thermodynamic property calculations. Several companies have presented commercial software for hydrate phase boundary prediction, such as HydraFlash® 2.2 which is developed by Hydrafact and has been used for all predictions in this work.

1.2 Gas Hydrate Inhibition

Hydrate formation can cause flow restriction or even interrupt the whole production at more severe conditions where a solid plug is formed. Depending on the location and extent of the blockage, remediation can be expensive and dangerous. Thus, implementing a strategy to prevent or manage hydrates to avoid production interruption and safety risks is essential.

Hydrate blockages can be avoided by removing one of the required elements for hydrate formation such as high pressure, low temperature (by flow line insulation or active heating) and supply of water (using dehydration), but these methods can be expensive, impractical and/or ineffective under severe conditions (Patel and Russum, 2010).

The most common technology implemented by the oil and gas industry to prevent gas hydrate problems is chemical injection. There are two main options for chemical hydrate inhibitors including thermodynamic inhibitors (methanol, ethylene glycol) and low dosage hydrate inhibitors. Thermodynamic Inhibitors (TIs) work by shifting the hydrate phase boundary to lower temperatures and/or higher pressures, so that the operating conditions of flow lines are outside of the hydrate formation zone. However, at more severe conditions such as exploration and production in deeper waters, the required TI concentration could reach as high as 60 mass%. Therefore as an economic alternative, Low Dosage Hydrate Inhibitors (LDHIs) have been developed and investigated during the past two decades (Koh et al., 2002; Patel and Russum, 2010).

The term "LDHI" was applied to these inhibitors because they can be used at concentrations as low as 0.1-1 mass% (active component) based on the water phase compared to 20-50 mass% for traditional thermodynamic inhibitors (Kelland, 2006). A further difference between LDHIs and TIs is the inhibition mechanism. Neither type of LDHI alters the hydrate equilibrium point, though recent investigations (Anderson et. al., 2011) shows there are Complete Inhibition and Slow Dissociation Regions in the presence of KHIs.

1.3 Low Dosage Hydrate Inhibitors

As mentioned before, Low Dosage Hydrate Inhibitors (LDHIs) are so called because they can be applied at very low concentrations compared to large quantities of thermodynamic hydrate inhibitors such as methanol and ethylene glycol (e.g. 30-60 mass %). They can mainly be classified into two categories of Kinetic Hydrate Inhibitors (KHIs) and Anti-Agglomerants (AAs) based on their inhibition mechanism.

Kinetic hydrate inhibitors are a new and evolving technology, where their first field trial goes back to 1995(Kelland, 2006). They are usually water-soluble polymers, often with added synergists to improve their performance. A large variety of compounds have been developed and claimed to act as kinetic hydrate inhibitors, but the most famous

examples of them includes Poly(N-Vinylcaprolactam), Poly(N-Vinylpyrrolidone) and their copolymers. These polymers are composed of polyethylene strands, from which a pendant group (typically a ring compound with an -N-C=O linkage) is suspended (Sloan and Koh, 2008). Although a vast variety of investigations has been carried out on different KHI polymers, the precise mechanism by which they work is still relatively poorly understood. The general belief however is that they work by adsorbing on the hydrate surface and the pendant group acts as a "pseudo guest" in the hydrate cage. Pendant groups fit in the cages and anchor the polymer to the surface of the growing crystal so force the hydrate surface to grow past the polymer backbone barrier. As the polymer KHI chains are adsorbed more closely together on the crystal surface, it becomes more difficult for the hydrate crystal to grow between them (Palermo and Sloan, 2011; Larsen et al., 1998).

Anti-Agglomerants (AAs) are surface-active agents. Different types including water in oil emulsifying AAs and AAs with "hydrate-philic" headgroup/hydrophobic tail have been reported (Kelland, 2006). An AA allows the hydrate crystals to form but keep them small and non-adherent, thus allowing the hydrates to be transported in the production fluids, as the viscosity remains low. It is commonly accepted that because of their inhibition mechanism - act as dispersants of the hydrate particles in the liquid hydrocarbon phase - AAs require the presence of liquid hydrocarbon phase in sufficient quantities. This requirement typically limits the AA to water cut not greater than 50% (Clark and Anderson, 2007), however some developments claim to be effective for water cuts as high as 80% (Alapati, 2008). Although this might be a limitation, AAs have the advantage of working at high subcoolings (above 40°F). They are also seen to perform well regardless of the system's residence time in the hydrate stability region (Clark and Anderson, 2007).

1.4 Kinetic Hydrate Inhibitors

The initial idea for Kinetic Hydrate Inhibitors came from the natural anti-freeze, which exists in some types of fish so that they have the ability to live in sub-zero temperatures (Franks et al., 1987). Inspired by this fact, many water-soluble polymers have been shown to work as KHIs. The chemistry of polymers predominantly controls their performance. A large variety of chemistries has been researched and claimed to have kinetic inhibition effect but only a small portion of them have found their way to oil field application. Lactam-based homopolymers and their copolymers and terpolymers

are the most widely used chemistry. There are two key structural features in a KHI polymer. First, the polymer needs functional groups - usually amide groups - that can hydrogen bond to water molecules or gas hydrate particle surfaces. The second key feature is a hydrophobic group adjacent to or bonded directly to each of the amide groups (Kelland, 2014).

Research on Kinetic Hydrate Inhibitors was initiated in the late 1980s by Colorado School of Mines (CSM) where the first promising kinetic hydrate inhibitor, polyvinylpyrrolidone (PVP) was introduced. Continuing the research, they came across three more effective polymers: Poly N-vinylcaprolactam (PVCap), a terpolymer, N-vinylpyrrolidone / N-vinylcaprolactam / N,N-dimethylaminoethylmeth- acrylate (V-713) and a copolymer of N-vinylpyrrolidone-co- N-vinylcaprolactam (VP-VC) (Lederhos et al., 1996). Structures of these KHI polymers as well as two other copolymers with KHI effect (N-methyl-N-vinylacetamide:vinyl caprolactam 1:1 copolymer (VIMA:VCap) and polyisopropylmethacrylamide:N-vinyl-N-methyl acetamide copolymer (VIMA:iPMA)) are shown in Figure 1.2. There are many KHIs based on the above-mentioned polymers but there are also other polymers, which are reported to have KHI effect (Fu, 2002).

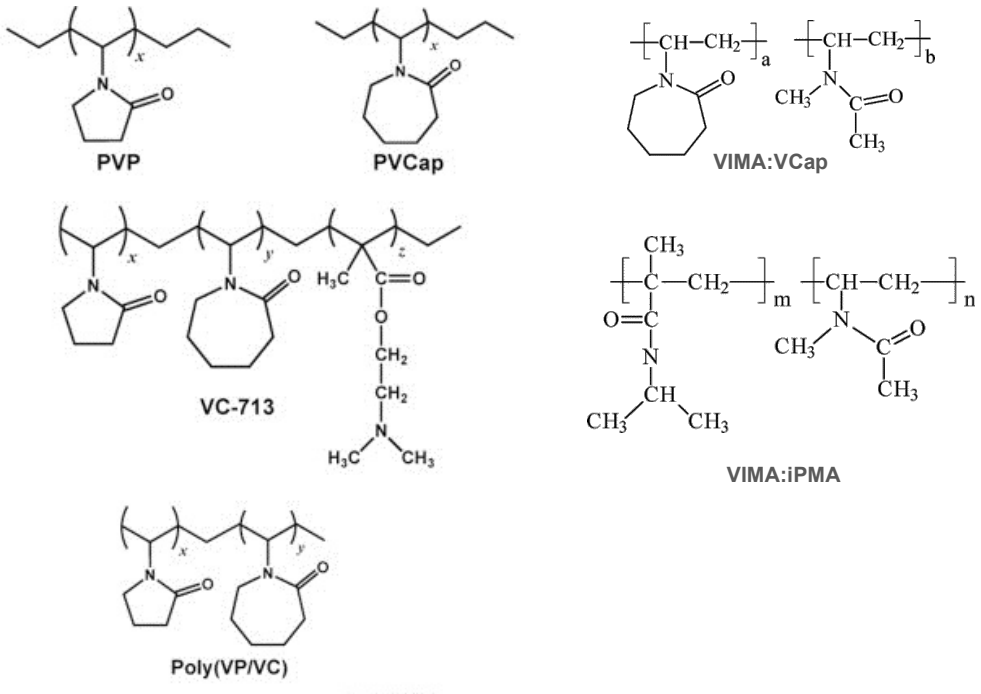

Figure 1.2 Structure of repeating chemical formulas for some kinetic hydrate inhibitors (Palermo and Sloan, 2011; Kelland, 2006)

Since these polymers' introduction as kinetic hydrate inhibitors, many studies have been conducted to determine their effectiveness at different pressures, concentrations and compositions, mainly in gas-dominated systems. The main question addressed in all tests is what test apparatuses and what test protocols adequately predict field performance. Over several years of tests, different procedures have been examined and applied to give accurate and reproducible results. Most of the research however has been focused on discovery of new inhibitors rather than quantification of their performance. A precise knowledge about different parameters affecting KHI performance will be very useful to understand their inhibition mechanism as well as for their effective design and application in real field.

1.5 Proposed Inhibition Mechanisms for KHI polymers

Kinetic hydrate inhibitors are generally believed to delay hydrate nucleation and also crystal growth for a period of time - induction or hold time - which depends on system subcooling and to some extent pressure; the period of time that passes at a specific subcooling (ΔT_{sub}, at pressure, P) within the hydrate stability zone (HSZ) before critical nuclei are achieved and hydrate nucleation proceeds to growth (Kelland, 2006; Sloan and Koh, 2008). In theory, if the KHI-induced induction time at a certain subcooling and pressure condition is greater than the pipeline fluid residence time at the same condition, then the KHI should be able to prevent hydrate nucleation/growth and enable pipeline fluid to be transported to the process facilities before hydrate formation and deposition in the line can occur.

Mechanisms by which KHIs work are still not completely understood, however two broad mechanisms which may be the case at different conditions are:

1- KHI polymers perturb the water structure by hydrophobic interactions to a degree that gas hydrate particles cannot grow to the critical nuclei size where growth becomes spontaneous (Kelland, 2014).

2- KHI polymers adsorb onto the surfaces of growing hydrate particles, limiting their growth and possibly deforming the hydrate cavities, which can occur before or after the particles reach the critical nucleus size so they can act as nucleation or growth inhibitors (Kelland, 2014). Larsen et al. (1998) believe that the complete growth inhibition is a result of polymer adsorption to the

crystal surface, with the adsorbed molecules acting as barriers to further growth. When the concentration is high enough, polymer molecules will sit closer on the surface than twice the critical radius for crystal growth at the corresponding temperature, and the crystal will not be able to grow between the polymer strands. The adsorption process is fairly rapid, as no measurable growth takes place after a crystal is transferred to an inhibited solution (Larsen et al., 1998).

1.6 Kinetic Hydrate Inhibitors Evaluation Equipment and Test Methods

The growing interest in kinetic hydrate inhibitor utilization has encouraged research groups to do extensive studies on KHI development, their performance under different field conditions and determining the inhibition mechanism. Several test procedures and types of equipment have been described for studying KHIs. The simplest technique could be investigating the growth pattern of tetrahydrofuran (THF) single crystal which can represent a similar case to gas hydrate. THF is structure II hydrate former; a structure that is normally formed in natural gas systems. The growth chamber in this case was a test tube containing THF hydrate melt with a glass pipette inserted, projecting into a cooling chamber within which a coolant is circulated to maintain a constant and controlled temperature (Makogon et al., 1997).

Testing equipment which is designed to simulate field conditions for hydrate formation and inhibitor testing typically include three major categories: rocking cells, autoclaves and flow loops. Rocking cells or ball-stop rigs are usually steel or sapphire (for visual observation) and may vary in size. In this case, mixing and turbulence is usually achieved by means a glass or steel ball which rocks forth and back in the cell (Lone and Kelland, 2013). When the ball stops moving is used to indicate that the cell has been plugged with hydrates. Induction time could also be measured when the liquid goes cloudy in the case of visual cell and/or the time gas consumption due to hydrate formation is detected (Kelland, 2006).

The performance of the hydrate inhibitor polymers can also be evaluated by using a high pressure stirred autoclave or cell which may have a sapphire window or be entirely made of sapphire for visual observation. For these set-ups, cell temperature is controlled by circulating coolant through a jacket surrounding the cell or by placing the cell in a cooling bath. There is a magnetic stirrer inside the cell whose speed could be controlled. Temperature, pressure and sometimes torque are recorded in this case. Tests

here are carried out by constant volume method and hydrate detection is by change in pressure due to gas consumption; since no further gas is delivered during hydrate formation, the experiments are not conducted under isobaric condition (Kelland, 2006; Fink, 2011; Anderson et al., 2011).

A flow loop is the most complicated setup to simulate field flow conditions. While all testing apparatuses are attempting to recreate the actual field condition, it is generally agreed that large flow loops make the closest match to real conditions. The relative size, flow regime and gas to oil ratio can be reproduced more accurately in flow loops. They can range from the mini-loop (e.g., 1/4 in. ID) to a very large loop of 4 in ID and several hundred feet in length (Kelland, 2006; Patel and Russum, 2010). The loop unit is mainly composed of a pipe, a pump and a storage tank and could be divided into several sections to monitor temperature and pressure drop over each individual section, which is indicative of gas hydrate formation (Fink, 2011; Peytavy et al., 2008).

In recent years, some instrumental methods have also been employed to investigate hydrate kinetic inhibition. These include NMR/Raman spectrometry, differential scanning calorimetry (DSC) and magnetic resonance imaging. Although each of these methods provides very useful and valuable information, none of them alone significantly reveals enough information on complex polymer/hydrate systems, transferring laboratory results to real field is also a challenge (Rojas et al., 2010; Daraboina et al., 2013a).

KHIs are reported to primarily act as hydrate anti-nucleators, so are usually evaluated by means of induction/hold time measurement (Kelland, 2006). Determining effectiveness of a kinetic hydrate inhibitor for different operating condition using induction time tests may not encourage operators to use these chemicals, because the stochastic nature of hydrate nucleation leads to scattered results which are poorly transferable to real conditions. To overcome this problem Duchateau et al. (2009) proposed a test procedure based on water memory. The procedure, which was driven from TOTAL test protocol for flow loops (Peytavy et al., 2008), uses the residual structures remaining in solution after a previous hydrate formation/dissociation cycle and leads to less-scattered results (Duchateau et al., 2009). The procedure termed as "Second Germination (SG)" was also applied to autoclave cells with respect to tackling the ongoing problem of stochasticity in laboratory KHI data (Duchateau et al., 2008).

Building on basic principles of SG technique, a new Crystal Growth Inhibition (CGI) based method for KHI evaluation was developed at Heriot-Watt University (Anderson et al., 2011; Glénat et al., 2011). The goal for development of the CGI method – which is fully described in Section 2.2.2 of this thesis - was to overcome stochasticity of induction time data and provide more reliable and repeatable results. This new approach is based on the determination of fundamental KHI-induced crystal growth inhibition (CGI) regions as a function of subcooling. As CGI regions are controlled primarily by thermodynamic rather than kinetic phenomena (or nucleation), test results are very repeatable and transferable, in contrast to traditional, commonly stochastic induction/hold time data. Furthermore, CGI regions correlate well with induction time trends, allowing the use of CGI methods to both rapidly approximate and support traditional induction time evaluation data.

1.7 Removal of Kinetic Hydrate Inhibitors from Produced Water

Kinetic hydrate inhibitors are gaining particular interest as an attractive alternative to thermodynamic inhibitors. Although they offer considerable operating and capital cost saving, there is the issue of handling/disposal of KHI-containing produced waters. The most problematic component of KHIs in this respect is the active polymeric component. Polymer miscibility with water is commonly quite sensitive to high temperature and salinity, which may cause it to precipitate and potentially leading to fouling. This can occur during re-injection and thus block perforations / pore spaces and so reducing injection efficiency. Furthermore, with the increasing interest in reducing levels of thermodynamic inhibitor used for hydrate prevention − particularly in the case of MEG − by combining these with KHIs as hybrid inhibition strategy, there is a potential for precipitation in MEG reclamation units, causing fouling and reduction in efficiency (Anderson et al., 2014).

In light of this as well as concerns over poor polymer biodegradability and regulations with respect to produced water disposal in the natural environment, there is an increasing interest in the industry to remove KHI polymers from produced waters. Various physical, chemical and biological treatment methods such as membrane separation, advanced oxidation, biotreatment and heated centrifugation have been examined, with the oxidation showing particular promise (Hussain et al., 2012; Adham et al., 2014). A simple polymer extraction method from produced water was also

recently developed in house for this purpose (see Chapter 4). The method removes KHI polymers from water by using small fractions of largely water immiscible fatty alcohols, which have a high affinity for KHI polymers. The polymer containing solvent then can be separated from treated water by means of common physical techniques such as gravity settling, centrifugal separation, coalescing separation (Anderson et al., 2014).

1.8 Thesis Outline

Previous studies demonstrate that KHI polymer effects extend well beyond the nucleation process, inducing a number of specific, well-defined growth/inhibition regions as a function of subcooling (Anderson et al., 2011; Mozaffar, 2013). Investigation of these regions provides a novel means to examine in detail the fundamentals of KHI inhibition mechanisms as a function of various parameters (gas and aqueous phase compositions, pressure, polymer type, presence of other pipeline chemicals). In this work, the newly developed Crystal Growth Inhibition based method has been utilized to investigate in detail the fundamental physiochemical controls governing KHI performance with the aim of improving inhibition strategies/formulation optimisation. The specific polymer-controlled hydrate crystal growth/inhibition PT regions were investigated as a function of polymer type and gas composition, with particular focus on:

- Acid/sour gases containing CO_2/H_2S
- The effect of pH
- Hybrid hydrate inhibition of thermodynamic hydrate inhibitors (methanol, ethanol and ethylene glycol)

Moreover, by increasing interest in application of KHIs in production operations, addressing problems associated with them is vital. These problems include KHI polymer coming out of solution at hot reservoir condition in the case of produced water re-injection, fouling problems in processing equipment such as MEG regeneration units in the event of KHI+MEG combination to prevent hydrate formation and KHI containing produced water disposal to natural environment, which is limited by environmental restrictions. To address these problems, a KHI removal technique has been evaluated in this work. This method is based on solvent extraction using fatty alcohols to remove polymer from the aqueous phase.

The largely water immiscible fatty alcohols have been shown to strip polymer from the aqueous phase by up to 100%. These properties were seen as a means to test the theory as to whether a KHI polymer could still work even though it was not in the aqueous phase by using fatty alcohols as a carrier solvent for KHI polymers. Therefore, the work has been expanded to examine 'water immiscible KHIs', i.e. to be used in a preventative manner (polymer is kept out of the aqueous phase) for certain applications such as where the salinity of produced waters would normally pose a problem in terms of causing KHI polymer precipitation.

As mentioned above, the in-house developed CGI method has been used throughout this work for KHI evaluation/investigation experiments. The experimental set-up and procedure for KHI evaluation tests are fully described in Chapter 2 of this thesis. Results from the work on the effects of H_2S and CO_2 within this study have shown that these two gases appear to be very important in KHI performance, therefore chapter 2 also will also be focused on the effect of acid and sour gases on KHI performance. Due to different processes which may be involved in acid and sour gas systems – including aqueous phase acidity, increased propensity for hydrate formation from dissolved gas and hydrate cage occupancy patterns - determining the potential effect of these systems on KHIs will be difficult. Therefore, besides looking at the effect of cage occupancy patterns and the issue of hydrate formation from dissolved gases by testing different concentrations of CO_2 and H_2S, the general effect of acidity was examined independently by working with hydrocarbon gases only (very low aqueous solubility and no pH effect) and aqueous solutions of known pH. The results are reported in Chapter 2.

Thermodynamic inhibitors such as methanol, ethanol and ethylene glycol have widespread use in industry but using them for more challenging systems with high subcooling and water cut can be quite expensive as the required effective dosage will be very high (10 to 60 % of water phase), while KHIs normal concentrations are less than 5%. Therefore replacing some of the high required volume of thermodynamic inhibitor by kinetic hydrate inhibitor and achieving a proper concentration of each will result in much lower injection rates while controlling hydrate formation. Some laboratory studies and field experiences has shown good synergy through the combination of KHIs and THIs in some multi-component hydrate forming systems; however Crystal Growth Inhibition (CGI) experiments revealed the negative effect of methanol and ethanol on

PVCap performance for single component methane systems (Mozaffar et al., 2014). Therefore, to better understand the impact of thermodynamic inhibitors on KHIs, in Chapter 3 of this thesis, CGI behaviour of different concentrations of THIs in combination with KHI polymers are investigated in a multi component gas system.

While KHI doses are low, there is a potential for accumulation at some point during produced water processing. This accumulation could lead to fouling with the most problematic component of KHIs in this respect being the active polymeric component. Polymer solubility in water can be quite tenuous and sensitive to increases in temperature and/or salinity, which may cause it to precipitate, resulting in fouling. To address this problem, chapter 4 concentrates on a simple solvent extraction method, which has been developed to remove KHI polymers from produced water. Different potential solvents are examined with the main focus on linear chain fatty alcohols such as normal hexanol, heptanol and octanol. The effects of various parameters such as polymer type and concentration, solvent type and quantity, liquid hydrocarbons, etc. on removal efficiency are also investigated.

Based on the above, there is the opportunity of having a novel immiscible KHI design to avoid problems associated in water processing and disposal. As detailed in chapter 5 of this thesis, excellent polymer removal properties of fatty alcohols were used to test the theory as to whether a KHI polymer could still work even though it was not in the aqueous phase by using fatty alcohols as carrier solvent for KHI polymers. Therefore, 'water immiscible KHIs' were evaluated for certain applications such as where the salinity of produced waters would normally pose a problem in terms of causing KHI polymer precipitation. Different gas systems were used to see to what extent immiscible KHIs would work. Their performance was also evaluated in the presence of NaCl and liquid hydrocarbons (liquid hydrocarbons caused displacement of the PVCap back into the aqueous phase in removal experiments).

Finally in Chapter 6, problems associated with application of KHIs are discussed and some possible options to address these problems are presented. To help understanding KHI inhibition mechanisms, in this work the possibility of having hydrate-polymer complexes and their stoichiometry were investigated. These investigations were conducted by measuring PVCap performance as a function of concentration as well as measuring CGI regions in the presence of different fractions of hydrate. Another concern regarding the use of KHIs is environmental restrictions limiting their

application. Based on this two biodegradable KHIs were also evaluated using the CGI method and results are presented in this chapter. Later in Chapter 6, KHI removal/recovery is considered as another option for future directions in the application of KHIs. The simple solvent extraction method – discussed in detail in Chapter 4 – is believed to open-up new opportunities for the use of KHIs and help to address environmental, technical and economic concerns associated with these hydrate inhibitors.

CHAPTER 2 – EFFECT OF ACID AND SOUR GASES ON KHI INDUCED HYDRATE CRYSTAL GROWTH PATTERNS

2.1 Introduction

Evident from the literature, hydrates crystals, which are formed from gas mixtures have a more complex behaviour compared to the ones formed from single gases or liquid hydrate formers (Rydzy et al., 2007; Nakagawa et al., 2008; Kumar et al., 2008). The addition of kinetic inhibitors to such a system will increase the complexity even more. Because of this complex behaviour understanding the effect gas composition might have on kinetic hydrate inhibitors' performance is important, but despite this importance few studies have been conducted on this topic (Daraboina et al, 2013b).

Darboina et al. (2011a, 2013c) have carried out various experiments on comparison of the formation and dissociation of mixed gas hydrates in the presence of commercial and biologically based kinetic hydrate inhibitors (KHIs). In their work, all inhibitors significantly delayed hydrate nucleation and reduced the hydrate growth. They also have looked at the formation of hydrates from a synthetic natural gas mixture consisting of methane, ethane and propane in the presence of different classes of KHIs. Using Raman spectroscopy they confirmed that hydrates in the chemical KHI experiments were heterogeneous in contrast to the seemingly homogeneous hydrates formed in water controls or biological AFP-III inhibitor experiments. Large hydrate cages formed in the presence of all the inhibitors showed a reduction in methane content. With the commercial inhibitors, these large cage methane guests appeared to be substituted by ethane, resulting in a decreased driving force for hydrate production. They speculated that the formed s-I hydrate was likely methane-ethane s-I. In contrast to the near full occupancy of total (methane + ethane + propane) large cages in chemical kinetic inhibitor experiments, almost 7% of the total large cages were not filled when hydrates were formed in the presence of AFP-III, possibly supporting an adsorption-inhibition mechanism (Daraboina et al, 2011b).

In a previous study as part of Heriot-Watt Institute of Petroleum Engineering Joint Industrial Project (JIP) (2009-2012), extensive work has been conducted on the effect of guest gas and hydrate structure on CGI regions of aqueous PVCap (Luvicap-EG base polymer); starting from single component gas systems of methane, ethane, propane and

carbon dioxide. The work then continued on various binary and ternary mixtures of the tested gases to gradually build up more complex systems toward a real natural gas. The results of this work have shown a typically superior performance of PVCap in s-II forming systems (both simple s-II and binary/multicomponent s-I/-sII) compared to s-I forming systems, which supports stronger polymer adsorption on s-II hydrate crystal surfaces. In the natural gas case, the presence of CO_2 appears to have a negative effect (notably at lower pressures of < 70 bar), while PVCap performance is considerably reduced in pure CO_2 (s-I) systems. Results for the natural gas systems showed that at pressures below 70 bar, PVCap performance is moderately reduced. The reasons for this observation are unclear but it is speculated it may be related to the fact that driving force deviates from its normal relationship with subcooling at this pressure range (Arjmandi et al., 2005) and/or cage occupancy patterns as a function of pressure, with results suggesting CO_2 is an important factor. Moreover, while presence of ethane apparently reduces the rate of hydrate growth within the SGR and shows general positive impact on PVCap performance, data suggested that ethane alone could not apparently be the reason for the good performance of PVCap in natural gas systems. Instead, the CO_2+C_2+C_1 combination in natural gas seems to give good PVCap performance at higher pressures, although CO_2 is at the same time responsible for the reduction in PVCap performance observed at lower pressures (Heriot-Watt Institute of Petroleum Engineering Joint Industrial Project (JIP), 2009-2012).

As discussed above, results show that gas composition plays a crucial role in governing KHI performance, most notably as a function of pressure, with CO_2 content highlighted as a significant factor in this.

Trends in the industry towards increasing production of sour gases (due to the fact that a large part of the remaining gas reserves are sour) means this issue is of growing importance; KHIs being favoured as a hydrate inhibition solution for gas and gas condensate systems. Information on KHI performance in sour gas systems is somewhat limited although studies have shown that these can offer a challenging environment for KHIs, especially in terms of compatibility with other pipeline chemicals such as corrosion inhibitors (Al-Adel and Cruz, 2011; Menendez et al., 2014). In work by Rithauddeen et al. (2014), the CGI approach was used to find an appropriate kinetic hydrate inhibitor for a sour lean gas field. Due to the feed gas composition, which requires high corrosion inhibitor (CI) concentrations and results in predominately

structure-I hydrate, they found it very challenging in terms of finding a suitable KHI (Rithauddeen et al., 2014).

There are number of factors that can potentially make sour systems difficult for KHIs. For example, sour gases are commonly quite lean (low in heavier s-II forming components such as propane and butane), meaning structure-I can be the most stable hydrate structure, posing a problem for KHIs that are designed primarily for inhibition of s-II hydrates. Then there is the issue of H_2S and CO_2 themselves; these can form quite high fractions of the gas phase and evidence suggests they are important factors in KHI performance, whether this is due to acidity or other fundamental processes such as cage occupancy patterns vs polymer surface adsorption strength. Finally, acidic solutions can change aqueous polymer conformation (Yu and Somasundaran, 1996), this possibly will cause coagulation / precipitation and could reduce hydrate inhibition performance and/or fouling problems. Results from the work on the effects of H_2S and CO_2 within this study have shown that these two gases appear to be very important in KHI performance, notably as a function of pressure. However, determining the processes involved is difficult as there are potentially up to three main factors that play a role, including aqueous phase acidity, increased propensity for hydrate formation from dissolved gas (due to much higher CO_2 and H_2S solubility in the aqueous phase compared to hydrocarbons), and hydrate cage occupancy patterns (thus strength of polymer adsorption) as a function of composition / pressure.

The number of potential effects CO_2 and H_2S could have directly or indirectly on KHI performance makes determining these experimentally problematic due to multiple variables involved. For example, a notable problem when it comes to singling out the effect of pH on KHIs is that pH is dependent on the level of CO_2 or H_2S dissolved in the aqueous phase. Thus the pH may vary depending on the CO_2 / H_2S fraction in the gas (and thus the water), pressure and fraction of hydrate present (hydrate formation can change the CO_2 and H_2S contents of the remaining aqueous and gaseous phases).

Due to the above detailed difficulties, the effect of cage occupancy patterns were investigated separately by looking at different concentration of CO_2 and H_2S. Meanwhile the general effect of acidity was examined independently by working with hydrocarbon gases only (very low aqueous solubility and no pH effect) and aqueous solutions of known pH.

2.2 Experimental Setup and Procedures

2.2.1 Experimental set-up

All the tests described in this thesis (except tests on H_2S containing gases) were conducted on Heriot-Watt University designed and built autoclave cells with volume of 280 ml. These autoclaves can be operated up to maximum pressure of 410 bar and temperature range between 233 K and 323 K. Cells were made of either stainless steel or titanium (salt compatible). Figure 2.1 shows a schematic of the cells used for the experiments. Although tests were performed using a constant volume method in autoclaves, constant pressure gas consumption tests in rocking cells have yielded identical results confirming transferability of data (Mozaffar, 2013). Temperature control in these autoclave cells was achieved by circulating coolant from a programmable cryostat through a jacket surrounding the cells. To maintain the temperature, the jacket was insulated with polystyrene board and the hoses connecting cryostat to jacket were covered with plastic foam. Temperature was determined by platinum resistance thermometers (PRT, ± 0.1 °C). The pressure was measured by either strain standard gauge (± 0.07 bar) or precision Quartzdyne (± 0.0007 bar) transducers which were regularly calibrated against a dead weight tester. Pressure and temperature of the cells were continually monitored and recorded by a computer connected to them

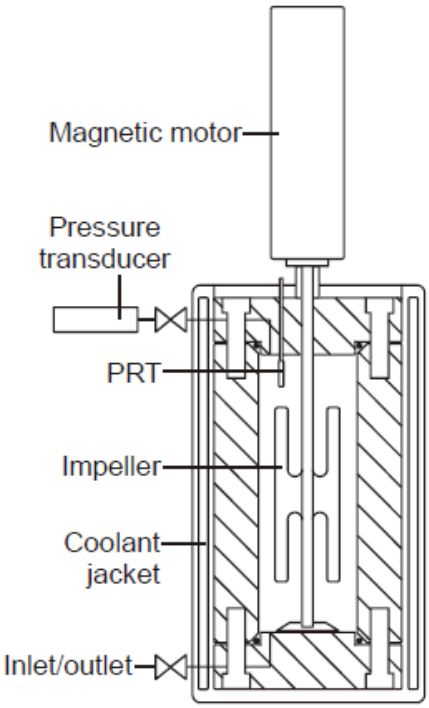

Figure 2.1 Schematic of the 280 ml autoclave cell used for the experiments; with maximum working pressure of 410 bar and working temperature between 233 to 323 K (Anderson et al., 2011).

In any phase behaviour study it is vital to create conditions where the various phases can interact with each other as much as possible. This allows phases to - within the timescales of interest - reach either stable or metastable equilibrium states which reflect current PTX conditions. Only by this approach will the data show good repeatability, irrespective of whether the process is kinetically and/or thermodynamically driven. Thus a mixing rate is not important per se, rather that the entirety of the internal surface of the test cell is regularly wetted by the KHI aqueous phase. However, there was a concern over the possibility of polymer having lower chances to interact and be adsorbed on crystal surfaces therefore having poorer performance at lower mixing rates; thus polymer performance was tested at different mixing rates from 25 to 750 rpm and results showed almost identical CGI region extents demonstrating this is not an issue.

A moderate mixing rate of 550 rpm (though it is likely to be a function of test setup, orientation and fluid loadings) was used as it intermingles the gas and the water, creating the most favourable conditions for hydrate growth, promoting stable or metastable equilibrium, and thereby presenting the mostly used testing conditions for KHIs. In order to reduce unmixed/dead volumes and possibility of having hydrate

formation from condensed water at dead volumes (a disequilibrium "top of line hydrates" type scenario) experiments were carried out with autoclave cells in horizontal position. Cell aqueous liquids volume fractions were also typically 0.80 (unless otherwise specified) to minimise dead volume/aqueous phase unwetted internal cell surfaces. Another reason for implementing such a high liquid fraction is to give high sensitivity for detection of hydrate (the smaller the gas head/moles of gas, the greater the pressure changes due to hydrate formation). By knowing accurate liquid and gas fractions, amount of hydrate formed during experiments could be calculated using simple PVT methods (Anderson et al., 2011). HydraFLASH® 2.2, a Hydrate/PVT prediction software developed by Hydrafact, was used to calculate amount of hydrate throughout all experiments in this work.

KHI polymer specification and composition of the gas used in each experiment is given separately in related chapters. Deionised water was used in all tests, with aqueous polymer solutions prepared gravimetrically.

Hydrogen sulphide experimental set-up and safety

H_2S experiments were carried out at the Hydrafact sour gas lab in standard high-pressure, 280 ml volume, acid gas compatible (hastelloy) stirred autoclaves which are located inside a fume cupboard equipped with H_2S detectors at sensitivity of 0.1 ppm. The fume cupboards are located in an isolated and negative pressure lab space. All the tests were carried out by two H_2S safety (course) and test procedure trained staff present and no unauthorized personnel were allowed in the lab during the experiments. Full face mask was worn whenever needed (e.g. during charging the cell with gas and depressurizing steps). Following loading and depressurizing, each cell was purged with nitrogen to ensure no H_2S was remaining in the system and flowing gas was passed through a scrubber column (sodium hypochlorite solution) for neutralization. All the tests were conducted according to Hydrafact work instruction "QWI021 Rev 0, Conducting Sour Gas Tests in H_2S Laboratory Work Instruction".

2.2.2 CGI experimental procedure

The Crystal Growth Inhibition (CGI) based method previously developed in-house has been used in all experiments (Anderson et al., 2011; Glénat et al., 2011). The primary aim in development of the CGI approach was to devise a reliable, repeatable, and

ideally rapid means to assess KHI performance. In this regard, the aim was to bypass the stochasticity inherent to nucleation processes (induction time measurements) and thus focus on KHI inhibition properties for evaluation, which were more repeatable and quantifiable. If such approach existed for KHIs, then their application in production operations could be greatly increased, offering potentially enormous cost savings.

Literature and observations demonstrate that the effect of KHIs extends well beyond the nucleation process (Makogon et al., 1997, Larsen et al., 1998, 1999; Habetinova et al., 2002; Svartaas et al., 2008). For an aqueous polymer to completely inhibit crystal growth at low subcoolings, and/or induce a large degree of metastability to hydrates where they would normally dissociate, suggests interaction with crystals occurs throughout the hydrate nucleation-growth-dissociation cycle. Assuming that this interaction is, as believed, through polymer crystal surface adsorption, then it must be controlled to a large extent by thermodynamics (adsorption being a thermodynamic process), and so quantifiable in a repeatable way. Particularly important is the observation that KHIs can completely inhibit further growth when hydrates are already present, i.e. when it might be considered that a KHI has 'failed'. Whatever the exact mechanisms are, KHI polymers apparently change the entire PT conditions of crystal growth, inhibition and dissociation. Data for a variety of different gas−water systems consistently show that aqueous KHI polymers induce a number of fixed, repeatable (and transferable between different setups) crystal growth/inhibition PT zones delineated by quite well defined 'phase boundaries'. These include (Anderson et al., 2011):

- A Slow Dissociation rate Region (SDR) which can extend quite significantly (e.g. up to 7 °C) beyond the hydrate phase boundary, where hydrate-polymer complexes (current understanding) may survive for weeks in a metastable state (orders of magnitude reduction in dissociation rates)
- A Complete Crystal Growth Inhibition Region (CIR) within the hydrate stability zone to quite high subcoolings (> 15 °C for some systems) where hydrate nucleation/growth is prevented indefinitely and even dissociation (typically in the case of hydrates initially formed at high subcoolings) can occur
- A Slow Growth rate Region (SGR) where hydrate growth can occur, but is varyingly inhibited in terms of growth rate; from nearly fully inhibited (orders of magnitude reduction in growth rates) to steady but still polymer-moderated growth

- A Rapid Growth Region (RGR) where rapid/catastrophic/uncontrolled hydrate growth occurs upon nucleation with growth rates being largely unaffected by the polymer, i.e. where the latter ceases to inhibit to any measurable extent

Table 2.1 shows CGI regions definition based on change in hydrate growth rate.

Table 2.1 Classification of crystal growth inhibition (CGI) regions based on orders of magnitude change in hydrate growth rates (% water converted to hydrate per hour), as commonly observed across region boundaries. Defining characteristics of the hydrate slow dissociation region (SDR) are also shown (Anderson et al., 2011).

Region name	**Growth rates order of magnitude (% water / hr)**	**Growth rate description**
CIR	0.00	No growth
SGR (VS)	0.01 (<0.05)	Very slow
(S)	0.1 (≥0.05 to <0.5)	Slow
(M)	1 (≥0.5 to <5)	Medium
RGR	10 (≥5)	Rapid
SDR	Dissociation rate one order of magnitude less than for no KHI	(Abnormally) Slow dissociation

In order to define the crystal growth inhibition (CGI) regions three scenarios were considered for each experiment, which are as follow:

1. *No hydrate history:* Hydrate history refers to the case that the aqueous phase has recently experienced hydrate phase and is believed to reduce hydrate formation subcooling (e.g. Sloan and Koh, 2008; Duchateau et al., 2009). Although the origin of hydrate history is unclear (might be related to the presence of remnant crystalline water structures and/or excess gas solubility potentially associated with the latter) but seems to be an important factor in KHI systems (Duchateau et al., 2009). To have some history free results for comparison with other scenarios cells were warmed up to temperature well above the hydrate phase boundary and left there for at least 2 hours before cooling to form hydrates.

2. *Hydrate history present:* To keep some hydrate history present in the system, cells were warmed up following hydrate formation at high

subcooling. The heating process beyond the hydrate phase boundary was stepwise and quite close to the phase boundary (about 3 to 6 °C maximum depending on the hydrate structure). The system was kept at this temperature for complete disappearance of any hydrate present. Then it was cooled down again into hydrate stability zone.

3. *Hydrate present:* In this scenario the critical nucleus has been exceeded and crystals with the potential to grow are already present, so in theory there is no induction time. Similar to other cases, hydrate was formed at high subcooling and then the system was warmed up to a few degrees above the phase boundary. However, prior to complete dissociation, with only a small fraction of hydrate remaining (<1 mass% of the aqueous phase, small pressure drop still remaining), the cell temperature was again reduced, bringing conditions back into the hydrate stability zone.

The standard CGI experimental procedure for all experiments based on above scenarios was as follows, however there were some variations (e.g. in heating and cooling rates, hydrate fraction present) depending on the system (Anderson et al., 2011; Glénat et al., 2011):

1. Gas was charged to the cell to the desirable initial pressure at a temperature well higher than the hydrate phase boundary. Following gas charging, the system was cooled rapidly to a high subcooling to induce hydrate formation and to generate the no-hydrate baseline.

2. After initial hydrate formation, the system was then warmed up in steps to dissociate most of the hydrate formed (or all in case of hydrate history runs), leaving only a small fraction remaining (typically < 0.5% of water converted), while assessing the extent of any anomalously slow dissociation behaviour.

3. The cell temperature was then reduced again at a constant cooling rate (typically 1.0 °C / hr, but both slower and faster rates were commonly employed as part of investigations) to observe clear changes in growth rate as a function of subcooling.

4. Steps 2-3 were repeated a number of times to examine repeatability.

5. Finally, following a repeat of Step 2, the system was step-cooled with a small fraction of hydrate present to confirm the extent of the complete inhibition region.

Data interpretation to define CGI regions

For the systems under study, the above procedure was used to generate some PT data. Based on the generated PT data and changes in relative growth rates (see Table 2.1) KHI-induced crystal growth inhibition regions were identified as follow (discussed in detail by Mozaffar (2013)):

1- CIR: The Complete Inhibition Region is defined by step cooling at the rate of 0.5 °C / day, while a small amount of hydrate is already present in the system (typically < 0.5% of water converted). Any step that a detectable growth (e.g. 0.05% water conversion detectable) could be observed is considered as the end of CIR region. Due to the 0.5 °C temperature drop for each step and considering only one step cooling run for each initial pressure, there is ± 0.5 °C uncertainty in CIR determination.

2- SGR: The Slow Growth region is determined by applying a 1.0 °C / hr constant cooling rate. Crystal growth is detected from the deviation of the cooling curve from the no-hydrate baseline. Depending on hydrate growth rates, this region may be subdivided into Very Slow growth SGR (VS), Slow SGR (S), and Moderate SGR (M) growth rate zones (see Table 2.1). Growth rate is calculated based on water converted to hydrate as a result of cooling; water conversion at a specific condition is calculated with HydraFLASH® 2.2 from system composition and volumetric data using pressure change due to hydrate formation, ΔP_h. PT data were recorded every 5 minutes, therefore in this case error in determining the regions are as low as ± 0.1 °C.

3- RGR: The Rapid Growth Region is defined where rapid/catastrophic growth occurs as a result of fast cooling runs (e.g. > 1.0 °C / hr). In this case to confirm repeatability, cooling runs are repeated several times for all three scenarios (no hydrate history, with hydrate history and with hydrate).

4- SDR: By step heating of the previously formed hydrate, which clearly demonstrates the abnormally slow dissociation, the extent of the Slow Dissociation Region can be determined.

Based on the above, CGI boundary points were measured for different system initial pressures. Using measured data points, the region boundaries were determined by applying the following steps:

1- For each initial pressure, temperature difference between structure-I hydrate phase boundary and measured data point is calculated and reported as ΔT_{s-I} (subcooling form s-I phse boundary). Hydrate phase boundaries – unless measured experimentally – are predicted using the HydraFlash® 2.2 thermodynamic model.
2- Using above-mentioned subcoolings, average ΔT_{s-I} is then calculated.
3- Predicted / measured Hydrate equilibrium points are shifted by average ΔT_{s-I} to determine CGI regions boundary points.
4- CGI region boundary curves are then interpolated from shifted hydrate phase boundary points.

2.3 Results and Discussions

As discussed earlier in this chapter, gas production systems containing hydrogen sulphide and carbon dioxide could be quite a challenging environment for kinetic hydrate inhibitors in terms of hydrate inhibition properties. In analysing the effect that these gases might have on KHI polymers' performance a number of different issues could be potentially involved; including cage occupancy patterns, hydrate formation from dissolved gas and acidity. Due to difficulties associated with considering all these issues at the same time, in this work, CGI experiments were carried at different concentrations of H_2S and CO_2 separately and in combination to see the effect of cage occupancy patterns on KHI performance. The effect of acidity was looked at independently by working with hydrocarbon gases only (very low aqueous solubility and no pH effect) and aqueous solutions of known pH. Modelling studies using HydraFLASH® 2.2 thermodynamic model conducted by Anderson (2013, 2014) are also presented as evidence for the effect of gas solubility.

2.3.1 Effect of carbon dioxide on KHI performance

All experiments were carried out in standard in-house high-pressure, 280 ml volume stirred autoclaves using the new CGI method, as described in Section 2.2. The purity of the gases used in preparing the gas mixture were: methane 99.995%, ethane 99.5%,

propane 99.5%, and CO_2 99.995%. Distilled water was used in all tests. Gas mixtures were prepared gravimetrically with compositions checked by GC where appropriate. Natural gas compositions used in tests are provided in Table 2.2. The PVCap used was Luvicap-EG base polymer (Kvalue = 25-8, average MW = 7000) supplied by BASF, with the ethylene glycol solvent removed by vacuum oven drying.

Table 2.2 Composition of natural gases used in CGI experiments on PVCap in previous studies (Mozaffar, 2013) and the gas with 12 mol% CO_2 (CO_2 added to the existing gas) used in this study.

Component	Mole%	
	Previous studies	This study
Methane	89.41	79.0
Ethane	5.08	5.4
Propane	1.45	1.8
i-Butane	0.18	0.2
n-Butane	0.26	0.3
i-Pentane	0.06	-
CO_2	1.55	12.0
Nitrogen	1.93	1.3
n-Pentane	0.06	-
n-Hexane	0.02	-

Methane-ethane-propane-carbon dioxide mixture with PVCap

Based on the conclusion from previous studies (Mozaffar 2013), the CO_2+C_2+C_1 combination in natural gas (NG) seems to give good PVCap performance at higher pressures, although CO_2 is at the same time apparently responsible for the significant reduction in PVCap performance observed at lower pressures in NG systems. However, to examine the effect of CO_2, while at the same time working towards the composition of a real natural gas, PVCap induced CGI behaviour in methane-ethane-propane-CO_2 systems were measured and are presented here.

Figure 2.2 shows CGI data and interpreted regions determined for the 91.5 mole% methane / 4.9 mole% ethane / 2 mole% propane / 1.6 mole% CO_2 gas mixture with 0.5 mass% PVCap aqueous. Data are tabulated in Table 2.3. As discussed previously and consistent with other s-I/s-II forming binary and multicomponent gas systems, CGI boundaries for this system appear related primarily through subcooling to the s-I phase boundary for the gas, i.e. hydrate growth is apparently the result of initial s-I formation.

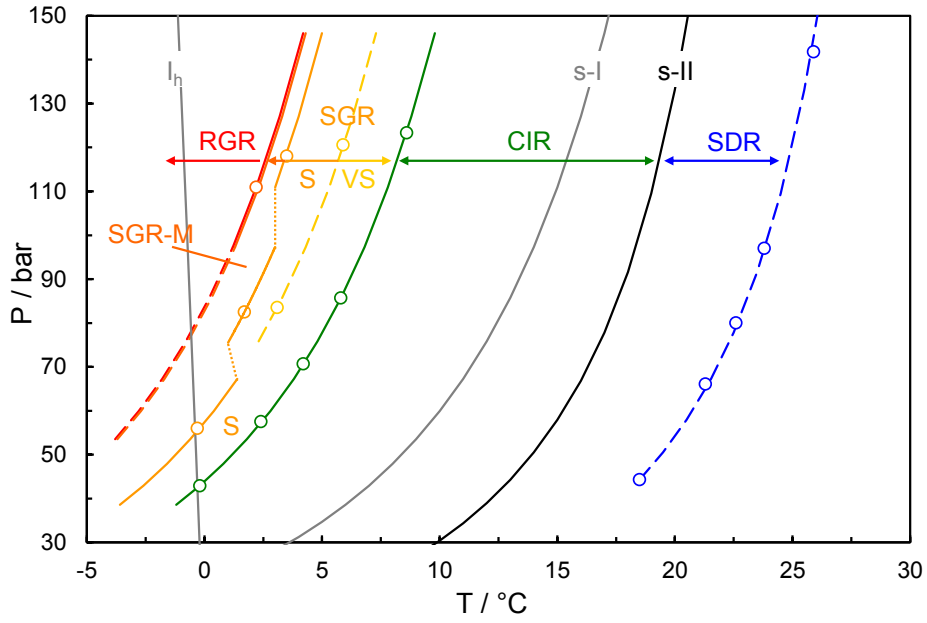

Figure 2.2 CGI data and interpreted regions determined for the 91.5 mole% methane / 4.9 mole% ethane / 2 mole% propane / 1.6 mole% CO_2 gas mixture with 0.5 mass% PVCap aqueous.

Table 2.3 Experimentally determined points on CGI region boundaries for the 91.5 mole% methane / 4.9 mole% ethane / 2 mole% propane / 1.6 mole% CO_2 gas mixture with 0.5 mass% PVCap aqueous.

CGR boundary	Growth rate	T / °C (± 0.5)	P / bar (± 0.2)	$\Delta T_{s\text{-}I}$ / °C (± 0.5)	$\Delta T_{s\text{-}II}$ / °C (± 0.5)
SDR	Slow dissociation	18.5	44.3	-	5.5
		21.3	66.1	-	5.4
		22.6	80.0	-	5.4
		23.8	97.0	-	5.5
		25.9	141.8	-	5.6
CIR-SGR(VS)	No growth	-0.2	42.9	-7.2	-13.0
		2.4	57.5	-7.2	-12.5
		4.2	70.7	-7.2	-12.2
		5.8	85.7	-7.2	-11.8
		8.6	123.3	-7.2	-11.0
SGR(VS-S)	Very slow	3.1	83.5	-9.7	-14.3
		5.9	120.6	-9.7	-13.6
SGR(S-M)	Slow	-0.3	56.0	-9.7	-15.1
		1.4	67.3	-9.6	-14.6
		1.7	82.5	-11.0	-15.6
		3.5	118.0	-12.0	-15.9
SGR(M)-RGR	Moderate	2.2	110.9	-12.8	-16.9

As noted, it is believed that CO_2 may be responsible for the moderately reduced performance of PVCap in natural gas systems at lower pressures. Studies on C_1-C_2-C_3 and C_1-CO_2 systems have lent support to this theory; the extent of CGI regions in the C_1-C_2-C_3 system increase modestly at lower pressures, while a clear reduction in the extent of CGI regions was observed at lower pressures in the C_1-CO_2 system. However, while the presence of CO_2 apparently reduces PVCap performance at lower pressures, it enhances performance at higher pressures; in both the natural gas and C_1-CO_2 systems (Mozaffar, 2013).

The addition of CO_2 to the C_1-C_2-C_3 system results in an overall significant improvement in PVCap performance (see Figure 2.6); the CIR region is the largest observed for all systems shown in Figure 2.6, extending apparently to $\Delta T_{s\text{-}I}$ = ~-7.2 °C across the pressure range studied (~50 to 130 bar). Likewise the SGR region is also the largest in extent observed; with CGI properties extending up to 12.8 °C subcooling from the s-I boundary for the C_1-C_2-C_3-CO_2 mixture. However, while the addition of CO_2 clearly improves PVCap performance compared to the C_1-C_2-C_3 system, a modest reduction in PVCap performance is still observed for the C_1-C_2-C_3-CO_2 below ~100 bar (SGR (VS) lost and SGR(S)-(M) boundary at lower subcoolings), as per the natural gas and C_1-CO_2 systems. Thus data would support previous conclusions that CO_2 content plays an important role in PVCap performance; increasing PVCap CGI properties at higher pressures, but with this being offset somewhat by it reducing performance modestly at lower pressures for the systems described.

The reasons as to why CO_2 has this effect are unclear. However, it is now clear that guest gas (presumably in terms of occupancy patterns in hydrate cages as a function of pressure and how this affects polymer adsorption on crystal surfaces) composition is as important as hydrate structure in terms of KHI polymer performance. For further work on the effect of CO_2, studies have been undertaken on a 12 mole% CO_2 natural gas, with results discussed below.

CO_2-rich natural gas with PVCap

In addition to the above, to continue work on the effect of CO_2, CGI studies have been undertaken on 0.5 mass% PVCap in a natural gas system with high CO_2 (12 mole%). Figure 2.3 shows example CGI method cooling and heating curves for the 12 mole% CO_2 natural gas with 0.5 mass% aqueous PVCap. Interpreted points on CGI boundaries are reported in Table 2.4 and plotted with interpolated CGI boundaries in Figure 2.4.

As shown in Figures 2.3 and 2.4, CGI region studies on 12 mole% CO_2 natural gas system with 0.5 mass% PVCap aqueous have demonstrated that PVCap performance is apparently better at lower pressures compared to higher pressures. This is opposite to the case for multicomponent systems where CO_2 is modest (e.g. 1.6 mole% CO_2 natural gas and C_1-C_2-C_3-1.6 mol% CO_2) and likewise in contrast to results for the binary 85 mol% CH_4 / 15 mol% CO_2 mixture (Mozaffar, 2013) where the effect of high CO_2 was to greatly reduce PVCap performance at lower pressures (see Figure 2.6). However, while for example the CIR region at 12% CO_2 is comparable in subcooling extent to that for natural gas with 1.6 mol% CO_2 at $\Delta T_{s\text{-}l}$ = ~5.2 °C, the total extent of the SGR region is reduced for 12 mol% at both high and low pressures, supporting a generally common negative effect of CO_2.

In conclusion, results suggest that CO_2 plays a very important role in PVCap performance, in particular with respect to the common changes in PVCap performance seen from lower (< 70 bar) to higher (>100 bar) pressures. However, while CO_2 is commonly associated with a negative effect, this is not ubiquitous across all gas systems at all pressures. Rather, the effect depends on the CO_2 concentration and other gas components in the system; speculatively this influencing cage occupancy patterns and thus the strength of adsorption on hydrate crystal surfaces.

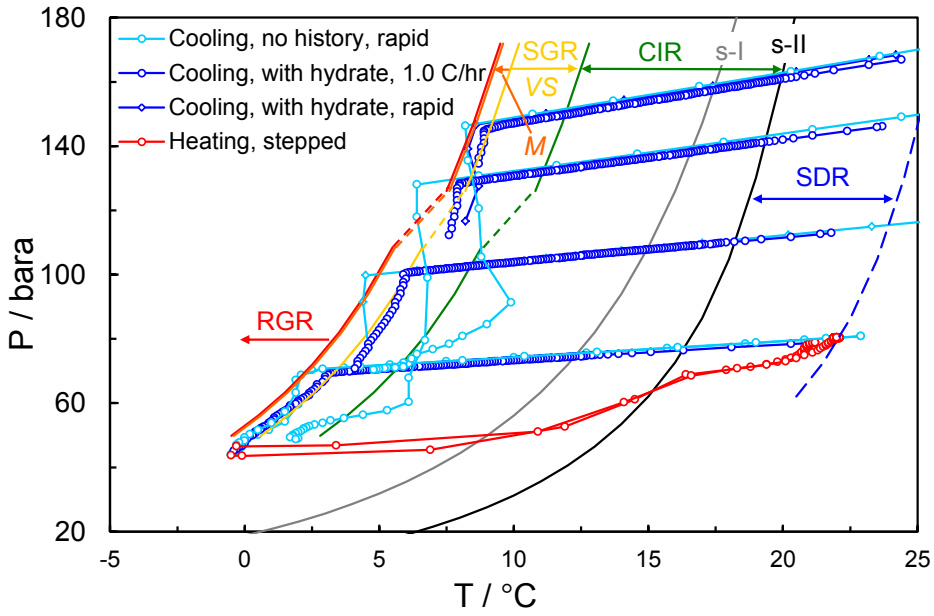

Figure 2.3 Example CGI method cooling and heating curves for the 12 mole% CO_2 natural gas with 0.5 mass% PVCap aqueous.

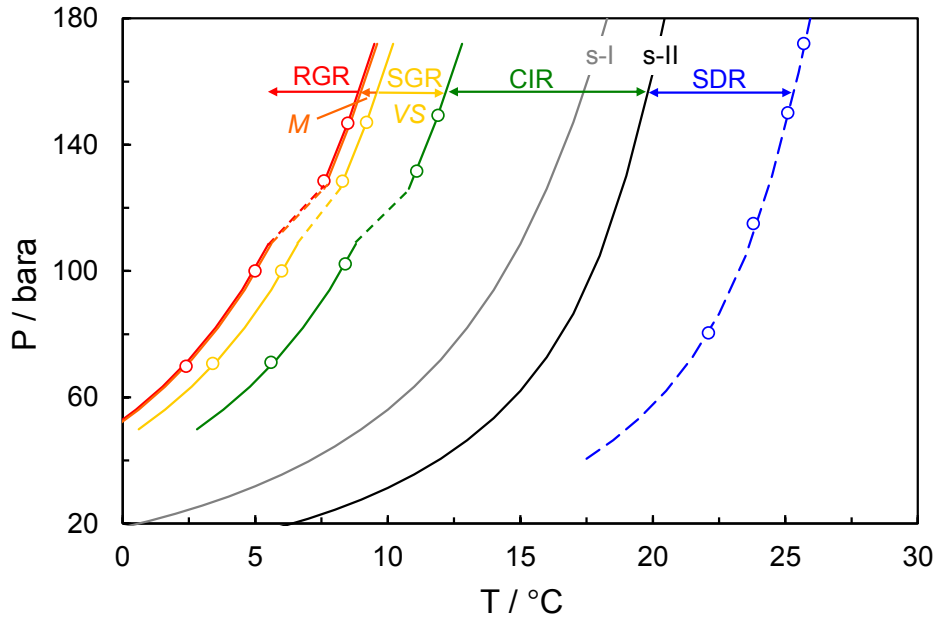

Figure 2.4 Interpreted CGI regions for 12 mole% CO_2 natural gas with 0.5 mass% PVCap aqueous.

Table 2.4 Experimentally determined points on CGI region boundaries for the 12 mole% CO_2 natural gas with 0.5 mass% PVCap aqueous.

CGR boundary	Growth rate	T / °C (± 0.5)	P / bar (± 0.2)	ΔT_{s-I} / °C (± 0.5)	ΔT_{s-II} / °C (± 0.5)
SDR	Slow dissociation	22.1	80.4	-	5.5
		23.8	115.0	-	5.4
		25.1	150.1	-	5.4
		25.7	172.0	-	5.4
CIR-SGR(VS)	No growth	5.6	71.0	-6.3	-10.2
		8.4	102.2	-6.2	-9.4
		11.1	131.6	-5.2	-8.0
		11.9	149.3	-5.2	-7.7
SGR(VS-M)	Very slow	3.4	70.7	-8.5	-12.7
		6.0	100.0	-8.4	-11.7
		8.3	128.4	-7.8	-10.6
		9.2	147.0	-7.8	-10.4
SGR(M)-RGR	Moderate	2.4	69.8	-9.4	-13.3
		5.0	100.0	-9.4	-12.7
		7.6	128.5	-8.5	-11.4
		8.5	146.8	-8.5	-11.1

Methane-carbon dioxide with PVCap

Following the contrasting effect of carbon dioxide between high CO_2 content natural gas (12 mol% CO_2) where pressure had a negative effect and C_1-CO_2 mixture containing 15 mol% carbon dioxide where pressure had a positive effect, CGI experiments were carried out on a C_1- CO_2 mixture with 90 mol% methane and 10 mol% carbon dioxide at pressures up to 140 bar to see if any change happens in this intermediate carbon dioxide concentration. Figure 2.5 shows determined CGI regions for this gas mixture, with data reported in Table 2.5.

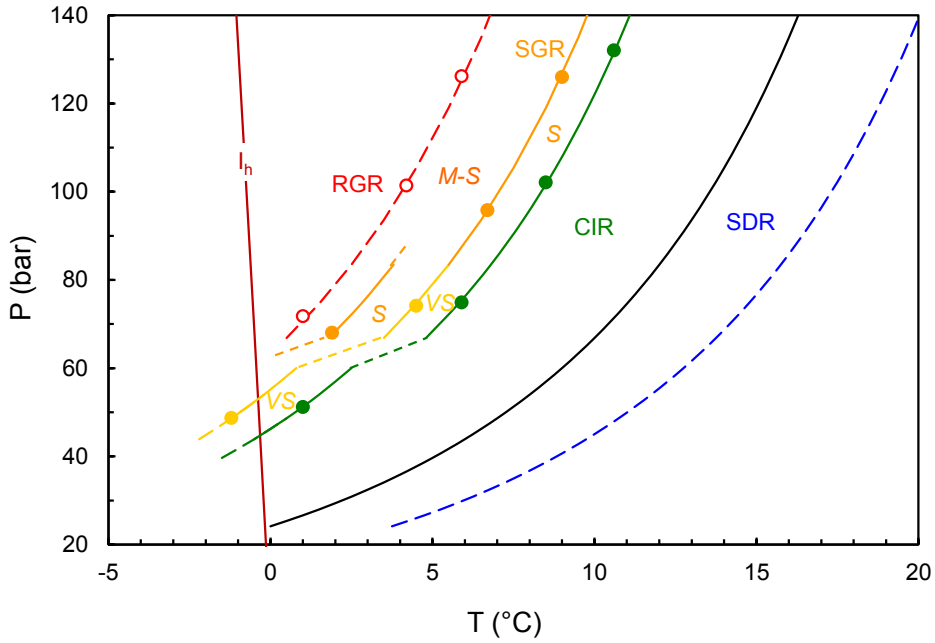

Figure 2.5 Determined CGI regions for 0.5 mass% PVCap with the 10 mol% CO_2 / 90 mol% CH_4 gas mixture.

Table 2.5 Experimentally determined points on CGI region boundaries for 0.5 mass% PVCap aqueous with the 10 mole% CO_2 / 90 mole% CH_4 mixture.

CGR boundary	Growth rate	T / °C (± 0.5)	P / bar (± 0.2)	ΔT_{s-I} / °C (± 0.5)
CIR-SGR(VS)	No growth	1.0	51.2	-6.5
		5.9	74.9	-5.1
		8.5	102.1	-5.2
		10.6	132.0	-5.2
SGR(VS-S)	Very slow	-1.2	48.7	-8.2
		4.5	74.1	-6.4
SGR(VS-M)	Slow	1.9	68.0	-8.3
		6.7	95.8	-6.5
		9.0	126.0	-6.5
SGR(M)-RGR	Moderate	1.0	71.8	-9.7
		4.2	101.4	-9.5
		5.9	126.2	-9.6

As can been seen in Figure 2.5, PVCap performance reduces with pressure in the 10% CO_2 / 90% CH_4 system which is also the case for H_2S-CH_4 systems (Section 2.3.2). Likewise, this reduction in extent of CGI regions occurs up to ~70 bar, beyond which region extents become largely constant. The results for 10% CO_2 / 90% CH_4 however contrast those for 15% CO_2 / 85% CH_4 where the opposite occurs, i.e. CGI regions are larger in extent at higher pressures.

Figure 2.6 shows a comparison of subcooling extents of CGI regions from the s-I phase boundary for the CO_2 containing gas mixtures compared to various single and mulitcomponent gas systems. The negative effect of high CO_2 content systems at low pressures is opposite to the result of natural gas with 12% CO_2 which like 10% CO_2 with methane, showed a positive effect at lower pressures. This means that for standard natural gases of modest CO_2 content (e.g. up to 5%), CO_2 is unlikely to be the primary source of the reduction in performance commonly observed at lower pressures. Instead, it seems more likely the combination of CO_2 and ethane is causing a positive effect at higher pressures. This can be seen in Figure 2.6 where ethane and CO_2 are both present alongside methane; the highest CGI subcooling extents are observed (important CIR and SGR(VS) specifically). Both of these are dominant s-I large cavity occupiers; ethane in particular only occupying the large $5^{12}6^2$ cavity. H_2S is similar (section 2.3.2), albeit of slightly lower molecular diameter, but this feature is the main one common to the three gases which seem to have the most influence on PVCap CGI performance in terms of gas composition and pressure.

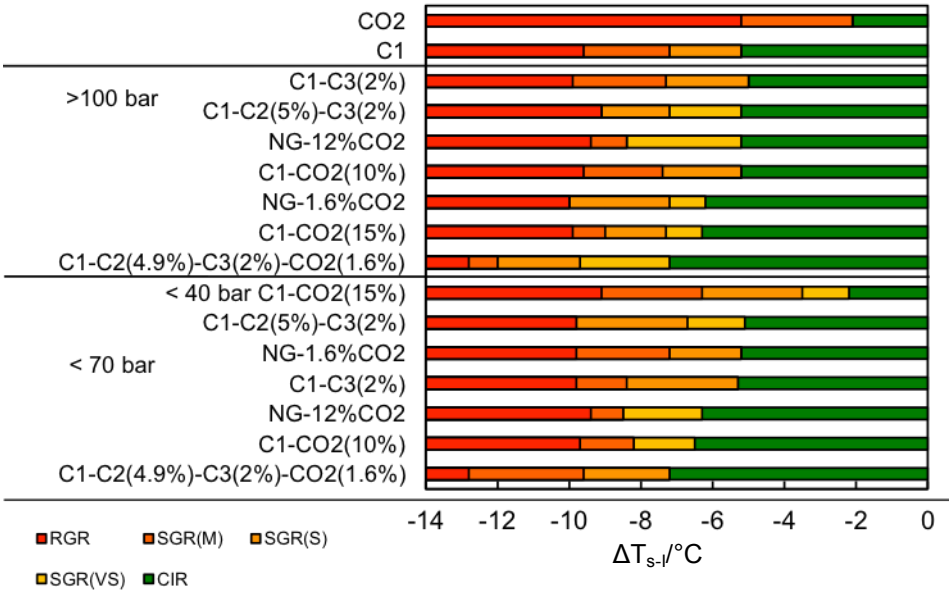

Figure 2.6 Comparison of subcooling extents of CGI regions from the s-I phase boundary for the CO_2 containing gas mixtures compared to various single and multi-component gas systems studied using the CGI method to date (Mozaffar, 2013). The plot sorts the data as a function of CIR region extent at < 70 bar and > 100 bar. NG compositions are given in Table 2.2.

The causes of this behaviour still remain somewhat elusive, although based on findings to date, hydrate cage occupancy patterns (as determined by gas composition and pressure) have emerged as the most likely controlling factor; investigations into gas solubility and acidity suggesting the former does not have an obvious influence and the latter actually increases PVCap inhibition (Sections 2.3.3 and 2.3.4).

2.3.2 Effect of hydrogen sulphide on KHI performance

H_2S experiments were carried out at the Hydrafact sour gas lab in standard high-pressure, 280 ml volume, acid gas compatible (hastelloy) stirred autoclaves using the Crystal Growth Inhibition (CGI) method (Anderson et al., 2011; Glénat et al., 2011). Hydrate dissociation point measurements were made using standard in-house constant volume, isochoric equilibrium step-heating techniques (Tohidi et al., 2000). All H_2S mixtures were supplied by BOC. Distilled water was used in all tests. The PVCap used was Luvicap-EG base polymer (K-value = 25-8, average MW = 7000) supplied by BASF, with the ethylene glycol solvent removed by vacuum oven drying.

90 mol% methane-10 mol% hydrogen sulphide with PVCap

Given the high solubility of H_2S in water, the hydrate phase boundary for a fixed molar gas to water ratio will be depressed at higher pressures as more H_2S is dissolved, reducing the fraction present in the vapour phase. This factor however only applies to a significant extent where water is greatly in excess of gas on a molar basis, i.e. in laboratory conditions where a significant volume of water is required to allow detection of hydrate formation (i.e. minimising the gas fraction, hence maximizing the pressure drop when gas is trapped in hydrate structure). In a real pipeline system, the gas normally dominates and is already in equilibrium with the water, so any dissolution effect is minimal.

As the cells used in experiments here are constant volume, adding more gas is normally the method used to increase pressure. Maintaining a constant gas to water molar ratio is problematic, unless the cell is loaded and unloaded each time; something to be avoided when working with H_2S which is a laborious process due to safety issues. This would also have the knock-on effect of shifting the phase boundary to lower temperatures/higher pressures as pressure was increased as noted; i.e. something which is not commonly applicable in real pipelines.

In light of the above, for H_2S tests, it was decided to maintain constant water content (50% of cell volume) and increase pressure by increasing the gas mole fraction as normal. This should, in theory, result in the vapour phase composition remaining roughly constant as the additional gas compensates for that going into solution as the pressure is increased. To confirm this and to ensure that the phase boundary for the system was known accurately, dissociation point measurements were conducted on the 10 mol% H_2S-90 mol% CH_4 gas for the pressure range of interest.

Figure 2.7 shows experimental equilibrium points with interpolation for gas hydrate dissociation conditions for the 10 mole% H_2S / 90 mole% CH_4 gas mixture, with measured dissociation points reported in Table 2.6. The phase boundary for the H_2S-CH_4 mixture is an interpolation, with the methane hydrate phase boundary shown for comparison.

As can be seen in Figure 2.7, the measured phase boundary shows an essentially constant temperature shift from that for methane across the pressure range, indicating a generally constant H_2S content of the vapour phase as a function of pressure as expected. The interpolated phase boundary derived from dissociation point data has been used as a reference for determining the extent of PVCap-induced CGI regions.

Table 2.6 Measured hydrate dissociation conditions for the 10 mole% H_2S / 90 mole% CH_4 gas mixture. Cell was 50 vol% aqueous phase.

T/°C	P/Bara
6.4	27.0
14.8	68.8
20.0	122.6

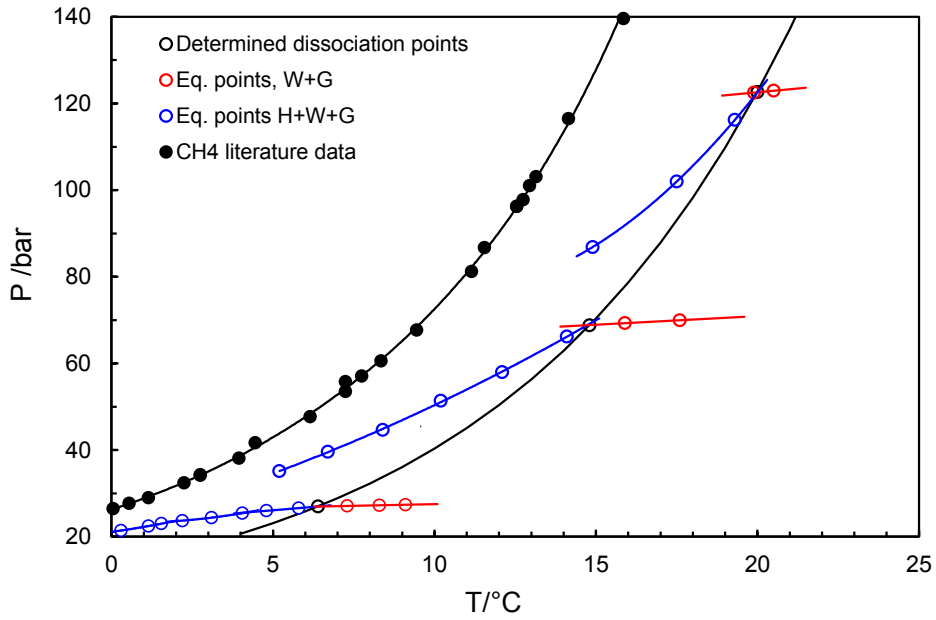

Figure 2.7 Experimental equilibrium points with interpolation for gas hydrate dissociation conditions for the 10 mole% H_2S / 90 mole% CH_4 gas mixture. The Phase boundary for the H_2S-CH_4 mixture is an interpolation. Shown for comparison is the methane hydrate phase boundary including literature data points (Deaton and Frost, 1946; McLeod and Campbell, 1961; Jhaveri and Robinson, 1965; Mohammadi et al., 2005).

Following hydrate dissociation point measurements, hydrate CGI regions have been investigated for 0.5 mass% aqueous PVCap with the 10 mole% H_2S / 90 mole% CH_4 mixture at pressures up to ~110 bar.

Figure 2.8 shows example CGI method cooling and heating curves for 0.5 mass% PVCap with the 10 mole% H_2S / 90 mole% CH_4 gas mixture. Experimentally determined points on CGI region boundaries are reported in Table 2.7 and presented with interpolated boundaries in Figure 2.9. Figure 2.10 shows a comparison of subcooling extents of CGI regions for 0.5 mass% PVCap aqueous with CO_2, methane, 10 mol% CO_2 / 90 mol% CH_4 and the 10 mol% H_2S / 90 mol% CH_4 mixture.

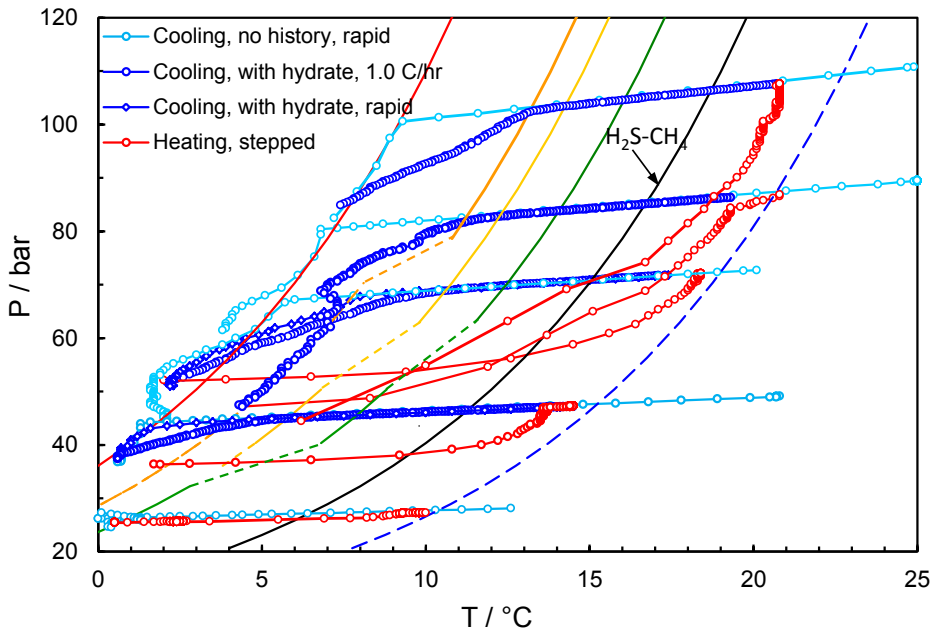

Figure 2.8 Example CGI method cooling and heating curves for 0.5 mass% PVCap with the 10 mole% H_2S / 90 mole% CH_4 gas mixture. The phase boundary for the system was determined experimentally.

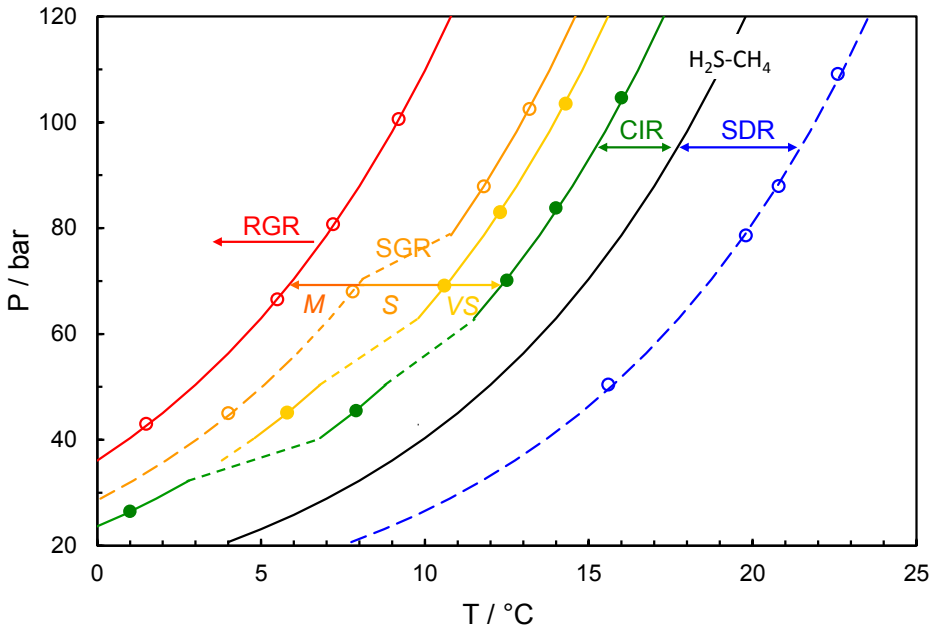

Figure 2.9 Experimentally determined points and interpolated CGI region boundaries for 0.5 mass% PVCap aqueous with the 10 mole% H_2S / 90 mole% CH_4 mixture. The phase boundary for the system was determined experimentally. Dashed lines indicate a degree of uncertainty.

Table 2.7 Experimentally determined points on CGI region boundaries for 0.5 mass% PVCap aqueous with the 10 mole% H_2S / 90 mole% CH_4 mixture.

CGR boundary	Growth rate	T / °C (± 0.5)	P / bar (± 0.2)	ΔT_{s-l} / °C (± 0.5)
SDR	Slow dissociation	10.8	28.9	3.8
		15.6	50.4	3.6
		19.8	78.6	3.8
		20.8	87.9	3.8
		22.6	109.1	3.7
CIR-SGR(VS)	No growth	1.0	26.5	-5.2
		7.9	45.5	-3.2
		12.5	70.1	-2.5
		14.0	83.8	-2.6
		16.0	104.6	-2.6
SGR(VS-S)	Very slow	5.8	45.1	-5.2
		10.6	69.1	-4.2
		12.3	83.0	-4.2
		14.3	103.5	-4.2
SGR(S-M)	Slow	4.0	45.1	-7.0
		7.8	68.1	-6.9
		11.8	87.9	-5.2
		13.2	102.5	-5.2
SGR(M)-RGR	Moderate	1.5	42.9	-9.1
		5.5	66.5	-9.0
		7.2	80.7	-9.0
		9.2	100.6	-9.0

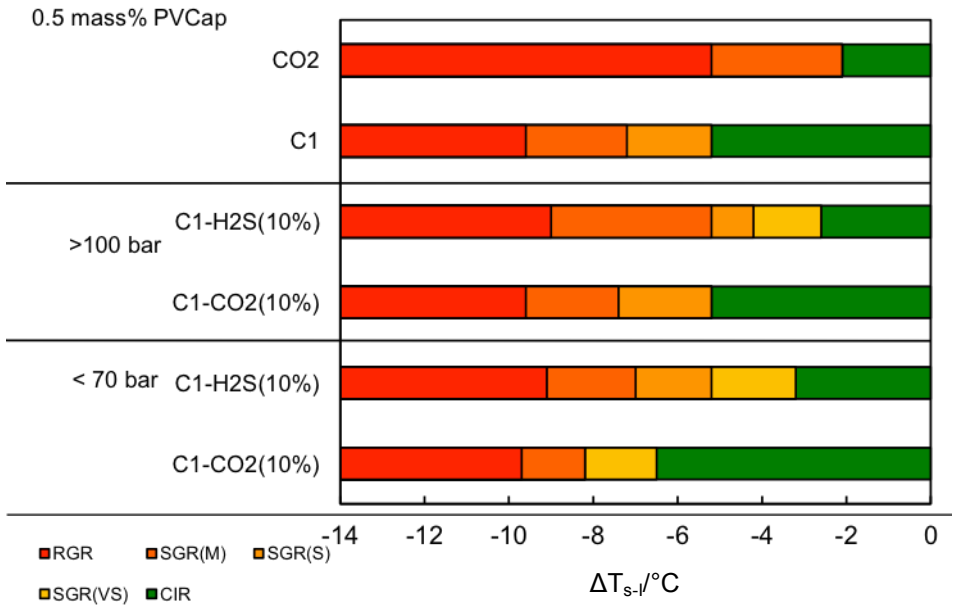

Figure 2.10 Comparison of determined subcooling extents of 0.5 mass% PVCap aqueous induced hydrate CGI regions for CO_2, methane (Mozaffar, 2013), 10% CO_2 / 90% CH_4 and the 10% H_2S / 90% CH_4 mixture.

As can been seen in Figures 2.9 and 2.10, data suggest H_2S has a negative effect on PVCap performance when compared with pure methane. The total extent of CGI regions across the pressure range studied is reduced from ~9.8 °C subcooling to 9.1 °C subcooling. The CIR is most strongly affected; whilst it extends to ΔT = -5.2 °C at pressures below ~35 bar, it reduces to ΔT = -3.2 °C at ~40 bar and to ΔT = -2.5 °C at pressures of 70 bar and above. This contrasts with methane, where the CIR remains at a subcooling of 5.2 °C across a similar pressure range. SGR(VS) and (S) regions also reduce with pressure; the SGR(M) conditions beginning at only 5.2 °C subcooling at 100 bar in the H_2S-CH_4 case.

The effect of H_2S somewhat is similar to that for the same concentration of CO_2 with methane. As noted, the negative effect of H_2S increases with pressure which is also the case for 10 mol% CO_2 with methane. In natural gases, an opposite case apparently applies for CO_2, at least at lower concentrations (1.6%); at higher concentrations (12%) increasing pressure has negative effect.

Data points for the two higher pressures show that while PVCap performance reduces with pressure up to ~80 bar, beyond this performance appears to become constant and further changes to the extent of CGI regions would be limited above ~80 bar which is also supported by modelling studies (Anderson, 2013, 2014). Further discussions of the suspected reasons for this are given in Section 2.3.3.

95 mol% methane-5 mol% hydrogen sulphide with PVCap

For the 5 mol% H_2S / 95 mol% CH_4 system, for the reasons given in the previous section, equilibrium hydrate dissociation conditions were again measured for the PVCap-free system first to ensure accuracy in subsequent determination of the extent of CGI regions. Figure 2.11 shows experimental equilibrium points with interpolation for gas hydrate dissociation conditions for the 5 mol% H_2S / 95 mol% CH_4 gas mixture, with measured dissociation points reported in Table 2.8. The phase boundary for the 5 mol% H_2S-95 mol% CH_4 mixture is an interpolation derived from dissociation point data and, as was the case for the 10 mol% H_2S / 90 mol% CH_4 system, has been used as a reference for determining the extent of PVCap-induced CGI regions.

Table 2.8 Measured hydrate dissociation conditions for the 5 mol% H_2S / 95 mol% CH_4 gas mixture. Cell was 50 vol% aqueous phase.

T/°C	P/Bara
4.9	26.4
13.3	69.8
19.2	133.5

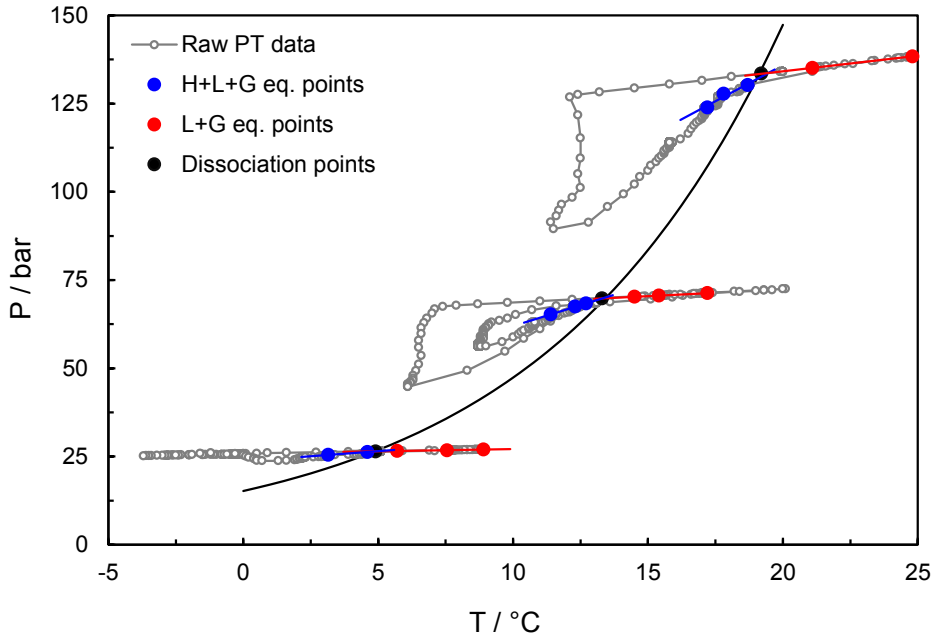

Figure 2.11 Experimental equilibrium points with interpolation for gas hydrate dissociation conditions for the 5 mol% H_2S / 95 mol% CH_4 gas mixture. The phase boundary is an interpolation.

Following hydrate dissociation point measurements, hydrate CGI regions were investigated for 0.5 mass% PVCap aqueous with the 5 mol% H_2S / 95 mol% CH_4 mixture at pressures up to ~140 bar. Figure 2.12 shows example CGI method cooling and heating curves for 0.5 mass% PVCap with the 5 mol% H_2S / 95 mol% CH_4 gas mixture. Figure 2.13 shows determined CGI regions for gas mixture, with Figure 2.14 showing a comparison of determined subcooling extents of 0.5 mass% PVCap aqueous induced hydrate CGI regions for CH_4, 5 mol% H_2S / 95 mol% CH_4 and 10 mol% H_2S / 90 mol% CH_4 mixtures at ~40 and >70 bar. Measured points on CGI region boundaries for the 5 mol% H_2S / 95 mol% CH_4 mixture are reported in Table 2.9.

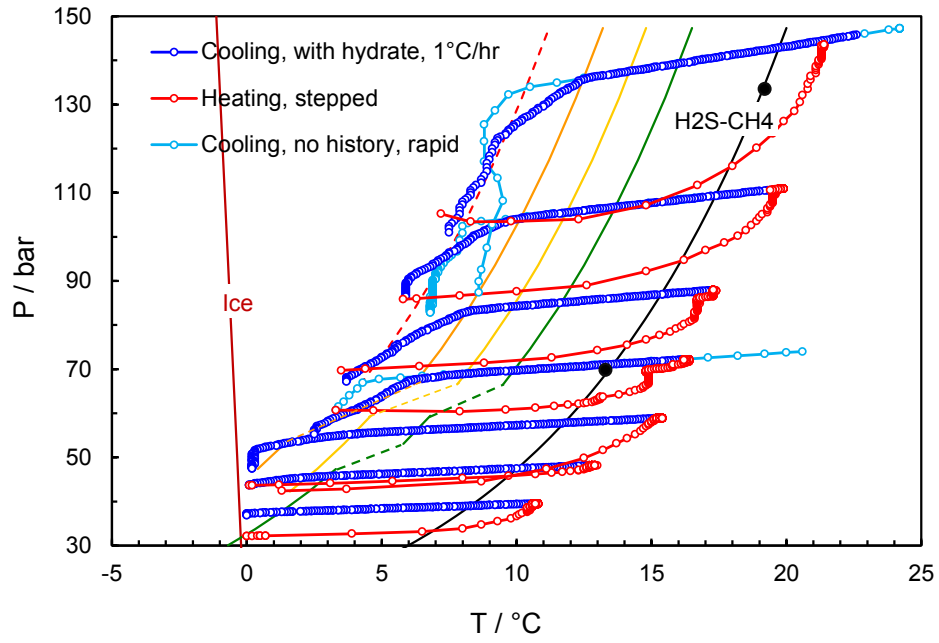

Figure 2.12 Example CGI method cooling and heating curves for 0.5 mass% PVCap with the 5 mol% H_2S / 95 mol% CH_4 gas mixture. The phase boundary for the system was determined experimentally.

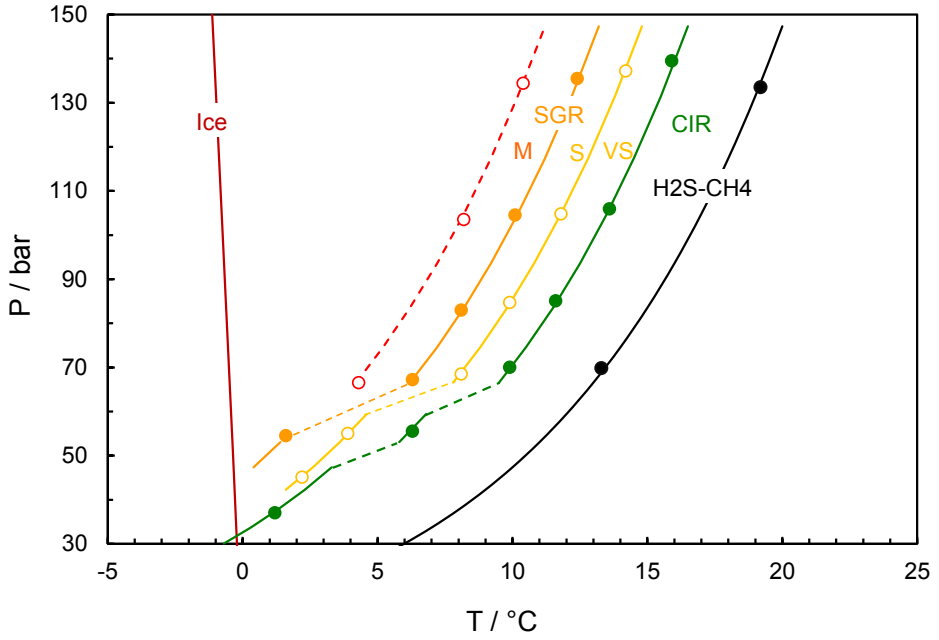

Figure 2.13 Determined CGI regions for 0.5 mass% PVCap with the 5 mol% H_2S / 95 mol% CH_4 gas mixture. The phase boundary for the system was determined experimentally.

Table 2.9 Experimentally determined points on CGI region boundaries for 0.5 mass% PVCap aqueous with the 5 mol% H_2S / 95 mol% CH_4 mixture.

CGR boundary	Growth rate	T / °C (± 0.5)	P / bar (± 0.2)	ΔT_{s-I} / °C (± 0.5)
CIR-SGR(VS)	No growth	1.2	37.0	-6.7
		6.3	55.5	-5.2
		9.9	70.0	-3.5
		11.6	85.1	-3.5
		13.6	105.9	-3.5
		15.9	139.5	-3.5
SGR(VS-S)	Very slow	2.2	45.1	-7.4
		3.9	55.0	-7.4
		8.1	68.5	-5.2
		9.9	84.7	-5.2
		11.8	104.8	-5.2
		14.2	137.2	-5.2
SGR(S-M)	Slow	1.6	54.5	-9.6
		6.3	67.2	-6.8
		8.1	83.0	-6.8
		10.1	104.5	-6.9
		12.4	135.5	-6.9
SGR(M)-RGR	Moderate	4.3	66.5	-8.7
		8.2	103.5	-8.7
		10.4	134.4	-8.8

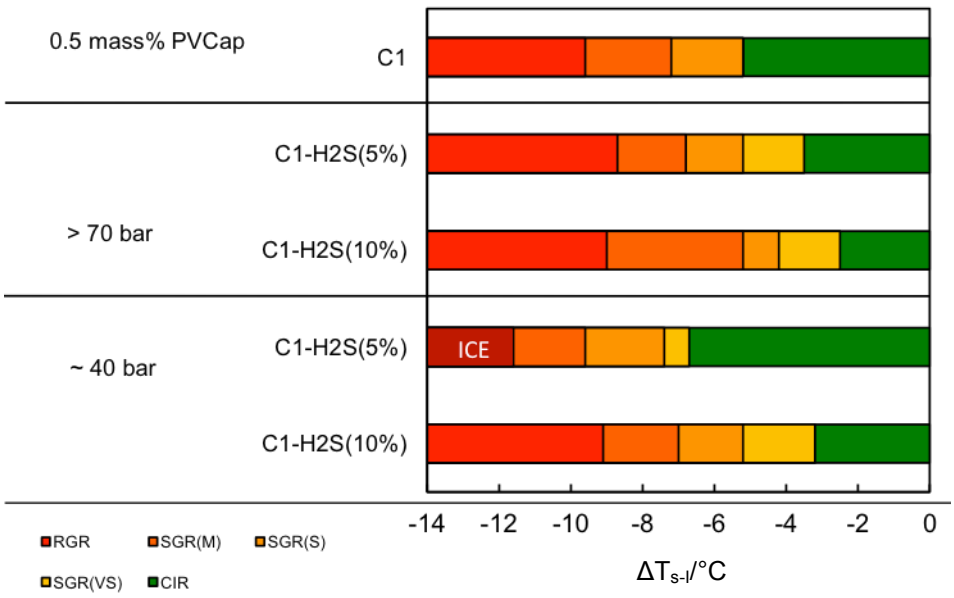

Figure 2.14 Comparison of determined subcooling extents of 0.5 mass% PVCap aqueous induced hydrate CGI regions for CH_4 (Mozaffar, 2013), 5 mol% H_2S / 95 mol% CH_4 and 10 mol% H_2S / 90 mol% CH_4 mixtures at ~40 and >70 bar.

As can been seen in Figures 2.12 to 2.14, as for 10 mol% H_2S, PVCap performance reduces with pressure in the presence 5 mol% H_2S. Likewise, in a similar manner to 10 mol% H_2S, this reduction in the extent of CGI regions occurs up to ~70-80 bar, beyond which region extents become largely constant. At both 5 and 10 mol% H_2S concentrations, the total extent of CGI behaviour is reduced compared to those for methane by up to ~1 °C subcooling, furthermore, the higher the H_2S content, the more the complete inhibition region is reduced.

As noted, the negative effect of H_2S increases with pressure. This is the opposite case to 15 mol% CO_2 with methane, where a negative effect is seen at lower pressures and a positive effect (relative to methane alone) at higher pressures while similar to 10 mol% CO_2 with methane where pressure had a negative effect. For natural gases with lower concentrations of carbon dioxide (e.g. 1.6%), a positive effect applies for CO_2; however increasing CO_2 content to higher concentrations (12%) shows a negative effect.

90 mol% methane-5 mol% hydrogen sulphide-5 mol% CO_2 with PVCap

Progressing to more complex mixtures, a 5 mol% CO_2 / 5 mol% H_2S / 90 mol% methane mixture with 0.5% PVCap was investigated. As a standard for H_2S systems where gas solubility in the aqueous phase is high, the phase boundary for this mixture was measured experimentally prior to CGI tests. Measured dissociation point data are reported in Table 2.10; points were found to be in good agreement with model predictions. Figure 2.15 shows determined CGI regions for 0.5 mass% PVCap with the 3 component mixture, with measured points on CGI region boundaries reported in Table 2.11.

Table 2.10 Experimentally determined dissociation points on the hydrate phase boundary for the 5 mol% CO_2 / 5 mol% H_2S / 90 mol% CH_4 mixture (no PVCap). Aqueous volume fraction in the cell was 50%.

T/°C	P/Bara
5.6	26.6
12.0	55.6
18.5	133.0

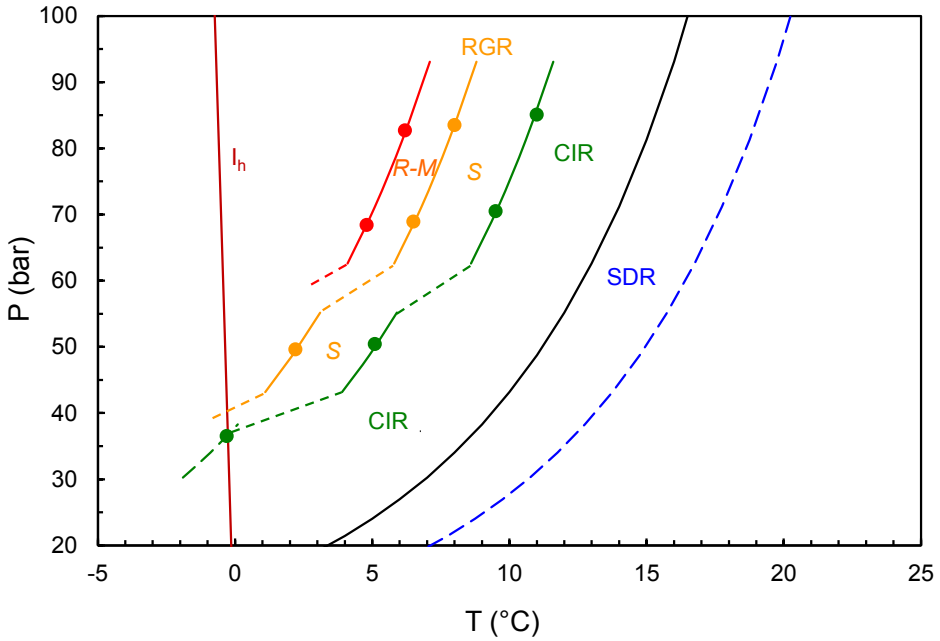

Figure 2.15 Determined CGI regions for 0.5 mass% PVCap with the 5 mol% CO_2 / 5 mol% H_2S / 90 mol% CH_4 gas mixture. The phase boundary is a model prediction which was found to be in agreement with measured hydrate dissociation points.

Table 2.11 Experimentally determined points on CGI region boundaries for 0.5 mass% PVCap aqueous with the 5 mol% CO_2 / 5 mole% H_2S / 90 mole% CH_4 mixture.

CGR boundary	Growth rate	T / °C (± 0.5)	P / bar (± 0.2)	ΔT_{s-I} / °C (± 0.5)
CIR-SGR(S)	No growth	-0.3	36.5	-8.9
		5.1	50.4	-6.2
		9.5	70.5	-4.4
		11.0	85.1	-4.3
SGR(S-M)	Slow	2.2	49.6	-8.9
		6.5	68.9	-7.2
		8.0	83.5	-7.2
SGR(M)-RGR	Moderate	4.8	68.4	-8.9
		6.2	82.7	-8.9

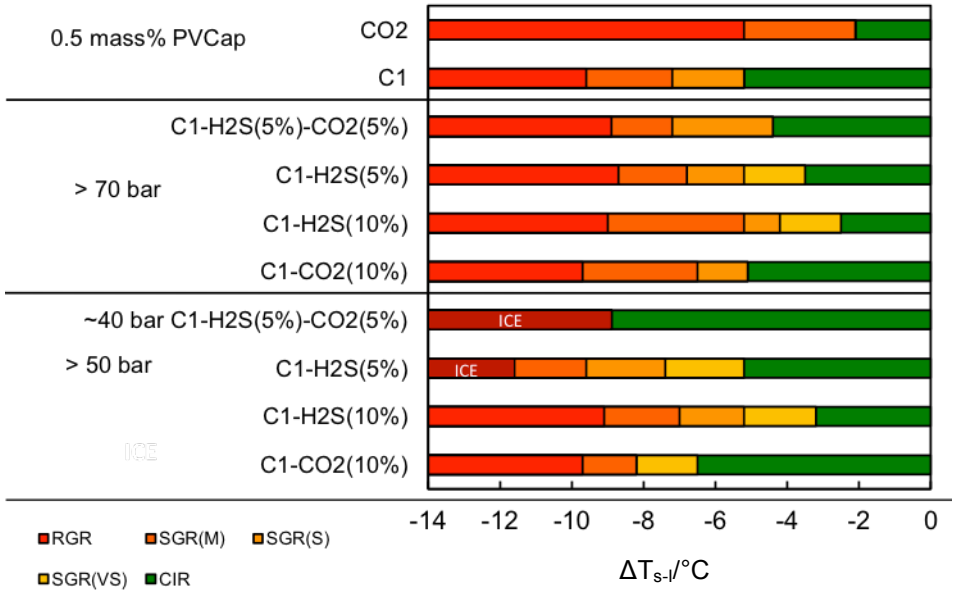

Figure 2.16 Comparison of determined subcooling extents of 0.5 mass% PVCap aqueous induced hydrate CGI regions for various single and binary/ternary mixtures of CH_4, CO_2 and H_2S measured during the course of the work. Single component CO_2 and CH_4 data from Mozaffar (2013).

Figure 2.16 shows a comparison of determined subcooling extents of 0.5 mass% aqueous PVCap induced hydrate CGI regions for various single and binary/ternary mixtures of CH_4, CO_2 and H_2S.

Similar to the 5 mol% H_2S-95 mol% CH_4 system and as seen for the 10 mol% CO_2 / 90 mol% CH_4 system, PVCap performance reduces with pressure in the ternary CO_2-H_2S-CH_4 mixture; CGI performance is very high at low pressures – the CIR extending at least to 8.9 °C subcooling – but reduces markedly above ~70 bar and regions appear constant in extent above this pressure. The results for the ternary mixture are therefore broadly in line with binary mixtures for similar CO_2 / H_2S ratios relative to CH_4. In both pressure ranges (Figure 2.16) adding CO_2 to H_2S-CH_4 mixture improves PVCap inhibition properties comparing to the 5 mol% H_2S-95 mol% CH_4 which is more pronounced at lower pressure (~40 bar).

The causes of H_2S and CO_2 behaviour remain elusive, with hydrate cage occupancy, solubility, and acidity all potentially playing a role. Modelling studies results (Anderson, 2013, 2014) are presented here to see if this can shed light on the processes involved (Section 2.3.3).

2.3.3 Modelling studies on the effect of cage occupancy and gas solubility

For CO_2 and H_2S with methane, as discussed previously in this chapter, the following factors stand out over the pressure range where significant changes in the PVCap performance are normally observed (~70-100 bar). These factors are small cage occupancy and gas solubility in the aqueous phase. Modelling studies using HydraFLASH® 2.2 (Anderson, 2013, 2014) are discussed here to see the effect of the above-mentioned factors. The thermodynamic model used in these studies was the Cubic Plus Association (CPA) equation of state. The Cubic-Plus-Association (CPA) model is an equation of state that combines a cubic equation of state (SRK in this case) and an association (chemical) term, which takes into account the specific site-site interactions due to hydrogen bonding (Haghighi, 2009). The model used for hydrate-forming condition was the solid solution theory of van der Waals and Platteeuw (1959) with Kihara Potential parameters (Kihara, 1953).

Figure 2.17 shows HydraFLASH® 2.2 predictions for CH_4 and H_2S solubility in the aqueous phase in the presence of hydrate along the phase boundary for the 10 mol% H_2S-90 mol% CH_4 system as a function of pressure. Figure 2.18 shows the same for CO_2 and CH_4 for the 15 mol% CO_2 system.

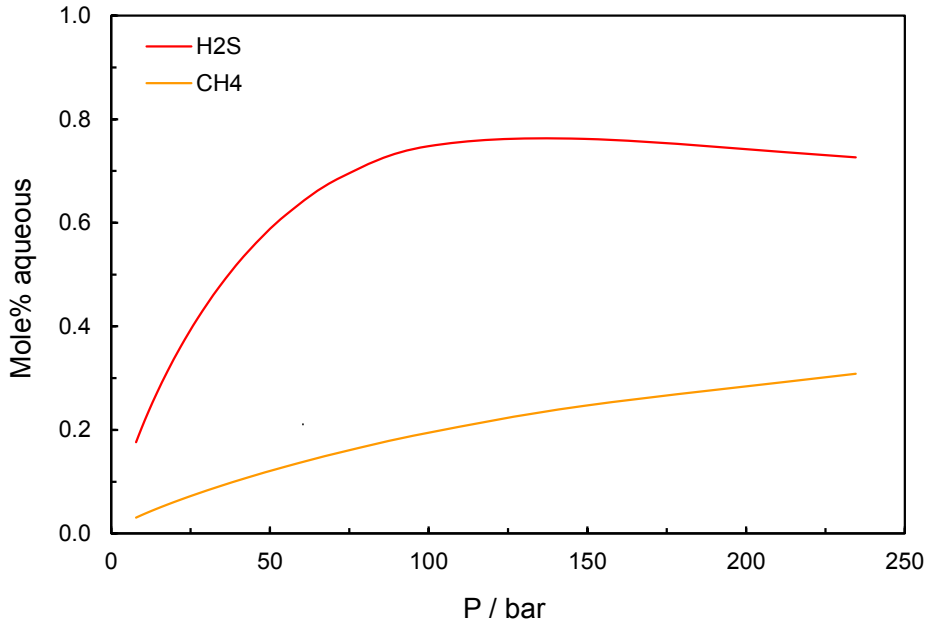

Figure 2.17 HydraFLASH® 2.2 predictions for CH_4 and H_2S solubility in the aqueous phase in the presence of hydrate along the phase boundary for the 10 mol% H_2S-90 mol% CH_4 system as a function of pressure (Anderson, 2013).

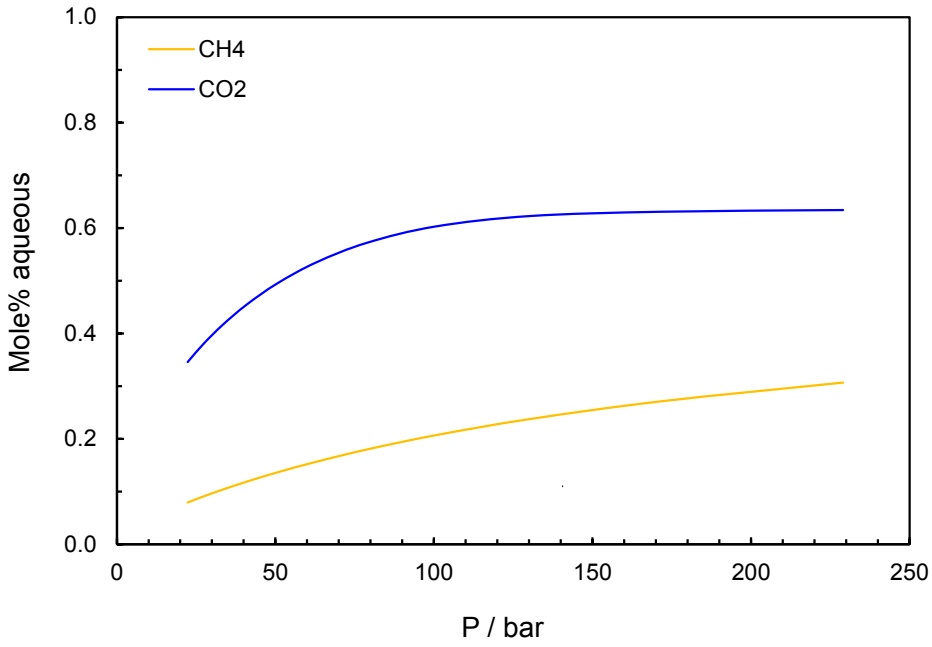

Figure 2.18 HydraFLASH® 2.2 predictions for CH4 and CO_2 solubility in the aqueous phase in the presence of hydrate along the phase boundary for the 15% CO_2 system as a function of pressure (Anderson, 2013).

As can be seen for both systems, the solubility of methane is very low and rises gently with pressure to just over 0.3 mol% as 250 bar is approached. No clear, significant changes are observed in the pressure range of interest (70- 100 bar). In contrast, for both CO_2 and H_2S, solubilities are quite low at lower pressures (0.17 mol% at 8 bar and 0.35 mol% aqueous at 20 bar for H_2S and CO_2 respectively), but rise quite rapidly with increasing pressure up to ~100 bar before levelling out. This is particularly true in the case of H_2S.

These rises in H_2S and CO_2 solubility could have two potential effects: an increase in acidity and an increase in potential for hydrate formation from dissolved gas (which PVCap may be weaker at inhibiting given increasing evidence that it acts predominantly at the gas-water interface). In the former case, increasing acidity may cause the polymer to curl up and/or coagulate, reducing propensity for crystal surface adsorption and thus effectiveness, although this would be expected to be much more of a factor in the H_2S system due to the greater acidity resulting from dissolved H_2S. Certainly, from the CGI data so far, for the H_2S system, it would appear that the reduction in PVCap

performance ceases above ~70 bar which may correlate with the levelling off of H_2S solubility (and thus associated acidity) in the aqueous phase.

However, while solubility patterns appear similar for both 10 mol% H_2S and 15 mol% CO_2 with methane, PVCap performance as a function of pressure is the opposite for these: it improves with pressure in the case of CO_2, but reduces in the case of H_2S. This implies that gas solubility (and thus potential acidity and/or growth from dissolved gas) cannot be the only factor involved.

Figures 2.19 and 2.20 show predicted s-I hydrate cage fractional occupancy (FO) along the phase boundary for the 10 mol% H_2S-CH_4 and 15 mol% CO_2-CH_4 systems respectively as a function of pressure. In this case, quite different patterns are seen for H_2S and CO_2.

At low pressures, H_2S dominates in both s-I small (5^{12}) and large cages ($5^{12}6^2$), occupying nearly 70% in both cases. This H_2S dominance occurs up to the 150-200 bar pressure range where methane then becomes dominant. Whilst the total large ($5^{12}6^2$) cage occupancy varies a little (from 0.98 to level off at ~0.99 as pressure increases past 100 bar), the change in small cage (5^{12}) occupancy over the same pressure range is considerably larger; it rises from 0.88 to 0.96 over the range 8 to 100 bar before starting to level off.

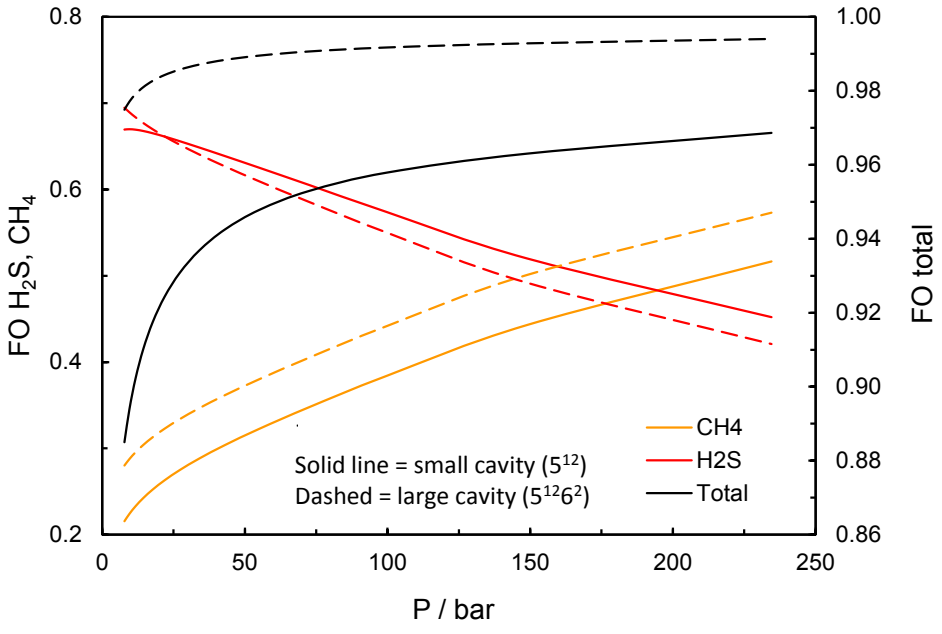

Figure 2.19 HydraFLASH® 2.2 predicted s-I hydrate cage fractional occupancy (FO) along the phase boundary for the 10 mol% H_2S-CH_4 system as a function of pressure (Anderson, 2013).

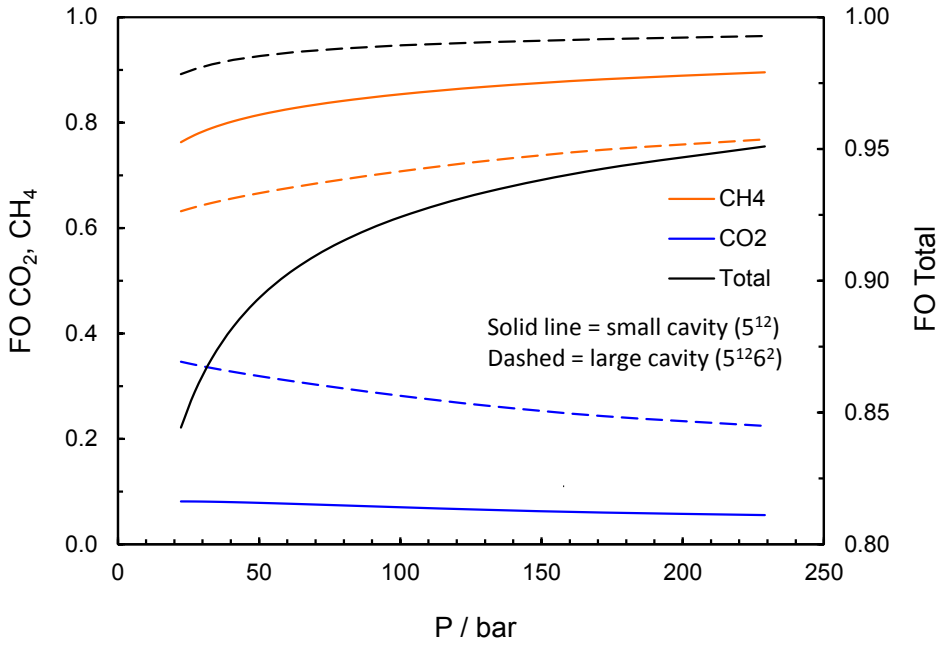

Figure 2.20 HydraFLASH® 2.2 predicted s-I hydrate cage fractional occupancy (FO) along the phase boundary for the 15 mol% CO_2-CH_4 system as a function of pressure (Anderson, 2013).

In contrast, for the CO_2-CH_4 system, while CO_2 occupancy also (as per H_2S) decreases with increasing pressure, methane dominates in both the large and small cages across the whole pressure range, which is in direct contrast to the H_2S-CH_4 system. Thus if cage occupancy is important – as results to date for single, binary and multicomponent gas mixtures suggest – then it might be expected results for PVCap - H_2S and CO_2 with methane to vary as they do.

In addition to relative occupancies for different components, total occupancies vary significantly between the different systems too, as can be seen in Figures 2.19, 2.20 and 2.21 (the latter showing total occupancies of each cage only). As can be seen in Figure 2.21, in addition to CO_2 not dominating cavities, total cage occupancies are considerably lower for the CO_2-CH_4 system, most notably for the small (5^{12}) cage and at lower pressures.

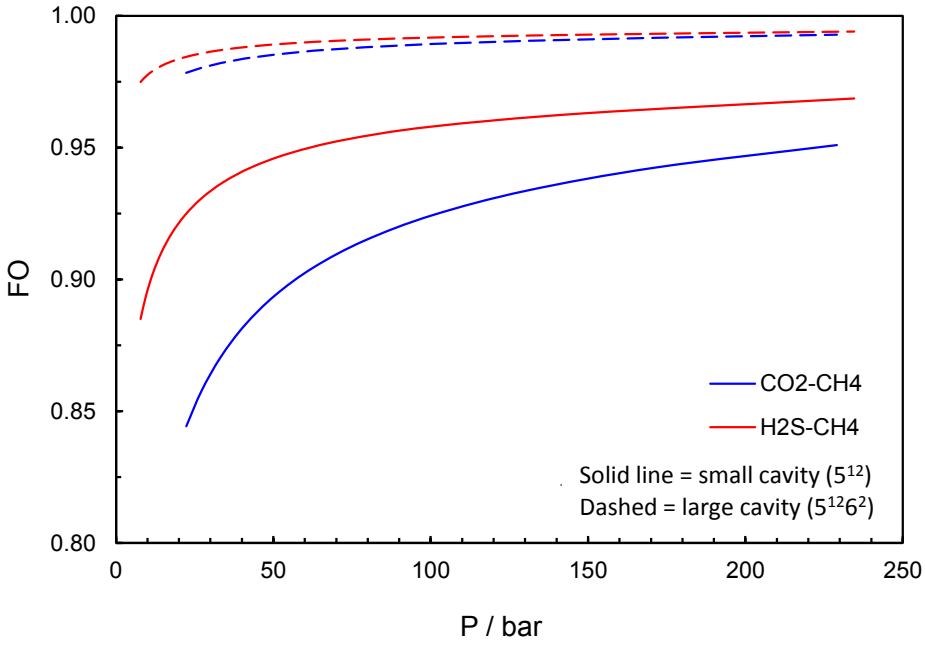

Figure 2.21 HydraFLASH® 2.2 predicted total s-I hydrate cage fractional occupancies (FO) along phase boundaries for the 15 mol% CO_2-CH_4 and 10 mol% H_2S-CH_4 systems as a function of pressure (Anderson, 2013).

In terms of the effect of cage occupancy, it has been speculated that the more stable the hydrate structure, the more stable the 'hydrate-polymer' complex formed following surface adsorption, the better the PVCap performance in terms of CGI. The loose correlation between KHI performance and extent of the SDR region adds some weight to this theory (increased metastability of polymer-hydrate complexes). Obviously, the stability of a hydrate depends on guest gas and occupancy; some formers need small cavities to be occupied in addition to the large (such as methane) whilst others do not (such as ethane). Considering this, the fact that PVCap shows better performance with ethane than with methane might be attributed to the former being more thermodynamically stable, with no need for 'help' gases filling the 5^{12} cages. In the case of methane, the structure is less stable and small cavities must be occupied to stabilise it; hence poorer PVCap performance. This theory certainly could help explain why PVCap is better with s-II than s-I; s-II is inherently a more stable structure (larger number of 5^{12} cavities with the ideal dihedral angle water bond orientations) and the most common s-II formers (e.g. propane or propane-ethane mixes, isobutane) do not require small cavity occupancy for stability. Applying this theory to the H_2S-CH_4 and CO_2-CH_4 systems discussed here, the following could be speculated.

For the 10 mol% H_2S-CH_4 case, PVCap performance at the lowest pressures (Figure 2.9) is seemingly as good as for methane, but performance reduces considerably with pressure. This could be the result of two processes; cage occupancy changes and increasing H_2S in the aqueous phase. At the lowest pressures, there is the lowest H_2S concentration in the aqueous phase thus it would be expected that acidity levels would be at their lowest, likewise the propensity for any formation from dissolved gas should be at its lowest (requires further study). The high cage occupancy by the strong hydrate stabilising H_2S could potentially explain the highest PVCap performance. As pressure is increased, while overall cage occupancy is also increased, H_2S is replaced by the less stabilising methane. At the same time, more H_2S dissolved in the aqueous phase causes an increasing negative effect due to increased propensity for hydrate formation directly from the aqueous phase (driven by further gas dissolution).

In the CO_2 system, due to the weak acidity, this is far less of a factor. Instead, cage occupancy is the controlling factor. As CO_2 does not do a great deal to stabilise hydrates compared to methane (phase boundaries for mixtures are nearly identical even to high CO_2 concentrations), total cage occupancy is more important, particularly small cage occupancy (this being crucial for methane and CO_2 hydrate for stability). As this rapidly decreases below ~100 bar, the hydrates formed are less stable, thus the hydrate-polymer complexes are less stable and hence PVCap performance in terms of CGI is reduced.

Figure 2.22 shows predictions for equilibrium aqueous H_2S solubility in the presence of hydrate as a function of subcooling for 10 mol% H_2S / 90 mol% CH_4 system. As can be seen, as the pressure increases along the phase boundary (zero subcooling), so does the gas solubility in equilibrium with hydrate. However, this increase largely stops above ~80 bar, as shown in Figure 2.22. Clearly, at all pressures, as subcooling increases, so the equilibrium solubility of H_2S in the presence of hydrate reduces, thus the driving force for hydrate formation from dissolved gas increases.

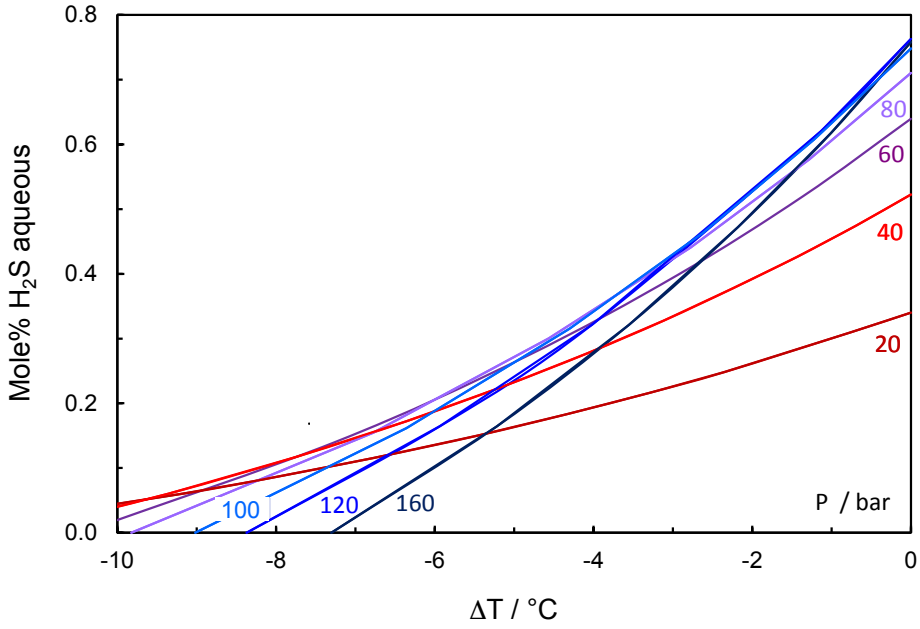

Figure 2.22 HydraFLASH® 2.2 predictions for equilibrium aqueous H_2S solubility in the presence of hydrate as a function of subcooling for 10 mol% H_2S / 90 mol% CH_4 system (Anderson, 2014).

Predictions do therefore suggest increasing propensity for hydrate formation from dissolved gas as pressure is increased up to ~80 bar, at which point this starts to stabilise. Likewise, as subcooling is increased, so the driving force for hydrate formation from dissolved gas increases. Such patterns would fit with experimental results for the H_2S-CH_4 system if it is assumed that hydrate formation from dissolved gas is a problem for PVCap; inhibition performance reducing as pressure increases up to ~80 bar then stabilising, i.e. increasing formation from dissolved gas reduces performance then this largely stops as the driving force for it reduces at higher pressures. However, this is not supported by results for CO_2-CH_4.

Figure 2.23 shows predictions for equilibrium aqueous CO_2 solubility in the presence of hydrate as a function of subcooling for 10 mol% CO_2 / 90 mol% CH_4 system. A similar pattern to that for the H_2S system is observed; as pressure increases, so does the solubility of CO_2 in the presence of gas hydrate at the phase boundary. Likewise, as subcooling is increased, so CO_2 solubility in the presence of hydrate decreases, thus propensity for hydrate formation from dissolved gas increases.

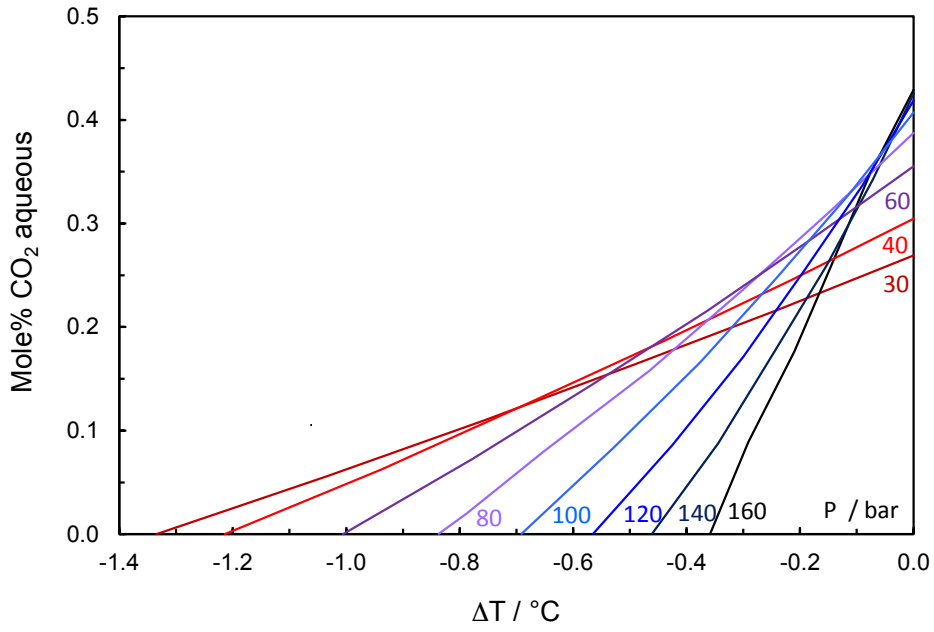

Figure 2.23 HydraFLASH® 2.2 predictions for equilibrium aqueous CO_2 solubility in the presence of hydrate as a function of subcooling for 10 mol% CO_2 / 90 mol% CH_4 system (Anderson, 2014).

However, there is a clear difference in the CO_2-CH_4 system; minimal CO_2 solubilities in the presence of hydrate – thus maximum propensity for formation from dissolved gas – occur at less than 1.4 °C subcooling for all pressures compared to over 10 °C subcooling for the H_2S system. At the highest pressure condition modelled of 160 bar, values are < 0.4 °C subcooling for the CO_2 system and > 7 °C subcooling for the H_2S system (this is because hydrate phase boundaries for pure CH_4 and CH_4-H_2S mixtures are much further apart in terms of temperature at a specific pressure than for CO_2-CH_4 mixtures where, for the compositions of interest, there is not a great deal of difference). This would imply that, if hydrate formation from dissolved gas is an issue for PVCap, then performance should be worse in CO_2-CH_4 systems (driving force for hydrate formation from dissolved gas peaks at much lower subcoolings) and worsen with pressure in both H_2S-CH_4 systems and CO_2-CH_4 systems, with the negative effect of CO_2 being greater than that for H_2S. This is not apparently the case though; instead PVCap performance improves in CO_2- CH_4 systems with pressure, at least for 15% CO_2 and natural gases with lower levels of CO_2. Likewise, tests on 10% CO_2 with 90% CH_4 and an immiscible PVCap KHI do not clearly support theoretically 'less hindered' growth from dissolved gas having a strong negative effect on PVCap performance.

2.3.4 Effect of pH and acidity on PVCap performance

The effect pH may have on KHI performance is not well established. The primary concern is acidity / low pH, namely that resulting from the aqueous dissolution and part ionic dissociation of CO_2 (forming carbonic acid, $CO_2 + H_2O \rightleftharpoons H_2CO_3 \rightleftharpoons HCO_3^- + H^+$) and H_2S (forming hydrosulfuric acid, $H_2S \rightleftharpoons HS^- + H^+$) from natural gases. The trend in the industry towards increasing production of sour gases means this issue is of growing importance. Changing pH is known to cause changes in polymer conformation (Yu and Somasundaran, 1996), this potentially leading to coagulation / precipitation which could lead to a reduction in hydrate inhibition performance and/or fouling problems.

Based on difficulties detailed earlier in this chapter (section 2.1), it was decided to look at the general effect of acidity independent of CO_2 and H_2S by working with hydrocarbon gases only (very low aqueous solubility and no pH effect) and aqueous solutions of known pH.

Experiments were carried out using high pressure stirred autoclaves employing the in-house CGI method. Purities of citric and acetic acid used were 99.5% supplied by SIGMA-ALDRICH. Deionised water was used in all tests. The purity of hydrochloric acid used was 10.0%. Methane was 99.995% pure and supplied by BOC. The PVCap used was standard Luvicap-EG base polymer – as used throughout the project – supplied by BASF with the ethylene glycol solvent removed by oven drying.

Citric acid and methane

Citric acid (Figure 2.24) was chosen initially for this purpose due to it being a mild acid with no particular corrosion risk (chelating agent for metals), and with a molecular diameter too large to potentially be involved in whole or partial hydrate enclathration. Furthermore, its weak, organic nature also makes arguably similar to naturally-occurring organic acids that may be found in hydrocarbon reservoir produced waters.

A citric acid solution of 0.04 mass% was prepared to give a moderately acidic pH of 3.0. This was achieved following preparation of a range of solutions of different citric acid concentrations to correlate mass% vs pH. The pH of solutions was measured with a VWR pH110 pH meter calibrated using manufacturer-supplied buffer solutions.

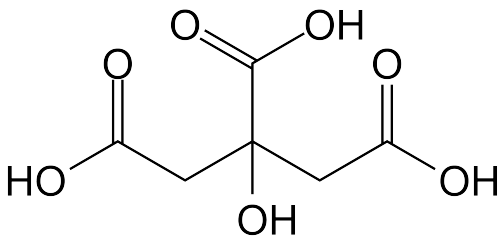

Figure 2.24 Molecular structure of citric acid

Example CGI method cooling and heating curves for 0.5 mass% PVCap (relative to aqueous phase) with 0.04 mass% citric acid (relative to water) - giving a pH of 3.0 – for the methane system are shown in Figure 2.25. Determined points on CGI region boundaries are reported in Table 2.12 and presented with interpolated boundaries in Figure 2.26. Figure 2.27 shows a comparison of subcooling extents of methane hydrate CGI regions at ~100 bar for the PVCap-citric acid system compared to that for PVCap with deionised water.

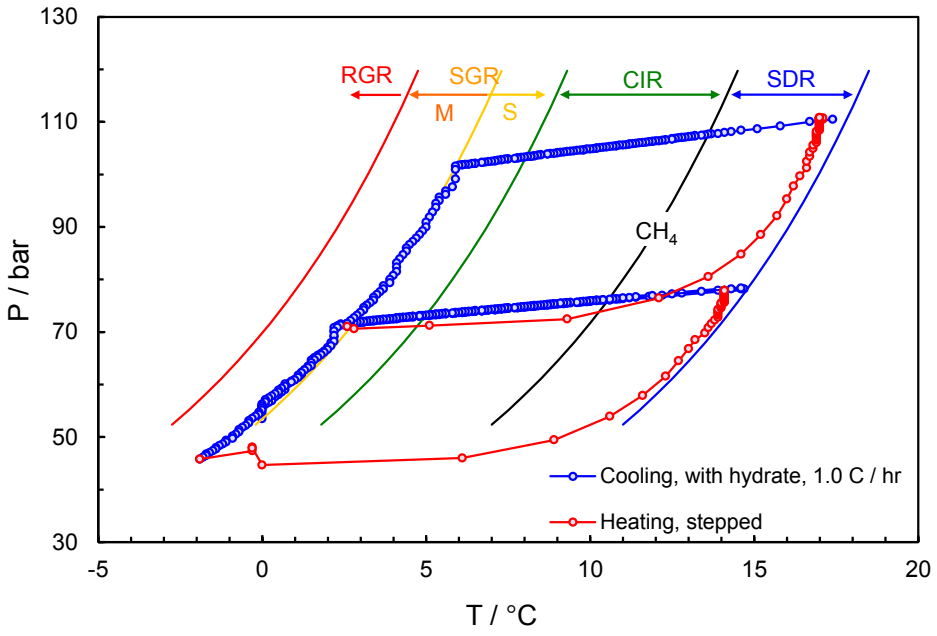

Figure 2.25 Example CGI method cooling and heating curves for 0.5 mass% PVCap / 99.5 mass % pH 3.0 citric acid solution (0.04 mass% citric acid) with methane.

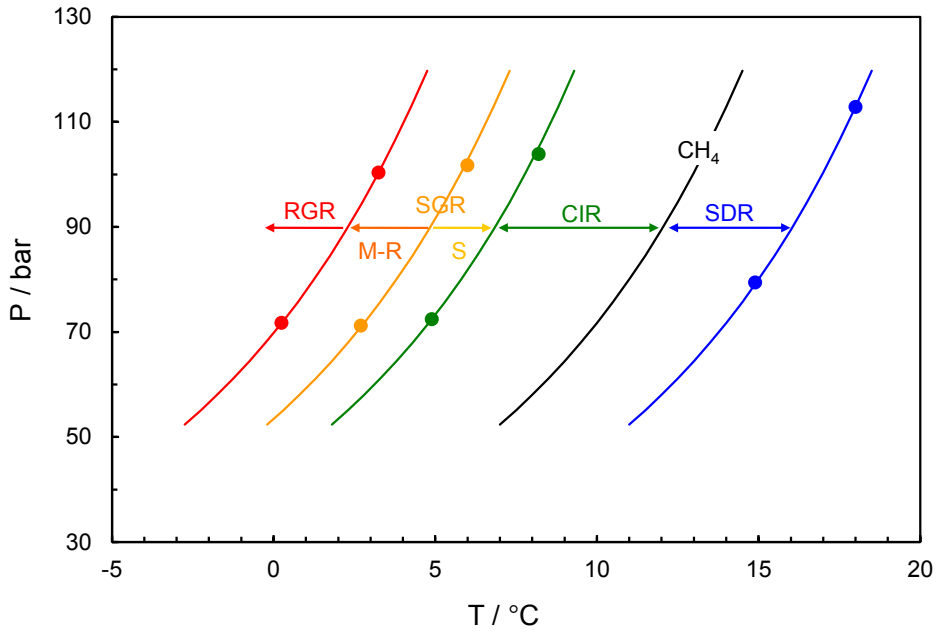

Figure 2.26 Experimentally determined methane hydrate CGI region data for 0.5 mass% PVCap / 99.5 mass % pH 3.0 citric acid solution (0.04 mass% citric acid).

Table 2.12 Experimentally determined methane hydrate CGI region data for 0.5 mass% PVCap (relative to aqueous phase) / 99.5 mass % pH 3.0 citric acid solution (0.04 wt% citric acid relative to water).

CGR boundary	Growth rate	T / °C (± 0.5)	P / bar (± 0.2)	ΔT_{s-I} / °C (± 0.5)
SDR	Slow dissociation	14.9	79.4	4.0
		18.0	112.8	4.0
CIR-SGR(S)	No growth	4.9	72.4	-5.2
		8.2	103.9	-5.1
SGR(S-M)	Slow	2.7	71.2	-7.2
		6.0	101.7	-7.1
SGR(M)-RGR	Moderate	0.3	71.7	-9.8
		3.3	100.3	-9.7

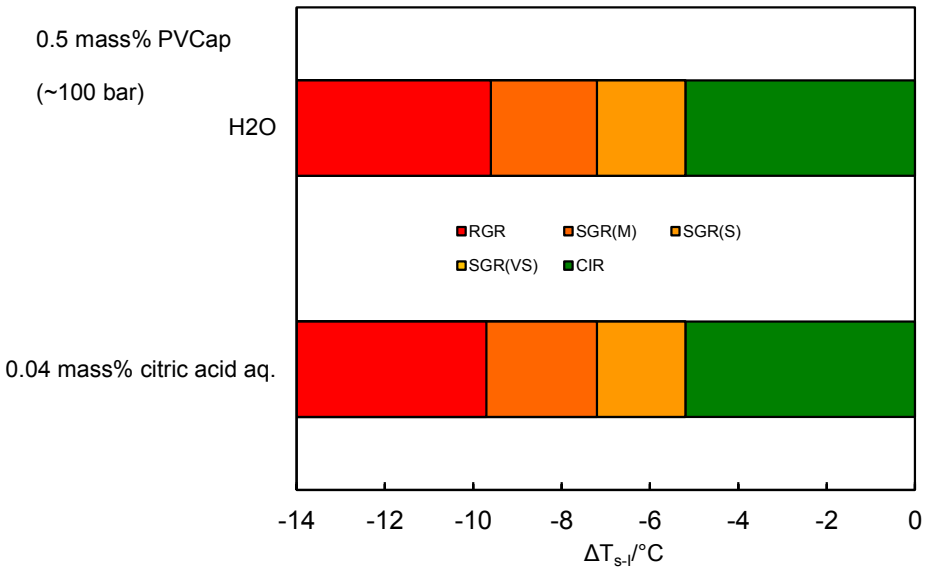

Figure 2.27 Comparison of subcooling extents of methane hydrate CGI regions for 0.5 mass% aqueous PVCap with deionised water and a 0.04 mass% citric acid solution with a pH of 3.0. CH_4-H_2O data from Mozaffar (2013).

As can be seen in Figures 2.25 to 2.27, CGI behaviour for PVCap in the citric acid system is effectively indistinguishable from that for deionised water, with region boundaries identical. There was some evidence that growth rates were slightly slower in the SGR(S) region in the citric acid system, but not enough to warrant changing region classification. Thus, if anything, the acidic nature of the aqueous phase at pH 3.0 had a slightly positive one.

With respect to a potential slight positive effect, during preparation of citric acid solutions it was noted that at higher citric acid concentrations / lower pH, polymer drop-out occurred (cloud point ~3.5 mass% citric acid at a pH of ~2.0). This ties in with the general rule of thumb that components dissolved in the aqueous phase which encourage polymer drop-out (e.g. salt, glycol ethers), unless levels actually cause precipitation, tend to have a positive effect on PVCap performance. A simple explanation for this is that hydrate crystal surface adsorption is more favoured when polymer miscibility with water is increasingly tenuous.

Acetic acid and methane

To further investigate the effect of pH on KHI-induced hydrate CGI patterns, acetic acid (common to reservoir waters) was tested to see if behaviour was the same as for citric acid. The effect of acetic acid solution of pH 3.0 (0.35 mass% acetic acid aqueous) on PVCap performance in a methane system was examined and the results are reported here. An acetic acid solution of 0.35 mass% was prepared to give a moderately acidic pH of 3.0. This was achieved following preparation of a range of solutions of different acetic acid concentrations and correlation of acetic acid mass% vs pH. The pH of solutions was measured with a VWR pH110 pH meter calibrated using manufacturer-supplied buffer solutions.

CGI method cooling curves for 0.5 mass% PVCap with 0.35 mass% acetic acid (relative to water) – giving a pH of 3.0 - in a methane system are shown in Figure 2.28. Determined points on CGI region boundaries are reported in Table 2.13 and presented with interpolated boundaries in Figure 2.29. Figure 2.30 shows a comparison of subcooling extents of CGI regions (from the s-I boundary) for 0.5 mass% aqueous PVCap with deionised water and with 0.04 mass % citric acid and 0.35 mass % acetic acid all tested with methane.

Table 2.13 Experimental methane hydrate CGI region data for 0.5 mass% PVCap aqueous / 99.5 mass % pH 3.0 acetic acid solution (0.35 mass% acetic acid relative to water).

CGR boundary	Growth rate	T / °C (± 0.5)	P / bar (± 0.2)	ΔT_{s-I} / °C (± 0.5)
SDR	Slow dissociation	13.6	72.6	3.6
		16.8	110.2	3.0
CIR-SGR(S)	No growth	2.4	67.3	-6.9
		5.9	101.8	7.2
SGR(S-M)	Slow	0.9	66.9	-8.3
		4.5	100.6	-8.5
SGR(M)-RGR	Moderate	0.1	66.5	-9.1
		3.6	100.1	-9.4

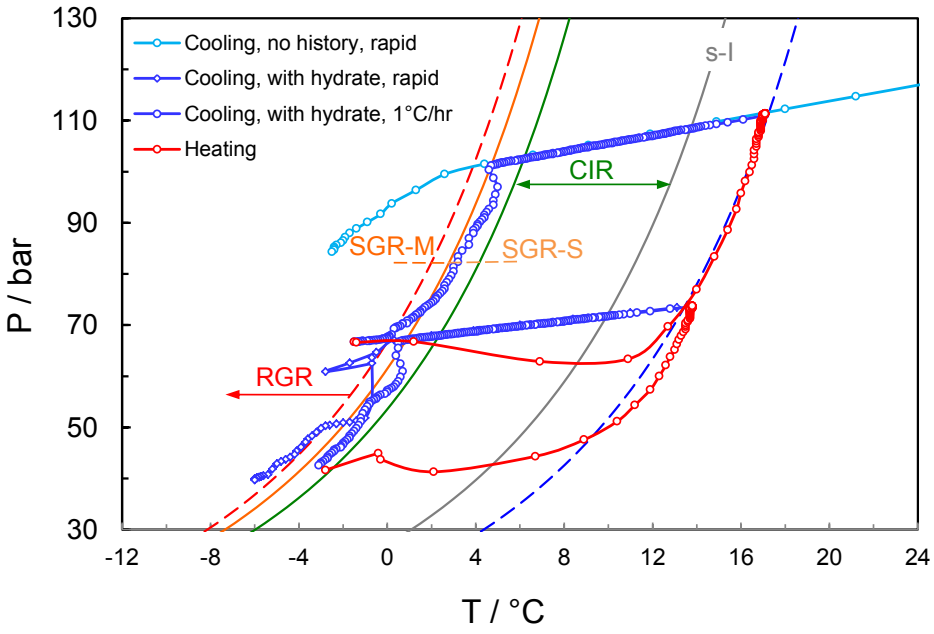

Figure 2.28 Example CGI method cooling and heating curves for 0.5 mass% PVCap aqueous / 99.5 mass % pH 3.0 acetic acid solution (0.35 mass% acetic acid) with methane.

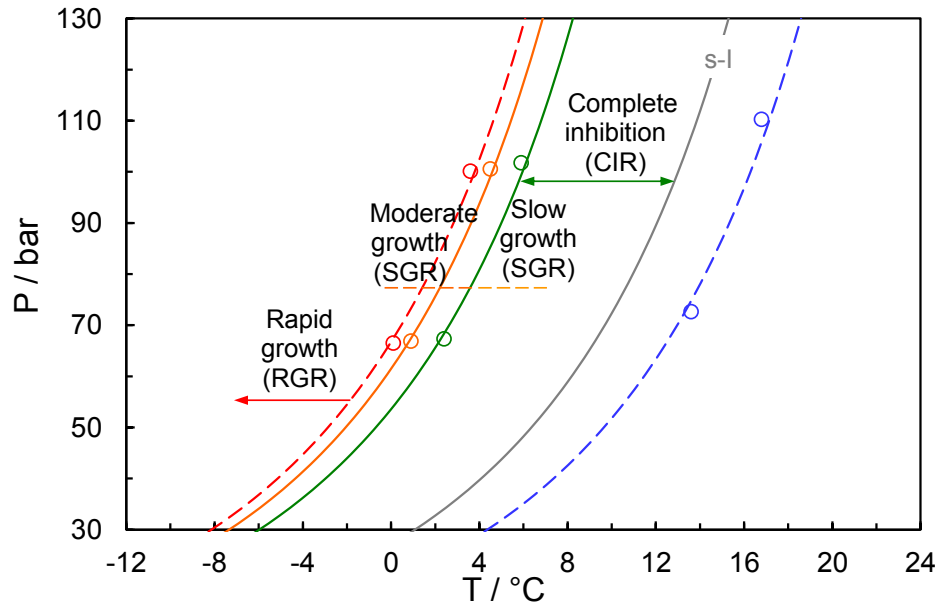

Figure 2.29 Experimental methane hydrate CGI region data for 0.5 mass% PVCap aqueous / 99.5 mass % pH 3.0 acetic acid solution (0.35 mass% acetic acid).

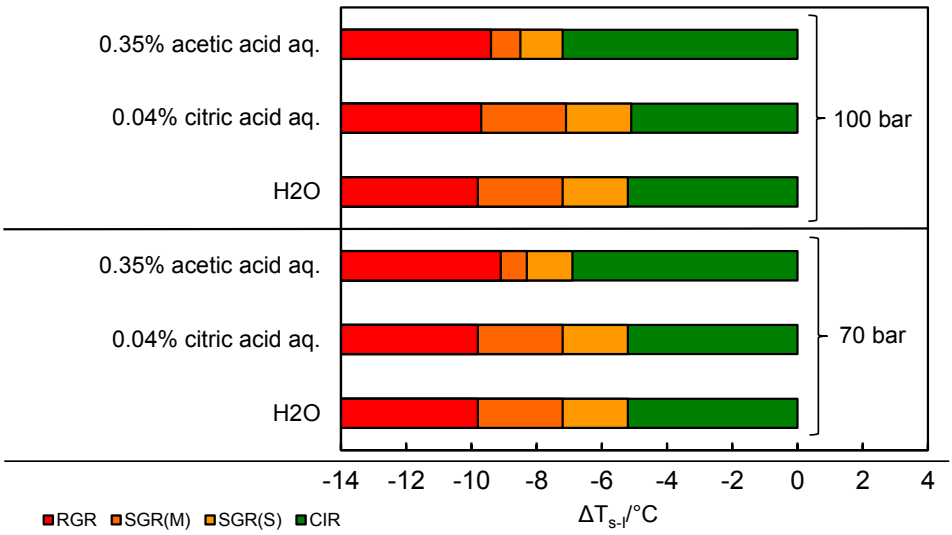

Figure 2.30 Comparison of subcooling extents of CGI regions from the s-I boundary for 0.5 mass% aqueous PVCap with deionised water and with 0.04 mass % citric acid and 0.35 mass % acetic acid, tests with methane. CH_4-H_2O data from Mozaffar (2013).

As mentioned above, for citric acid experiments, there was some evidence that growth rates were slightly slower in the SGR(S) region and therefore a slight positive effect on PVCap performance could be seen. In the case of acetic acid, however the positive effect clearly can be observed at least in terms of CIR and SGR-VS. Even though pH is the same as the previous citric acid test (pH = 3.0), both CIR and SGR-S regions are increased to -7.1 and -8.4°C respectively, but there is a slight reduction in total inhibition extent.

In a similar case to citric acid, it was observed that at higher acetic acid concentrations / pH, polymer drop-out occurred (cloud point ~7.2 mass% acetic acid at a pH of ~2.3).

Hydrochloric acid and methane

For the two tested systems, results do suggest that pH may not be a major factor in KHI performance, and even can have some positive effect. To provide further evidence for this theory, tests were carried out with hydrochloric acid at the same pH. A hydrochloric acid solution of 0.0037 mass% was prepared to give a moderately acidic pH of 3.0. The pH of the solution was checked with a VWR pH110 pH meter calibrated using manufacturer-supplied buffer solutions.

Determined points on CGI region boundaries for 0.5 mass% PVCap with 0.0037 mass% hydrochloric acid (relative to water) – giving a pH of 3.0 - in a methane system are

reported in Table 2.14 and presented with interpolated boundaries in Figure 2.31. Figure 2.32 shows a comparison of subcooling extents of CGI regions (from the s-I boundary) for 0.5 mass% aqueous PVCap with deionised water and with 0.04 mass % citric acid, 0.35 mass % acetic acid and 0.0037 mass % hydrochloric acid all tested with methane and all at pH 3.0.

Table 2.14 Experimental methane hydrate CGI region data for 0.5 mass% PVCap aqueous / 99.5 mass % pH 3.0 hydrochloric acid solution (0.0037 mass% hydrochloric acid relative to water).

CGR boundary	Growth rate	T / °C (± 0.5)	P / bar (± 0.2)	ΔT_{s-I} / °C (± 0.5)
SDR	Slow dissociation	12.3	67.1	3.0
CIR-SGR(VS)	No growth	4.1	62.2	-4.5
SGR(VS-S)	Very slow	4.0	62.7	-4.6
SGR(S-M)	slow	-1.1	58.1	-9.0
SGR(M)-RGR	Moderate	-1.4	60.6	-9.7

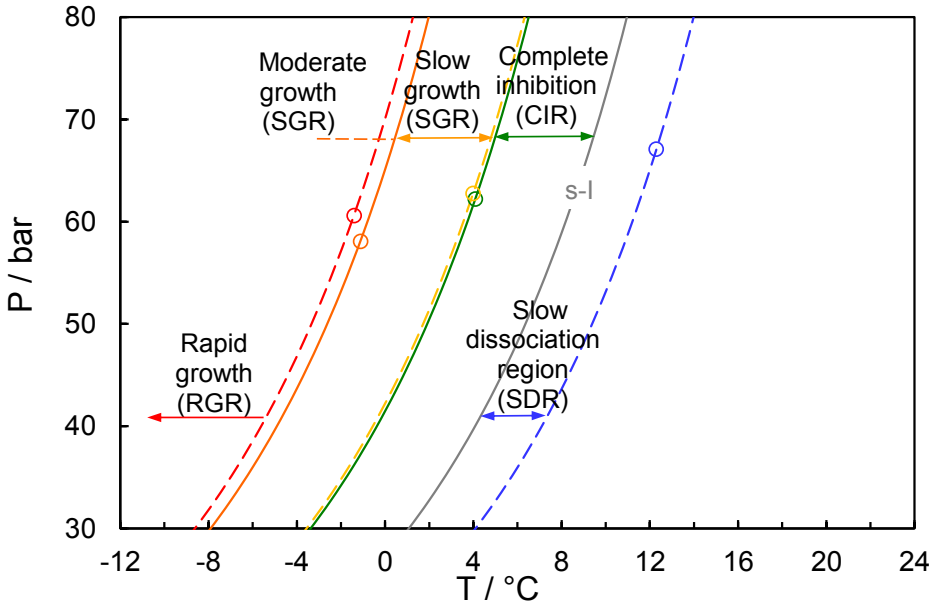

Figure 2.31 Experimental methane hydrate CGI region data for 0.5 mass% PVCap aqueous / 99.5 mass % pH 3.0 hydrochloric acid solution (0.0037 mass% hydrochloric acid).

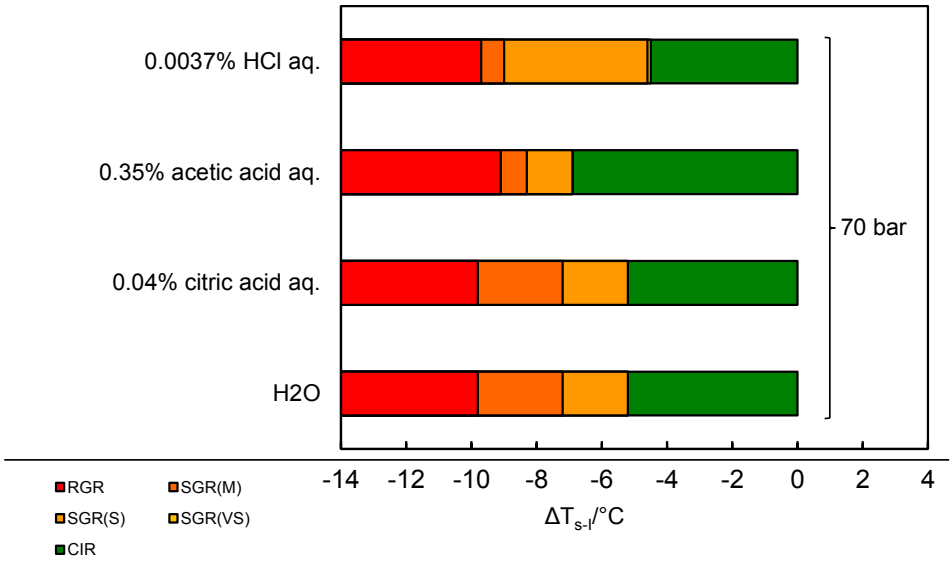

Figure 2.32 Comparison of subcooling extents of CGI regions from the s-I boundary for 0.5 mass% aqueous PVCap with deionised water and with 0.04 mass % citric acid, 0.35 mass % acetic acid and 0.0037 mass % hydrochloric acid tests with methane. CH_4-H_2O data from Mozaffar (2013).

Similar to what was observed for the two previous acids, hydrochloric acid at the pH of 3.0 does not show a significant effect on PVCap-methane CGI behaviour. There is a slight reduction in CIR extent which is -4.6°C comparing to -5.2°C PVCap in deionized water. Despite this slight negative effect on CIR, SGR-S region extent is increased to -9.0°C, while introducing a very narrow SGR-VS region. The Rapid Growth Region is however preserved at ~-9.7°C.

2.4 Conclusions

As discussed earlier, guest gas composition and presumably cage occupancy patterns play an important role in KHI performance, the specific mechanisms of this however is unclear. In light of this to further understand the underlying mechanism, the newly developed CGI method was utilised to assess this effect particularly when acid and sour gases are present in the system.

Results suggest that CO_2 plays a very important role in PVCap performance, in particular with respect to the common changes in PVCap performance seen from lower (< 70 bar) to higher (>100 bar) pressures. However, while CO_2 is commonly associated with a negative effect, this is not ubiquitous across all gas systems at all pressures. Rather, the effect depends on the CO_2 concentration and other gas components in the

system; speculatively this influencing cage occupancy patterns and thus the strength of adsorption on hydrate crystal surfaces.

CGI studies on a 91.5 mole% methane / 4.9 mole% ethane / 2.0 mole% propane / 1.6 mole% CO_2 gas mixture with 0.5 mass% PVCap aqueous confirm that the addition of CO_2 to the C_1-C_2-C_3 (Mozaffar, 2013) mixture causes a significant improvement in PVCap induced crystal growth inhibition, notably at higher pressures (>100 bar), however it also introduces the pattern of reduced (relatively, compared to higher pressures) CGI extents/PVCap performance at lower pressures, supporting the theory that CO_2 is likely responsible for this in natural gas systems. However, overall the performance of PVCap is better in this mixture than for a real natural gas (Mozaffar, 2013), suggesting that while CO_2 is responsible for reduced PVCap performance in NGs at low pressure, it is not the sole cause of this.

Addition of more CO_2 to the natural gas composition - to see the effect of higher concentration - with 0.5 mass% PVCap aqueous reveals that at 12 mol% CO_2, PVCap performance is better at lower pressures compared to higher pressures; the opposite case for when CO_2 is modest (1.6 mole%) and likewise in contrast to tests for 85% CH_4 / 15% CO_2, where the effect of high CO_2 was to significantly reduce PVCap performance at lower pressures (Mozaffar, 2013). However, the presence of 12 mol% CO_2 does reduce the overall total extents of CGI regions compared to 1.6% CO_2, supporting a generally negative effect.

The data for 10 mol% CO_2 contrasts that for 15 mol% CO_2 which found the opposite, suggesting a reversal in effect between 10 and 15 mol%. For 10 mol% CO_2 with methane, a similar trend to H_2S is observed as the extent of regions decrease by pressure. Overall CO_2 is less negative, with PVCap performance more comparable to simple methane systems and even a slight improvement at lower pressures.

Based on CGI studies of PVCap in 5 and 10 mol% H_2S / 90 mol% CH_4 system, studies of CO_2-CH_4 and other binary to multicomponent systems (Mozaffar, 2013), H_2S appears to have a markedly negative effect on PVCap performance, most notably as pressure increases past ~80 bar, although above this pressure CGI regions appear to stop reducing / performance becomes constant. This agrees with the similar CO_2-CH_4 system and contrasts the effect of higher 15 mol% CO_2 with methane where performance improves with increasing pressure.

PVCap performance for the 5 mol% H_2S / 5 mol% CO_2 / 90 mol% CH_4 mixture somewhat mirrored results for H_2S-CH_4 and CO_2-CH_4 (10 mol%) in that CGI regions were particularly extensive at low pressures (CIR 9 °C subcooling or greater), but likewise considerably reduced at higher pressures (> 70 bar).

Initial modelling studies (Anderson, 2013, 2014) in combination with experimental results offer some indications – speculatively – of what may lie behind this contrasting behaviour and could help explain patterns seen in natural gas systems. In the case of H_2S containing systems, H_2S may act to stabilise hydrates at lower pressures, thus stabilising hydrate-polymer complexes and so improving PVCap performance. At higher pressures though, this effect is lost as methane begins to dominate cages, while at the same time increasing H_2S in the aqueous phase may be responsible for the reduced performance presumably due to increasing acidity (causing polymer conformational changes and or coagulation) and/or by increasing propensity for hydrate formation from dissolved gas, which PVCap may be less able to prevent. However modelling studies of gas solubility in the presence of hydrate vs subcooling and pressure (Anderson, 2013, 2014) (and immiscible KHI results in Chapter 5) do not show clear support for hydrate formation from dissolved gas being a problem for KHIs. Likewise, studies on the effect of pH do not suggest that acidity, at least moderate acidity (pH 3.0), has a negative effect. Thus, speculatively, with acidity and hydrate formation from dissolved gas looking not to be major factors, this would leave cage occupancy patterns - and presumably how that affects the strength of polymer adsorption on hydrate crystal surfaces / stability of polymer-hydrate complexes – as the most likely factor controlling PVCap performance in terms of CGI. A similar case may apply for CO_2 at lower concentrations (e.g. 10 mol%), although the origins of the reversal of the effect on performance vs pressure at higher (15 mol% CO_2) remains unclear. However, in higher concentration of 15 mol% a significant reduction in total hydrate cage occupancy – notably for the 5^{12} cage – causing a reduction in polymer-hydrate complex stability and thus PVCap performance at pressures below 100 bar may explain observed patterns.

Results of CGI region studies on 0.5 mass% PVCap in a methane system with 0.04 mass% citric acid, 0.35 mass% acetic acid and / pH 3.0 aqueous undertaken show that:

- A moderately acidic pH of 3.0 appears to have no effect on KHI performance

- There is a slight positive pH effect with growth rates reduced a little in the SGR(S) region and the extent of this region increased in some cases
- A positive effect might be related to more acidic pH making PVCap miscibility in water more tenuous, thus crystal surface adsorption more favoured

For the tested systems, results do suggest that pH may not be a major factor in KHI performance.

CHAPTER 3 – HYBRID HYDRATE INHIBITION; EFFECT OF THERMODYNAMIC HYDRATE INHIBITORS ON KHI PERFORMANCE

3.1 Introduction

Methanol, ethanol and mono ethylene glycol (MEG) are the most widespread used Thermodynamic Hydrate Inhibitors (THIs) and an extensive amount of research has been conducted on their effect on the hydrate phase boundary. They work by shifting the hydrate phase boundary to lower temperatures and keep the system out of hydrate stability zone. While thermodynamic inhibitors can be very effective under certain conditions, using them to treat the systems with high subcooling and/or water cut can be quite expensive as the required effective dosage will be very high (10 to 60 mass% of water phase). MEG is usually recovered downstream and recycled while methanol is not and causes some environmental problems. Methanol also accelerates equipment and pipeline corrosion due to acidic impurities and dissolved oxygen and increases the chance of scale problems by lowering solubility of salts in water (Budd et al., 2004).

Laboratory studies and field experiences have shown synergy could be achieved through the combination of Kinetic Hydrate Inhibitors (KHIs) and THIs which is termed as Hybrid Hydrate Inhibition (HHI) (Budd et al., 2004; Szymczak et al., 2006; Allenson and Scott, 2010; Pakulski, 2011; Cha et al., 2013). Thermodynamic inhibitors like MEG and methanol are known to be used as KHI solvents and having various degrees of synergistic effect on their performances. As mentioned above THIs are usually used at concentration ranges from 10 to 60 mass% of water phase while KHIs normal concentrations are less than 5 vol%. So that replacing some of the high required volume of thermodynamic inhibitor by kinetic hydrate inhibitor and achieving an optimised concentration of each will result in much lower injection rates while controlling hydrate formation. This will lead to a significant cost reduction for gas companies.

Although there is some evidence of positive effect for THIs and KHIs combination – as mentioned above – Sloan et al. (1998) showed that methanol appears to have a negative effect on PVCap subcooling and this negative effect was more significant for lower molecular weight PVCap. They concluded that increasing methanol concentration from

0 to 15 mass% in presence of 0.5 wt% PVCap will decrease its subcooling in linear proportion to methanol concentration (Sloan et al., 1998).

A systematic laboratory study by Bud et al. (2004) showed a possible synergistic effect between methanol and LDHI. They found a certain LDHI to methanol ratio in which a strong synergistic effect between methanol and a low molecular weight oligomer type hydrate inhibitor was observed. They tested LDHI/methanol ratios from 0 to 30 mass% and recorded the beginning of hydrate formation time and 5% gas to hydrate conversion time; which was considered as failure. Results showed that by increasing the amount of LDHI in the formulation, the time difference between the beginning of hydrate formation and 5% gas conversion increased. With a larger portion of LDHI present in the system, hydrate may form earlier but it is very slow; while in a methanol only system hydrate formation after onset will be catastrophic. Field results for the discovered LDHI/methanol ratio also showed up to 80% reduction in inhibitor dosage comparing to the original methanol dosage (Budd et al., 2004). In a similar test procedure, Pakulski (2011) explained a series of tests on several mixtures of polymeric and non-polymeric KHIs and THIs to find the best performing combination of hydrate inhibitors. The work resulted in the discovery of a few KHI/KHI/THI combinations that outperformed any previously used product (Pakulski, 2011).

In a field study in the Gulf of Mexico, Szymczak et al. (2006) applied a hybrid hydrate inhibition (HHI) technology to reduce the cost. The field operator was initially using approximately 120 gal/day of methanol to ensure hydrate inhibition. In this study, some of the required methanol was replaced with low dosage hydrate inhibitor (LDHI) and the pressure difference between wellhead pressure (chemical injection line) and the flow line pressure at the platform was tracked. This differential pressure could be a measure of the flow resistance offered by hydrates in the line. While using methanol as hydrate inhibitor, differential pressure varied typically between 150 to 250 psi. After changing the inhibition strategy to an HHI approach, they were able to reduce the pressure drop to 50 psi while decreasing inhibitor injection to only 16 gal /day (Szymczak et al., 2006).

There are some limited research works on the combination of KHIs and MEG as thermodynamic hydrate inhibitors. In some laboratory evaluations, the effect of different MEG concentrations and VC-713 as KHI polymer on natural gas system hydrate formation was tested by Wu et al. (2007). Although the results of field application showed that V-713 had better efficiency and good application prospect but

they concluded that in practice combination of kinetic and thermodynamic hydrate inhibitors is better (Wu et al., 2007).

In another work, Allenson and Scott (2010) worked on deployment of KHI within a MEG stream and optimization of a combination of MEG/KHI when applied to an offshore gas/condensate field in the Mediterranean Sea. During the trial they were able to reduce the MEG rate by 70% by adding some KHI to the system therefore reducing footprint/capacity of handling/storage and recovery systems (Allenson and Scott, 2010).

Kinetic inhibition performance of MEG has been investigated and proven at least a concentration of 30 wt% by Cha et al. (2013). Kinetic hydrate inhibitors such as PVP and PVCap delay hydrate onset, therefore it might be possible to obtain synergistic kinetic inhibition by mixing both MEG and KHI in the aqueous phase. In light of this, Cha et al. (2013) carried out more experiments to measure the induction time of 30 mass% MEG and 1 mass% PVP aqueous solution with a synthetic natural gas. They suggested that, this combination further delayed induction time and they presumed that PVP increases the energy barrier for hydrate nucleation and incurs a synergistic inhibition effect with MEG. Their study suggests that it is feasible to incorporate the kinetic inhibition performance of MEG into current hydrate inhibition strategies which will be able to save the operational expenditure of MEG injection by reducing MEG requirement (Cha et al., 2013).

Methane hydrate crystal growth patterns in the presence of different concentrations of methanol, ethanol and MEG (2.5 to 50 mass %) were investigated by Mozaffar et al. (2014). They used the Crystal Growth Inhibition (CGI) technique for KHI evaluation (Anderson et al., 2011). They concluded that methanol overall had a detrimental effect on the subcooling extent of all CGI regions at all concentrations tested compared to aqueous PVCap alone for methane as hydrate former. Ethanol also showed a negative effect on PVCap performance for all tested concentrations, although was less negative than methanol. Based on the results of this work, in contrast to methanol and ethanol, MEG generally has a positive synergistic effect on PVCap for the concentrations tested (Mozaffar et al., 2014). They showed that MEG enhances PVCap performance by reducing hydrate growth rates, extending the slow growth region, and acts as a full ‘top-up’ inhibitor, meaning the combination of MEG + PVCap offers far better inhibition by mass/volume inhibitor than MEG alone, at least up to 50 mass% MEG (Mozaffar et al., 2014).

As mentioned above, laboratory studies and field experiences have shown good synergy through the combination of Kinetic hydrate inhibitors (KHIs) and THIs in some multi-component hydrate forming systems; but Crystal Growth Inhibition (CGI) experiments revealed the negative effect of methanol and ethanol on PVCap performance in the presence of methane as hydrate former (Mozaffar et al., 2014). Therefore, to better understand the impact of thermodynamic inhibitors on KHIs, in this work the CGI behaviour of different THIs with different concentrations in combination with KHI polymers are investigated in a multi component gas system.

All experiments were carried out in high pressure stirred autoclaves using the new CGI method, as described in chapter 2 of this thesis. All experiments were carried out with 0.5 mass % PVCap and 0.5 mass% active polymer of T1441. The PVCap used was Luvicap-EG base polymer (K-value = 25-8, average MW = 7000) supplied by BASF, with the ethylene glycol solvent removed by vacuum oven drying. T1441 is commercial KHI containing a co-polymer dissolved in water and was supplied by Champion Technologies. The specific structure of this co-polymer is unknown but it is known that T1441 is 50 mass% active polymer in water so a concentration of 1 mass% total KHI was used in all experiments to reach 0.5 mass% active polymer in the system. The biodegradable KHI used in this work was Bio-800 (30 mass% active ingredient in water) supplied in ethylene glycol butyl ether (EGBE / 2-butoxyethanol) from Ashland (provided by Champion Technologies). The concentration of KHI solution used was 1.67 mass% in water to get 0.5 mass% Bio-800 in total. The purities of the methanol and ethanol used were 99.9% and 99.5 % , which were supplied by Fisher Scientific. The purity of MEG used was 99.5% supplied by Fluka Analytical. Distilled water was used in all tests. The composition of the gas mixture used in tests is given in Table 3.1 and this was supplied by BOC. This gas composition was used to simulate a typical North Sea natural gas. The composition of the North Sea natural gas used for a PVCap only system in another work (Mozaffar, 2013) is also given for comparison.

Table 3.1 Composition of natural gases used in CGI experiments on PVCap alone and PVCap or T1441 with Methanol/Ethanol/MEG.

Component	Mole%	
	PVCap	PVCap/T1441-Methanol/Ethanol/MEG
Methane	89.41	87.93
Ethane	5.08	6.00
Propane	1.45	2.04
i-Butane	0.18	0.20
n-Butane	0.26	0.30
i-Pentane	0.06	-
CO_2	1.55	2.03
Nitrogen	1.93	1.50
n-Pentane	0.06	-
n-Hexane	0.02	-

3.2 Results and Discussions

Research shows that although methanol is a good thermodynamic inhibitor, by increasing its concentration the rate and amount of hydrate formation will clearly increase, when the system is under-inhibited (Yousif, 1998). Other research also showed that methanol generally does not act as a synergist for PVCap in a methane system (Mozaffar et al., 2014). On the other hand, some studies and field trials confirm a synergistic effect of methanol in the presence of LDHIs (Budd et al., 2004; Szymczak et al., 2006). Based on this, it is essential to better understand methanol behaviour in combination with KHIs, especially in multi-component gas systems, which are close to the real field condition. Therefore, this chapter presents various experimental results for a range of methanol concentration (2.5 to 25 mass%) in a multi-component system to evaluate the synergistic effect of methanol on PVCap as a well-known KHI base polymer and one other commercial polymer to see if there is a synergistic effect and to what extent it is applicable.

Ethanol is another thermodynamic hydrate inhibitor that could potentially be used in combination with KHIs to increase their subcooling extent. Despite having thermodynamic hydrate inhibition effect, experimental phase equilibrium and compositional data provide evidence for the formation of binary ethanol-methane clathrate hydrates at ambient temperatures and elevated pressures (Anderson et al., 2009). Hence, the fact that ethanol can enter the hydrate structure may affect its

behaviour in a system with KHI polymer present. In light of this, a series of experiments have been reported in this chapter for different ethanol concentrations with PVCap and one commercial KHI to fundamentally understand its effect on KHI inhibition performance.

Mono ethylene glycol (MEG) is the most common thermodynamic inhibitor, which is also used as carrier solvent for some KHI polymers. Previous studies using the CGI method have shown a synergistic effect of MEG on PVCap performance in a single component methane system (Mozaffar et al., 2014) but whether this could be extended to the multi-component system and does the behaviour follow a similar pattern for different MEG concentrations is investigated in this chapter. PVCap, a commercial KHI as well as a Bio KHI were used to observe the effect. The possibility of forming top of line hydrate in presence of MEG was also looked at.

3.2.1 Methanol / KHI combination CGI behaviour

Effect of Methanol on PVCap

Enhancement or diminution of PVCap performance at concentration of 0.5 mass% was investigated by adding 2.5, 5.0 and 25.0 mass% of methanol (relative to water + PVCap) to the aqueous phase using natural gas as hydrate former. Investigations were normally carried out at a range of pressure between 60 and 140 bar using the CGI method. CGI regions data points for all three methanol concentrations and subcooling extents from both structures I and II hydrate phase boundaries are reported in Tables 3.2, 3.3 and 3.4.

Table 3.2 Experimental natural gas hydrate CGI region data for 0.5 mass% PVCap aqueous (relative to water) with 2.5 mass % methanol (relative to water + PVCap).

CGR boundary	Growth rate	T / °C (± 0.5)	P / bar (± 0.2)	ΔT_{s-I} / °C (± 0.5)	ΔT_{s-II} / °C (± 0.5)
CIR-SGR(S)	No growth	4.1	66.7	-6.1	-11.3
		7.1	100.7	-6.3	-10.9
		8.9	130.8	-6.4	-10.5
SGR(S-M)	Slow	2.5	65.4	-7.5	-12.8
		5.0	98.5	-8.3	-12.9
		6.3	126.7	-8.7	-12.9
SGR(M)-RGR	Moderate	0.8	64.6	-9.1	-14.5
		3.7	98.2	-9.5	-14.1
		5.5	126.1	-9.5	-13.7

Table 3.3 Experimental natural gas hydrate CGI region data for 0.5 mass% PVCap aqueous (relative to water) with 5.0 mass % methanol (relative to water + PVCap).

CGR boundary	Growth rate	T / °C (± 0.5)	P / bar (± 0.2)	ΔT_{s-I} / °C (± 0.5)	ΔT_{s-II} / °C (± 0.5)
CIR-SGR(S)	No growth	3.2	66.3	-6.0	-11.1
		6.0	98.3	-6.3	-10.7
		8.1	129.3	-6.2	-10.1
SGR(S-M)	Slow	1.3	64.5	-7.7	-12.8
		3.9	96.0	-8.2	-12.7
		5.4	126.5	-8.8	-12.7
SGR(M)-RGR	Moderate	-0.4	65.7	-9.5	-14.6
		2.3	95.7	-9.8	-14.2
		4.2	124.6	-9.8	-13.8

Table 3.4 Experimental natural gas hydrate CGI region data for 0.5 mass% PVCap aqueous (relative to water) with 25.0 mass % methanol (relative to water + PVCap).

CGR boundary	Growth rate	T / °C (± 0.5)	P / bar (± 0.2)	ΔT_{s-I} / °C (± 0.5)	ΔT_{s-II} / °C (± 0.5)
CIR-SGR(S)	No growth	-5.2	60.4	-3.8	-9.4
		-1.8	94.3	-3.6	-8.5
		0.1	119.3	-3.2	-7.7
SGR(S-M)	Slow	-6.6	60.8	-5.2	-10.8
		-4.7	91.4	-6.2	-11.2
		-2.8	115.1	-5.9	-10.4
SGR(M)-RGR	Moderate	-8.4	60.9	-7.0	-12.6
		-5.7	89.9	-7.1	-12.1
		-3.9	113.6	-6.9	-11.4

Example cooling curves along with experimentally determined CGI regions for 2.5 and 5.0 mass % methanol and 0.5 mass % PVCap are presented in Figures 3.1 and 3.2. Figure 3.3 also shows experimentally determined CGI regions for 25.0 mass% methanol. Cooling runs were repeated several times to be sure of the repeatability.

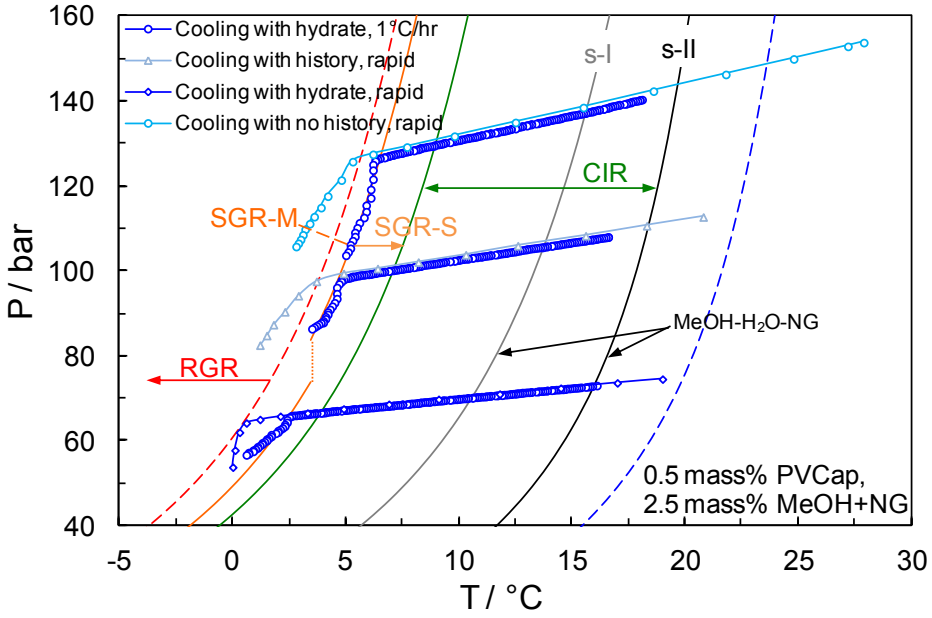

Figure 3.1 Example CGI method cooling curves and experimentally determined CGI regions for 0.5 mass% PVCap / 2.5 mass % methanol aqueous with natural gas.

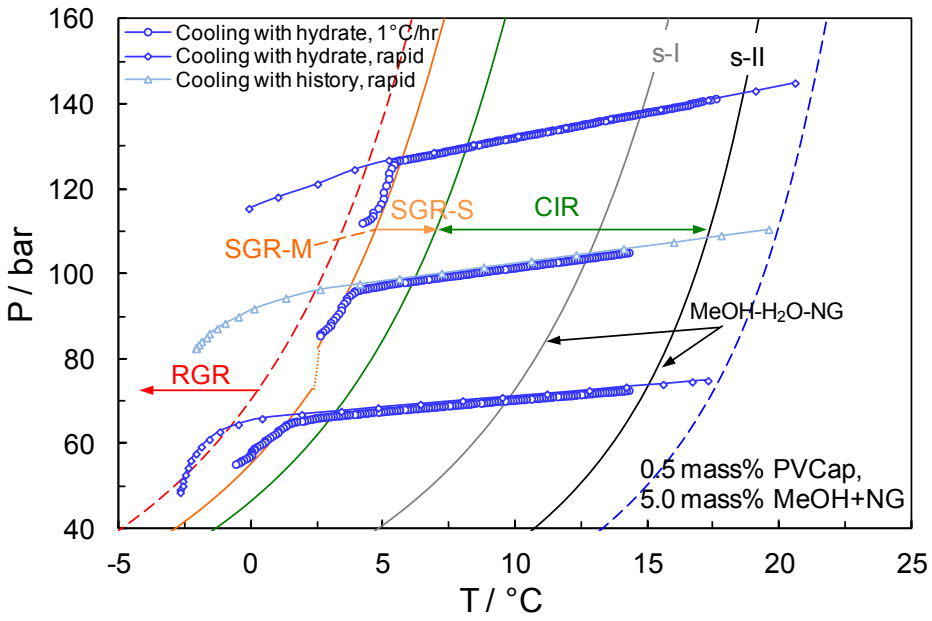

Figure 3.2 Example CGI method cooling curves and experimentally determined CGI regions for 0.5 mass% PVCap / 5.0 mass % methanol aqueous with natural gas.

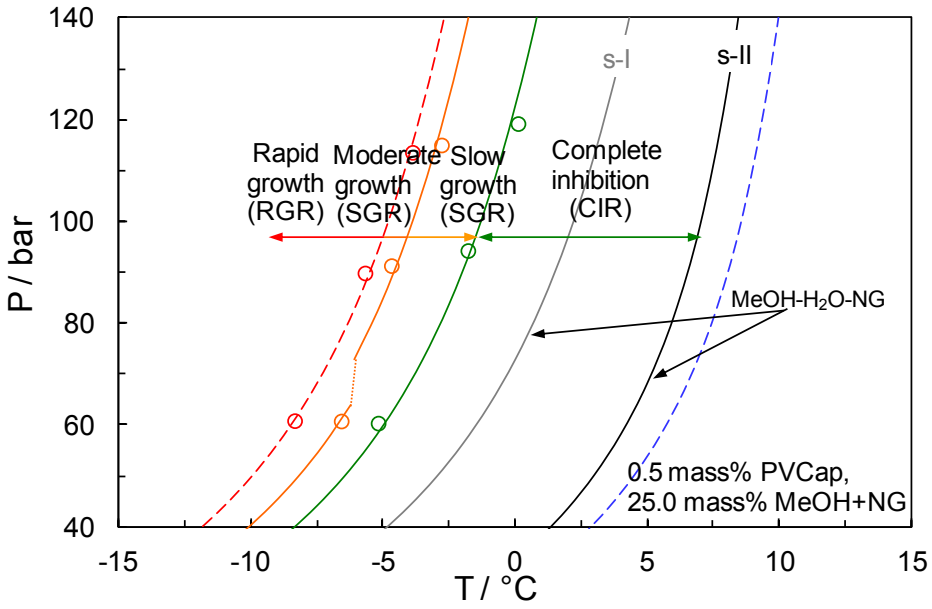

Figure 3.3 Experimental natural gas hydrate CGI region data for 0.5 mass% PVCap aqueous with 25 mass % methanol (relative to water + PVCap) showing CGI regions determined from changes in relative hydrate growth rates.

As noted, it was previously concluded that 2.5 mass% to 50 mass% methanol have an overall negative effect on PVCap performance in s-I forming methane systems (Mozaffar et al., 2014). In contrast, results for tests on 0.5 mass% PVCap and 2.5 and 5.0 mass% methanol with natural gas do not show a negative effect, with methanol instead showing a moderate positive effect and acting as a top-up inhibitor for PVCap for the concentrations tested. In the presence of 2.5 mass% methanol, complete inhibition region (CIR) is increased to ΔT_{sub}=−6.1°C from the structure I phase boundary at lower pressures (~70 bar), comparing −5.2 °C for the PVCap-water system. The same improvement in CIR can also be observed for 5.0 mass% methanol which increases to −6.0°C. For the two higher pressures tested however, the extent of CIR is almost the same as PVCap-water alone with a natural gas system (Mozaffar, 2013).

Similarly, the slow growth region (SGR) increased to $\Delta T_{s\text{-}I}$ =−8.2 °C with the RGR preserved at −9.4 °C for 2.5 mass % methanol (Figure 3.4). However, while the top-up effect is clear, the additional positive effect observed compared to the NG system with no methanol could potentially be in part related to NGs being of slightly different composition (Table 3.1). For the higher methanol concentration of 25.0 mass%, in agreement with data for methane systems, a consistently negative effect on the performance of PVCap is observed; the extent of CGI region subcoolings are

considerably reduced at 25.0 mass %. For example, the PVCap induced CIR decreased to $\Delta T_{s\text{-}I} \approx -3.5$ °C compared to −5.2 °C for PVCap with natural gas and distilled water. Similarly, the SGR decreased to $\Delta T_{s\text{-}I} \approx -5.2$ °C at lower pressures (~ 70 bar) with the RGR boundary reduced to ~7.0 °C subcooling from the s-I boundary (Figure 3.4). Certainly, the reduction in the extent of the SGR region observed for the three methanol concentrations tested at lower pressure (~ 70 bar) is consistent with other natural gas systems and is likely related to the effect of CO_2; highlighting the apparent importance of guest gas/cage occupancy patterns to polymer performance.

Figures 3.4 and 3.5 show average PVCap induced CGI regions and total hydrate inhibition offered by the combination of PVCap-methanol for the natural gas as a function of methanol concentration.

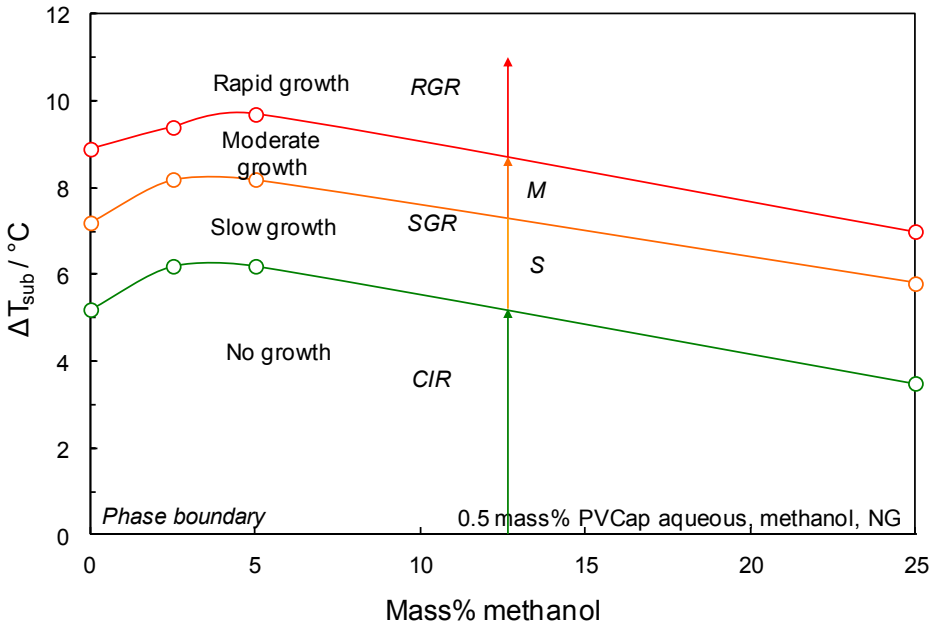

Figure 3.4 Average (60 to 150 bar) PVCap induced CGI regions for 0.5 mass% PVCap aqueous in the natural gas system as a function of methanol mass% (relative to water + PVCap) from s-I phase boundary. 0.5 mass% PVCap-NG data from Mozaffar (2013).

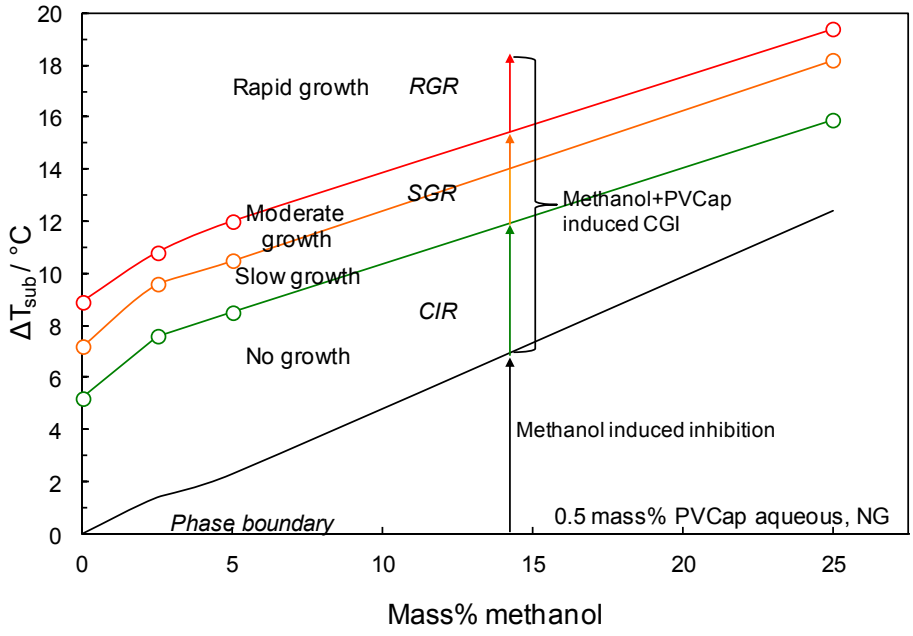

Figure 3.5 Total hydrate inhibition offered by 0.5 mass% PVCap aqueous + Methanol at different concentrations (relative to water + PVCap) in the natural gas system; subcoolings are calculated from s-I phase boundary. 0.5 mass% PVCap-NG data from Mozaffar (2013).

Comparison of the data from 0.5 mass% PVCap in a multi-component natural gas system (Mozaffar, 2013) with the same concentration of PVCap in the presence of 2.5 and 5.0 mass% methanol in a natural gas system shows a general improvement in PVCap performance in terms of CGI behaviour for these two concentrations of methanol.

By increasing methanol concentration up to 5.0 mass% there is an increase in all CGI regions, as illustrated in Figure 3.4; a peak can be distinguished in the PVCap performance at 5.0 mass% methanol which was also the case for PVCap-methanol-methane system in terms of the slow growth region (Mozaffar et al., 2014). Bud et al. (Bud et al., 2004) have also reported a performance peak at certain LDHI/MeOH ratio for their case of a multicomponent field gas. Beyond 5.0 mass% however, CGI regions reduce again to levels lower than PVCap alone by increasing methanol content to 25.0 mass%.

Although by increasing methanol concentration to 25.0 mass% PVCap performance is decreasing, the combination of PVCap-methanol still offers better inhibition than methanol alone. From Figure 3.5 it is clear that 0.5 mass% PVCap along with 25.0 mass% methanol can completely inhibit hydrate formation and growth up to subcooling

of 15.9°C compared to 12.4 °C for 25.0 mass% methanol without any PVCap. To achieve an inhibition equivalent to 25.0 mass% methanol, a hybrid inhibitor containing 0.5 mass% PVCap and ~15.0 mass% would be sufficient.

In terms of understanding the effect of methanol on KHI performance, the finding that the effect is very different in s-I forming methane systems compared to s-II/s-I forming multicomponent gases is significant in that it strongly suggests methanol involvement in hydrate growth/nucleation, e.g. potentially though temporary cage occupation. The reasoning for this is that if the effect of methanol was confined to interactions in the liquid (or gaseous phases) alone, then intuitively negative or positive effects might be expected to be largely independent of gas composition. Certainly, methanol has a molecular diameter sufficiently small to enter gas hydrate cavities and can participate in hydrate formation as a guest at cryogenic temperatures (Shin et al., 2013).

Effect of Methanol on T1441

Previous studies have shown different polymers can act very differently in terms of hydrate inhibition (Larsen et al., 1998; Larsen et al., 1999; Habetinova et.al, 2002). Investigation of the effect of another polymer type on hydrate CGI behaviour can produce consistent information to see whether this is the case in presence of alcohols. CGI regions have been determined for 0.5 mass% T1441 active polymer supplied by Champion Technologies with 5.0 and 25.0 mass % methanol aqueous and a standard natural gas; the aim being to see if the effect of methanol on KHI performance is similar for different polymer types.

Example CGI method cooling/heating curves and interpolated boundaries for 0.5 mass% T1441 / 5.0 and 25.0 mass % methanol aqueous with natural gas are shown in Figures 3.6 and 3.7. Determined points on CGI region boundaries are reported in Tables 3.5 and 3.6.

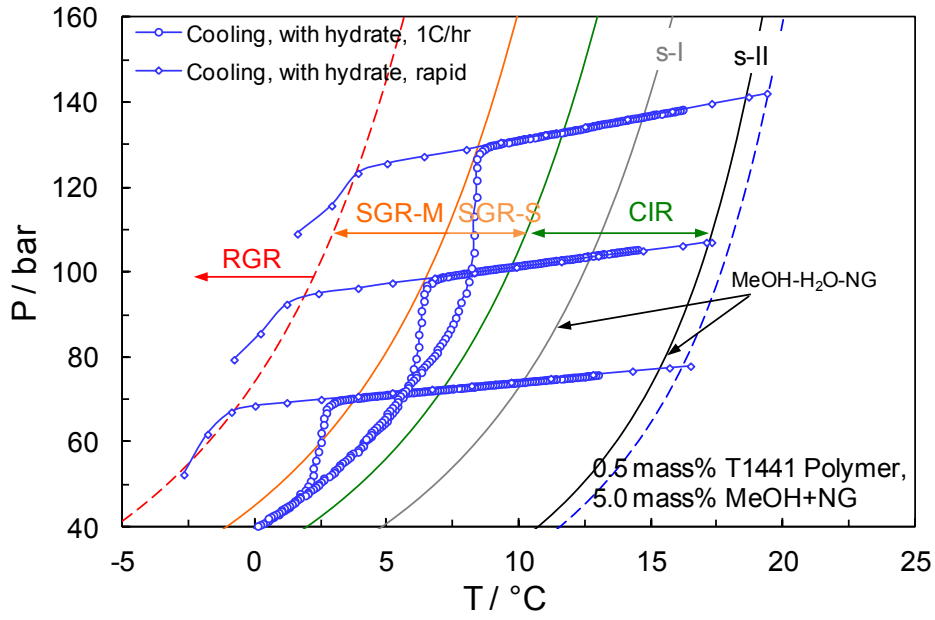

Figure 3.6 Example CGI method cooling curves and interpolated boundaries for 0.5 mass% T1441 / 5.0 mass % methanol aqueous with natural gas.

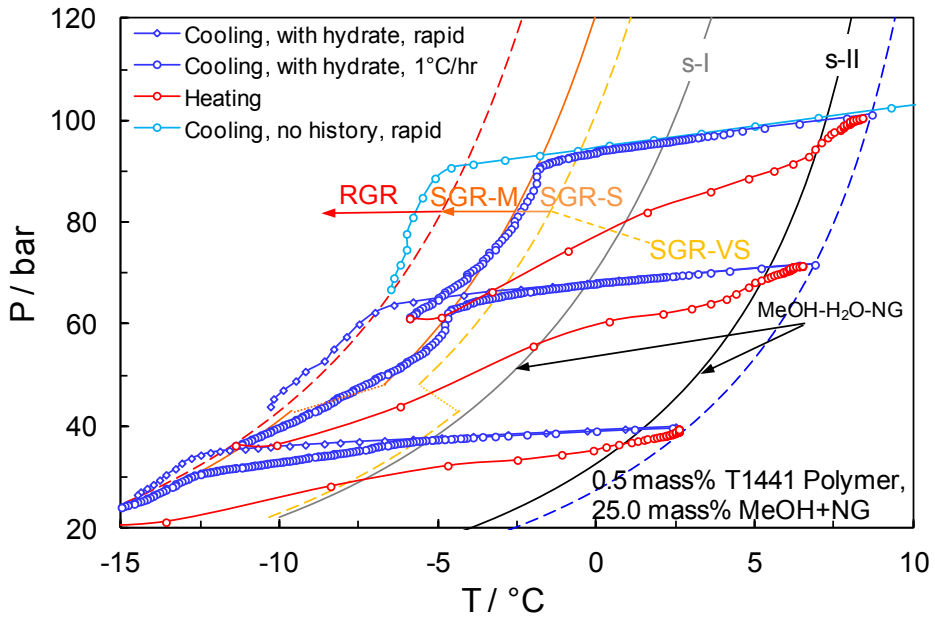

Figure 3.7 Example CGI method cooling/heating curves and interpolated boundaries for 0.5 mass% T1441 / 25.0 mass % methanol aqueous with natural gas.

Table 3.5 Experimental natural gas hydrate CGI region data for 0.5 mass% T1441 polymer aqueous (relative to water) with 5.0 mass % methanol (relative to water + T1441).

CGR boundary	Growth rate	T / °C (± 0.5)	P / bar (± 0.2)	ΔT_{s-I} / °C (± 0.5)	ΔT_{s-II} / °C (± 0.5)
CIR-SGR(S)	No growth	6.9	71.2	-2.9	-7.9
		9.6	100.3	-2.9	-7.2
		11.7	131.6	-2.7	-6.6
SGR(S-M)	Slow	3.2	69.5	-6.4	-11.4
		6.7	97.8	-5.6	-10.0
		8.7	129.4	-5.6	-9.5
SGR(M)-RGR	Moderate	-1.0	67.5	-10.4	-15.4
		1.7	94.5	-10.3	-14.8
		4.2	125.5	-9.9	-13.8

Table 3.6 Experimental natural gas hydrate CGI region data for 0.5 mass% T1441 polymer aqueous (relative to water) with 25.0 mass % methanol (relative to water + T1441).

CGR boundary	Growth rate	T / °C (± 0.5)	P / bar (± 0.2)	ΔTs-I / °C (± 0.5)	ΔTs-II / °C (± 0.5)
CIR-SGR(VS)	No growth	-4.3	37.1	-	-5.3
		0.4	67.7	-	-4.8
		2.2	94.5	-	-4.8
SGR(VS-S)	Very slow	-5.5	37.2	-0.3	-6.5
		-3.0	65.8	-2.4	-8.0
		-0.8	92.9	-2.7	-7.7
SGR(S-M)	Slow	-12.4	31.3	-5.6	-12.0
		-4.8	62.7	-3.9	-9.5
		-1.8	90.9	-3.6	-8.6
SGR(M)-RGR	Moderate	-12.0	35.2	-6.4	-12.6
		-6.5	64.6	-5.8	-11.4
		-4.1	90.7	-5.8	-10.9

As can be seen in Figures 3.6, crystal growth inhibition properties for 0.5 mass% T1441 and 5.0 mass % methanol can be observed up to a total subcooling of ~9.9 (150 bar) to ~10.4 °C (70 bar) from the s-I phase boundary, beyond which rapid failure was observed. The CIR remained relatively constant for the pressure range studied at $\Delta T_{s-I} \approx -2.8$ °C, following which an SGR(S) was extended between 5.6 and 6.4 °C subcooling from the s-I boundary. T1441 behaviour at this concentration of methanol is quite different from that observed for 0.5 mass% PVCap and the same level of methanol. In the latter case, the growth PT pattern tends to follow the SGR(M) boundary up to a modest concentration of hydrate present in the system. In contrast, in the case of 0.5

mass% T1441 once a small fraction of hydrate is formed, the growth rate increases up to a few mass% of hydrate (~1-2 mass%) where the growth pattern follows a boundary parallel to the SGR(M) boundary. A similar behaviour was evident for 0.5 mass% T1441 with natural gas (Data for 0.5 mass% T1441 and natural gas were generated as part of this work for comparison and are presented in Appendix A, Table A.1) and methane (Mozaffar, 2013).

It is clear that 5.0 mass% methanol has an overall negative effect on T1441 performance and the results for 25.0 mass% methanol support this negative effect showing all CGI regions are reduced compared to 5.0 mass% methanol and the complete inhibition region is totally lost. Similar to other natural gas systems, the negative effect is much more apparent at lower pressures (below ~60 bar) where only a narrow SGR-VS region could be distinguished.

Figure 3.8 shows a comparison of subcooling extents of CGI regions (from the s-I boundary) for 0.5 mass% aqueous PVCap and T1441 alone and with 5.0/25.0 mass % methanol, all tested with natural gases for different pressures.

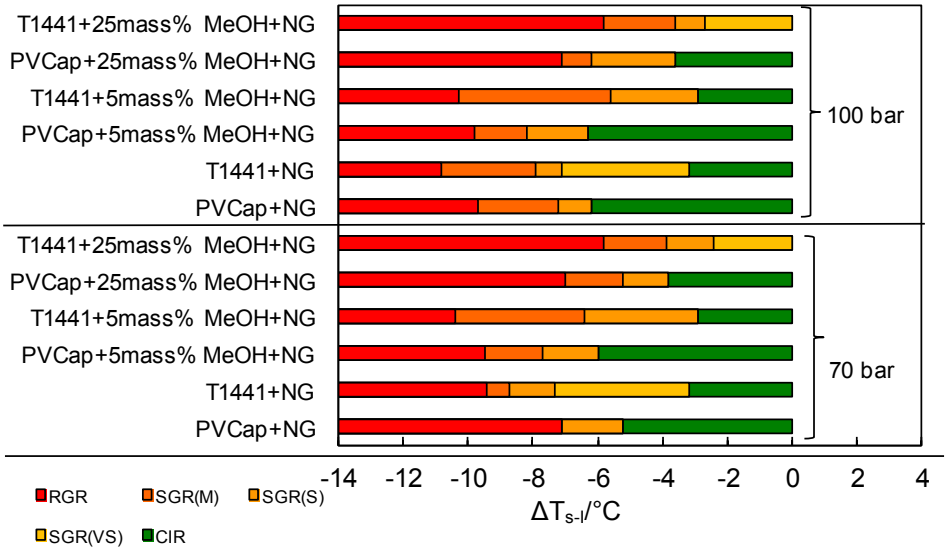

Figure 3.8 Comparison of subcooling extents of CGI regions for 0.5 mass% aqueous PVCap and T1441 alone and with 5.0 and 25.0 mass % methanol, tests with natural gas at various pressures. Data for 0.5 mass% T1441 and natural gas were generated as part of this work for comparison and are presented in Appendix A, Table A.1.

Compared to data for T1441 alone (Figure 3.8), T1441 with methanol performed more poorly at all pressures tested (all CGI regions smaller in extent relative to the s-I boundary, except around a 1°C shift of the RGR to higher subcoolings for 5.0 mass% methanol at ~70 bar). In general, the presence of methanol has a negative effect on T1441 at both the low and high concentrations tested, similar to that observed for PVCap at higher methanol concentrations, and in contrast to PVCap with lower methanol concentrations in which CGI regions were preserved or increased in some cases. As seen from the results (Figure 3.8), the negative impact of methanol at higher concentration (25.0 mass%) is apparently stronger for T1441 compared to PVCap. Consistent with behaviour observed for T1441 in natural gas systems, data support T1441 as less powerful than PVCap, but this is offset by the potential benefit of it having a much higher cloud point of 90 °C at 0.5 mass% aqueous compared to 38−39 °C for PVCap (Mozaffar, 2013); which makes T1441 less problematic in terms of drop-out and 'gunking' for wellhead hot injection cases.

3.2.2 Ethanol / KHI combination CGI behaviour

Effect of ethanol on PVCap in natural gas system

Following the tests on different methanol concentrations, experiments were carried out on 0.5 mass% PVCap aqueous with 5.0, 13.1 and 25.0 mass % ethanol (relative to water + PVCap). Figures 3.9, 3.10 and 3.11 show example CGI method cooling curves and boundaries for PVCap−natural gas systems with three ethanol concentrations. CGI boundary data points for all systems are reported in Tables 3.7, 3.8 and 3.9.

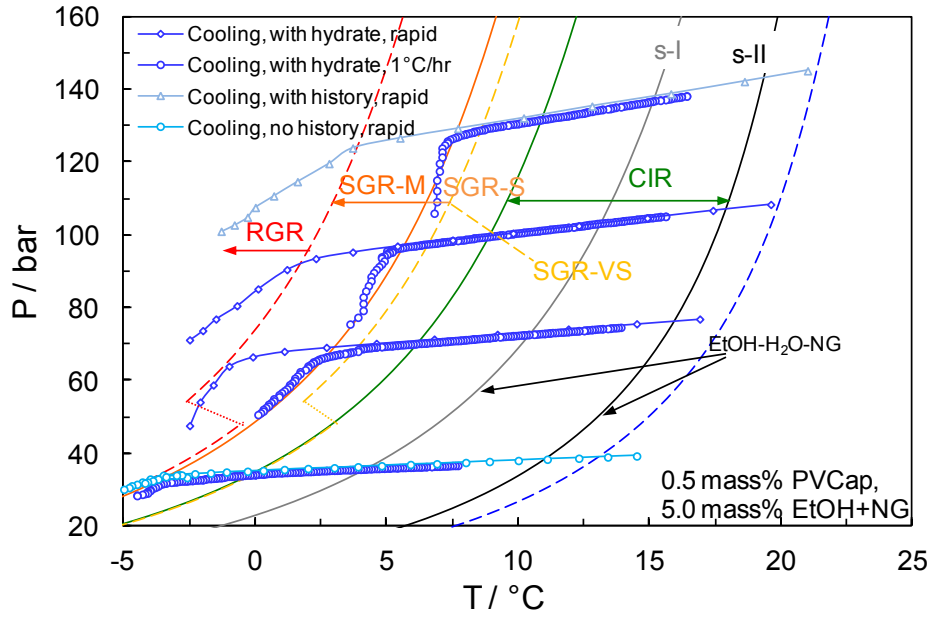

Figure 3.9 Example CGI method cooling curves and interpolated boundaries for 0.5 mass% PVCap / 5.0 mass % ethanol aqueous with natural gas.

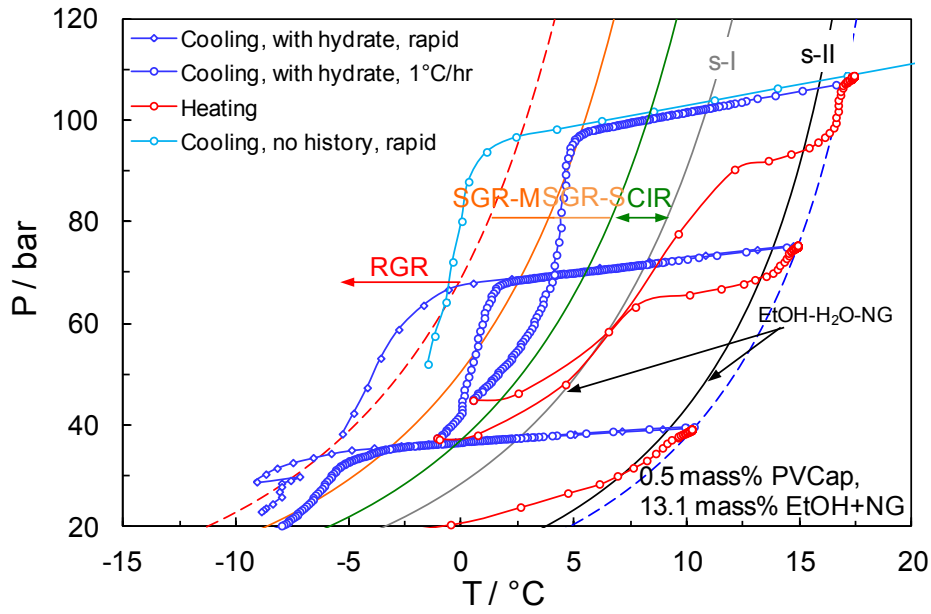

Figure 3.10 Example CGI method cooling curves and interpolated boundaries for 0.5 mass% PVCap / 13.1 mass % ethanol aqueous with natural gas.

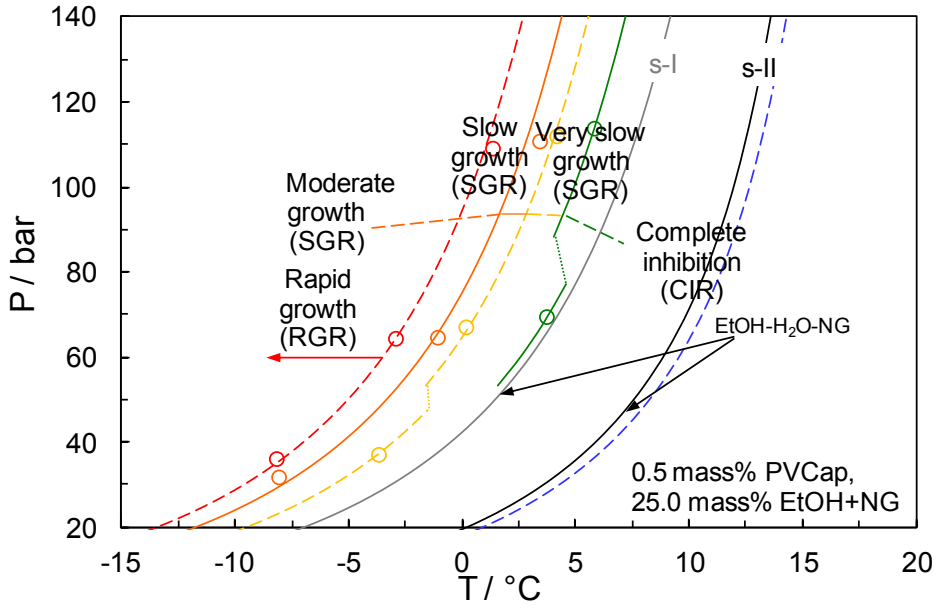

Figure 3.11 Experimental natural gas hydrate CGI region data for 0.5 mass% PVCap aqueous with 25.0 mass % ethanol (relative to water + PVCap) showing CGI regions determined from changes in relative hydrate growth rates.

Table 3.7 Experimental natural gas hydrate CGI region data for 0.5 mass% PVCap aqueous (relative to water) with 5.0 mass% ethanol (relative to water + PVCap).

CGR boundary	Growth rate	T / °C (± 0.5)	P / bar (± 0.2)	ΔT_{s-I} / °C (± 0.5)	ΔT_{s-II} / °C (± 0.5)
CIR-SGR(VS)	No growth	0.3	34.2	-3.7	-9.9
		5.8	69.9	-4.4	-9.5
		8.6	100.0	-4.2	-8.9
		11.0	131.1	-3.8	-7.9
SGR(VS-S)	Very slow	0.1	34.3	-3.9	-10.1
		3.7	67.9	-6.2	-11.5
		6.6	97.8	-6.1	-10.7
		8.5	129.0	-6.2	-10.3
SGR(S-M)	Slow	-3.2	32.0	-6.5	-12.9
		2.2	65.2	-7.4	-12.7
		5.5	96.3	-7.1	-11.8
		7.4	126.8	-7.2	-11.3
SGR(M)-RGR	Moderate	-3.5	34.1	-7.5	-13.7
		-1.1	63.9	-10.5	-15.9
		1.8	93.9	-10.6	-15.3
		3.7	123.9	-10.7	-14.9

Table 3.8 Experimental natural gas hydrate CGI region data for 0.5 mass% PVCap aqueous (relative to water) with 13.1 mass % ethanol (relative to water + PVCap).

CGR boundary	Growth rate	T / °C (± 0.5)	P / bar (± 0.2)	ΔT_{s-I} / °C (± 0.5)	ΔT_{s-II} / °C (± 0.5)
CIR-SGR(S)	No growth	-0.6	35.1	-2.6	-9.0
		5.4	69.8	-2.5	-7.9
		8.3	98.7	-2.3	-7.0
SGR(S-M)	Slow	-2.9	35.4	-5.0	-11.4
		2.2	68.1	-5.5	-10.9
		5.3	97.1	-5.2	-9.9
SGR(M)-RGR	Moderate	-5.6	34.9	-7.5	-14.0
		-0.5	67.3	-8.1	-13.5
		2.4	96.6	-8.0	-12.8

Table 3.9 Experimental natural gas hydrate CGI region data for 0.5 mass% PVCap aqueous (relative to water) with 25.0 mass % ethanol (relative to water + PVCap).

CGR boundary	Growth rate	T / °C (± 0.5)	P / bar (± 0.2)	ΔT_{s-I} / °C (± 0.5)	ΔT_{s-II} / °C (± 0.5)
CIR-SGR(VS)	No growth	0.0	38.4	-	-5.6
		3.7	69.6	-0.5	-6.1
		5.8	113.9	-2.0	-6.8
SGR(VS-S)	Very slow	-3.7	37.2	-2.5	-9.1
		0.2	67.2	-3.7	-9.4
		4.2	112.1	-3.5	-8.3
SGR(S-M)	Slow	-8.1	31.9	-5.5	-12.3
		-1.1	64.7	-4.7	-10.4
		3.4	110.9	-4.2	-9.0
SGR(M)-RGR	Moderate	-8.2	36.2	-6.8	-13.8
		-3.0	64.5	-6.5	-12.7
		1.3	109.2	-6.1	-11.3

Previous studies showed that in a similar case to methanol, ethanol had a consistently negative effect on the performance of PVCap in methane systems; the extent of CGI regions subcooling reduced as ethanol concentration increased (Mozaffar et al., 2014). Particularly the CIR region was reduced up to the point that it was completely lost for 50.0 mass%. Likewise, for the natural gas system with 0.5 mass% PVCap, a negative effect could be seen for 5.0, 13.1 and 25.0 mass% ethanol, although this is much more apparent at 25.0 mass% EtOH. At 5.0 mass% ethanol, the complete inhibition region has been reduced to $\Delta T_{s-I} \approx -4$ °C. The main negative effect for this level of ethanol is on the CIR; the SGR is preserved at $\Delta T_{s-I} \approx -7.1$°C and the RGR boundary is actually at a slightly higher subcooling than for PVCap alone. In contrast, for 25.0 mass% EtOH

the negative effect is apparent across all CGI regions; the complete inhibition region has been reduced to $\Delta T_{s\text{-}I} \approx -2$ °C at higher pressures, reducing to ~ −0.5°C at medium pressures, and finally at lower pressure (below ~60 bar) it is totally lost. The slow and rapid growth region boundaries are being reduced from $\Delta T_{s\text{-}I} \approx -7.2$ °C and ~−8.9 °C for water-PVCap, to ~ −4.8 °C and ~ −6.5 °C for water-ethanol-PVCap respectively (Figure 3.12). Finally, as seen for PVCap with NG alone, pressure again has an effect; with performance reduced at lower pressures (below ~ 60 bar) compared to higher pressures in PVCap-ethanol systems for 5.0 and 25.0 mass% ethanol.

Experimental phase equilibrium and compositional data provide conclusive evidence for the formation of binary ethanol-methane clathrate hydrates at ambient temperatures and elevated pressures for aqueous molar ethanol fractions of greater than 0.056, which are stable over a wide PT range (Anderson et al., 2009). Therefore, following the tests on 5.0 and 25.0 mass% EtOH, experiments were carried out on 0.5 mass% PVCap aqueous with 13.1 mass% (5.56 mol%) ethanol (relative to water + PVCap) to see if this ideal stoichiometric ratio for ethanol hydrates corresponded to a 'peak' in CGI extents or a clear change in them.

For this stoichiometric concentration, in agreement with data for other concentrations, a consistently negative effect on the performance of PVCap is observed; for example, the PVCap induced CIR decreased to $\Delta T_{s\text{-}I} \approx -2.5$ °C compared to −5.2 °C for PVCap with natural gas and distilled water. Similarly, the SGR decreased to $\Delta T_{s\text{-}I} \approx -5.2$ °C with the RGR boundary reduced to ~ −7.9 °C subcooling from the s-I boundary. As evident in Figure 3.12, data for 13.1 mass% ethanol and 0.5 mass% PVCap with NG do not correspond to a clear change in CGI region extents with all regions reduced compared to 5.0 mass% ethanol in the same PVCap-NG system.

As illustrated in Figure 3.12, for all concentrations tested, ethanol had a detrimental effect on PVCap performance but unlike methanol there is not a peak in the performance for any of the ethanol concentrations. As evident from the figure the higher the concentration of ethanol the smaller the CIR becomes. In a similar manner, SGR and RGR also decrease as function of ethanol concentration with the only exception of larger RGR in the presence of 5.0 mass% ethanol.

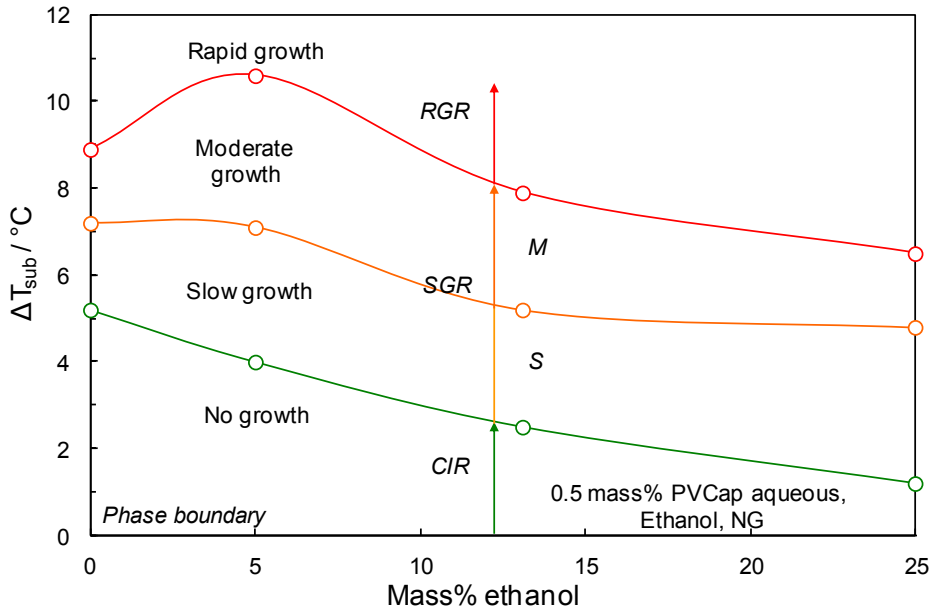

Figure 3.12 Average (60 to 150 bar) PVCap induced CGI regions for 0.5 mass% PVCap aqueous in a natural gas system as a function of ethanol mass% (relative to water + PVCap). 0.5 mass% PVCap-NG data from Mozaffar (2013).

Although ethanol has a negative effect on PVCap performance in terms of CGI properties, the combination of 0.5 mass% PVCap and ethanol still offers better inhibition by mass of inhibitor in comparison to ethanol alone.

Effect of Ethanol on PVCap in ethane system

An ongoing question with respect to the negative effect of ethanol on PVCap performance was whether ethanol enclathration was a factor; ethanol being known to form binary hydrates in both methane and ethane systems (Anderson et al., 2009). In light of this, tests were carried out on the effect of ethanol on PVCap performance in an ethane system. Although ethane s-I hydrate system shares the same CGI boundaries as methane s-I hydrate system, the hydrate growth rate in SGR is much higher in the case of methane, so that PVCap is able to inhibit ethane hydrate growth much more effectively than methane (Mozaffar, 2013). The effect of 5.56 mole% ethanol (the stoichiometric ratio for ethanol entry into the hydrate lattice, which is equal to 13.1 mass%)) on 0.5 mass% PVCap inhibition in an ethane system was briefly examined. The ethane used was 99.99% pure and supplied by BOC gases.

Due to the uncertainty in model predictions for ethane-ethanol systems, the phase boundary for the 5.56% mole% ethanol system was estimated based on ice point

depression data. This was additionally confirmed through experimental measurement (for a PVCap-free system), with good agreement being observed (Figure 3.13). The hydrate dissociation point measurement for the KHI-free ethanol-water-ethane system was made using the reliable constant volume, isochoric equilibrium step heating technique previously developed in-house (Tohidi et al., 2000) as standard. The measured dissociation point is reported in Table 3.10. Figure 3.13 shows example CGI method cooling and heating curves for 0.5 mass% PVCap with 5.56 mole% ethanol (relative to water) and ethane, including interpreted CGI boundaries. Experimental ethane hydrate CGI regions data measured for the system are reported in Table 3.11. Figure 3.14 shows a comparison of subcooling extents of PVCap-induced CGI regions from the s-I boundary for water-methane, water-ethane, water-natural gas, 5.56 mole% ethanol aqueous with ethane and with natural gas and 4.81 mole% ethanol aqueous with methane.

Table 3.10 Experimentally determined equilibrium hydrate dissociation conditions for 5.56 mol% ethanol aqueous with ethane.

T / °C (± 0.5)	P / bar (± 0.2)
8.4	23.4

Table 3.11 Experimental ethane hydrate CGI region data for 0.5 mass% PVCap with 5.56 mole% thanol (relative to water).

CGR boundary	Growth rate	T / °C (± 0.5)	P / bar (± 0.2)	ΔT_{s-I} / °C (± 0.5)
CIR-SGR(VS)	No growth	6.7	22.2	-1.2
SGR(VS-S)	Very slow	5.3	22.0	-2.5
SGR(S-M)	Slow	3.2	21.5	-4.5
SGR(M)-RGR	Moderate	-2.2	20.1	-9.4

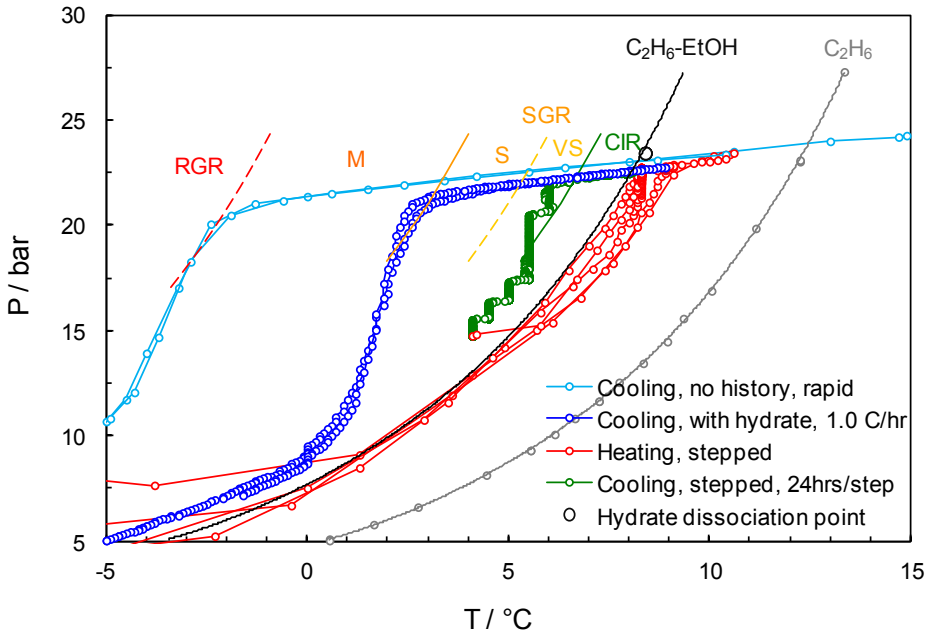

Figure 3.13 Example CGI method cooling and heating curves for 0.5 mass% PVCap with 5.56 mole% ethanol (relative to water) and ethane, including interpreted CGI boundaries. The hydrate phase boundary for the system was estimated based on ice melting point depression data and confirmed experimentally.

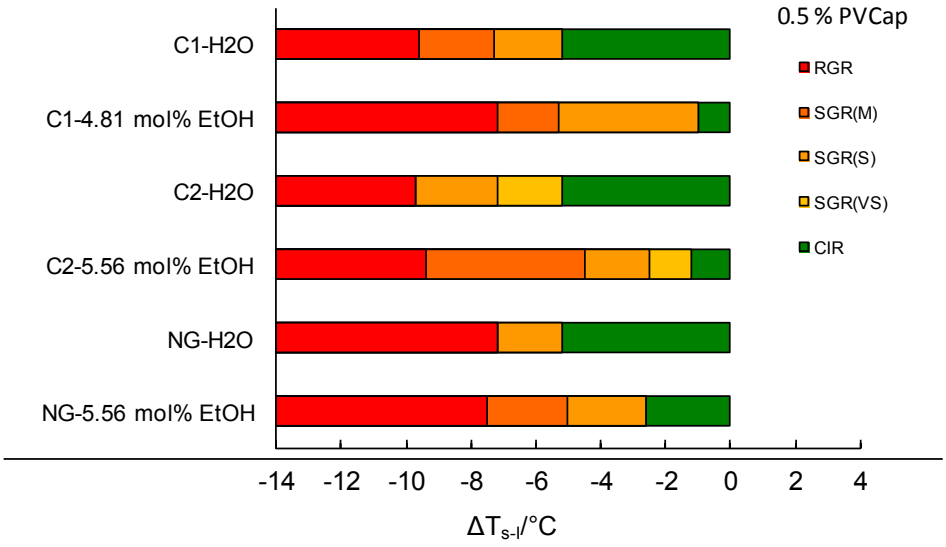

Figure 3.14 Comparison of subcooling extents of PVCap-induced CGI regions from the s-I boundary for water-methane, water-ethane and water-natural gas (Mozaffar, 2013), 5.56 mole% ethanol aqueous with ethane and with natural gas (this work), 4.81 mole% ethanol aqueous with methane (Mozaffar, 2013).

As can be seen in Figures 3.13 and 3.14, while PVCap does show some ethane hydrate CGI inhibition in the ethanol system, the latter, as might be expected, has a strongly negative effect; while the total extent of CGI inhibition remains largely constant, the CIR, SGR(VS) and (S) regions are greatly reduced in extent compared to data for deionised water. A similar negative effect could be observed for 0.5 mass% PVCap and 5.56 mol% ethanol with natural gas; adding ethanol to the system does not show a massive effect on total inhibition extent while largely decreases both the CIR and SGR(S) regions extent; however the negative effect on CIR is not as big as in the case of ethane. The negative effect of ethanol is however less for ethane than for methane with slightly lower aqueous concentration of 4.81 mol% (equal to 11.4 mass%) (Mozaffar, 2013).

Ethane, due to its large molecular diameter, stabilises s-I hydrates much more readily than methane. In that sense, given ethane is a stronger hydrate former, it might be expected that PVCap would be less able to inhibit ethane hydrate growth compared to methane hydrate. However, the opposite is the case, at least for the pressures studied to date (Mozaffar, 2013). This behaviour is seen in the data for ethanol systems too; in the systems where hydrate stability is greatest, i.e. ethane-ethanol, the negative effect of ethanol is more subdued. Due to the enhanced PVCap performance in presence of ethane, this component may also be a factor in the improved CGI behaviour of natural gas either alone or in presence of ethanol.

These findings are consistent with the emerging picture of the (gas composition therefore) composition of molecules occupying cages being likely the single biggest factor in governing the ability of a polymer to inhibit crystal growth as a function of pressure and composition. Somewhat paradoxically, often the more ‘thermodynamically stable’ the hydrate is (or at least the more the molecular diameter of guests lends stability to cages), the more PVCap has the ability to inhibit growth. Although it is important to remember that results to date do suggest hydrates formed in KHI-inhibited systems are not ‘normal’ hydrates, but hydrate polymer complexes, so this is maybe less contradictory that it at first might seem (see Chapter 6).

Effect of Ethanol on T1441 in natural gas system

As mentioned earlier, different polymers can act very differently in terms of hydrate inhibition. Results for T1441 in the presence of methanol also showed different

behaviour comparing to PVCap. Based on this and to further investigate the effect of ethanol, Champion Technologies T1441 KHI performance in a natural gas system was examined briefly. Crystal growth inhibition data were generated for 0.5 mass% T1441 with 25.0 mass% ethanol (relative to T1441+water) and natural gas at ~70 bar. CGI method cooling curves and interpolated boundaries are shown in Figure 3.15. Determined points on CGI region boundaries are reported in Table 3.12.

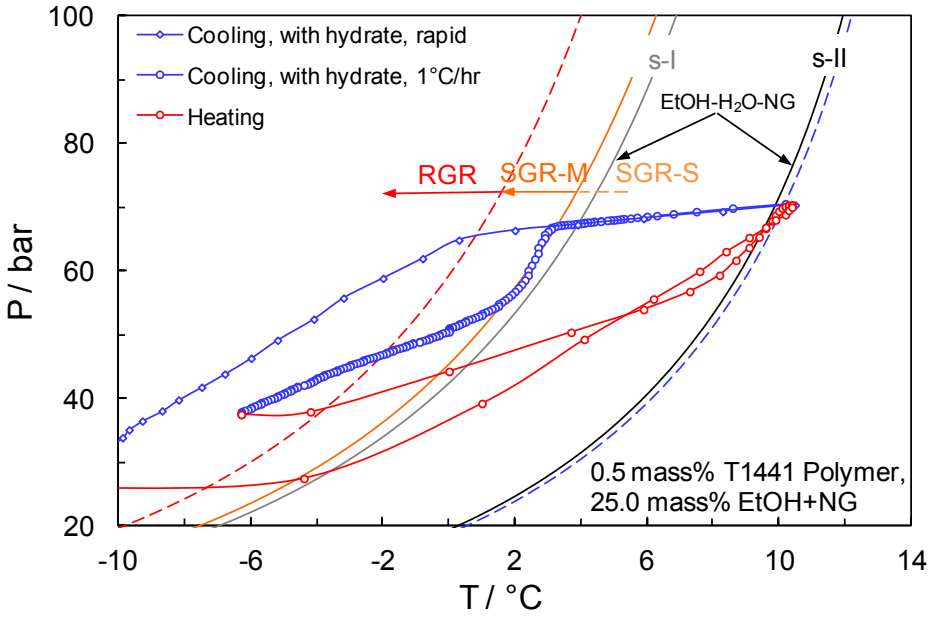

Figure 3.15 Example CGI method cooling and heating curves for 0.5 mass% T1441 (relative to water) / 25.0 mass % ethanol aqueous (relative to T1441+water) with natural gas.

Table 3.12 Experimental natural gas hydrate CGI region data for 0.5 mass% T1441 aqueous (relative to water) with 25.0 mass % ethanol (relative to water + PVCap).

CGR boundary	Growth rate	T / °C (± 0.5)	P / bar (± 0.2)	ΔT_{s-I} / °C (± 0.5)	ΔT_{s-II} / °C (± 0.5)
SDR	Slow dissociation	10.0	69.9	–	0.3
CIR-SGR(S)	No growth	4.9	67.6	–	-4.6
SGR(S-M)	Slow	3.2	66.7	-0.6	-6.1
SGR(M)-RGR	Moderate	0.8	65.5	-2.9	-8.6

It was previously shown that methanol has an overall negative effect on T1441 performance which can also be seen for 25.0 mass% ethanol and T1441; all CGI regions are reduced compared to T1441 alone (data for 0.5 mass% T1441 and natural gas were generated as part of this work for comparison and are presented in Appendix A, Table

A.1) and the complete inhibition region from s-I is totally lost. In general, presence of alcohols (methanol and ethanol) has a negative effect on T1441 at both the low and high concentrations tested similar to what was observed for PVCap in the presence of ethanol and methanol at higher concentrations.

Figure 3.16 illustrates the comparison of polymer (PVCap/T1441) induced inhibition regions for both polymers alone and with alcohols, all for 0.5 mass% polymer with natural gas and at ~70 bar. As seen from the results (Figure 3.16), poorer performance of T1441 at the high ethanol concentration (25.0 mass %) is clear compared to a similar concentration of methanol. The negative impact of ethanol at 25.0 mass% is apparently stronger for T1441 compared to PVCap. Consistent with behaviour observed for T1441 alone and with methanol in natural gas systems, data support T1441 as less powerful than PVCap, but this is offset by the potential benefit of it having a much higher cloud point (90 °C at 0.5 mass% aqueous compared to 38−39 °C for PVCap).

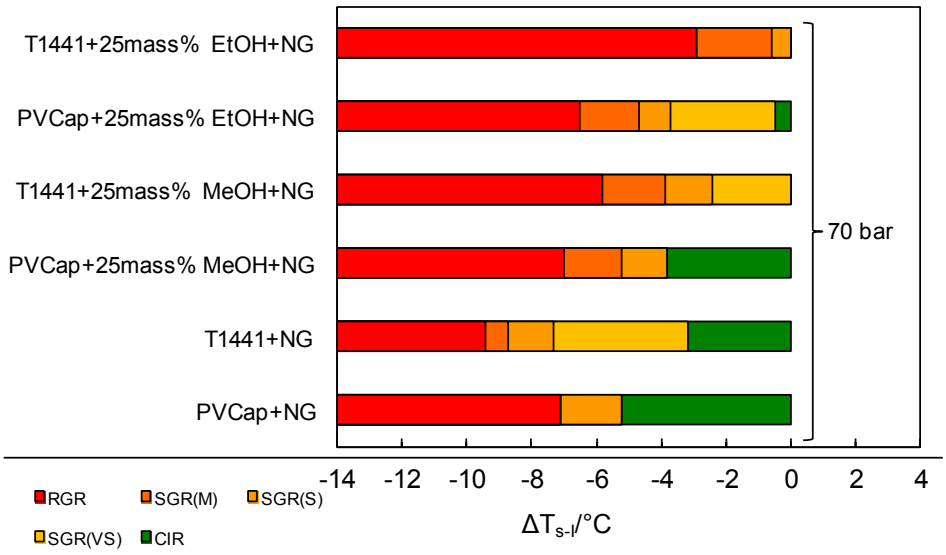

Figure 3.16 Comparison of subcooling extents of polymer induced CGI regions from the s-I boundary for 0.5 mass% aqueous PVCap and T1441 co-polymer alone and with 25.0 mass % methanol and ethanol, tested with natural gas at 70 bar. 0.5 mass% PVCap-NG data from Mozaffar (2013) Data for 0.5 mass% T1441 and natural gas were generated as part of this work for comparison and are presented in Appendix A, Table A.1.

3.2.3 MEG / KHI combination CGI behaviour

Effect of MEG on PVCap in natural gas system

As previously discussed, presence of MEG has a very positive effect on PVCap performance and the combination of MEG + PVCap offers far better inhibition by mass/volume of inhibitor than MEG alone in a methane hydrate forming system. As MEG enhances PVCap performance by reducing hydrate growth rate and acts to all intents and purposes as a full 'top-up' inhibitor to PVCap to at least 50 mass%, it could in theory be used to extend the subcooling of KHIs and/or significantly reduce required MEG thermodynamic inhibitor volumes (Mozaffar et al., 2014).

Taking into account results for alcohols, glycol ethers (2-butoxyethanol) and salts (NaCl) with methane (Mozaffar, 2013), it could be concluded that a general rule of thumb seems to be that water soluble compounds which act to reduce PVCap solubility (e.g. salts, glycol ethers) commonly have a positive effect on PVCap performance (unless polymer precipitation occurs) possibly by encouraging its adsorption. The exception to this rule is MEG; which is a very good synergist/top-up inhibitor for PVCap with methane, but does not reduce polymer aqueous solubility. The reason for this behaviour is however unclear. In light of this the effect of different MEG concentrations (5.0, 10.0 and 20.0 mass %) for PVCap and natural gas was investigated to see whether the results of single component systems are extendable to multi-component systems.

Figures 3.17, 3.18 and 3.19 show example CGI method cooling/ heating curves and CGI boundaries for MEG−PVCap−natural gas (0.5 mass% PVCap with 5.0, 10.0 and 20.0 mass% MEG). Experimental data delineating regions are reported in Tables 3.13, 3.14 and 3.15.

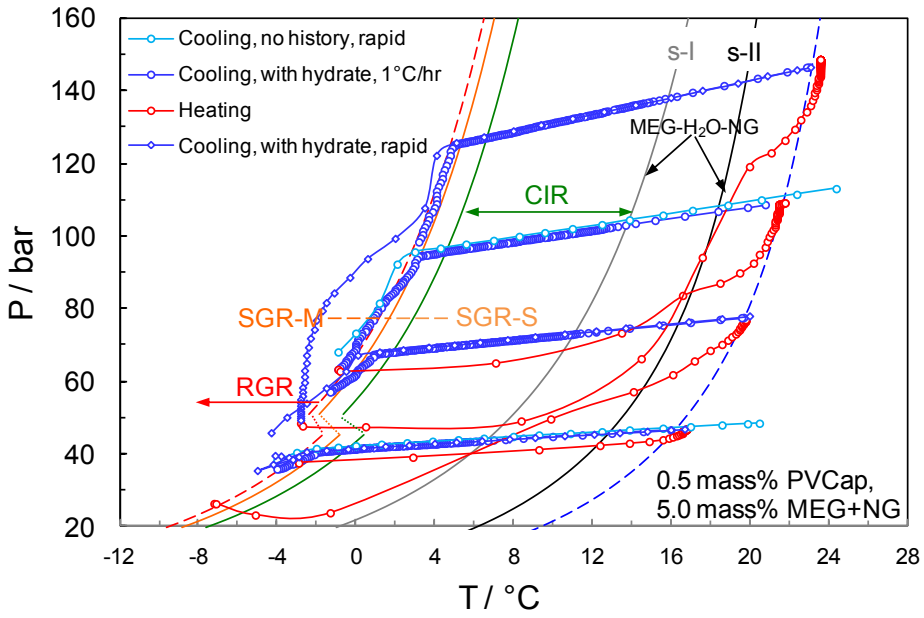

Figure 3.17 Example CGI cooling/heating runs and experimentally determined boundaries for 0.5 mass% PVCap (relative to water) / 5.0 mass% MEG (relative to water + PVCap) aqueous with natural gas.

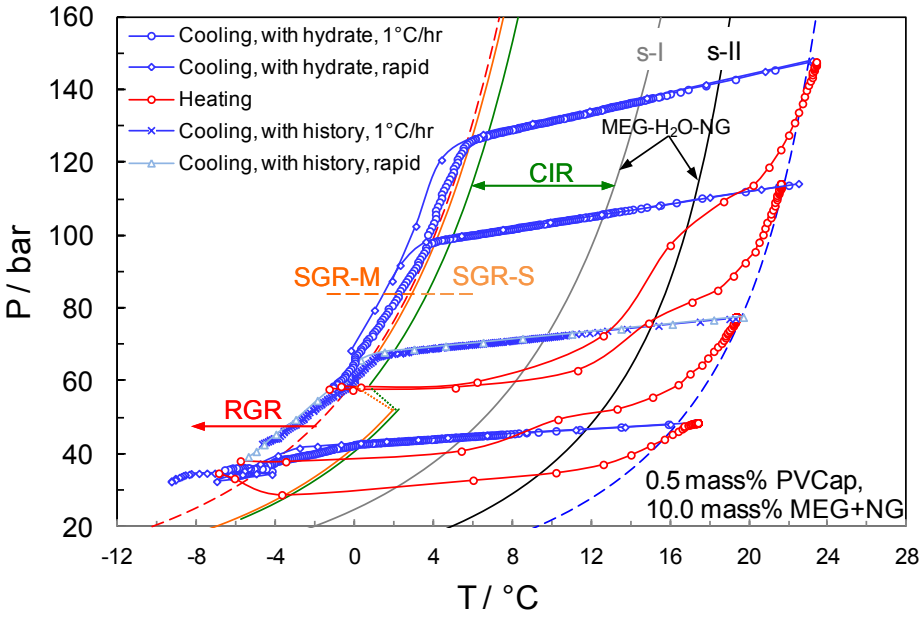

Figure 3.18 Example CGI cooling/heating runs and experimentally determined boundaries for 0.5 mass% PVCap (relative to water) / 10.0 mass% MEG (relative to water + PVCap) aqueous with natural gas.

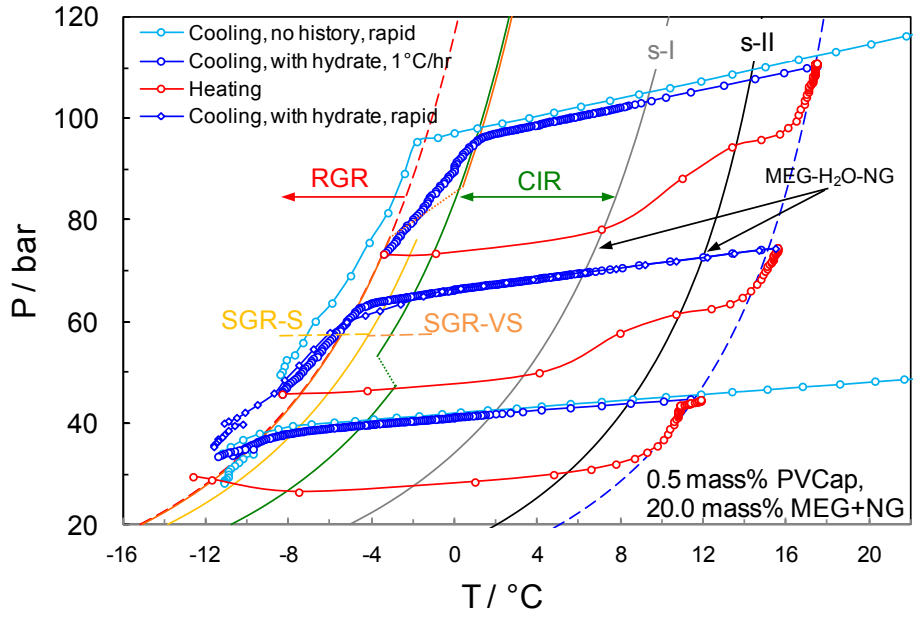

Figure 3.19 Example CGI cooling/heating runs and experimentally determined boundaries for 0.5 mass% PVCap (relative to water) / 20.0 mass% MEG (relative to water + PVCap) aqueous with natural gas.

Table 3.13 Experimental natural gas hydrate CGI region data for 0.5 mass% PVCap aqueous (relative to water) with 5.0 mass % MEG (relative to water + PVCap).

CGR boundary	Growth rate	T / °C (± 0.5)	P / bar (± 0.2)	ΔT_{s-I} / °C (± 0.5)	ΔT_{s-II} / °C (± 0.5)
SDR	Slow dissociation	16.8	46.5	–	3.8
		19.6	77.4	–	3.2
		21.3	108.7	–	2.9
		22.9	146.3	–	3.0
CIR-SGR(S)	No growth	-0.5	40.7	-6.6	-12.5
		1.6	67.3	-8.8	-13.9
		4.4	94.9	-8.7	-13.2
		6.8	126.4	-8.4	-12.4
SGR(S-M)	Slow	-1.7	41.0	-7.8	-13.7
		0.8	67.3	-9.6	-14.7
		3.2	94.3	-9.8	-14.4
		5.0	125.1	-10.1	-14.1
SGR(M)-RGR	Moderate	-2.6	40.5	-8.7	-14.5
		0.1	67.1	-10.2	-15.4
		3.0	95.4	-10.1	-14.7
		4.3	124.6	-10.8	-14.8

Table 3.14 Experimental natural gas hydrate CGI region data for 0.5 mass% PVCap aqueous (relative to water) with 10.0 mass % MEG (relative to water + PVCap).

CGR boundary	Growth rate	T / °C (± 0.5)	P / bar (± 0.2)	ΔT_{s-I} / °C (± 0.5)	ΔT_{s-II} / °C (± 0.5)
SDR	Slow dissociation	16.8	48.0	–	4.8
		19.1	76.6	–	4.0
		21.6	113.3	–	4.3
		23.1	147.0	–	4.5
CIR-SGR(S)	No growth	0.4	42.4	-4.8	-10.7
		2.0	67.7	-7.2	-12.3
		5.0	98.8	-7.2	-11.6
		6.7	127.1	-7.3	-11.2
SGR(S-M)	Slow	0.2	42.5	-5.0	-10.9
		1.3	66.9	-7.8	-12.9
		3.8	97.7	-8.2	-12.7
		6.1	126.1	-7.8	-11.8
SGR(M)-RGR	Moderate	-2.8	41.9	-7.8	-13.8
		1.1	67.4	-8.1	-13.2
		3.6	98.6	-8.5	-12.9
		5.5	125.7	-8.4	-12.3

Table 3.15 Experimental natural gas hydrate CGI region data for 0.5 mass% PVCap aqueous (relative to water) with 20.0 mass % MEG (relative to water + PVCap).

CGR boundary	Growth rate	T / °C (± 0.5)	P / bar (± 0.2)	ΔT_{s-I} / °C (± 0.5)	ΔT_{s-II} / °C (± 0.5)
SDR	Slow dissociation	11.6	44.6	-	3.0
		15.3	74.8	-	3.2
		17.4	110.2	-	3.0
CIR-SGR(VS)	No growth	-4.3	39.5	-5.8	-11.9
		-2.1	64.9	-7.7	-13.3
		1.1	96.8	-7.6	-12.5
SGR(VS-S)	Very slow	-7.4	38.5	-8.6	-14.8
		-3.4	64.4	-9.0	-14.5
		-	-	-	-
SGR(S-M)	Slow	-9.2	37.2	-10.2	-16.7
		-4.6	63.2	-10.0	-15.6
		1.1	96.3	-7.6	-12.8
SGR(M)-RGR	Moderate	-9.0	38.4	-10.2	-16.4
		-4.3	64.5	-9.9	-15.4
		-1.8	95.4	-10.4	-15.3

Results from application of the CGI method to natural gas−PVCap−ethylene glycol−water systems (up to 20.0 mass % MEG) agree with previous findings (Mozaffar et al., 2014) in that ethylene glycol has a positive, synergistic effect on PVCap hydrate crystal growth inhibition properties. As shown in Figures 3.17 to 3.19, MEG generally acts as a 'top-up' inhibitor for PVCap for the concentrations tested. The PVCap-induced CIR from s-I boundary is increased to $\Delta T_{sub} \approx$ -8.6, -7.2 and -7.7 °C for 5.0, 10.0 and 20.0 mass% MEG respectively compared to -5.2 °C for PVCap alone. However, while complete inhibition and slow to moderate growth regions boundaries are extended to higher subcoolings at 5.0 mass% MEG, these return to lower values at 10.0 mass % MEG but are still larger than PVCap alone. The onset of rapid growth at the RGR boundary is decreased to slightly lower subcoolings at 10.0 mass% MEG compared to PVCap alone.

For 20.0 mass% MEG, as shown in figure 3.19, an additional very slow growth region extending to subcoolings about -9.0 °C appears for pressures lower than 80 bar but for higher pressure of 110 bar this does not seem to be the case. This region was also observed for PVCap alone with natural gas (Mozaffar, 2013). This additional region however could not be distinguished for lower MEG concentrations in the same natural gas system. The onset of rapid growth at the RGR boundary is increased to slightly higher subcoolings at 20 mass% MEG compared to PVCap alone. Moderate growth region behaviour at this concentration of MEG is different from the other concentrations; increases in extent at pressures below 80 bar but at higher pressures, comes close to the CIR boundary.

Finally, as seen for PVCap with NG alone, pressure again has an effect, with KHI performance reduced at lower pressures (below ~60 bar) compared to higher pressures especially in terms of CIR which was decreased in all three tested MEG concentrations as is common to this type of NG system.

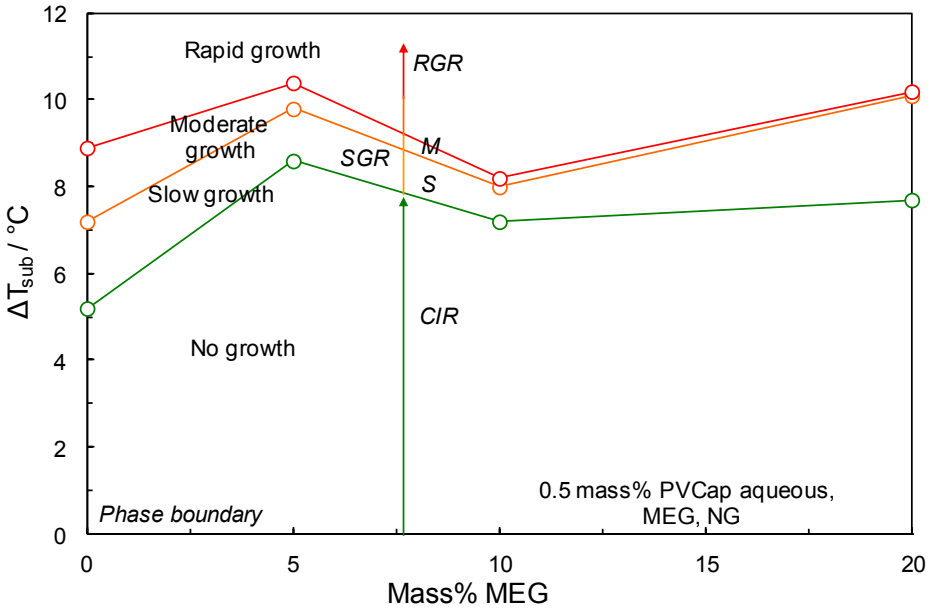

Figure 3.20 Average (60 to 150 bar) PVCap induced natural gas CGI regions from the s-I phase boundary for 0.5 mass% PVCap aqueous as a function of MEG mass% (relative to water + PVCap). 0.5 mass% PVCap-NG data from Mozaffar (2013).

Figures 3.20 and 3.21 show PVCap induced and total PVCap + MEG natural gas hydrate inhibition regions as a function of MEG concentration respectively. As can be seen in Figure 3.21, 0.5 mass% PVCap with 20.0 mass% MEG offers complete crystal growth inhibition (CIR region) more than twice the thermodynamic inhibition offered by ~20.0 mass% MEG. Although PVCap with 10.0 mass % MEG induced total CGI is smaller than PVCap alone, it seems to be larger by increasing MEG concentration to 20.0 mass% and the combined total CGI of 15.8°C is far greater than PVCap alone. As MEG acts as a 'top-up' inhibitor up to 20.0 mass% with PVCap, then it could in theory be used to extend the subcooling of KHIs and/or significantly reduce thermodynamic inhibitor volumes through the hybrid inhibition strategies. MEG volume reduction is even higher considering total inhibition offered form s-II structure phase boundary rather than s-I - shown in Figures 3.20 and 3.21 as the few degrees of subcooling which lies between s-I and s-II phase boundaries will be added to the offered inhibition.

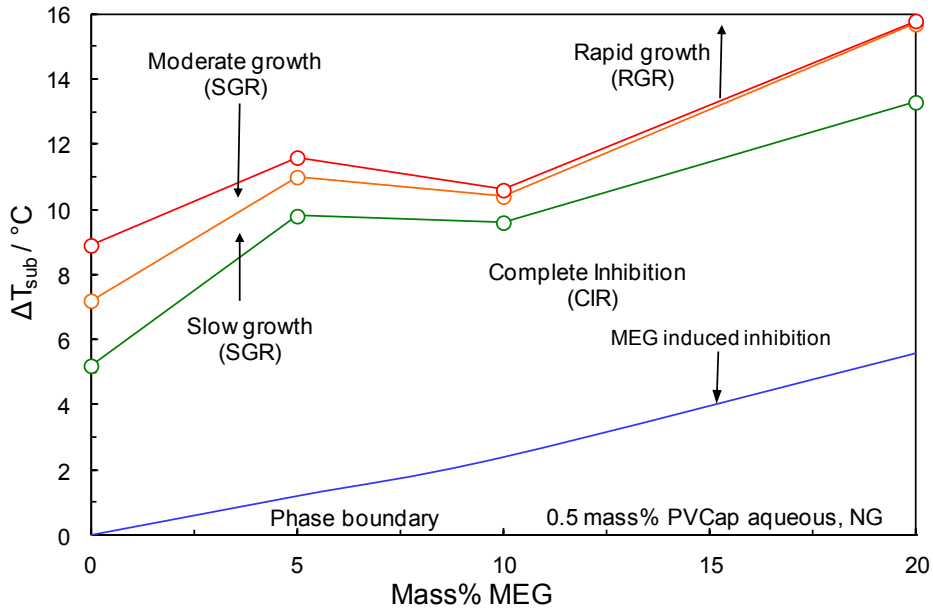

Figure 3.21 Total natural gas hydrate inhibition from the s-I boundary offered by 0.5 mass% PVCap and MEG as a function of MEG concentration. 0.5 mss% PVCap-NG data from Mozaffar (2013).

Effect of MEG on T1441 in natural gas system

Following the tests on PVCap, experiments were carried out on 0.5 mass% Champion technologies T1441 aqueous with 5.0 mass% MEG. Figure 3.22 shows example CGI method cooling and heating curves of the system. CGI boundary data points are reported in Tables 3.16 and presented in Figure 3.23.

The CIR for T1441 with 5.0 mass% MEG decreases from about 4.5°C to 2.5°C relative to the s-I phase boundary with increasing pressure, while it was relatively constant at about 3.2°C for T1441 alone in the same natural gas system. The complete inhibition region is followed by a SGR(S) region up to subcoolings of about 8.2 °C from the s-I boundary (up to 13.4 °C from s-II depending on pressure) which diminishes in extent from $\Delta T_{s\text{-}I} \approx$-8.2 °C at pressures below 90 bar to $\Delta T_{s\text{-}I} \approx$ -6.2°C by 130 bar. Finally, a SGR (M) region extends to a subcooling of 15.3 °C from the s-II boundary beyond which rapid growth invariably occurs. At the lowest pressure, the extent of SGR slow and moderate regions could not be determined as ice formation occurred before any detectable hydrate formation.

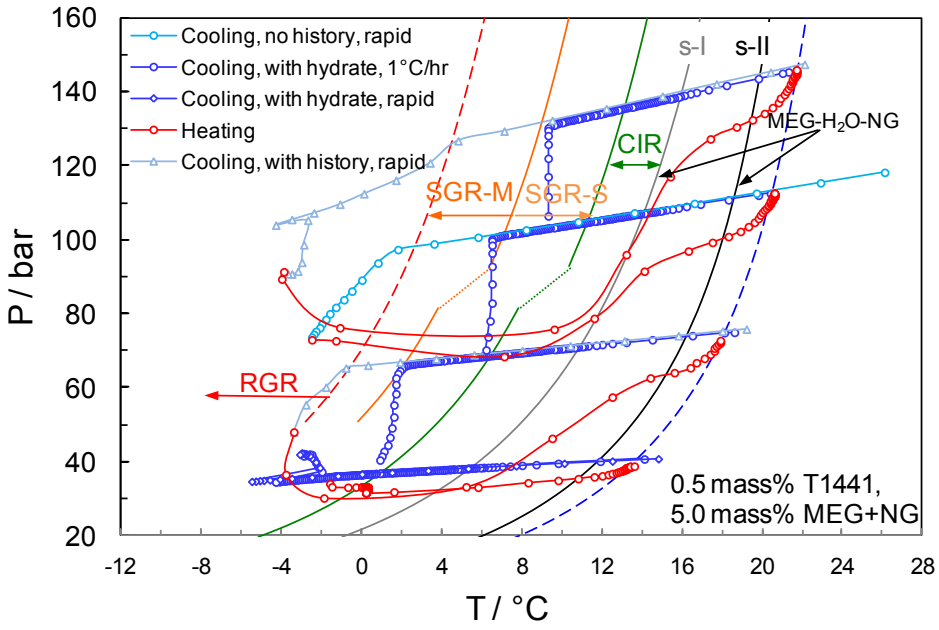

Figure 3.22 Example CGI method cooling/heating curves for 0.5 mass% T1441 aqueous (relative to water) with 5.0 mass % MEG (relative to water + polymer) in a natural gas system. Points are every five minutes.

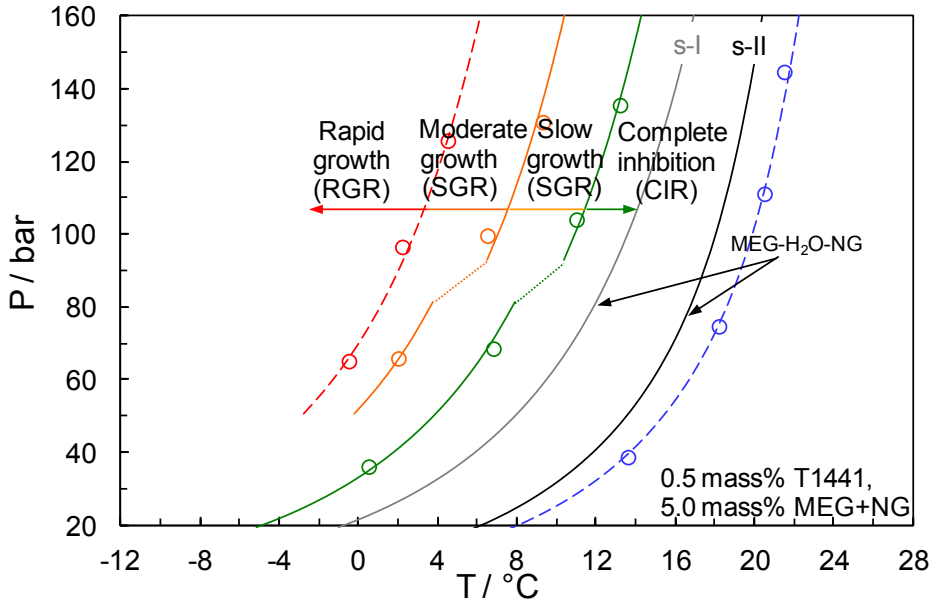

Figure 3.23 Experimental natural gas hydrate CGI region data for 0.5 mass% T1441 aqueous (relative to water)- with 5.0 mass % MEG (relative to water + polymer) showing CGI regions determined from changes in relative hydrate growth rates.

Table 3.16 Experimental natural gas hydrate CGI region data for 0.5 mass% T1441 aqueous (relative to water) with 5.0 mass % MEG (relative to water + PVCap).

CGR boundary	Growth rate	T / °C (± 0.5)	P / bar (± 0.2)	$\Delta T_{s\text{-}I}$ / °C (± 0.5)	$\Delta T_{s\text{-}II}$ / °C (± 0.5)
SDR	Slow dissociation	13.6	38.7	–	2.0
		18.2	74.7	–	2.0
		20.5	111.2	–	2.0
		21.5	144.8	–	1.6
CIR-SGR(S)	No growth	0.5	36.1	-4.5	-10.6
		6.8	68.6	-3.7	-8.9
		11.0	104.1	-2.8	-7.2
		13.2	135.6	-2.5	-6.4
SGR(S-M)	Slow	–	–	–	–
		2.0	65.9	-8.2	-13.4
		6.5	99.7	-6.9	-11.4
		9.3	130.9	-6.2	-10.1
SGR(M)-RGR	Moderate	–	–	–	–
		-0.5	65.2	-10.6	-15.8
		2.2	96.6	-11.0	-15.5
		4.5	125.8	-10.7	-14.7

Although the top-up effect is apparent at pressures below 90 bar, pressure seems to have a negative effect in the 5.0% MEG system by reducing CGI region extents compared to T1441 alone (Data for 0.5 mass% T1441 and natural gas were generated as part of this work for comparison and are presented in Appendix A, Table A.1). This behaviour somehow contrasts that for PVCap at a similar MEG concentration, where a negative effect is seen at lower pressures and a positive effect at higher pressures.

Figure 3.24 shows a comparison of subcooling extents of CGI regions (from the s-I boundary) for 0.5 mass% aqueous PVCap alone and with 5.0 mass % MEG, 0.5 mass % T1441 co-polymer alone and with 5.0 mass % MEG, all tested with natural gases for a range of pressures.

As can be seen, for the lower pressure of 70 bar, T1441 with MEG shows comparable performance with polymer alone or better; while the CIR is slightly larger by ~ 0.5 °C, SGR conditions extend up to 10.6 °C. T1441-MEG combination has the poorest performance of the three pressures at 150 bar; the CIR extending only to 2.5 °C subcooling from the s-I boundary before SGR(S) conditions occur.

Consistent with behaviour observed for T1441 in natural gas systems (Data for 0.5 mass% T1441 and natural gas were generated as part of this work for comparison and are presented in Appendix A, Table A.1), data support T1441 as less powerful than PVCap, but with this offset by the potential benefit of it having a much higher cloud point (90 °C at 0.5 mass% aqueous compared to 38−39 °C for PVCap).

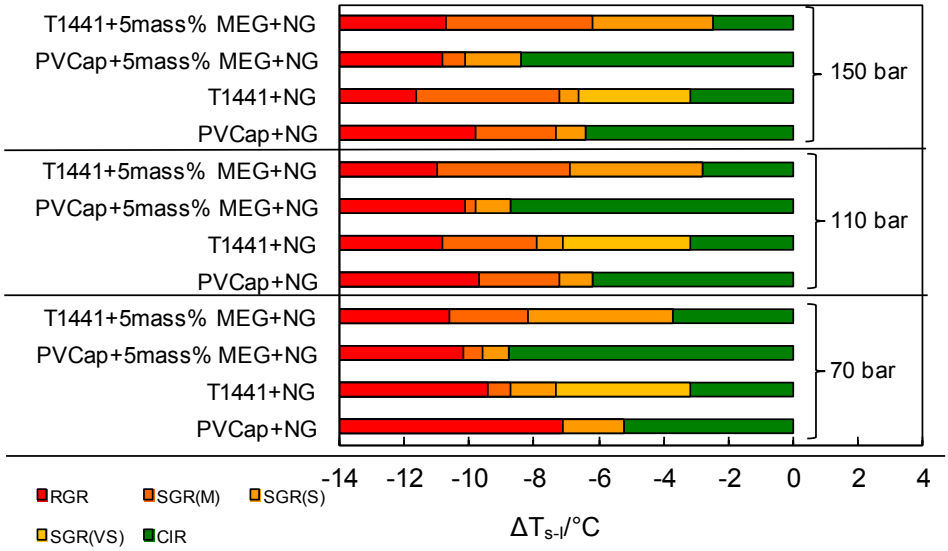

Figure 3.24 Comparison of determined subcooling extents of 0.5 mass% PVCap and T1441 aqueous induced hydrate CGI regions alone and with 5.0 mass % MEG at different pressures. 0.5 mass% PVCap-NG data from Mozaffar (2013). Data for 0.5 mass% T1441 and natural gas were generated as part of this work for comparison and are presented in Appendix A, Table A.1.

Effect of MEG on Bio-800 in natural gas system

Although KHIs can offer significant CAPEX and OPEX advantages comparing to other conventional hydrate inhibition strategies (e.g. thermodynamic inhibition with glycols, methanol, heating and/or insulation), environmental issues are emerging regarding their application, particularly where produced water is released into the sea. The fact that active polymers in KHI formulations have very large molecular size makes their breakdown difficult for microorganisms thus make them poorly biodegradable. Another issue that restricts polymers biodegradability can be due to their low reactivity.

Increasing environmental restriction on KHI biodegradability in the cases that produced waters are disposed to natural environment has forced the oil and gas industry to seek bio-KHIs. In some regions (such as Norwegian waters), because of environmental issues, conventional KHI polymers cannot be applied. Therefore to compare with

PVCap, CGI data were generated for 0.5 mass% Bio-800 – a biodegradable KHI from Ashland - aqueous with 5.0 mass% MEG (relative to water + polymer) in a natural gas system. Figure 3.25 shows example CGI method cooling curves and experimentally determined CGI boundaries for the system. CGI boundary data points are reported in Table 3.17.

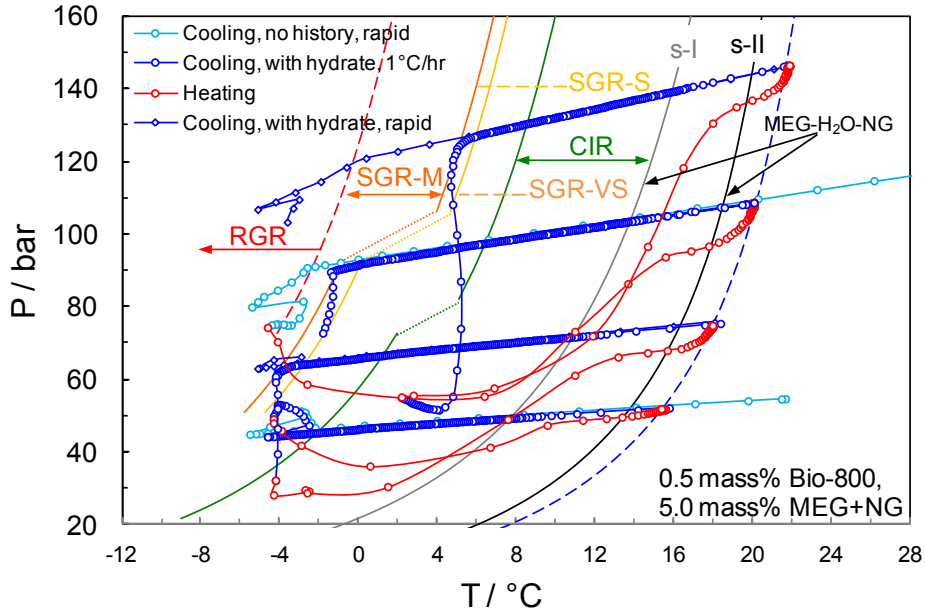

Figure 3.25 Example CGI method cooling/heating curves and experimentally determined CGI boundaries for 0.5 mass% Bio-800 (relative to water) / 5.0 mass % MEG (relative to water + polymer) aqueous with natural gas.

Table 3.17 Experimental natural gas hydrate CGI region data for 0.5 mass% Bio-800 aqueous (relative to water) with 5.0 mass % MEG (relative to water + polymer).

CGR boundary	Growth rate	T / °C (± 0.5)	P / bar (± 0.2)	ΔT_{s-I} / °C (± 0.5)	ΔT_{s-II} / °C (± 0.5)
SDR	Slow dissociation	15.5	51.6	-	1.7
		18.1	74.9	-	1.7
		20.0	107.8	-	1.5
		21.5	145.4	-	1.4
CIR-SGR(VS)	No growth	-2.0	44.5	-8.8	-14.7
		0.9	65.3	-9.2	-14.5
		6.1	96.4	-7.1	-11.7
		8.4	125.8	-6.8	-10.9
SGR(VS-S)	Very slow	-	-	-	-
		-3.0	63.6	-12.9	-18.2
		0.2	91.6	-12.6	-17.3
		5.9	126.7	-9.3	-13.4
SGR(S-M)	Slow	-	-	-	-
		-4.1	61.8	-13.8	-19.1
		-1.3	89.4	-13.8	-18.6
		5.0	123.5	-10.0	-14.2
SGR(M)-RGR	Moderate	-	-	-	-
		-	-	-	-
		-2.8	89.9	-15.4	-20.2
		-0.1	120.5	-14.9	-19.1

The CIR for Bio 800 extends between 6.8 and 9.2°C from the s-I boundary, and depending on the pressure, can extend to up to 14.7 °C subcooling from the s-II boundary. For the complete pressure range studied, this is followed by a SGR(VS) region up to subcoolings of ~12.9 °C from the s-I boundary (up to 18.2 °C from s-II depending on pressure). Beyond this, a SGR(S) region is present, however this diminishes in extent from $\Delta T_{s-I} \approx$ -13.8 °C at pressures below 90 bar to $\Delta T_{s-I} \approx$ -10 °C by 130 bar while for the lowest tested pressure (~50 bar) no growth was detected until ice formation. Finally, a SGR-(M) region where performance is poor yet the KHI is still active extends to a subcooling of 15.4 °C from the s-I boundary where rapid growth invariably occurs. No detectable growth was observed beyond the SGR-(M) region for pressures below 70 bar before ice formation. Comparing to the data for 0.5 mass% Bio-800 alone (data for 0.5 mass% Bio-800 and natural gas are presented in Appendix A, Table A.3), the top-up effect of 5.0 mass% MEG is apparent at all tested pressures (Figure 3.26). Unlike what was observed for 0.5 mass% PVCap and same concentration of MEG, in this case pressure has a negative effect on CGI behaviour reducing the

extent of regions by increasing pressure (above 80 bar) which was also the case for 0.5 mass% T1441 and 5.0 mass% MEG.

Figure 3.26 shows a comparison of subcooling extents of CGI regions (from the s-I boundary) for 0.5 mass% aqueous PVCap alone and with 5.0 mass % MEG, 0.5 mass % Bio-800 alone and with 5.0 mass % MEG, all tested with natural gases for a range of pressures. Despite the negative effect of pressure, the positive effect of 5.0 mass% MEG on Bio-800 is still clear at higher pressures of 110 and 150 bar at least in terms of CIR and SGR(S) which are increased comparing to Bio-800 alone.

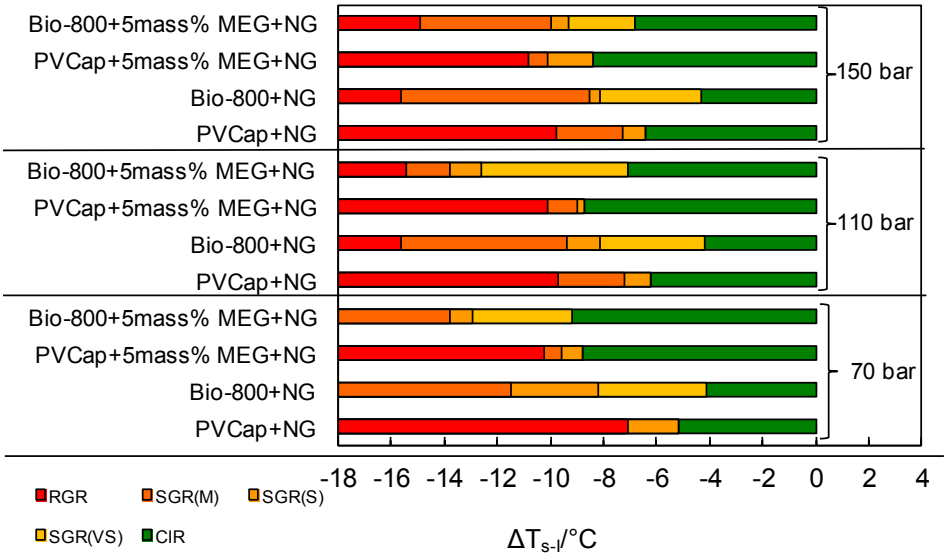

Figure 3.26 Comparison of determined subcooling extents of 0.5 mass% PVCap and Bio-800 aqueous induced hydrate CGI regions alone and with 5.0 mass % MEG at different pressures. 0.5 mass% PVCap-NG data from Mozaffar (2013). Data for 0.5 mass% Bio-800 and natural are presented in Appendix A, Table A.3.

As can be seen from Figure 3.26, for the lower pressures (under 80 bar), Bio 800 shows better performance compared to PVCap with the same MEG concentration; while the CIR is slightly larger and SGR(M) conditions extend beyond the ice point. A poorer performance of this polymer could be seen comparing to PVCap + 5.0 mass % MEG at pressures higher than 100 bar in terms of CIR, however the total inhibition offered is still better.

Top of line hydrates; PVCap-MEG systems

Hydrate formation at top of a pipeline which is experiencing stratified flow can be a serious design / operational consideration, particularly in sour gas systems. It is believed that the inhibitor present in the liquid phase can prevent hydrate formation, while water condensation at top of line, which is not in contact with inhibitor in the liquid phase, can present a potential risk of hydrate formation and cause line corrosion. An experimental work by Nazeri et al. (2012) has demonstrated that hydrate can readily grow directly from the vapour phase in simulated 'top of line' scenarios although the extent to which hydrate formation by this process presents a blockage risk is still poorly understood.

During the course of this work, it was observed that hydrates which have grown from the vapour phase in a top of line situation will stop growing or even dissociate if they come into contact with the KHI inhibited bulk aqueous phase, at least so long as conditions are within the KHI-induced CIR region. However, this behaviour was limited to very small fractions of top of line hydrates (only a few% water conversion at most), and what happens if hydrate fractions are larger and/or contact the aqueous phase in RGR regions remains unknown.

In simple PVCap-water-gas tests, the formation of top of line hydrates was found to be limited (Mozaffar, 2013), and primarily an occasional inconvenience in terms of interpreting what was happening with respect to hydrate growth in the bulk aqueous phase. Methods were adjusted to reduce unmixed/dead volumes in cells to eliminate this (e.g. by running autoclaves in a horizontal configuration). In this work during the tests on MEG-KHI combinations (Section 3.1.3), it was noted that evidence for top of line hydrate formation appeared to be more frequently observed. As a result, to investigate KHI behaviour in such 'non-ideal' systems (as occurs in real pipelines), tests have been performed on this phenomenon for a PVCap-MEG-natural gas system.

Top of line hydrate tests were undertaken on a 0.5 mass% PVCap (relative to water) and 10.0 mass% MEG (relative to water + PVCap) at a pressure of ~110 bar where CGI behaviour had already been established as part of this work (results presented in Section 3.1.3) . For the purposes of encouraging top of line hydrate formation, the autoclave cell was operating in vertical configuration and the aqueous phase occupied 25% of the cell volume (as opposed to normal 80%) to create a possible dead/unmixed volume at the top of the cell.

Figures 3.27 and 3.28 show example CGI method cooling and heating curves for the 0.5 mass% PVCap / 10.0 mass % MEG top of line system. Also shown in Figure 3.27 is example data for the same system where the experimental set-up was designed to avoid any top of line hydrate formation along with determined CGI boundaries. For the system where top of line hydrate formation is avoided, CGI regions are clear and repeatable, with hydrate growth only occurring when conditions exit the CIR at higher subcoolings.

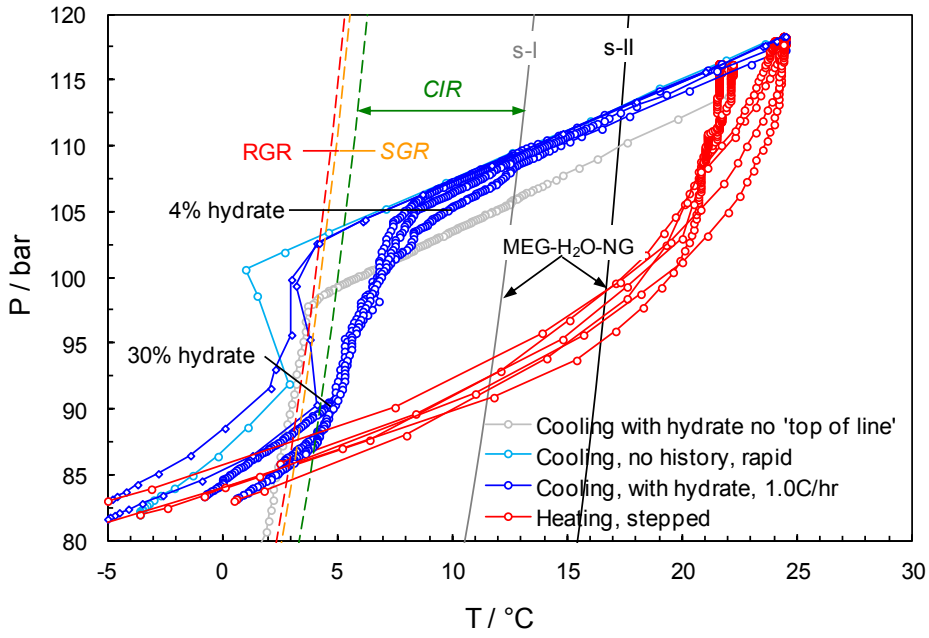

Figure 3.27 Example CGI method cooling and heating curves for 0.5 mass% PVCap (relative to water) and 10.0 mass % MEG (relative to water + PVCap) aqueous with natural gas for top of line hydrate tests. Also shown is example data for the same system where the experimental set-up was designed to avoid any top of line hydrate formation, with CGI boundaries for these tests (applicable to the bulk aqueous phase) shown.

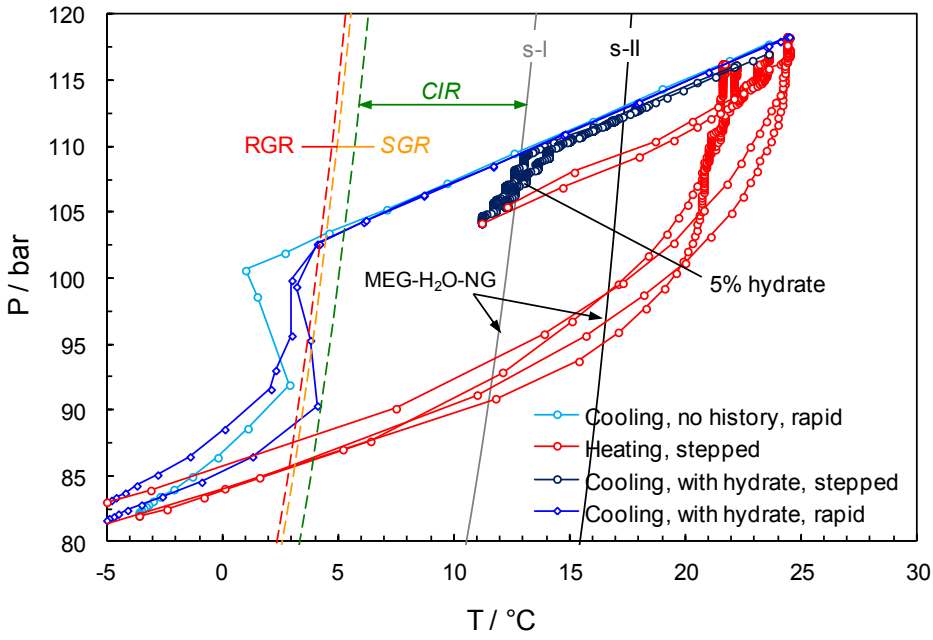

Figure 3.28 Example CGI method cooling and heating curves, including step-cooling run data, for 0.5 mass% PVCap (relative to water) and 10.0 mass % MEG (relative to water + PVCap) aqueous with natural gas for top of line hydrate tests. CGI boundaries shown here are for the no 'top of line' case.

For the top of line encouraging system, results are quite different; while fast cooling with hydrate present results in rapid growth from the bulk aqueous phase at the RGR boundary (for the bulk aqueous phase) as expected, slow cooling with hydrate present runs show considerable hydrate formation (up to 30% water converted) within what should be the CIR region (Figure 3.27). This is most pronounced when conditions enter the s-I stability region for the gas, although step-cooling runs show very slow growth can occur where only s-II hydrates are stable (Figure 3.28).

While tests were conducted in a non-visual cell so it is not possible to know where the observed hydrate formation is occurring, the fact that creating a 'dead/unmixed' volume at the top of the cell has such a dramatic effect on the ability of hydrate to grow in the system strongly implies top of line formation, as has been observed visually in other tests (Nazeri et al., 2012). As noted, this phenomenon does not occur to anywhere near this extent for PVCap only systems, which implies it is likely more related to MEG than to the polymer.

3.3 Conclusions

In this chapter results for the most common thermodynamic hydrate inhibitors including methanol, ethanol and MEG were presented when being applied as a hybrid hydrate inhibition strategy in combination with different KHI polymers specially PVCap. Investigations were carried out using the crystal growth inhibition (CGI) technique developed by Anderson et al. (2011).

CGI region studies on 0.5 mass% PVCap aqueous with different methanol concentrations and natural gas revealed that, in contrast to the previous data for PVCap with methanol and methane where a strongly negative effect of methanol was observed, results for the natural gas system show that methanol acts as a full 'top-up' thermodynamic inhibitor at lower concentrations of 2.5 and 5.0 mass%, with CGI regions increased slightly or preserved. However, increasing the concentration to 25.0 mass% will deteriorate the positive effect and all crystal growth inhibition regions are reduced comparing to PVCap alone. This contrasting behaviour between single and multi-component gas systems - at least at lower concentrations of methanol- strongly suggests methanol involvement in hydrate growth/nucleation, e.g. potentially through temporary cage occupation as opposed to it acting solely within liquid (or gas) phases; as it has a molecular diameter sufficiently small to enter gas hydrate cavities (Shin et al., 2013) and may potentially compete with polymer pendant groups to enter open cages on the crystal surface and encouraging hydrate growth at higher concentrations. Data suggest that for richer gases at least, methanol at lower concentrations could potentially be used as a top-up inhibitor for KHIs and/or KHIs could be used to reduce methanol requirements in terms of hydrate inhibition.

It is clear from work to date that results for PVCap in terms of the effects of various factors are not necessarily directly applicable to other polymers. Therefore other than PVCap, CGI studies on 0.5 mass% T1441 co-polymer in a natural gas system with 5.0 mass% methanol were undertaken and results were contradictory to PVCap. Methanol does not act as a 'top-up' thermodynamic inhibitor for this co-polymer at this concentration; all crystal growth regions are reduced with the exception of a slight shift of the RGR boundary to higher subcoolings at lower pressures. Results for 0.5 mass% T1441 and 25.0 mass% methanol also support the negative effect, as for this concentration of methanol all crystal growth regions are reduced and CIR is totally lost. The total extent of CGI regions for T1441 and 5.0 mass% MeOH were greater than

those for (a similar) natural gas with PVCap and MeOH, but had a smaller CIR with higher growth rates within the SGR region (e.g. large SGR(M) region). For 25.0 mass% MeOH, the total extent of CGI regions were apparently smaller than those for (a similar) natural gas with PVCap and MeOH. As evidenced by the results, T1441 is overall less well performing than PVCap in terms of CGI properties.

In addition to methanol, the ethanol effect on KHI performance was investigated as a potential thermodynamic inhibitor. Low and high concentration systems of 5.0 and 25.0 mass% ethanol were first tested with 0.5 mass% PVCap and natural gas. Results for 5.0 and 25.0 mass% EtOH support previous studies in the methane system (Mozaffar et al., 2014) that ethanol generally has a negative effect on PVCap performance and does not act as a 'top-up' thermodynamic inhibitor; except a slight increase in RGR region extent at 5.0 mass% ethanol, all other regions are reduced. The overall negative effect at higher concentrations of both methanol and ethanol could, to some extent, be explained by PVCap having a higher solubility with increasing alcohol concentration, thus reducing its affinity for surface adsorption on hydrates. In addition to this, ethanol is known to form s-II type gas hydrates at the conditions under study (Anderson et al., 2009) and the ideal stoichiometric ratio for these hydrates would be EtOH·17H2O or 5.56% mole% alcohol aqueous which would equate to 13.1 mass% ethanol. Results for this stoichiometric concentration confirmed the data for the other two concentrations, showing a detrimental effect on PVCap performance. Although ethanol is known to form s-II type gas hydrates at the conditions under study, the ideal stoichiometric concentration of 13.1 mass% ethanol (equal to 5.56% mole% alcohol aqueous) does not correspond to a clear change in CGI region extents, suggesting that if ethanol enclathration does play a role, that role is subtle.

Other than PVCap, a high concentration of ethanol was also examined briefly with 0.5 mass% T1441. Results for 25.0 mass% ethanol with this co-polymer and natural gas at one pressure also indicate a strong negative effect, as the CIR region is totally lost.

Moreover, a simple ethanol + ethane system with stoichiometric concentration of 5.56 mol% ethanol also support the previous data for PVCap and T1441 in various gas systems: that ethanol has a strongly negative effect on PVCap inhibition of hydrate growth. Results are consistent with the emerging picture that the nature of molecules occupying cages being likely the single biggest factor in governing the ability of a particular polymer to inhibit crystal growth as a function of pressure and composition.

The generally greater negative effect of ethanol compared to methanol is likely down to ethanol occupation of hydrate cavities and it may be that partial bonding of the ethanol OH group with the water lattice distorts the latter, making polymer surface adsorption weaker.

The reasons for the observed effects of ethanol and methanol are unclear. But the fact that PVCap has higher solubility at higher alcohol concentration, which reduces its affinity for surface adsorption on hydrates, could not be the only explanation. Because if this is this case, the same behaviour should be observed for PVCap-MEG combinations, yet previous studies show that MEG is generally a 'top-up' thermodynamic inhibitor in methane systems with crystal growth inhibition regions larger or equal to those for PVCap alone, at least up to concentrations of 50 mass% MEG (Mozaffar et al., 2014). CGI studies for MEG-PVCap systems for three MEG concentrations of 5.0, 10.0 and 20.0 mass% with natural gas generally confirm previous results of single component methane system. It is evident from the results that MEG acts primarily as a 'top-up' thermodynamic inhibitor for PVCap and NG; crystal growth inhibition regions are larger or equal to those for PVCap alone, at least up to concentrations of 20.0 mass% MEG. Besides, the combination of MEG + PVCap offers far better inhibition by mass/volume inhibitor than MEG alone as 0.5 mass% PVCap and 20.0 mass% MEG offers complete crystal growth inhibition (CIR region) more than 2 times the thermodynamic inhibition offered by ~20 mass% MEG. Increase in CGI region subcoolings resulting from the MEG+PVCap combination strongly suggest an increase in the strength of polymer adsorption on hydrate crystal surfaces in presence of MEG.

T1441 was another polymer which was studied in the presence of MEG. The total extent of CGI regions for T1441 and 5.0 mass% MEG were apparently smaller than those for (a similar) natural gas with PVCap and MEG, which made it overall less well performing than PVCap in terms of CGI properties. Pressure shows a negative effect on T1441+MEG performance; the CIR is smaller at higher pressure compared to T1441 alone therefore the top-up effect of 5.0 mass% MEG on this co-polymer is no longer the case at least in terms of CIR.

Bio-800 CGI properties were also studied in the presence of 5.0 mass% MEG. The total extent of CGI regions for this bio-KHI were larger than PVCap with the same concentration of MEG and natural gas, but pressure apparently has a negative effect on performance by reducing CIR which was also the case for T1441. Unlike T1441,

although the negative effect of pressure, the top-up effect of 5.0 mass% MEG on CIR is still apparent at higher pressure. However reduction in CIR extent at higher pressures makes it less well performing than PVCap in terms of CIR.

In general, MEG shows less top–up effect on PVCap with increasing concentration (which was also the case for methane systems (Mozaffar et al., 2014)) and on T1441 and Bio-800 with increasing pressure.

Furthermore, some preliminary tests have been conducted on top of line hydrate formation in a 0.5 mass% PVCap- 10.0 mass% MEG system with natural gas. Results revealed that in the presence of a dead/unmixed volume, considerable volumes of hydrate can grow in quite short timescales in a MEG-PVCap system, apparently in the dead volume direct from the vapour phase as 'top of line' hydrates. MEG seems to encourage this to occur, even though MEG is an excellent synergist and top-up inhibitor for KHIs, at least in the bulk aqueous phase. While results are preliminary, findings are very important with respect to potential KHI-MEG (and possibly other KHI-thermodynamic inhibitor) combinations.

CHAPTER 4 – KINETIC HYDRATE INHIBITOR REMOVAL FROM PRODUCED WATER

4.1 Introduction

The main advantage of kinetic hydrate inhibitors is that a very low dosage is required to prevent hydrate formation which cause considerable capital and operating cost savings in comparison to thermodynamic inhibitors. Thermodynamic inhibitors injection rate could be as high as 60 mass %, thus they are normally recovered/reclaimed for re-injection. In contrast to this, kinetic hydrate inhibitors are considered as once through inhibitors.

Despite the low doses required, there are potential problems associated with kinetic hydrate inhibitors injection which include (Anderson et al., 2014):

- Polymer precipitation in MEG reclamation units, causing fouling ('gunking'), a reduction in efficiency and the need for shut down/clean out
- Polymer precipitation when produced waters are re-injected into warm/hot reservoir formations, blocking perforations/pore space and so reducing injection efficiency
- Polymer precipitation in water handling facilities such as storage tanks
- Concerns over polymer biodegradability/regulations with respect to produced water disposal in the natural environment

The active polymer present in KHI formulation is the most problematic component with respect to the above-mentioned issues. KHI formulations normally contain about 20% of active polymer and the remainder is common solvents / synergists such as mono ethylene glycol (MEG) and ethylene glycol butyl ether (EGBE). Polymer solubility in water commonly decreases by increasing temperature and salinity, which can ultimately cause precipitating and possibly leads to fouling at more severe condition.

In order to address the problems associated with active polymer present in KHI formulations, there has been increasing interest in the removal of the polymers from produced waters prior to common treatments (e.g. MEG reclamation) or disposal/re-injection. Various physical, chemical and biological treatment methods such as membrane separation, advanced oxidation, biotreatment and heated centrifugation have

been examined, with the oxidation showing particular promise (Hussain et al., 2012; Adham et al., 2014). Tian and Bailey (2011) also introduced some immiscible solvents in order to avoid polymer precipitation in produced water, but not necessarily removing the polymer from the aqueous phase.

KHI removal could encourage more KHI use as an alternative to thermodynamic inhibitors (TI) which could be a significant concern in terms of operating and capital cost particularly at late reservoir life when water cut is high. In such scenarios, KHI-TI combinations could be another possibility to reduce TI injection dose by 20-40 mass % based on experimental work at Heriot-Watt University (Mozaffar et.al, 2014).

In light of this, during an attempt to develop a method for determining low concentrations of polymer in produced water – research at Hydrafact Ltd. – a simple polymer extraction method from produced water was developed (Anderson et al., 2013). In challenging measurement conditions such as low polymer concentrations, using conventional measuring devices such as High-Performance Liquid Chromatography (HPLC) or Fourier Transform Infrared Spectroscopy (FTIR) could be problematic. Based on this, the initial idea was to find a chemical which caused significant displacement of polymer from the aqueous phase and concentrating in the treatment chemical (TC). With the polymer enriched in the TC, the polymer content of the TC then could be measured accurately. With a known mass of TC, known mass of produced water and calibration for partitioning as a function of polymer content, then the polymer content of the original solution could in theory be determined from measurement of the polymer content of the TC following contact and separation from the produced water phase (Anderson et al., 2014).

In the course of finding an appropriate solvent, different treatment chemicals were tested and one family was found to apparently displace almost all (depending on the sample used) PVCap from the aqueous phase. To calculate the amount of polymer displacement, calibrations were carried out and it was found that up to 100% of the polymer had been displaced into the TC. Subsequent drying of the separated aqueous phases confirmed this; within accuracy up to 100% of the polymer had been removed from the aqueous phase at ambient conditions (Anderson et al., 2014). The TCs belong to the family of fatty alcohols, with the main focus on linear chain normal hexanol, heptanol and octanol which have been patented as the first group of polymer removal solvents (Anderson et al., 2013). The general features of fatty alcohols are that they are:

- Common, naturally occurring chemicals
- Produced synthetically in large volumes for several industrial purposes
- Of low toxicity (typically known as irritants), low volatility
- Safe to handle
- Having good biodegradability

The main desirable feature however is their very low solubility in water in the sense that some of them could be considered as immiscible in water. In addition to having very little solubility in water, fatty alcohols are excellent solvents for KHI polymers so that the amount required for polymer (mainly PVCap) displacement from water phase is very low. Table 4.1 summarizes the main physical properties of the most effective n-fatty alcohols as treatment chemicals. With the test on a number of fatty alcohols showing good polymer displacement properties, formulating different mixtures with respect to improving displacement effectiveness, density and viscosity seems to be promising.

Table 4.1 Boiling point, density and aqueous solubility of n-fatty alcohols as a function of their carbon numbers (C_n).

C_n	Description	Boiling point (°C)	Density (g/cm^3)	Aq. solubility (mass %)
5	1-pentanol	138	0.811	2.15
6	1-hexanol	157	0.814	0.59
7	1-heptanol	176	0.819	0.17
8	1-octanol	195	0.824	0.05
9	1-nonanol	214	0.827	0.01
10	1-decanol	233	0.829	< 0.01

4.2 Experimental Method

As mentioned above, normally the required dosage of treatment chemicals for polymer displacement from produced water is very low. The typical dose would be about at least two parts (mass or volume) per about one part polymer or two part TC per five parts KHI formulation (polymer is typically about 20% of a KHI formulation) to yield an immiscible TC liquid phase capable of extracting the polymer whilst remaining fluid (Anderson et al., 2014). With such a low dosage required, the basic procedure for polymer extraction is relatively simple and straightforward. Preliminary studies have focused on PVCap due to it being one of the most effective and widely used KHI

polymers and for all polymer removal tests in this chapter, normal TC dose is 4 parts per 1 part polymer to yield an immiscible separated polymer-rich TC phase of volume and viscosity similar to the original KHI. The following experimental procedure has been used to determine removal efficiency:

- KHI solutions to be treated are prepared gravimetrically at a known mass % of polymer aqueous (Figure 4.1 A)

- The treatment chemical is then injected into the aqueous solution which is being mixed in a moderately turbulent conditions and this causes immediate clouding of the aqueous phase as polymer is displaced from solution (Figure 4.1 B)

- After a short period of mixing, which enhances polymer displacement to the TC phase, the mixture is left static to separate by gravity. Commonly, more than 80 mass% of the TC phase readily separates by gravity over the first 10 minutes at static conditions due to immiscibility and different densities; the TC+polymer phase is typically of lower density so moves upwards. However, depending on the system and TC chemistry, a moderate fraction of the TC+polymer phase may remain suspended as a cloudy, microdroplet emulsion in the aqueous phase, requiring additional physical separation (Figure 4.1 C)

- If gravity separation is not sufficient to clear out the TC+polymer mixture from the aqueous phase, centrifugal separation of the microdroplet emulsion is then used and has shown to be effective to achieve full physical separation (Figure 4.2 A)

- Coalescing separation has also proven particularly effective as another option for full separation. In some cases the cloudy aqueous phase is simply passed through a fine polyurethane foam which can result in complete removal of remnant TC+polymer microdroplets as they coalesce on foam surfaces, producing a clear, polymer-free aqueous phase (Figure 4.2 B)

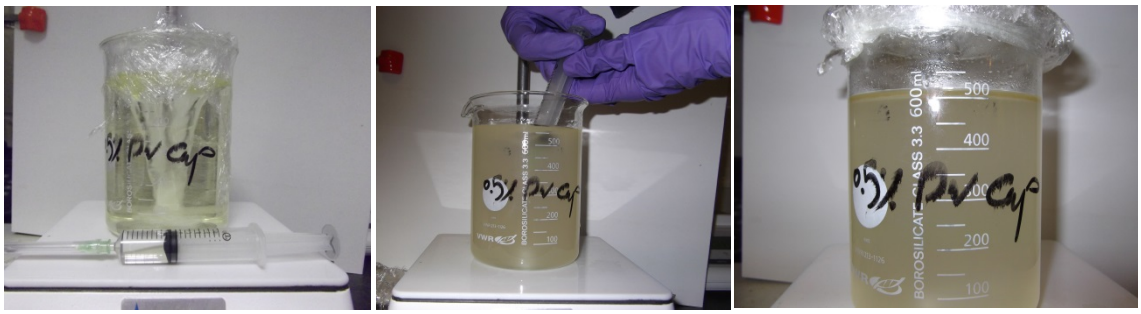

A B C

Figure 4.1 (A) 0.5 mass% PVCap / 99.5 mass% water being mixed turbulently by a magnetic stirrer prior to TC injection; The TC is the clear liquid in the syringe. (B) Injection of the TC into the 0.5 mass% PVCap / 99.5 mass% water under turbulent mixing conditions. (C) TC and 0.5 mass% PVCap / 99.5 mass% water solution following TC injection/mixing after 10 minutes at static conditions. The bulk of the TC + separated polymer (which has turned the TC yellow/orange in colour at the top of the aqueous phase) has gravity separated (Anderson et al., 2014).

A B

Figure 4.2 (A) Centrifuge separated TC+PVCap and aqueous phases, in this case for initial aqueous solutions containing 25 mass% MEG / 0.5 mass% PVCap / 74.5 mass% water. The yellow-orange PVCap-rich separated TC phase is seen sitting on top of the treated MEG-water phase. (B) Cloudy aqueous phase with remnant TC+PVCap microdroplets being passed through a simple polyurethane foam coalescing medium. Clear, polymer-free water flows freely out of the foam as the TC+PVCap coalesces on foam surfaces.

Following centrifugation, the removal level could be determined either by a gravimetric method or using UV-Vis. Using gravimetric method, the 'treated' water is drained, weighed, and then oven dried to evaporate the water. Once the water has been dried off, the sample is weighed again to determine the mass of any polymer which was not removed by treatment. All steps of the experimental procedure for tests reported in this chapter were conducted at ambient temperature and pressure and the removal levels reported are determined using the gravimetric method, unless specified.

The second approach to determine the remaining polymer level in the aqueous phase is using a high precision Hitachi U-3010 dual beam UV-Vis spectrometer. The strong absorbance of UV by double bonds makes UV-Vis spectroscopy ideal for detection of polymers such as PVCap in water, particularly as water itself is a poor UV absorber (as opposed to Infra-Red (IR) where the opposite is the case; water strongly absorbing but polymers only weakly). In light of this, calibrations were undertaken to assess how accurately UV-Vis could be used to determine the PVCap concentration of aqueous solutions. Figure 4.2 shows UV-Vis spectra for different PVCap concentrations in a water solution, with water as baseline.

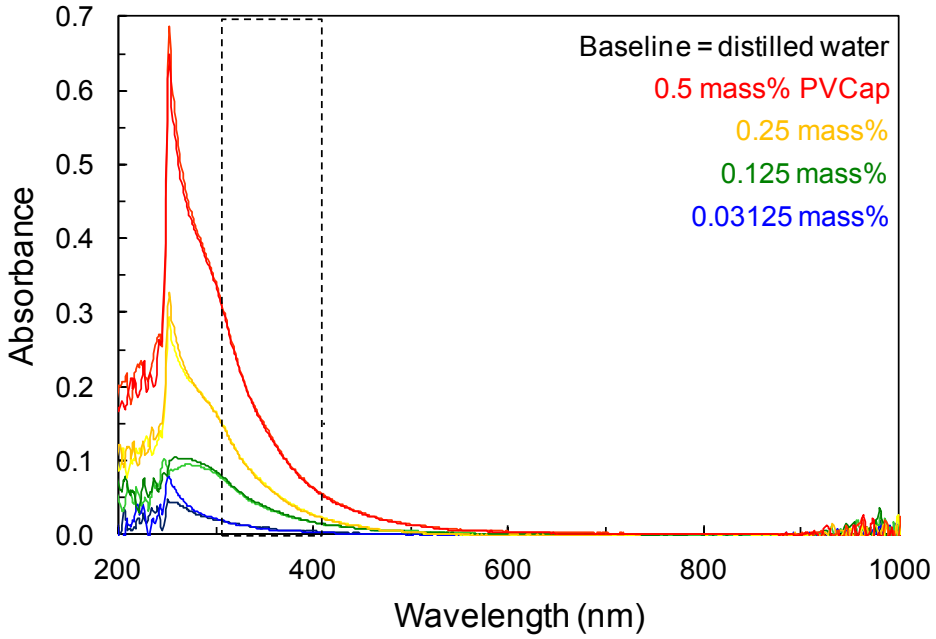

Figure 4.3 (A) UV-Vis spectra for different PVCap concentrations in water (water baseline) showing the region where calibration for aqueous concentration is possible (Anderson et al., 2014).

As can be seen using the UV-Vis technique, the concentration of PVCap even at very low levels (0.03125 mass% or less) could be readily detected from absorbance in the range 300-400 nm wavelength. In light of this, calibrations were undertaken to assess how accurately UV-Vis could be used to determine the PVCap concentration of aqueous solutions.

Figure 4.4 shows an example calibration for PVCap in distilled water using absorbance at 320 nm. Calibration data show the maximum absolute deviation on test samples to be ± 0.004 mass% PVCap (Anderson et al., 2014). Thus, for an initial solution containing 0.5 mass% PVCap, post treatment, the effectiveness of removal can be assessed to within ± 0.8%.

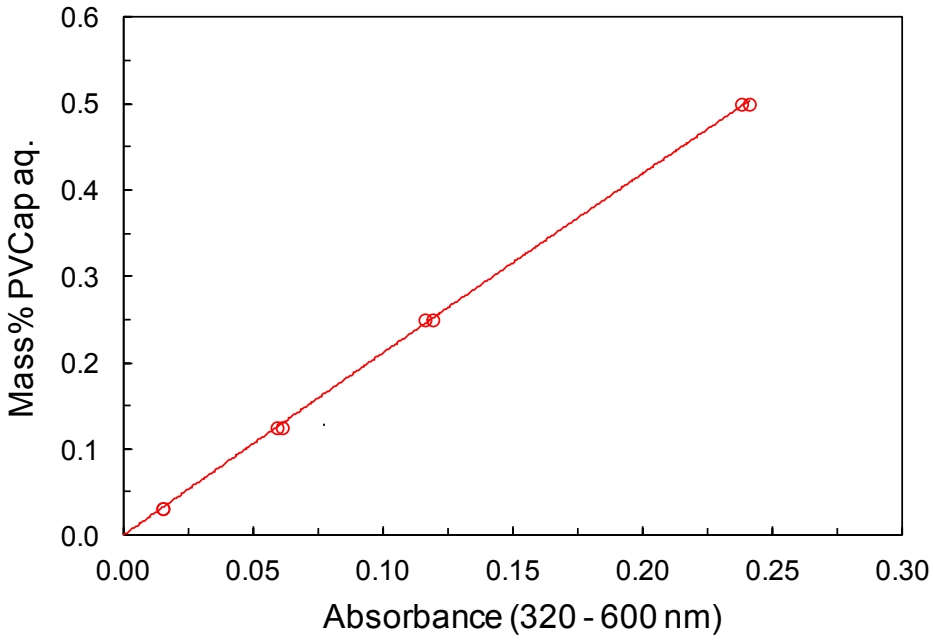

Figure 4.4 UV-Vis spectra calibration (absorbance at 320 nm compared to baseline at 600 nm wavelength) derived for PVCap-water solutions (Anderson et al., 2014).

All removal tests reported in this chapter are performed at standard temperature and pressure; however treatment at higher temperature – such as those associated with MEG regeneration – could improve removal levels. Some initial tests showed that high pressure can also aid physical separation. Figure 4.5 shows an image of 0.5 mass% PVCap with 2.0 mass% 1-octanol relative to water under 70 bar North Sea natural gas pressure at 20 °C in a visual autoclave cell at static conditions. During mixing, the TC+polymer phase was readily entrained to yield a cloudy suspension in the aqueous phase. When mixing was stopped, the amber 1-octanol + PVCap phase gravity-settled within a short timescale (almost fully clear in 10-20 minutes). It is suspected that this rapid gravity settling may be due to gas dissolution in the 1-octanol-PVCap phase, aiding buoyancy (and potentially altering water-TC+PVCap phase interfacial properties), thus physical separation. While findings are preliminary, results suggest that treating the aqueous phase prior to de-gassing may be beneficial in terms of physical separation part of the polymer removal process.

The PVCap used in all experiments was Luvicap-EG base polymer (K-value = 25-8, average MW = 7000) supplied by BASF, with the ethylene glycol solvent removed by vacuum oven drying. Purity of MEG used was 99.5% and supplied by Fluka Analytical. Purities of 1-octanol and 1-heptanol used as main treatment chemicals, were 99% and 98% and supplied by Sigma-Aldrich. Distilled water was used in all tests.

Figure 4.5 Image of 0.5 mass% PVCap with 2.0 mass% 1-octanol relative to water under 70 bar North Sea natural gas pressure at 20 °C in a visual autoclave cell (window is ~15 mm across). When mixing is stopped, the amber 1-octanol + PVCap phase gravity settles within a short timescale (almost fully clear in 10-20 minutes).

4.3 Results and Discussions

Since initial discovery, work has focussed on confirming the ability of the TC family to displace PVCap from aqueous solutions and the effect of various factors on the effectiveness of polymer removal from aqueous solution have been investigated, including the effect of TC type and quantity, presence of liquid hydrocarbons, scale inhibitor, corrosion inhibitor, common pipeline chemicals and KHI solvents etc. Work has primarily focussed on PVCap due to it being one of the most effective, widely used and studied KHI polymers. Initial tests on other KHI polymers/formulations have shown some success, however so far it seems to be most effective for PVCap-type chemistry. Given that MEG and PVCap show excellent synergism with respect to kinetic hydrate inhibition, with small fractions of PVCap (0.5 to 1.0 mass%) offering the equivalent inhibition of 10's of mass% MEG (Mozaffar et.al, 2014; Tohidi et al., 2014), work has also focussed particularly on potential use of the technology for polymer removal where PVCap is used to significantly reduce MEG volumes required for hydrate inhibition.

4.3.1 Effect of polymer type and concentration

As mentioned above, work has primarily been focussed on PVCap as KHI polymer and method effectiveness was evaluated for solutions at different PVCap concentrations. For this, the technique has been found to be effective in removing up to 100% PVCap from the aqueous phase at ambient temperature and pressure, depending on the nature of the PVCap and sample average molecular weight in particular. Table 4.2 summarizes removal results for a range of PVCap concentrations using 1-octanol as the treatment chemical and in the presence of salt. Results suggest that the method is equally effective in pure water (e.g. condensed water) and NaCl solutions (produced water). Produced water salinity enhances KHI performance but can cause polymer drop out from the aqueous phase when the salt level is high which, means presence of salt in the system can possibly even promote removal performance. For all the tests reported here the dosage of added TC is 4 parts per 1 part polymer in mass.

Table 4.2 Polymer mass % removed from different PVCap concentrations treated by 1-octanol and in presence of salt.

Solution treated (values in mass %)	Treatment Chemical	% PVCap Removed
0.10 % PVCap	1-octanol	88-100
0.25 % PVCap	1-octanol	88-100
0.50 % PVCap	1-octanol	88-100
0.50 % PVCap+3.5 % NaCl	1-octanol	90

While focused on PVCap, the removal technique also showed some degree of success on some other commercial polymers and KHI formulations, suggesting the technique is not confined to PVCap alone. Figure 4.6 shows a comparison of removal effectiveness between different polymer types.

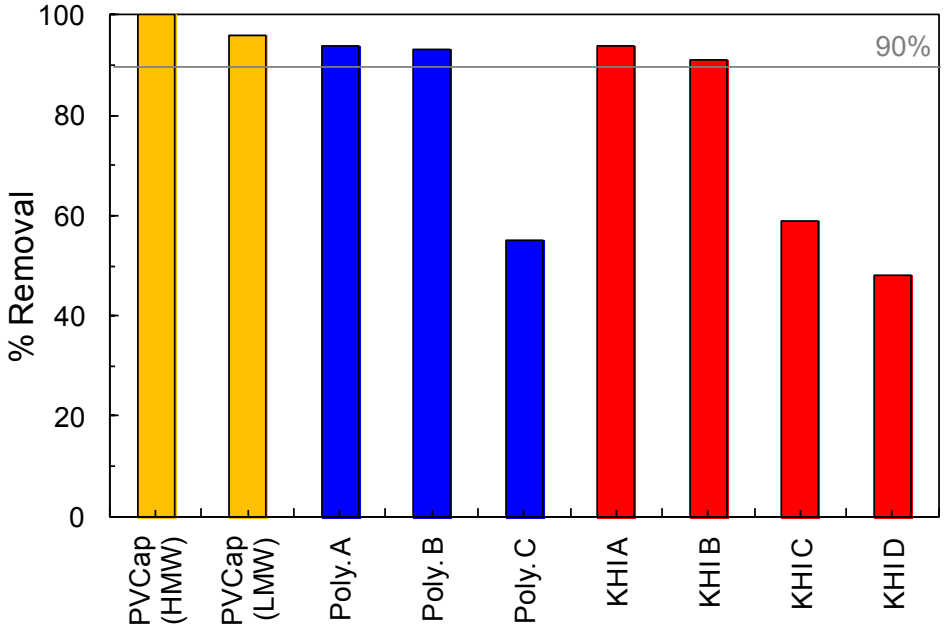

Figure 4.6 Comparison of Removal efficiency between PVCap, three commercial base polymers (A,B,C) and four commercial KHI formulations (A,B,C,D) (Anderson et al., 2014).

In some cases after PVCap solution treatment, a small fraction of some remnant solids have been detected (removal efficiencies were less than 100%) which is suspected to be either:

- Low molecular weight polymer strands which have a much higher water solubility
- Contaminants in polymer samples, e.g. unpolymerised monomers

To both examine whether the above would precipitate out of solution at higher temperatures and to confirm removal of PVCap from solutions, some initial cloud point studies on treated and untreated samples have been performed. These tests confirmed the effectiveness of the method for polymer removal.

In these tests, both treated and untreated samples were heated up to 90°C. Untreated samples showed the typical behaviour of polymer clouding, drop-out and coagulation at moderate temperatures (aqueous PVCap cloud point is normally around 40 °C). Moderate amounts of MEG do not change this behaviour greatly unless systems become MEG-dominated solution when the cloud point can increase significantly. In contrast, treated fluids typically remained clear up to the maximum temperature of the apparatus used (90 °C). Only where the treatment was not completely effective due to some lower molecular weight strands potentially remaining (as mentioned above), slight clouding

was observed at higher temperatures, but with no solid drop-out/surface adherence/coagulation. Some examples are shown in Figures 4.7 and 4.8.

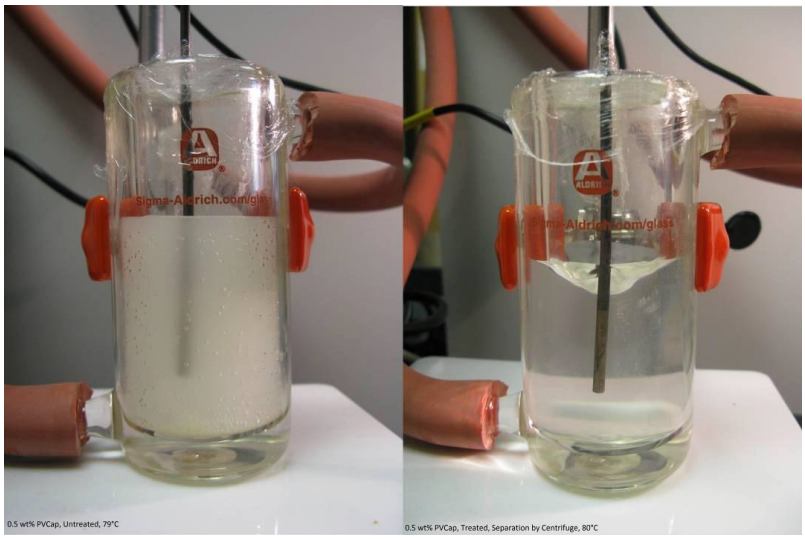

Figure 4.7 Images of 0.5 mass% PVCap / 99.5 mass% water at 80 °C (left) and the same solution post polymer-removal treatment also at 80 °C (right). In the untreated case, effectively complete polymer drop-out/clouding has occurred with coagulation of settled polymer causing the stirrer to become stuck. In contrast, the treated fluid remains clear due to the PVCap having being removed (Anderson et al., 2014).

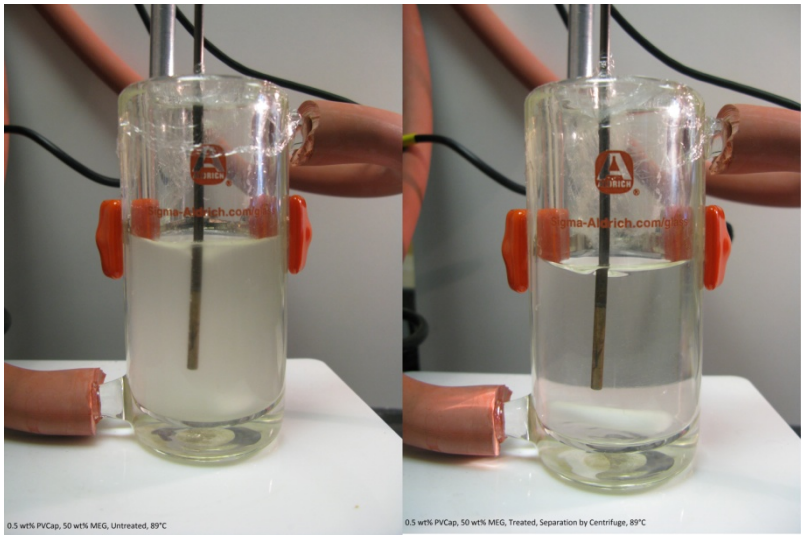

Figure 4.8 Images of 50 mass% MEG / 0.5 mass% PVCap / 49.5 mass% water at 89 °C (left) and the same solution post polymer-removal treatment also at 89 °C (right). In the untreated case, polymer drop-out/clouding is observed whereas the treated fluid remains clear due to the PVCap having been removed (Anderson et al., 2014).

4.3.2 Effect of treatment chemical type

As noted, the fatty alcohols family with the ability of polymer removal contains a range of members, all with similar physiochemical properties. In the previous section, removal tests were focused on 1-octanol as TC (that initially discovered as having excellent PVCap displacement properties). But other members of the TC family with different carbon numbers have also been examined for effectiveness.

Table 4.3 shows mass% PVCap polymer removed from aqueous solution by the TC method for a range of fatty alcohols from 1-pentanol to 1-decanol. Figure 4.9 shows these data compared to TC aqueous solubility (Table 4.1). In all the tests reported here the dosage of added TC is 4 parts per 1 part polymer (in mass).

Table 4.3 Mass % polymer removed from PVCap aqueous solutions by TC method for fatty alcohols with different carbon number.

Solution (values in mass %)	Treatment Chemical (by mass)	% PVCap Removed
0.5 % PVCap	100% 1-pentanol	93
0.5 % PVCap	100% 1-hexanol	96
0.5 % PVCap	100% 1-heptanol	97
0.5 % PVCap	100% 1-octanol	95
0.5 % PVCap	100% 1-decanol	89

As can be seen, 1-pentanol to 1-octanol (and likely 1-nonanol) all show greater than 90% PVCap removal from aqueous solution. These preliminary results suggest that 1-hexanol to 1-octanol are the most effective at greater than 95% displacement. As mentioned before, suspected remnant polymer is likely to be low molecular weight strands with a higher miscibility with water; PVCap samples invariably containing a range of molecular weights.

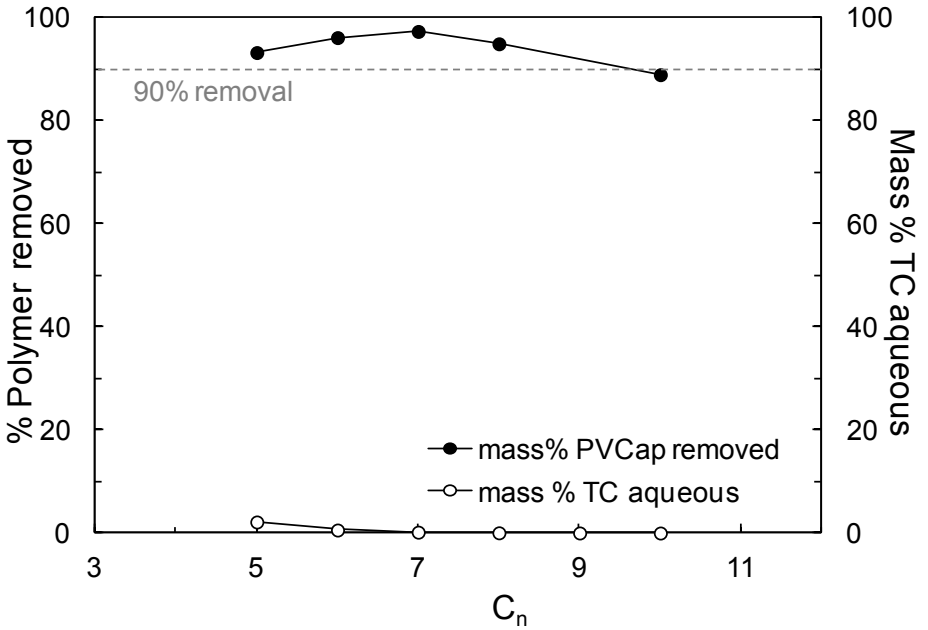

Figure 4.9 Mass% PVCap polymer removed from aqueous solution by the TC method for TCs of different carbon numbers compared to TC aqueous solubility.

4.3.3 Effect of treatment chemical quantity

In the previous section, different members of the fatty alcohols family with different molecular weights have been examined for effectiveness. Although this family shows quite high effectiveness, there is a concern about the amount of TC required to achieve a desirable level of removal. Based on this, evaluation work on the effect of TC quantity has been done using 1-heptanol (TC7), which has excellent PVCap displacement properties and very little water solubility, as the treatment chemical. In addition to chemical partitioning, good physical separation of the water and the TC+polymer phase is required for the treatment to work well within the context of fluids processing. By using 1-heptanol as the treatment chemical, physical separation can occur readily due to gravity or quickly during centrifuge.

Table 4.4 shows the mass% PVCap removed from aqueous solution by the TC method for 1-heptanol at different quantities. This data is also shown in Figure 4.10. As can be seen, TC7 shows greater than 96% PVCap removal from aqueous solution by adding as little as 1 mass% treatment chemical relative to water. It is clear from the results that no polymer removal is achieved until added 1-heptanol reaches its saturation point in aqueous phase at ~0.175 mass%.

Table 4.4 Mass% PVCap polymer removed from aqueous solution by the TC method for 1-heptanol at different quantities.

Solution treated (Values in mass %)	Added 1-heptanol relative to water (by mass)	% Polymer removed
0.5 % PVCap	0.05%	0.0
0.5 % PVCap	0.1%	0.0
0.5 % PVCap	0.175%*	25.6
0.5 % PVCap	0.5%	74.0
0.5 % PVCap	1%	96.7
0.5 % PVCap	2%	97.7
0.5 % PVCap	3%	97.7

*1-heptanol aqueous solubility

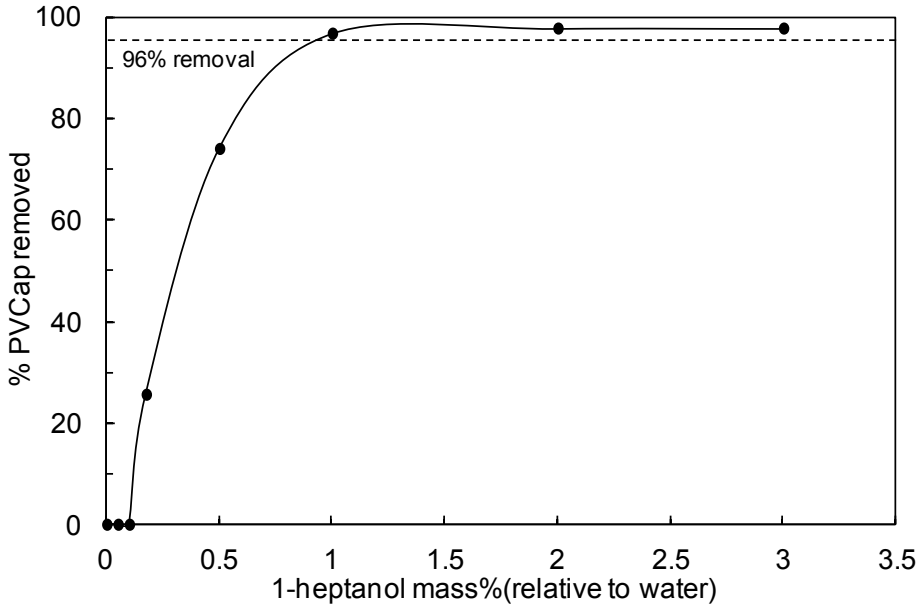

Figure 4.10 Mass% PVCap polymer removed from aqueous solution by the TC method for 1-heptanol at different quantities.

4.3.4 Effect of liquid hydrocarbons

Produced waters commonly contain trace liquid hydrocarbons either in solution at low levels or carried over as immiscible droplets in suspension. The TC family are miscible with liquid hydrocarbons and while it is envisaged that treatment would be applied post water/oil separation, it is likely that they will mix with – and potentially be affected by – small volumes of liquid hydrocarbons.

Initial tests were carried out on the effect of heptane – simulating condensate – on TC performance. To simulate extremes, TCs were mixed with varying levels of heptane and the polymer removal (displacement to the TC + heptane phase) properties evaluated. Results are reported in Table 4.5. Figure 4.11 shows mass% PVCap removed from aqueous solution by the TC method as a function of heptane content of the Treatment Formula (TF); the remainder of the TF in this instance being 1-heptanol. In all the tests reported here the dosage of added TC is 4 parts per 1 part polymer (in mass).

Table 4.5 Mass% PVCap polymer removed from aqueous solution by the TC method in presence of heptane in TC formula for two TCs and relative 1-heptanol/heptane combinations.

Solution treated (Values in mass %)	Treatment formula (by mass)	% Polymer removed
0.5 % PVCap	100.0 % 1-heptanol	97.7
0.5 % PVCap	50.0% 1-heptanol / 50.0% heptane	93
0.5 % PVCap	37.5% 1-heptanol / 62.5% heptane	87
0.5 % PVCap	25.0% 1-heptanol / 75.0% heptane	53
0.1 % PVCap	50.0% 1-decanol / 50.0% heptane	87

To further investigate the effect of liquid hydrocarbons, a real condensate (typical North Sea condensate) was tested and the polymer removal efficiency evaluated using 1-heptanol as TC. Results are reported in Table 4.6. The mass% PVCap removed from aqueous solution as a function of condensate content of the Treatment Formula (TF) is also shown in Fig 4.11 along with results of adding heptane to treatment formula.

Table 4.6 Mass% PVCap polymer removed from aqueous solution by the TC method for 1-heptanol at different condensate levels.

Solution treated (Values in mass %)	Treatment formula (by mass)	% Polymer removed
0.1 % PVCap	100.0% 1-heptanol	97.7
0.5 % PVCap	50.0% 1-heptanol / 50.0% cond.	92.7
0.5 % PVCap	37.5% 1-heptanol / 62.5% cond.	85.5
0.5 % PVCap	25.0% 1-heptanol / 75.0% cond.	70.5
0.5 % PVCap	7.5% 1-heptanol / 92.5% cond.	16.0

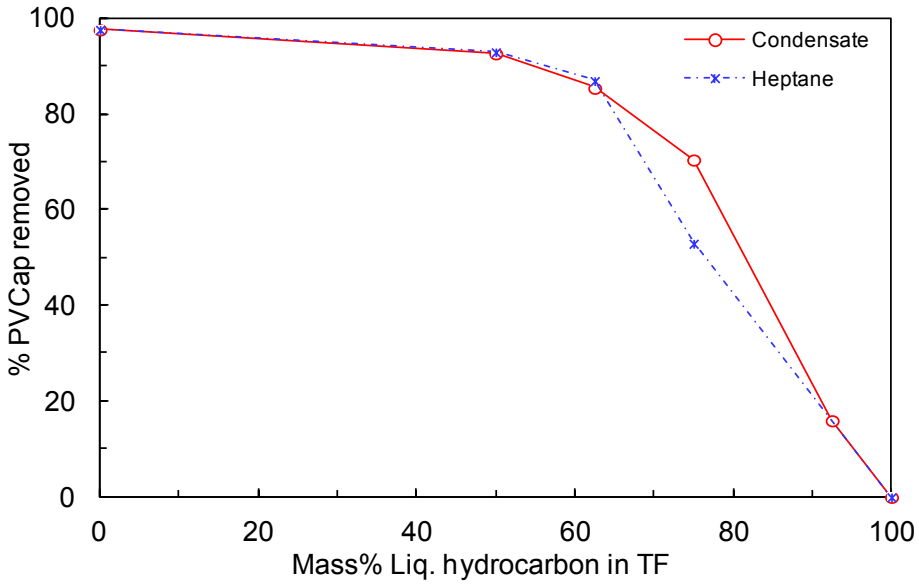

Figure 4.11 Mass% PVCap polymer removed from aqueous solution by the TC method as a function of condensate/heptane content of the Treatment Formula (TF); the remainder of the TF being 1-heptanol.

As can be seen, for both heptane and condensate present in the treatment formula, up to quite high levels of heptanes/condensate – up to 50% by mass relative to TC − the TC remains very effective, removing 90% and more of the PVCap from solution. Above this level of heptane/condensate, performance is reduced as the miscibility of the KHI polymer in the TC + heptanes/condensate phase reduces. This result suggests trace hydrocarbons should not present a problem for the TC treatment.

The observed behaviour also has some further benefits. The addition of heptane to the TC had the effect of reducing the TF phase density and thus the TF + polymer phase density. This aided considerably in the physical phase separation of the TC + polymer (+ heptane = TF) phase from the treated water both under gravity and centrifugal separation situations.

A further benefit is that liquid hydrocarbons are of lower cost than the TC (although TCs are not expensive themselves being relatively simple to produce) meaning a TC formulation could potentially be reduced in cost while providing greater ease of physical separation from treated water.

4.3.5 Effect of common KHI solvents and thermodynamic hydrate inhibitors

Methanol and ethylene glycol are the two most common thermodynamic hydrate inhibitors in addition to being used as solvents in KHI formulations and as a 'top-up' inhibitor to increase the subcooling to which KHIs can be used. Results for TC performance in the presence of methanol are shown in Table 4.7. Tests demonstrate that the TC removal effectiveness, even in the presence of high concentrations of methanol is still good, but less at higher concentrations apparently with 78% removal at 50 mass% methanol aqueous (Figure 4.12).

To further evaluate the effect of thermodynamic hydrate inhibitors removal tests were done in presence of different concentrations of mono ethylene glycol (MEG) using 1-octanol as the treatment chemical. Results are presented in Table 4.7. As shown in Figure 4.12, TC is able to remove PVCap effectively even in the presence of quite high concentrations of MEG and methanol; at 50% MEG about 90% of the PVCap is still removed. At higher MEG concentration of 75 mass% − equal to 46.5 mole% − however, there was a slight reduction in effectiveness but not a huge effect.

Table 4.7 Mass% PVCap polymer removed from aqueous solution by the TC method for different thermodynamic inhibitors and KHI solvents.

Solution treated (Values in mass %)	Treatment chemical (by mass)	% Polymer removed
0.50 % PVCap+25 % Methanol	1-octanol	94
0.50% PVCap+50 % Methanol	1-octanol	78
0.50 % PVCap+25 % MEG	1-octanol	95
0.50% PVCap+50 % MEG	1-octanol	89
0.50% PVCap+75 % MEG	1-octanol	85
0.50% PVCap+3.5 % NaCl+10 % MEG	1-octanol	79*
0.50% PVCap+3.5 % NaCl+20 % MEG	1-octanol	72*
0.50% PVCap+2% % Ethylene glycol butyl ether	1-heptanol	99
0.50% PVCap+2% % Ethylene glycol butyl ether	50% 1-heptanol/ 50% heptane	96

*Results from UV-Vis spectrometer

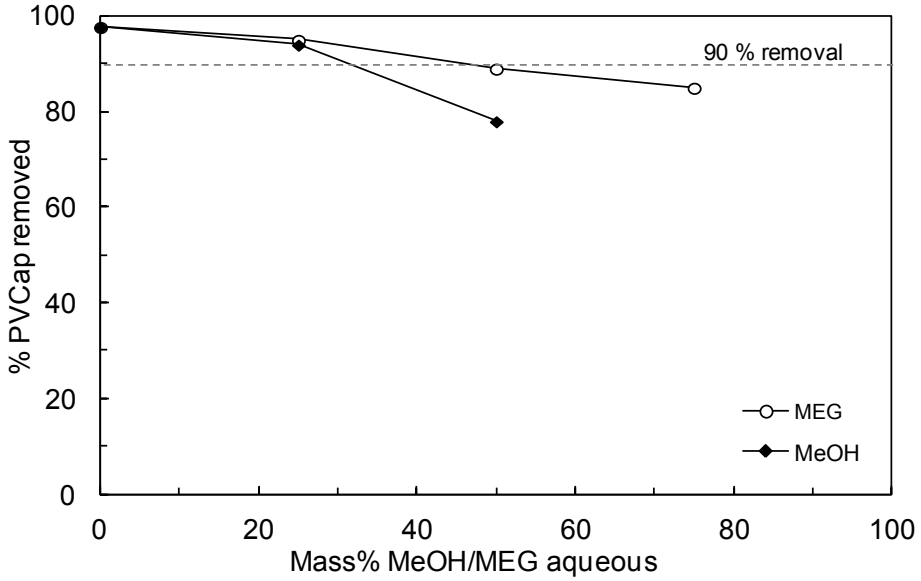

Figure 4.12 Mass% PVCap polymer removed from aqueous solution by the TC method as a function of aqueous methanol (MeOH) and MEG concentration for 1-octanol.

With respect to water salinity, previous results showed that salt does not affect the TC removal effectiveness and can even promote higher removal levels. Based on this and findings on the effect of MEG presence in the system, some tests were done to evaluate the effect of different MEG concentrations present in saline systems. Although salt showed some improvements on removal efficiency, adding MEG to the salt systems appears to have slightly negative effect on removal performance. Results are summarized in Table 4.7. It should be mentioned that in this case removal levels were determined using the UV-Vis method (as described in Section 4.2).

Some tests have also been carried out on the effect of the TC treatment in the presence of ethylene glycol butyl ether (EGBE or 2-butoxyethanol). This was examined because PVCap is supplied by vendors as a KHI formulation in both MEG and EGBE, with both being good synergists for KHI polymers in terms of inhibition performance. Tests were performed for 2.0 mass% EGBE with 0.5 mass% PVCap simulating a simple KHI polymer + synergist formulation dosed at 2.5 mass% aqueous. As shown in Table 4.7, the EGBE was found to have no effect on TC performance at levels that might be expected in produced waters.

4.3.6 Effect of scale and corrosion inhibitors

Scale and corrosion inhibitors (SI and CI respectively) are the two most common pipeline chemicals in the oil and gas industry. To assess the possible effect they may have on removal effectiveness, various commercial scale and corrosion inhibitors were studied with different treatment chemicals. Table 4.8 shows the results for mass% PVCap polymer removed by the TC method for various TC formulations at different levels of SI and/or CI in the aqueous phase, results are also summarised in Figure 4.13. As can be seen, neither the CI nor the SI appear to have any significant impact on TC performance for the concentrations tested. Only at higher, less typical concentrations of CI (≥1000 ppm) and/or SI (≥200 ppm), did performance reduce below 90%.

Table 4.8 Mass% PVCap polymer removed from aqueous solution by the TC method for different SIs and CIs at different levels.

Solution treated (Values in mass %)	Treatment chemical (by mass)	% Polymer removed
0.5 % PVCap, 70 ppm SI-A	1-heptanol	99
0.5 % PVCap, 200 ppm SI-A	1-heptanol	89
0.5 % PVCap, 50 ppm SI-A	50% 1-heptanol / 50% heptane	93
0.5 % PVCap, 230 ppm SI-A	50% 1-heptanol / 50% heptane	85
0.5 % PVCap, 50 ppm SI-A	1-octanol	95
0.5 % PVCap, 50 ppm SI-A, 200ppm CI-B	1-octanol	94
0.5 % PVCap, 180 ppm SI-B	1-heptanol	94
0.5 % PVCap, 50 ppm SI-C	1-heptanol	90
0.5 % PVCap, 220 ppm SI-C	1-heptanol	89
0.5 % PVCap, 200 ppm SI-D	1-heptanol	94
0.5 % PVCap, 220 ppm SI-E	1-heptanol	94
0.5 % PVCap, 1020 ppm CI-A	1-heptanol	91
0.5 % PVCap, 1000 ppm CI-B	50% 1-heptanol / 50% heptane	86

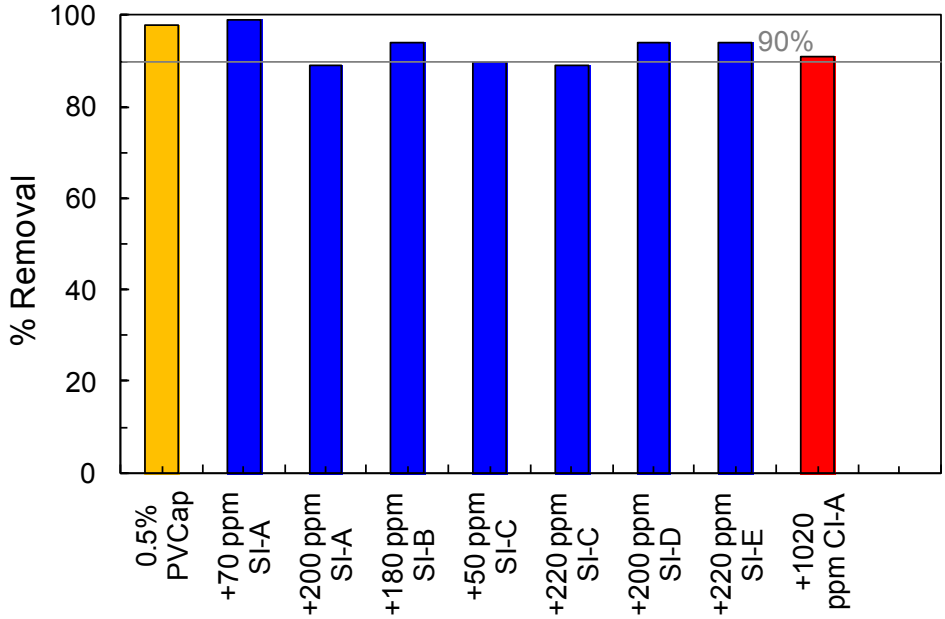

Figure 4.13 Mass% PVCap removed from aqueous solution in presence of different commercial corrosion and scale inhibitors using 1-heptanol as treatment chemical.

4.3.7 Polymer removal from liquid hydrocarbons

As mentioned earlier fatty alcohols are soluble in liquid hydrocarbons. Thus in the pipeline systems containing liquid hydrocarbons, in the case of using treatment chemical as KHI polymer carrier solvents e.g. to create an immiscible KHI (Chapter 5), polymer can transfer to the TC-liquid hydrocarbon phase. In such a case, the liquid hydrocarbon could be contaminated by both the TC and polymer. While the TC itself is less of a concern (hydrocarbon-like with high boiling point and low vapour pressure), the polymer could be, in terms of liquid hydrocarbon processing. Hence some initial tests were carried out to see if PVCap could be removed from TC-hydrocarbon mixtures by MEG washing.

As concluded in Section 4.3.4, liquid hydrocarbons up to 50 mass% - relative to TC – don't show significant effect on treatment chemical removal properties, and polymer displacement to the TC phase for both heptane and condensate case is more than 90%. By increasing the amount of liquid hydrocarbon to more than 50%, polymer tends to come out of the TC-hydrocarbon phase. Therefore, one possibility for washing polymer out of TC-hydrocarbon could be contacting the mixture with ethylene glycol, polymers having an affinity for MEG that hydrocarbons do not (very low solubility in MEG).

In light of this, some tests have been carried out on the effect of heptane on polymer displacement from TC-heptane mixtures to MEG. Initially 10 mass % PVCap in 1-heptanol solution was mixed with different levels of heptane in the presence of high MEG level (74 mass % relative to TC) and polymer displacement to the MEG phase evaluated. As detailed in Section 4.2 a Hitachi U-3010 dual beam UV-Vis spectrometer was used for determining PVCap concentration in MEG. Results are reported in Table 4.9.

Table 4.9 Mass% PVCap in MEG phase as a result of contacting 10 mass% PVCap in 1-heptanol solution with heptane in presence of 74 mass% MEG relative to TC.

Heptane (mass %)	PVCap in MEG (mass%)	% PVCap transferred to MEG
20	1.1	28.3
40	2.5	66.0
50	3.0	78.0
60	3.7	95.0

After initial tests showing promising results, further tests have been carried out on lower MEG levels (50 mass % relative to TC) to simulate a commercial (e.g. immiscible) KHI formulation (20 mass% polymer in MEG). In these set of tests, 20 mass% PVCap in 1-heptanol solutions were contacted with different levels of heptane in the presence of MEG, and polymer concentrations in MEG were measured by FT-IR.

Figure 4.14 shows mass% PVCap in the MEG phase as a function of mass % heptane added to the solution (relative to TC) for both MEG concentrations and also mass% of PVCap recovery to the MEG phase for higher MEG content (74 mass %).

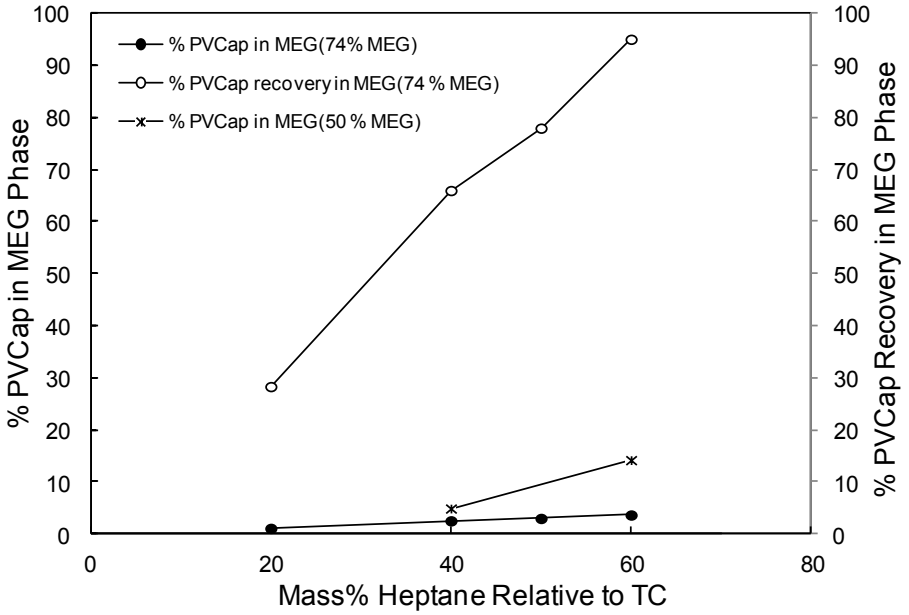

Figure 4.14 Mass% PVCap polymer in MEG for 50 and 74 mass % MEG contacting with 10 and 20 mass% polymer in 1-heptanol solution and mass % PVCap recovery in the MEG phase for 74 mass % MEG as a function of heptane content.

As can be seen, at levels of 60% by mass of heptane - relative to TC – more than 90% of the PVCap is removed from the solution and polymer concentration is increasing in the MEG phase. However, for calculating polymer recovery in the MEG phase it has been assumed no MEG is present in TC-Heptane phase since it was not detectable at higher MEG level. At the lower MEG level however, the amount of MEG dissolved in the top phase specifically when contacted with lower than 40 mass % heptane was noticeable. But increasing the heptane level to 60 mass % reduces miscibility of MEG in the TC + heptane phase while increases PVCap concentration in MEG which shows a higher polymer recovery in the MEG phase. Thus results do show promise for washing hydrocarbons contaminated by TC+polymer with MEG to extract the polymer component.

4.3.8 Viscosity of polymer + TC mixtures

In section 4.3.3 it was shown that by adding as little as 1 mass % of treatment chemical relative to water more than 96% removal efficiency could be achieved (in terms of minimum TC doses / TC to polymer ratio, for 1-heptanol and PVCap, 1 g of 1-heptanol was needed to remove 96% and more of 0.5 g PVCap from 100 g of solution to yield a PVCap-TC mixture of about 33 mass% PVCap). Therefore, as the polymer and TC showed complete mutual miscibility, limits of TC polymer uptake would mostly likely

be governed by the viscosity of the mixture and how this impacts on the ability to handle it (mainly in terms of pumping) practically; if the TC absorbed too much polymer it would eventually become semi-solid.

To assess this, the viscosity of TC + polymer mixtures was measured. Viscosity measurements were carried out on an Anton-Paar rheometer (Figure 4.15) using parallel plates. Two sets of measurements have been conducted; in the first set solutions of different PVCap concentrations in 1-octanol were prepared and viscosities measured at two shear rates. Table 4.10 and Figure 4.16 show the measured viscosities as a function of PVCap concentration.

(A) **(B)** **(C)**

Figure 4.15 Image of Anton-Paar rheometer (A) and double plates (B, C) used for viscosity measurements.

Table 4.10 Viscosity of PVCap + 1-octanol mixtures at different PVCap levels.

PVCap mass% (in 1-octanol)	Viscosity (cp) at shear rate = 100 s^{-1}	Viscosity (cp) at shear rate = 500 s^{-1}
0	4.6	4.6
10	25.3	10.8
20	81.1	51.5
30	318.4	288.1
40	1545.5	1739.0

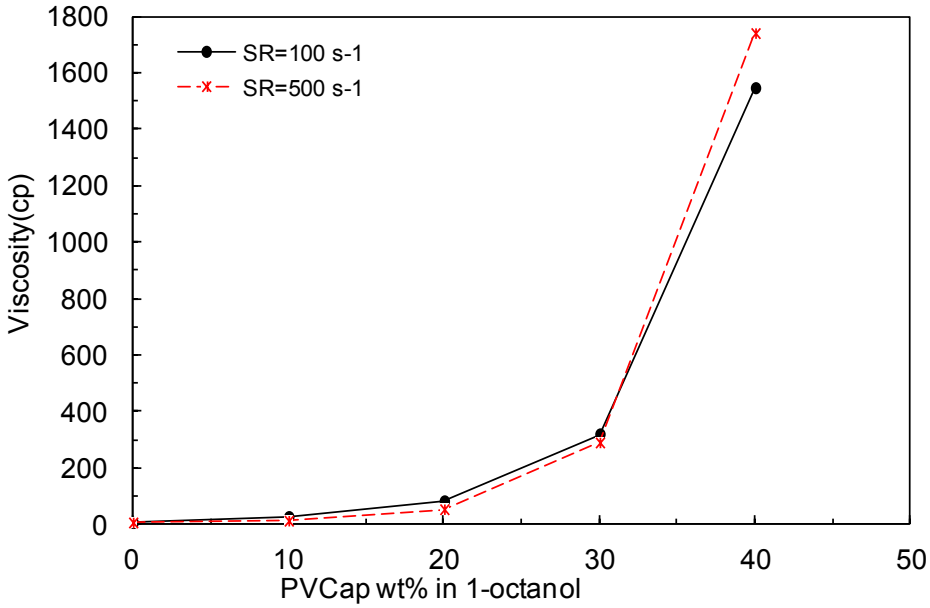

Figure 4.16 Viscosity of PVCap + 1-Octanol mixtures as a function of PVCap concentration at two shear rates.

As can be seen, there is not a large difference between measured viscosities at two shear rates and in both cases, a large increase in viscosity could be observed by increasing PVCap concentration to 40 mass%. For concentrations up to 30 mass% PVCap in TC, however, viscosity seems to be quite reasonable in terms of handling.

In the second set of measurements, the treatment procedure was carried out as normal; 0.5 mass % PVCap in water solutions were prepared and different quantities of 1-octanol were injected into them. The amount of treatment chemical injected was equal to achieve 10 to 40 mass% PVCap in TC assuming greater than 96% removal efficiency. Table 4.11 shows TC quantities added to the solution and desired polymer concentration in TC phase for each. TC + Polymer phase which also may contain some water, was drawn off after centrifuge and the viscosity of the separated phase was measured using Anton-Paar rheometer (at shear rate = 100 s^{-1}). Table 4.11 and Figure 4.17 show the measured viscosities as a function of TC quantity.

Table 4.11 Viscosity of PVCap + 1-octanol mixtures at different TC quantities.

Solution treated (Values in mass%)	Added 1-octanol relative to water (by mass)	Desired PVCap concentration in 1-octanol (mass%)	Viscosity (cp)
0.5% PVCap	0.8	40	332.1
0.5% PVCap	1.2	30	163.6
0.5% PVCap	2.0	20	51.6
0.5% PVCap	4.3	10	14.1

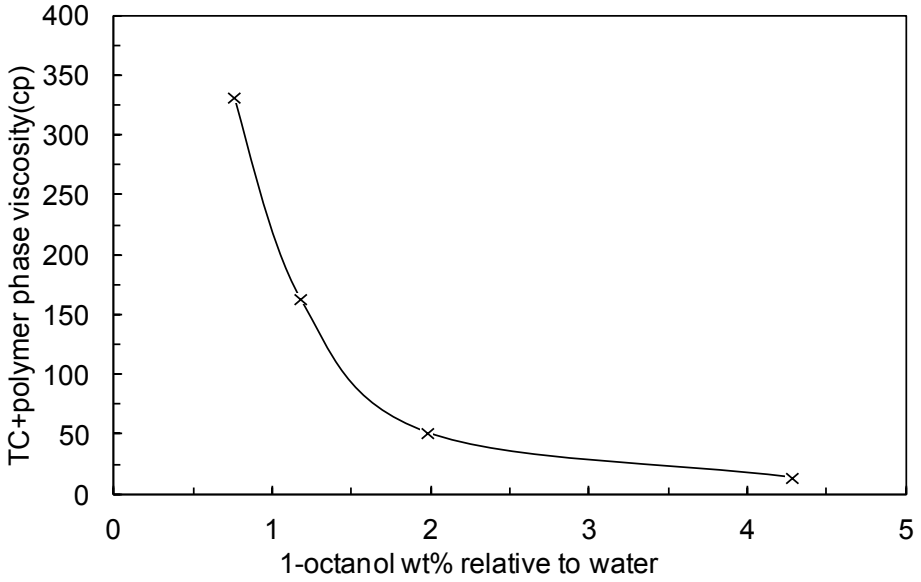

Figure 4.17 Viscosity of TC + Polymer phase separated from treated solution as a function of 1-octanol quantity (shear rate=100 s^{-1}).

Measured viscosities in this case are considerably lower comparing to the previous case, which is likely related to the presence of some water in the TC + polymer phase after separation from the water phase. This makes them much easier in terms of handling (pumping).

4.4 Conclusions

To address problems associated with kinetic hydrate inhibitors a KHI removal method was developed based on a simple solvent extraction technique. To remove KHI polymers from produced waters − which is the most problematic KHI ingredient − the method uses a very small quantity of fatty alcohols, with the main focus on linear chain normal hexanol, heptanol and octanol, and leaves the remaining aqueous phase largely or wholly polymer free. The physical separation post treatment chemical injection is easily possible by existing methods such as gravity settling, centrifugation or coalescing separation.

During the course of this work, the effects of several pipeline chemicals were examined and showed no significant effect on polymer removal efficiency. The main pipeline chemicals evaluated were salt, modest quantities of liquid hydrocarbons, corrosion and scale inhibitors. With the main focus on PVCap as KHI polymer, removal effectiveness was also evaluated for other commercial polymers. Treatment was effective for most of them, however for others with lower efficiency the treatment chemical can be adjusted to optimise effectiveness and facilitate physical separation.

As the method effectiveness remains largely unaffected in presence of thermodynamic inhibitor such as MEG and methanol, there is an opportunity of combining KHI and MEG; while by applying polymer removal the risk of precipitation in a MEG regeneration facility is removed. Furthermore, considering the fact that 1% KHI can replace about 20 to 40 mass% MEG (Mozaffar et.al, 2014), the removal technique can significantly decrease field MEG requirement.

Based on the above, applying the removal technique also can lead to some opportunities for KHI recovery as well as the opportunity of having a novel immiscible KHI design to address fouling problems associated with KHI polymers in water processing and disposal facilities.

CHAPTER 5 – EVALUATION OF IMMISCIBLE KINETIC HYDRATE INHIBITORS

5.1 Introduction

Kinetic hydrate inhibitors (KHIs) are generally formulated to prevent gas hydrate formation from the aqueous phase so it is assumed that the best way for them to do this is to be soluble and active within the aqueous phase. Therefore commercially available KHIs are normally designed to be water miscible formulations.

Previous studies in this lab for the effect of liquid hydrocarbons on KHI performance showed that potential partitioning of KHI polymer could occur, which will reduce the polymer concentration in aqueous phase. However, from the results it was speculated that any reduction in polymer concentrations in the aqueous phase is because of displacement of a modest fraction from the aqueous phase to the hydrocarbon-water interface, with negligible polymer entering the liquid hydrocarbon phase due to the immiscibility of the former with the latter (Mozaffar, 2013).

In some commercial studies at Hydrafact it was noted that KHIs could work very well for highly saline / salt saturated drilling muds. This behaviour is somehow in contrast with the fact that very high salinities involved should severely limit the amount of KHI polymer which could be miscible with the aqueous phase; salt typically greatly reducing the cloud/polymer drop-out temperature, whereby reducing hydrate inhibition performance. To find out the reason behind this behaviour, some tests were undertaken to see if small quantities of KHI could work well in combination with high salinities, however results demonstrated this not to be the case. This raises the question as to how KHIs could be working well for high salinity muds.

In another commercial work on the thermodynamic inhibition properties of muds, centrifuging of samples to remove solids prior to dissociation point measurements (solid minerals causing problems for equipment) revealed some muds to contain, in addition to the dominant water phase, an immiscible hydrocarbon-affinitive phase. This led to the question as to whether the KHI entered such a phase in muds yet was still able to prevent hydrate formation from the aqueous phase even though it was not present in the latter.

Based on the above, the opportunity of having a novel immiscible KHI design to avoid problems associated with water processing and disposal has opened up. As detailed in chapter 4 of this thesis, the largely water immiscible fatty alcohols have been shown to strip polymer from the aqueous phase by up to 100%. These properties were seen as a means to test the theory as to whether a KHI polymer could still work even though it was not in the aqueous phase by using fatty alcohols as carrier solvent for KHI polymers. Therefore, the work has been expanded to examine 'water immiscible KHIs', i.e. be used in a preventative manner (polymer is kept out of the aqueous phase) for certain applications such as where the salinity of produced waters would normally pose a problem in terms of causing KHI polymer precipitation.

Tests were carried out to examine whether KHI polymers do need to be miscible with / predominantly within the aqueous phase to inhibit hydrate growth. Contrary to what might have been expected – i.e. Treatment Chemicals (TCs) remove KHI from the aqueous phase so it might be imagined that they would reduce hydrate inhibition performance – tests on TC-PVCap 'immiscible' KHIs in different gas-water systems have shown this not to be the case; performance instead is generally comparable with aqueous PVCap.

All experiments were carried out in high pressure stirred autoclaves using the new CGI method, as described in Chapter 2 of this thesis. All experiments were carried out with 0.5 mass % PVCap. The PVCap used was Luvicap-EG base polymer (K-value = 25-8, average MW = 7000) supplied by BASF, with the ethylene glycol solvent removed by vacuum oven drying. The purity of the 1-octanol used was 99.0% and was supplied by Sigma Aldrich. Distilled water was used in all tests. Methane and Carbon dioxide were 99.995% pure and supplied by BOC.

5.2. PVCap/1-Octanol Immiscible KHI Formulation with Methane

A 'water immiscible KHI' comprising of 0.5 mass% PVCap / 2.0 mass% TC (1-octanol) relative to water − i.e. equivalent to 0.5 mass% PVCap aqueous but with the polymer almost wholly in the TC phase − was examined using the CGI method for a methane system.

Figure 5.1 shows example CGI method cooling and heating curves for 0.5 mass% PVCap / 2.0 mass% 1-octanol 'water immiscible KHI' (both relative to water) with

water and methane. Figure 5.2 shows a comparison of subcooling extents of CGI regions from the s-I methane phase boundary at ~70 bar for 0.5 mass% PVCap aqueous and 0.5 mass% PVCap / 2.0 mass% 1-octanol 'water immiscible KHI' formulation. As can be seen, the CGI behaviour for the 'immiscible KHI' is essentially identical to that for 0.5 mass% PVCap aqueous, demonstrating that PVCap can strongly inhibit hydrate growth even if not present in the aqueous phase. It should be noted that the possibility of the polymer being transferred back to the aqueous phase under gas pressure was also tested and seems to be unlikely; results are discussed in Section 5.5. Visual observations also showed the TC phase to retain its strong amber colour consistent with a high PVCap content under methane pressure throughout the test.

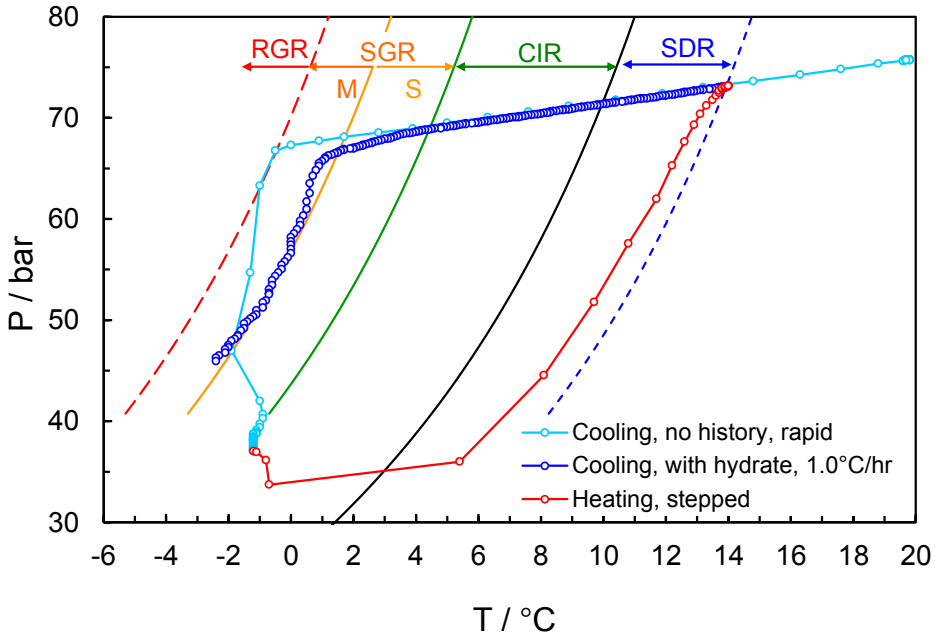

Figure 5.1 Example CGI method cooling and heating curves for 0.5 mass% PVCap / 2.0 mass% 1-octanol 'water immiscible KHI' with water and methane. Points are every 5 minutes.

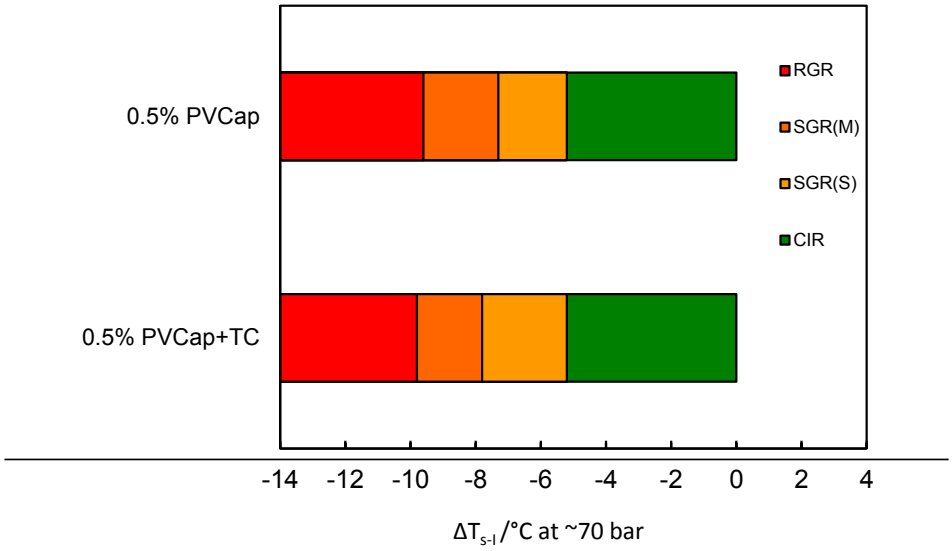

Figure 5.2 Comparison of subcooling extents of CGI regions from the s-I methane phase boundary at ~70 bar for 0.5 mass% PVCap aqueous (Mozaffar, 2013) and 0.5 mass% PVCap / 2.0 mass% 1-octanol 'water immiscible KHI' formulation.

These findings suggest that KHI polymers may very likely be most active at the hydrocarbon-water interface (be the latter gas or liquid hydrocarbon) rather than within the bulk aqueous phase. Given the low solubility of hydrocarbons in water, hydrate growth would be expected to be dominantly at water-hydrocarbon interfaces so ultimately KHIs being active at that location in the system would make sense.

Secondly, the results would potentially explain the ability of KHIs to inhibit hydrate growth in highly saline drilling muds; if the polymer is present in an immiscible, more hydrocarbon-affinitive phase, then they can still work by interfering with growth at water-hydrocarbon (like) interfaces.

5.3 PVCap/1-Octanol Immiscible KHI Formulation with NaCl in a Methane System

As mentioned before, for highly saline systems where KHIs are immiscible with the aqueous phase, water immiscible KHIs could be a potential solution to solve polymer drop-out problem from the aqueous phase. Therefore, to further investigate the potential of water immiscible KHIs, CGI tests have been undertaken on an 'immiscible' KHI comprised of 0.5 mass% PVCap relative to an aqueous phase of 20 mass% NaCl with

methane, but with the PVCap dissolved in 1-octanol (20 mass% PVCap / 80 mass% 1-octanol by mass).

Figure 5.3 shows example CGI method cooling and heating curves for 0.5 mass% PVCap / 2.0 mass% 1-octanol with a 20 mass% NaCl aqueous phase (all relative to water) and methane. Figure 5.4 shows experimentally determined points and interpolated CGI region boundaries for the system with data reported in Table 5.1.

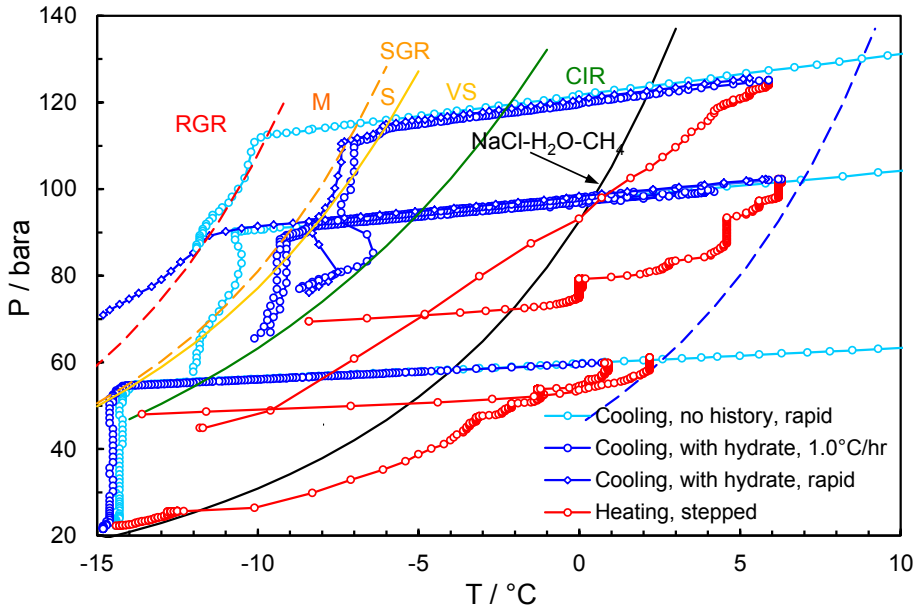

Figure 5.3 Example CGI method cooling and heating curves for 0.5 mass% PVCap / 2.0 mass% 1-octanol with a 20 mass% NaCl aqueous phase and methane. Points are every 5 mins.

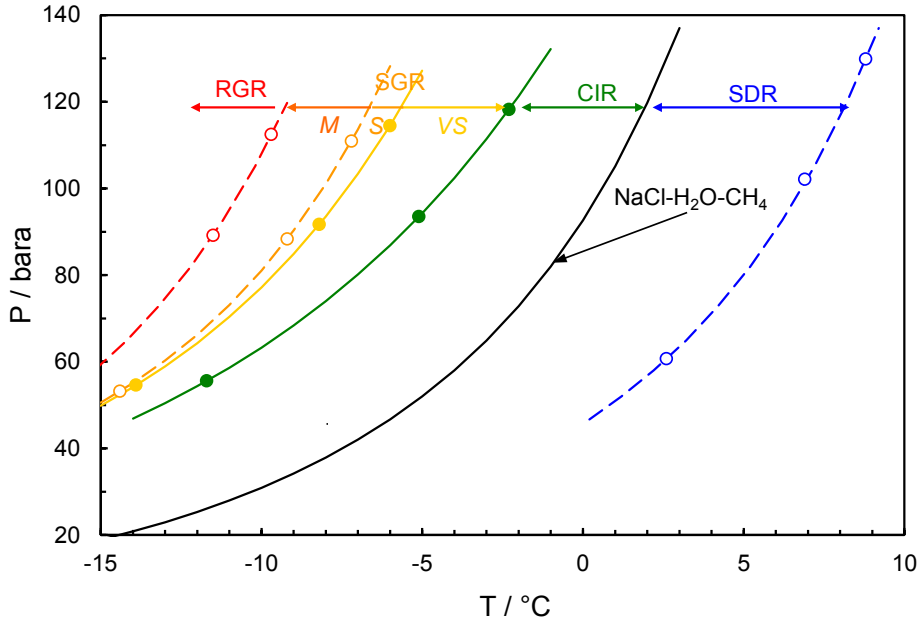

Figure 5.4 Experimentally determined points and interpolated CGI region boundaries for 0.5 mass% PVCap / 2.0 mass% 1-octanol with a 20 mass% NaCl aqueous phase and methane.

Table 5.1 Experimentally determined points on CGI region boundaries for 0.5 mass% PVCap / 2.0 mass% 1-octanol with a 20 mass% NaCl aqueous phase and methane.

CGR boundary	Growth rate	T / °C (± 0.5)	P / bar (± 0.2)	ΔT_{s-I} / °C (± 0.5)
SDR	Slow dissociation	2.6	60.7	6.3
		6.9	102.1	6.1
		8.8	129.9	6.2
CIR-SGR(S)	No growth	-11.7	55.6	-7.1
		-5.1	93.5	-5.2
		-2.3	118.2	-4.2
SGR(VS-S)	Very slow	-13.9	54.6	-9.1
		-8.2	91.7	-8.1
		-6.0	114.5	-7.7
SGR(S-M)	Slow	-14.4	53.2	-9.4
		-9.2	88.3	-8.8
		-7.2	110.9	-8.6
SGR(M)-RGR	Moderate	-11.5	89.2	-11.2
		-9.7	112.5	-11.2

Figure 5.5 shows a comparison of subcooling extents of CGI regions from the s-I methane phase boundary at ~70 bar for 0.5 mass% PVCap aqueous, 0.5 mass% PVCap / 2.0 mass% 1-octanol 'water immiscible KHI' formulations with water and with a 20 mass% NaCl aqueous solution.

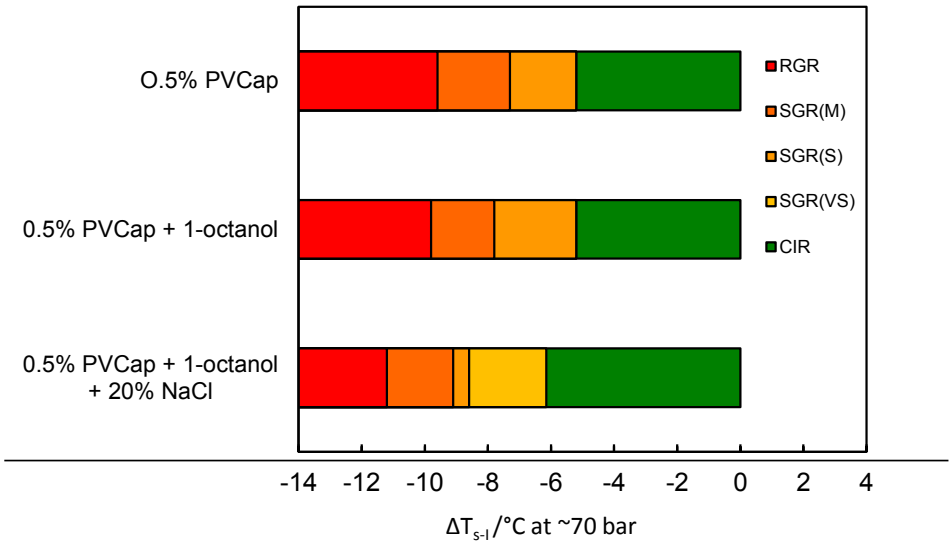

Figure 5.5 Comparison of subcooling extents of CGI regions from the s-I methane phase boundary at ~70 bar for 0.5 mass% PVCap aqueous (Mozaffar, 2013), 0.5 mass% PVCap / 2.0 mass% 1-octanol 'water immiscible KHI' formulations with water and with a 20 mass% NaCl aqueous solution (subcoolings for the last case are relative to NaCl+CH_4 phase boundary).

As can be seen, the 'water-immiscible KHI' offers very good crystal growth inhibition for the system with the 20 mass% NaCl apparently acting as a synergist; CGI region extents being the most extensive in this case. The fact that the PVCap is present in the 1-octanol phase means no polymer precipitation occurs and it is able to strongly inhibit hydrate nucleation/growth, presumably by acting at water–TC/PVCap-gas interfaces. Based on these results, such a KHI formulation could thus offer a novel inhibition method for lean/dry (low or condensate-free) systems, including those with saline produced waters. How the inhibition behaviour will be affected if the water immiscible formulation is heavily diluted with liquid hydrocarbons is discussed in Section 5.6. TCs used here are hydrocarbon miscible, thus in presence of liquid hydrocarbons, some of PVCap may disperse in the condensate rich phase containing dilute TC and hence hydrate inhibition efficiency could decrease.

5.4 Immiscible KHI in Carbon Dioxide - Methane System

One potential factor which may play a role in CO_2 and H_2S systems in terms of KHI performance is hydrate growth from dissolved gas. CO_2 and H_2S are considerably more soluble in the aqueous phase than hydrocarbon gases, and as the solubility of hydrate formers in water are reduced in the presence of gas hydrates, so there is greater potential for hydrate formation directly from dissolved gas in systems containing CO_2 and H_2S. As detailed in Section 2.3.3, the higher the subcooling, the lower the gas solubility in equilibrium with hydrate thus the higher the propensity for hydrate to grow directly from the aqueous phase.

From the experiments on 'immiscible' KHIs (discussed in Sections 5.2 and 5.3) it could be concluded that these can work well even though the bulk of the PVCap is not in the aqueous phase, suggesting that the polymer is most active at preventing hydrate formation at hydrocarbon-water interfaces. In light of this, one particular issue is that if the growth from dissolved gas is a factor in CO_2 and H_2S containing systems, then the immiscible KHI performance will be affected as polymer is not present in the aqueous phase. Some experiments therefore were carried out to test this theory by looking at an immiscible KHI performance in a CO_2-CH_4 system compared to one with the PVCap dissolved in the aqueous phase. A 10 mole% CO_2 / 90 mole% methane mixture was chosen for this purpose to provide data for comparison; studies being conducted with 0.5 mass% PVCap / 2.0 mass% 1-octanol (relative to water) as an immiscible KHI.

Figure 5.6 shows experimentally determined points and interpolated CGI region boundaries for 0.5 mass% PVCap (relative to water) in an immiscible KHI with the 10 mole% CO_2 / 90 mole% CH_4 gas mixture. Figure 5.7 shows a comparison of determined subcooling extents of 0.5 mass% PVCap aqueous induced hydrate CGI regions for CH_4, 10% CO_2 / 90% CH_4, and for 0.5 mass% PVCap as an immiscible KHI with 10% CO_2 / 90% CH_4 mixture at ~70 and ~100 bar.

As can be seen, the immiscible KHI performs well in the CO_2 system, giving a total CGI of ~8.2 °C across the pressure range studied. There is a modest reduction in performance with pressure, both in the extent of the CIR region and the SRG(S) region. As is common, this change mainly occurs in the ~70 to 100 bar pressure range.

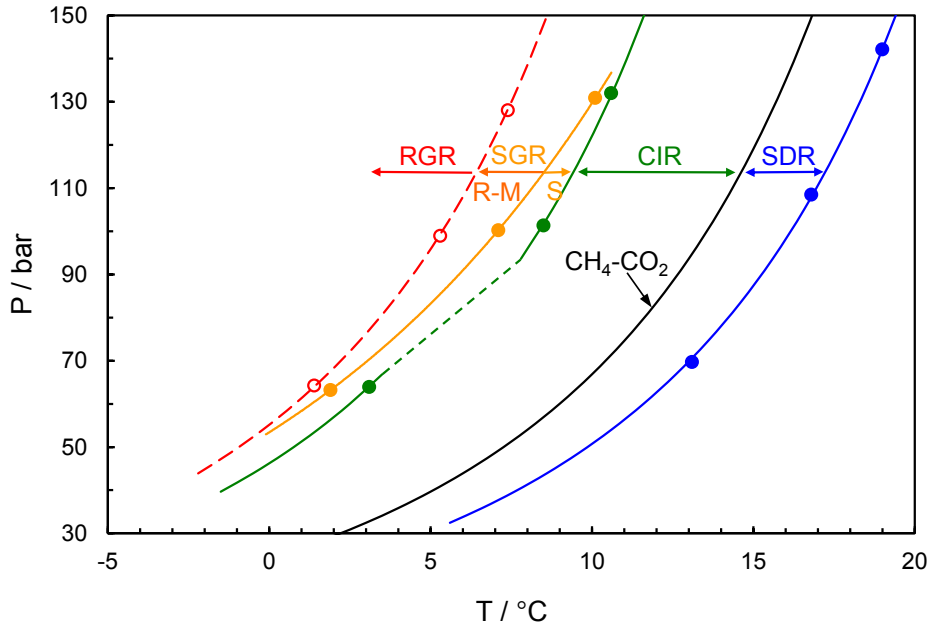

Figure 5.6 Experimentally determined points and interpolated CGI region boundaries for 0.5 mass% PVCap (relative to water) in an immiscible KHI (20 mass% PVCap / 80 mass% 1-octanol) with a 10 mole% CO_2 / 90 mole% CH_4 gas mixture.

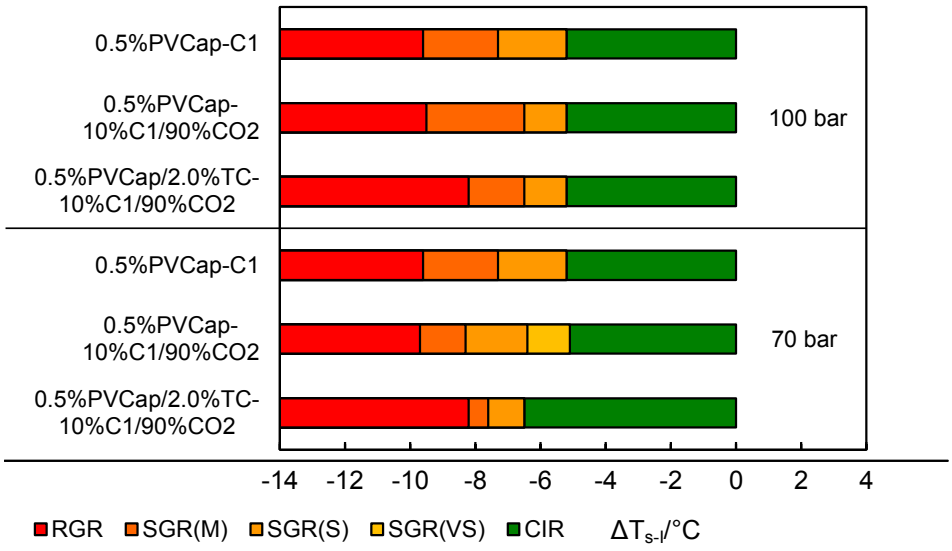

Figure 5.7 Comparison of determined subcooling extents of 0.5 mass% PVCap aqueous induced hydrate CGI regions for CH_4 (Mozaffar, 2013), 10% CO_2 / 90% CH_4 (data from Table 2.5.), and for 0.5 mass% PVCap as an immiscible KHI (TC) with 10% CO_2 / 90% CH_4 mixture at ~70 and ~100 bar.

When compared with data for aqueous PVCap with methane and with 10% CO_2 / 90% CH_4 (Figure 5.7), the PVCap not being in the water phase does not seem to pose a major issue in terms of performance; the CIR region for the immiscible KHI with 10% CO_2 /

90% CH_4 is larger at lower pressure (~70 bar) and identical at higher pressure (~100 bar) to that for methane, with only the SGR region reduced in extent. This would suggest that if formation from dissolved gas is an issue for KHIs in CO_2 containing systems, then the effect is not major.

5.5 Effect of Dissolved Gas; Immiscible KHI in a CO_2-CH_4 System

In the previous section, results on an immiscible KHI (PVCap + 1-octanol) with a 10 mole% CO_2 / 90 mole% CH_4 mixture showed that behaviour seems very similar whether the KHI is in the aqueous phase or not. However, there is a concern whether PVCap will definitely not transfer into the aqueous phase (or at least the bulk of it will not) under gas pressure. Previous visual studies indicated this was not the case but to confirm, it was checked by analysing the water phase under gas pressure.

In this regard, 0.5 mass% PVCap (relative to water) in an immiscible KHI (PVCap + 1-octanol) was pressurized to ~92 bar with the 10 mole% CO_2 / 90 mole% CH_4 gas mixture. The system was mixed for 24 hrs and then settled for another 24 hrs. The liquid phase was drawn off afterwards, centrifuged and filtered twice. Initial attempts at using UV-Vis spectrometry to determine amount of PVCap in the water seemed to be unsuccessful since small particles of graphite (from motor bearings) present in the water were clearly affecting spectra. Therefore a traditional dry-out method was used and result showed that only a very tiny amount of 0.0034 mass % PVCap was dissolved in water, confirming KHI immiscibility.

5.6 Effect of Liquid Hydrocarbon on Immiscible KHI Performance

The above findings suggest that as long as the KHI is close to the hydrocarbon-water interface (as it is if concentrated in an immiscible TC phase), then it can still perform as a KHI. This was found to be the case in methane systems, methane-CO_2 systems (where results show growth of hydrates from dissolved gas does not seemingly present a problem for a non-aqueous KHI) and highly saline systems (20 mass% NaCl) where polymers such as PVCap would normally drop-out / foul, but do not when dissolved in the TC phase. However, the behaviour in the presence of liquid hydrocarbons needs further investigation.

Work on removal effectiveness showed that dilution of the immiscible PVCap-rich TC phase with heptane or condensate caused displacement of the PVCap back into the

aqueous phase due to TC dilution (TCs being typically miscible with liquid hydrocarbons). In light of this, the effect such a dilution would have on an immiscible KHI in terms of hydrate inhibition performance was tested.

To examine this, CGI measurements have been undertaken on a 0.5 mass% PVCap + 2 mass% 1-octanol (both relative to water) 'immiscible' KHI diluted with a typical North Sea condensate (10 volume% condensate to 90 volume% water) with methane. Figure 5.8 shows determined CGI regions for the system and data are reported in Table 5.2.

Table 5.2 Experimentally determined points on CGI region boundaries for 0.5 mass% PVCap + 2 mass% 1-octanol (both relative to water) with a typical North Sea condensate (10 volume% condensate to 90 volume% water) and methane.

CGR boundary	Growth rate	T / °C (± 0.5)	P / bar (± 0.2)	ΔT_{s-l} / °C (± 0.5)
CIR-SGR(S)	No growth	4.4	68.1	-5.1
		7.8	100.1	-5.2
		10.7	139.5	-5.1
SGR(S-M)	Slow	3.9	67.6	-5.6
		6.8	99.8	-6.1
		9.1	137.6	-6.6
SGR(M)-RGR	Moderate	1.2	66.9	-8.2
		4.7	97.1	-8.0
		7.6	135.5	-7.9

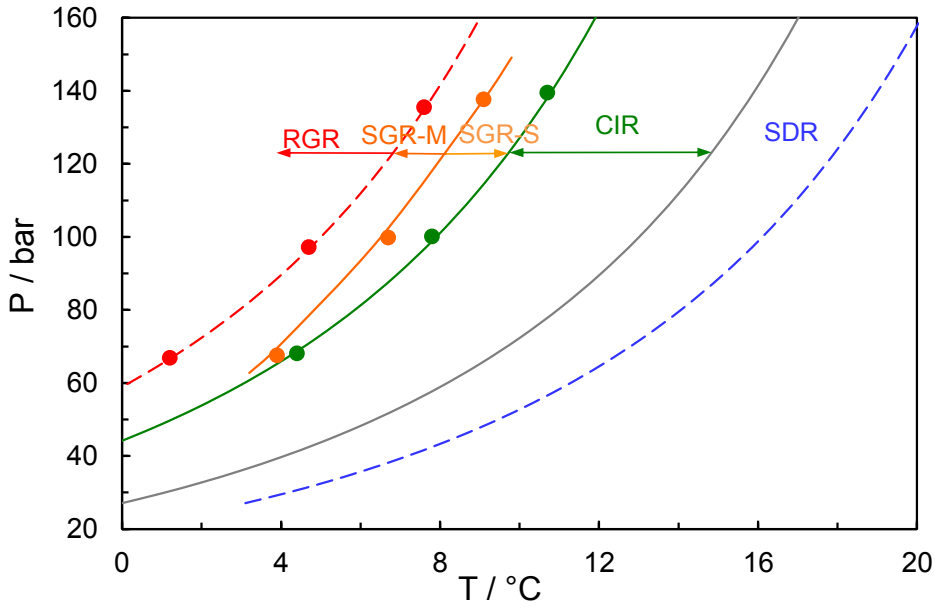

Figure 5.8 Determined CGI regions for 0.5 mass% PVCap + 2 mass% 1-octanol (both relative to water) with a typical North Sea condensate (10 vol% condensate to 90 volume% water) and methane.

Figure 5.9 shows a comparison of determined subcooling extents for the immiscible KHI with condensate compared to those for 0.5 mass% PVCap alone, with 1-octanol, and with 1-octanol + 20 wt% NaCl, all with methane at ~70 bar.

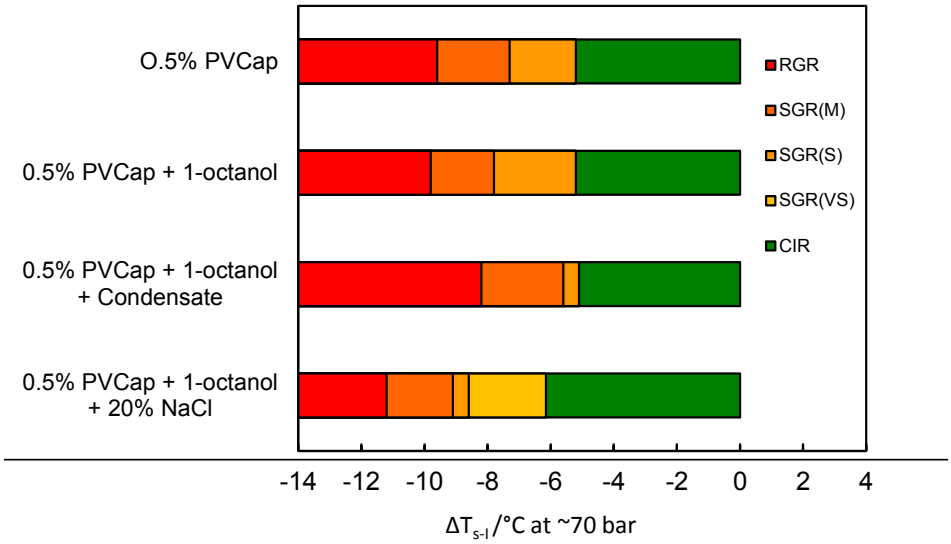

Figure 5.9 Comparison of determined subcooling extents for 0.5 mass% PVCap + 2 mass% 1-octanol (both relative to water) with a typical North Sea condensate (10 volume% condensate to 90 volume% water) compared to those for 0.5 mass% PVCap alone (Mozaffar, 2013), with 1-octanol, with 1-octanol and 20 wt% NaCl, all with methane at ~70 bar.

The presence of condensate does reduce PVCap CGI inhibition measurably, although the most important CIR is consistently retained across the pressure range tested. The reasons for the modest reduction of the SGR is unclear, but might suggest the effective PVCap dose has been reduced, possibly as some is dispersed in the condensate rich phase containing dilute TC. The condensate dilution would mean the hydrocarbon liquid phase would be ~20% 1-octanol. Based on removal testing, this could mean up to half the PVCap was dispersed in the condensate phase; if this proportion of the PVCap was not close to the hydrocarbon / water interface, then it might be less effective at hydrate inhibition.

5.7 Conclusions

Work on 'immiscible KHI's has demonstrated that these could work apparently very effectively for dry/lean gas systems, even in the case of highly saline produced waters. Initial tests of an immiscible KHI formulation in a simple methane system showed that the CGI behaviour for this formulation is essentially identical to that for 0.5 mass% PVCap aqueous. Further experiments on a highly saline solution containing 20 mass% NaCl also confirmed the ability of immiscible KHIs to prevent hydrate growth although they are not in the bulk aqueous phase.

These findings suggest that KHI polymers may be mostly active at the hydrocarbon-water interface rather than within the bulk aqueous phase. Given the low solubility of hydrocarbons in water, hydrate growth would be expected to be dominantly at water-hydrocarbon interfaces so ultimately KHIs being active at that location in the system would make sense.

For CO_2 and H_2S containing gas systems, which are considerably more soluble in the aqueous phase than hydrocarbon gases, there is a particular issue of hydrate formation from dissolved gas. Immiscible KHI tests – where the PVCap is not dissolved in the aqueous phase – for a 10 mol% CO_2 / 90 mol% CH_4 mixture do not show clear support for hydrate formation from dissolved gas being a problem for such KHI formulations. The concern over KHI polymer being transferred back to aqueous phase under gas pressure was also investigated for the same gas mixture and results confirmed immiscibility of KHI, showing only very little polymer was dissolved in water.

To see CGI behaviour in the presence of liquid hydrocarbons, an 'immiscible KHI' was tested with a typical North Sea condensate (10 volume % condensate to 90 volume% water) and methane. Results showed that PVCap still shows good KHI performance, even though the TC phase has been strongly diluted (~80%) by condensate. The presence of condensate does however reduce PVCap CGI inhibition measurably (compared to condensate free systems) although the important CIR is consistently retained for the pressure range studied (up to 140 bar).

Overall, the results of this study open up the possibility of water immiscible KHIs for which there might be some benefits for certain systems. For example, a non-water miscible KHI would not present gunking problems upon hot injection if the KHI

polymer remains miscible with its carrier solvent (the TC used has a high boiling point of 195°C). Likewise, the KHI formulation could be readily removed on arrival at the processing facilities by conventionally skimming/gravity separation/centrifuge methods as currently employed for water-hydrocarbon separation. In addition, a water immiscible KHI could potentially be used for highly saline systems where KHIs are immiscible with the aqueous phase. This could provide a potential novel solution where the use of thermodynamic inhibitors (MEG, methanol) was not favourable due to cost and/or concerns over salt deposition (due to thermodynamic inhibitors reducing salt solubility). Obviously for such a KHI to work, good suspension of it in the aqueous phase would be a prerequisite to ensure the polymer was well distributed. The TCs seem to offer that property, forming cloudy suspensions which gravity settle with time when mixing is stopped.

CHAPTER 6 – FUTURE DIRECTIONS IN APPLICATION OF KINETIC HYDRATE INHIBITORS

6.1 Introduction

In challenging conditions such as deep water production, long tiebacks and high water cuts, the cost of implementing thermodynamic inhibitors could be very high as per high required volume (e.g. > 50 mass%). Therefore research in the oil and gas industry continues to find a cheaper option while offering reasonable inhibition. Kinetic hydrate inhibitors (KHIs) can be an alternative technology for gas hydrates prevention, which have some clear advantages over thermodynamic inhibitors. The most pronounced advantage in this regard is reducing operating and capital expenses and optimizing production. Due to the low dosage required and reduction in inhibitor volume, production platforms can be downsized (Kulkarni, 2003). Kinetic hydrate inhibitors could also be combined with other pipeline chemicals such as corrosion inhibitors, which will reduce the requirement for storage thanks, injection pumps and transport of individual chemicals (McDonald et al., 2006).

Despite recent advances in developing new KHIs with high performance and economic benefits comparing to thermodynamic inhibitors (Perrin et al. 2013), there are still major concerns in their application. The main concerns in this regard include inconsistencies in performance, environmental issues, KHI disposal and produced water handling (Tohidi et al., 2014). These concerns could be addressed by:

- Better understanding of involved mechanisms by implementing reliable evaluation techniques such as the CGI method (Anderson et al., 2011)
- Development and application of environmentally friendly Bio-KHIs
- KHI removal from produced water and introducing novel designs such as immiscible KHIs

6.2 Mechanism of Kinetic Hydrate Inhibition

The mechanisms involved in KHIs inhibition still are not completely understood and somehow depend on each particular polymer. However the most favoured mechanism is adsorption of polymer on to the crystal surface thus restriction of further crystal growth.

By studying crystal growth and morphology in the presence and absence of kinetic hydrate inhibitors, Larsen et al. (1998) concluded that complete growth inhibition is a result of polymer adsorption to the crystal surface. They believed that adsorbed molecules act as barriers to further growth (Larsen et al., 1998). Small angle neutron scattering studies by King et al. (2000) showed conformational change in KHI polymers, which was believed to be a sign of adsorbed polymer layer on the hydrate crystal surface. Yang and Tohidi (2011) utilized attenuation and Fast Fourier Transform (FFT) analysis of ultrasound on PVCap and VP/BA (vinyl pyrrolidone/ butylacrylate) and resulted in two kinds of inhibition mechanisms including nucleation and growth inhibition. Then they concluded that adsorption of KHI molecules on the growth and nucleation sites could explain the inhibition achieved (Yang and Tohidi, 2011).

Molecular dynamic simulation also suggest that inhibitor molecules bind to the surface of the hydrate crystal and retard further growth (Anderson et al., 2005; Kvamme et al., 2005; Yagasaki et al., 2015)

6.2.1 Adsorption of KHIs on hydrate crystals

Despite various experimental and computational modelling studies on adsorption of kinetic hydrate inhibitors on hydrate crystal, less attention has been paid to the thermodynamics of this (Anklam and Firoozabadi, 2005). One suggested idea to explain crystal growth inhibition is that the adsorbed inhibitor on the crystal growth surface slows the growth through the mechanism of step pinning (Hutter et al, 2000). Based on this, the crystal is forced to grow between adsorbed inhibitors thus curvature of the crystal steps between adsorbed sites will decrease the growth rate or even completely inhibit the growth when adsorption sites are close enough (Anklam and Firoozabadi, 2005; Hutter et al, 2000). Another approach to explain the inhibition mechanism could be due to changes in interfacial tension and specific edge energy. Some non-hydrate crystals nucleation and growth studies showed that increase in specific edge energy associated with nucleation and increased interfacial tension for the crystal nuclei with adsorbed inhibitor could be the reason for increased induction time in the presence of inhibitor (van der Leeden et al., 1992; He et al., 1995). However van der Leeden et al.(1992) also noted this was not consistent with thermodynamics, and thus offered that the additives behave as active centres for nucleation and do not alter the surface free

energy and edge free energy of the nuclei by adsorption on them inhibitor (van der Leeden et al., 1993).

Anklam and Firoozabadi (2005) proposed an interfacial energy mechanism for complete crystal growth inhibition as a result of polymer adsorption. According to their model, adsorption of inhibitor will cause a reduction in interfacial tension or edge energy for the crystal surface or step, respectively. Therefore, the work to add a layer or grow a step increases due to the difference in interfacial tensions or edge energies for surfaces with and without an adsorbed inhibitor. For a large enough difference in interfacial tensions or edge energies, complete inhibition of growth is realized when the total work does not decrease as more crystals are formed (Anklam and Firoozabadi, 2005).

Zhang et al. (2009) presented the adsorption behaviour of PVCap and PVP on cyclopentane hydrates. They could fit PVP and PVCap adsorption data to the Langmuir and BET-type isotherms. Although the two isotherms were overlapping at low concentrations of polymer (< 50 μM), at higher concentrations PVCap showed superior performance. The reason for this superior performance was suggested to be the multilayer adsorption of PVCap as well as the large molecule size. They concluded that the affinity of polymers to the hydrate surface is not simply proportional to the free energy of binding of their monomers, but it is affected by both the number of monomers bound to the surface and the configuration of the adsorbed polymers (Zhang et al., 2009)

The ability to model hydrate crystal growth in presence of KHI polymers and predicting the inhibition offered by them will save time and reduce the inherent risks associated with screening processes. However achieving this goal, needs precise understanding of involved mechanisms – e.g. adsorption as the most favoured mechanism – and the nature of crystal formation/growth when inhibitor is present in the system. Daraboina et al. (2011a) suggest that very effective KHIs have a high probability to get anchored on hydrate crystal surface by means of a chemical group, which fits an empty cage and inhibit crystals from growing any further. Over the course of this work, it has also been speculated that in the presence of KHI polymers some form of polymer-hydrate complex develops rather than ‘normal’ hydrates forming. If this is the case, it raises the question as to whether these complexes have any stoichiometry.

6.2.2 Hydrate-polymer complex stoichiometry

In previous work in this lab, Mozaffar (2013) measured PVCap performance as a function of concentration for 0.25, 0.5, 1.0 and 5.0 mass% PVCap aqueous with methane. The focus was however on to what extent increasing the polymer content will increase the total subcooling of CGI regions. Increasing the level of detail in data (data points for different concentrations) can help confirm whether there is any stoichiometry involved in polymer-hydrate complex.

Therefore CGI region boundary subcoolings have been measured for a range of additional PVCap concentrations for methane at 70 bar as part of Heriot-Watt Institute of Petroleum Engineering Joint Industrial Project (JIP) (Progress report, April 2013) and this work (0.03 mass% PVCap) to increase detail in the relationships. Experiments were carried out in high pressure stirred autoclaves using the new CGI method, as described in Chapter 2 of this thesis. The PVCap used was Luvicap-EG base polymer (K-value = 25-8, average MW = 7000) supplied by BASF, with the ethylene glycol solvent removed by vacuum oven drying. Tests were performed with 99.995% pure methane. Distilled water was used in all tests.

Figure 6.1 shows all experimentally determined subcoolings of CGI region boundaries plotted as a function of aqueous PVCap concentration for methane at ~70 bar. For some PVCap concentrations, two SGR(S-M) features are seen, with PT pathways on cooling following one boundary then retreating in terms of subcooling to follow another as the fraction of hydrate increases. It is clear from the data that different polymer concentrations have similar subcooling features. However by increasing PVCap concentration, the extent of CGI boundaries do not follow a progressive trend but they change more in a step-wise manner.

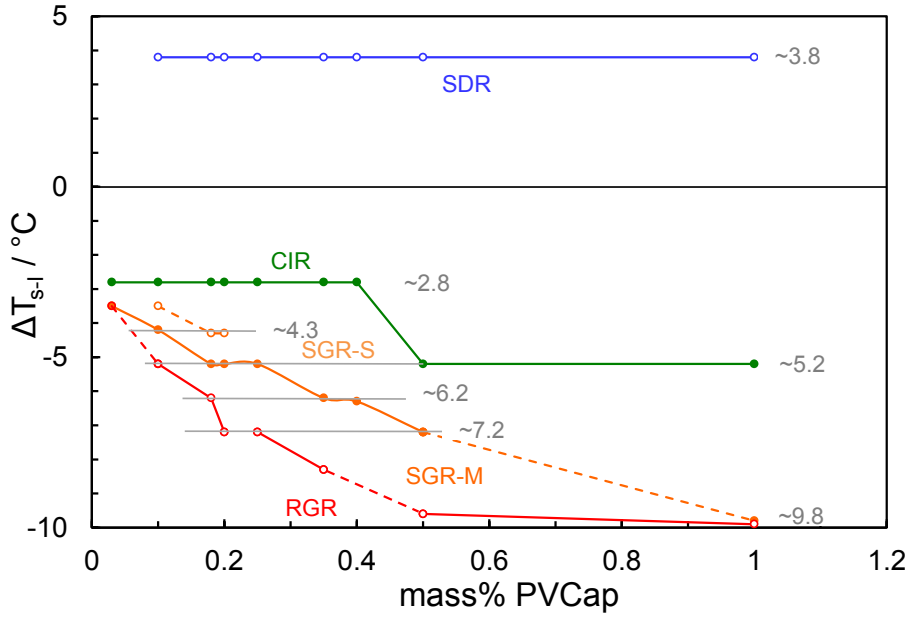

Figure 6.1 Experimentally determined subcoolings of CGI region boundaries as a function of aqueous PVCap concentration for methane at ~70 bar pressure.

Results clearly demonstrate how small changes in polymer concentration have a marked change in performance. For example, the CIR is constant at ~2.8 °C subcooling from 0.03 to 0.4 mass% PVCap before stepping abruptly to ~5.2 °C subcooling at 0.5 mass% and above. A similar case applies for SGR and RGR boundaries. Such behaviour can be very important in terms of dose selection, since small change in dosage could have a major impact on KHI subcooling extent.

The fact that different concentrations of PVCap share CGI subcooling boundary positions (most commonly relative to s-I phase boundary) strongly supports the theory that there is an underlying feature of crystal growth patterns as a function of subcooling rather than being polymer induced. For example, it could be speculated that each shared subcooling boundary represents a change in which crystal faces are favourable for growth, which, in the absence of the KHI, would determine growth rates and crystal morphologies as function of subcooling. In the presence of KHI polymer, the polymer preferentially adsorbs on some of these faces, whereby limiting or completely restricting growth (Larsen et al., 1998). Certainly the data support the generally accepted surface adsorption theory.

With respect to potential stoichiometry, one feature that supports this as a possibility is the apparently unchanged extent of the SDR region. As seen in Figure 6.1, the SDR is

completely independent of PVCap concentration, which might suggest that if this does represent a region where hydrate-polymer complexes can exist in a metastable state, then these complexes are of the same composition irrespective of aqueous PVCap concentration. But, in terms of using the extent of the SDR region as means to screen KHIs; these findings suggest that this is unlikely to be fruitful given that the SDR extent is unrelated to the extent of CIR regions/PVCap concentration/inhibition performance.

It was hoped that if PVCap performance as a function of concentration was known in detail, then CGI cooling runs with different fractions of hydrate could be potentially used to estimate PVCap-hydrate stoichiometry, if any. Initial attempts at the latter however did not meet with success due to the fractions of hydrate formed in tests being apparently too small to alter remaining PVCap concentration noticeably. Attempts using UV-Vis spectroscopy to sample the water in the presence of hydrate were also unfruitful, again due to the small fractions of hydrate (<1%) formed apparently not changing the remaining aqueous PVCap concentration, and also due to problems getting clear UV spectra; sample cloudiness (with it is suspected is down to the presence of mixer's motor bearing carbon dust) being a particular problem.

Based on this to encourage greater hydrate formation, the volume of aqueous phase in the cell was reduced to 50 vol% (instead of the standard 80 vol%) and this allowed greater than 10% water conversion to hydrate for 'hydrate present' re-cooling runs, before ice formation began to interfere with CGI region determination due to reduced system pressure (~ 80 bar). Figure 6.2 shows experimentally determined CGI regions for 0.5 mass% PVCap aqueous with methane for increasing initial fractions of water converted to hydrate. Tabulated results are given in Table 6.1.

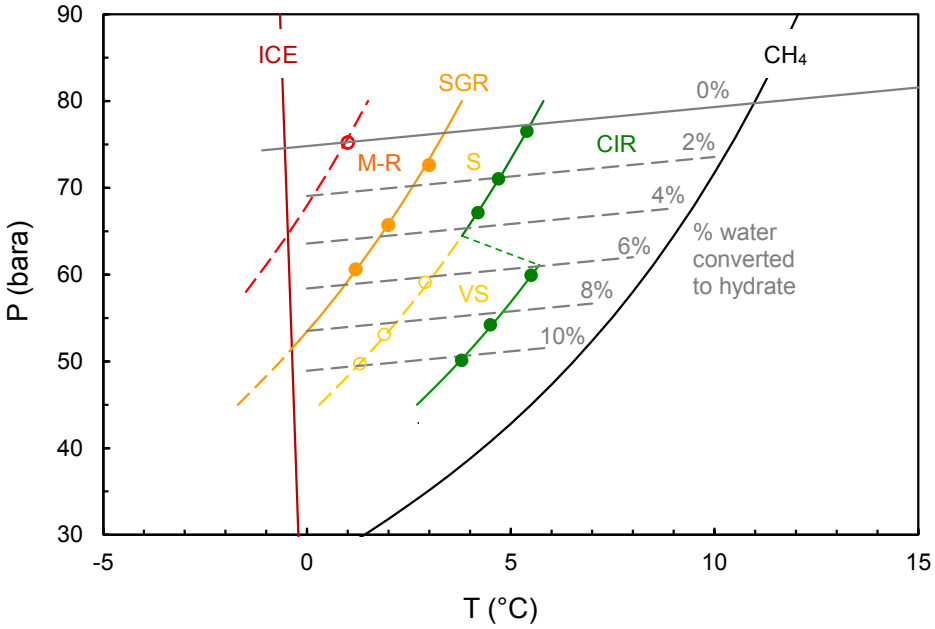

Figure 6.2 Determined CGI regions for 0.5 mass% PVCap aqueous with methane for increasing initial fractions of water converted to hydrate ahead of 'hydrate present' re-cooling runs. Aqueous phase volume was 50% of cell volume. Water converted to hydrate (on a molar basis) calculated by HydraFLASH® 2.2.

Table 6.1 Experimentally determined CGI region data for 0.5 mass% PVCap aqueous with methane for increasing initial fractions of water converted to hydrate ahead of 'hydrate present' re-cooling runs. Aqueous phase volume was 50% of cell volume. Water converted to hydrate (on a molar basis) calculated by HydraFLASH® 2.2.

CGR boundary	Growth rate	T / °C (± 0.5)	P / bar (± 0.2)	ΔT_{s-I} / °C (± 0.5)	%water as hydrate
CIR-SGR(S)	No growth	3.8	50.1	-2.8	10.2
		4.2	67.1	-5.2	3.4
		4.5	54.2	-2.8	8.6
		4.7	71.0	-5.2	2.0
		5.4	76.5	-5.2	0.2
		5.5	59.9	-2.8	6.4
SGR(VS-S)	Very slow	1.3	49.7	-5.2	9.9
		1.9	53.1	-5.2	8.6
		2.9	59.1	-5.3	6.2
SGR(S-M)	Slow	1.2	60.6	-7.2	5.3
		2.0	65.7	-7.2	3.5
		3.0	72.6	-7.1	1.2
SGR(M)-RGR	Moderate	1.0	75.2	-9.4	0.0

To grow even larger hydrate fractions and examine patterns without ice forming, further tests were carried out for 0.5 mass% PVCap and methane, with increased system pressure to ~ 130 bar and the same aqueous phase level (50 vol %). Figure 6.3 shows determined CGI regions for this case. Tabulated results for the higher pressure test are given in Table 6.2.

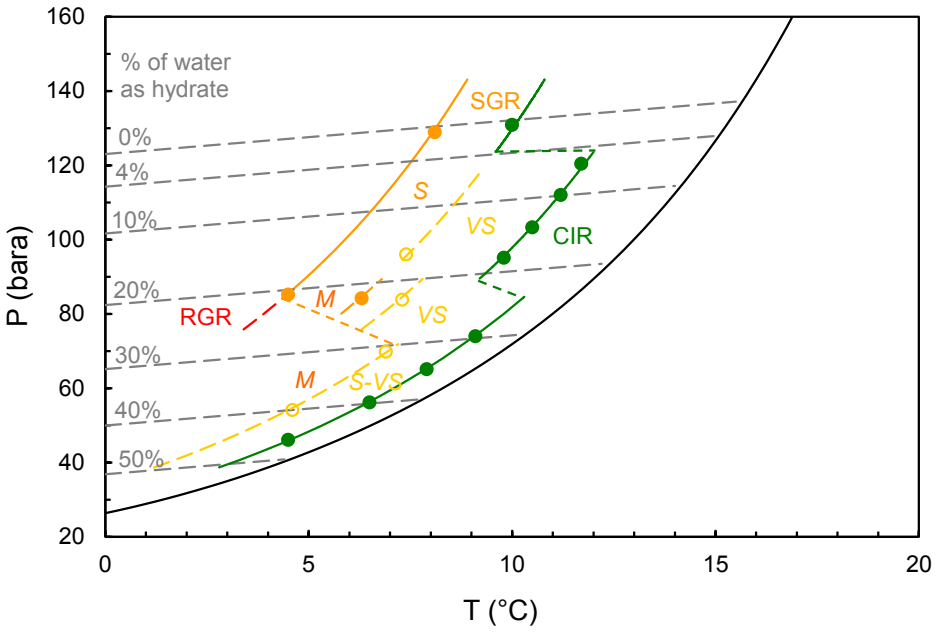

Figure 6.3 Determined CGI regions for 0.5 mass% PVCap aqueous with methane for increasing initial fractions of water converted to hydrate ahead of 'hydrate present' re-cooling runs. Aqueous phase volume was 50% of cell volume with an initial pressure of ~130 bar. Water converted to hydrate (on a molar basis) calculated by HydraFLASH® 2.2.

Table 6.2 Experimentally determined CGI region data for 0.5 mass% PVCap aqueous with methane for increasing initial fractions of water converted to hydrate ahead of 'with hydrate' re-cooling runs. Aqueous phase volume was 50% of cell volume with an initial pressure of ~130 bar. Water converted to hydrate (on a molar basis) calculated by HydraFLASH® 2.2.

CGR boundary	Growth rate	T / °C (± 0.5)	P / bar (± 0.2)	ΔT_{s-I} / °C (± 0.5)
CIR-SGR	No growth	4.5	46.1	-1.2
		6.5	56.2	-1.2
		7.9	65.1	-1.2
		9.1	74.0	-1.2
		9.8	95.1	-2.7
		10.5	103.3	-2.8
		11.2	112.0	-2.8
		11.7	120.4	-2.9
		10.0	130.9	-5.3
SGR(VS-S or M)	Very slow	4.6	54.1	-2.7
		6.9	69.8	-2.9
		7.3	83.8	-4.1
		7.4	96.0	-5.2
SGR(S-M)	Slow	6.3	84.2	-5.2
		4.5	85.2	-7.1
		8.1	128.9	-7.0

As can be seen in Figures 6.2 and 6.3, CGI behaviour was observed on all runs up to 50% water converted and beyond, demonstrating, aside from any possible stoichiometry aspects, that low concentrations of PVCap (0.5 mass%) can inhibit very large fractions of hydrate to varying degrees. In terms of CGI, initially, for lower hydrate fractions, regions were found to be largely unchanged, however, beyond ~4% water converted to hydrate in both test systems, regions started to reduce with this most clearly observed for the CIR, which dropped from the standard (for methane at 0.5 mass% PVCap) ~5.2 °C subcooling abruptly to ~2.8 °C subcooling; then for the higher pressure test, to around 1.2 °C subcooling at ~25% water conversion to hydrate. By this point, for the lower pressure test, higher subcoolings were reaching ice formation conditions so the full extent of CGI regions could not be determined, although some detail on SRG conditions could be delineated. In the higher pressure test (Figure 6.3), testing beyond ~50% hydrate was stopped by blockage – the aqueous phase becoming solid hydrate dominated.

The abrupt reduction in the extent of the CIR beyond ~4% water converted to hydrate could also be seen in data for PVCap concentration versus extent of CGI regions (Figure 6.1) where aqueous PVCap concentration drops from 0.5 mass% to 0.4 mass%. In light of this, the observed behaviour is suggestive of a comparable reduction in remnant aqueous PVCap as this is lost from the aqueous phase due to adsorption on the increasing fraction of hydrate present. If it is assumed that the reduction in the CIR at ~5% water converted to hydrate corresponds to a drop in PVCap concentration from ~0.5 mass% to 0.4 mass%, then we can use this data to estimate a potential PVCap to water ratio for the fraction of 'hydrate-polymer complexes' formed. Likewise, the same can be done for the CIR reduction at around 25% water converted to hydrate in the higher pressure test case.

However the extent of the SGR regions in Figures 6.2 and 6.3 at ~5% hydrate converted / 0.4 mass% PVCap remaining in solution (based on CIR data) do not seem to match closely the data for 0.4% PVCap in Figure 6.1. The fact that these are larger in the system with 5% hydrate might suggest a higher PVCap concentration than 0.4 mass%. However, it must be remembered that the system is different due to the high concentration of already inhibited hydrate that is present.

If it is assumed that first 4%+ of hydrate is fully inhibited by the polymer adsorbed on it, then it might be expected that this hydrate behaves as if in the presence of a higher concentration of PVCap thus remains completely inhibited until 5.2 °C subcooling, with SGR regions as appropriate, and this affects the overall bulk CGI patterns observed, at least in terms of SGR behaviour. In contrast, 'new' hydrate forming with total converted water of 6% or greater is in contact with water containing less PVCap which offers less inhibition, thus the CIR for this newly forming hydrate is markedly reduced, i.e. this new hydrate is growing as if it is in a solution of lower PVCap concentration with existing hydrate 'invisible' to it.

The above is somewhat speculative and needs further investigation. However, data show that crystal growth in PVCap systems, even at high hydrate fractions, is remarkably ordered and data does provide quite compelling evidence for a PVCap to water stoichiometric ratio.

6.3 Biodegradable Kinetic Hydrate Inhibitors

Although offering significant CAPEX and OPEX advantages over traditional thermodynamic inhibitors, there are environmental concerns regarding KHI application, particularly where produced water is released into the sea. Due to typical low reactivity and large molecular sizes which restrict breakdown by microorganisms, active polymers in KHI formulations are typically poorly biodegradable. By increasing environmental restrictions in use of KHIs, there is a growing interest in 'green' KHIs. Historically, development of such chemicals with good KHI properties as well as relatively good biodegradability has not met great success. However in recent years research within academia and the industry has resulted in the emergence of new hybrid polymers which apparently do offer good KHI properties combined with improved biodegradability (Musa and Cuiyue, 2010; Perrin et al., 2013).

Luvicap-bio is a biodegradable KHI (supplied by BASF and contains 30 mass% active ingredient in water) which has previously shown relatively good performance in terms of CGI regions in a methane s-I hydrate forming system (Mozaffar, 2013). Daraboina et al. (2015) have also reported a significant reduction in hydrate nucleation temperature in presence of this polymer for a natural gas system. Natural gas tests using the CGI method in this work also shows good performance for Luvicap-bio. Figure 6.4 shows experimentally determined points on CGI region boundaries (data points are reported in Appendix A Table A.2) and interpolated boundaries for 0.5 mass% aqueous Luvicap-bio in a typical north sea natural gas system.

The composition of natural gas used in bio-KHI tests as well the one used for PVCap experiments are given in Table 6.3. Distilled water was used in all bio-KHI tests. All experiments were carried out in high pressure stirred autoclaves using the new CGI method, as described in Chapter 2 of this thesis.

Table 6.3 Composition of natural gases used in CGI experiments on PVCap, Luvicap-bio and Bio-800.

Component	Mole%	
	PVCap	Luvicap-bio/Bio-800
Methane	89.41	87.93
Ethane	5.08	6.00
Propane	1.45	2.04
i-Butane	0.18	0.20
n-Butane	0.26	0.30
i-Pentane	0.06	-
CO_2	1.55	2.03
Nitrogen	1.93	1.50
n-Pentane	0.06	-
n-Hexane	0.02	-

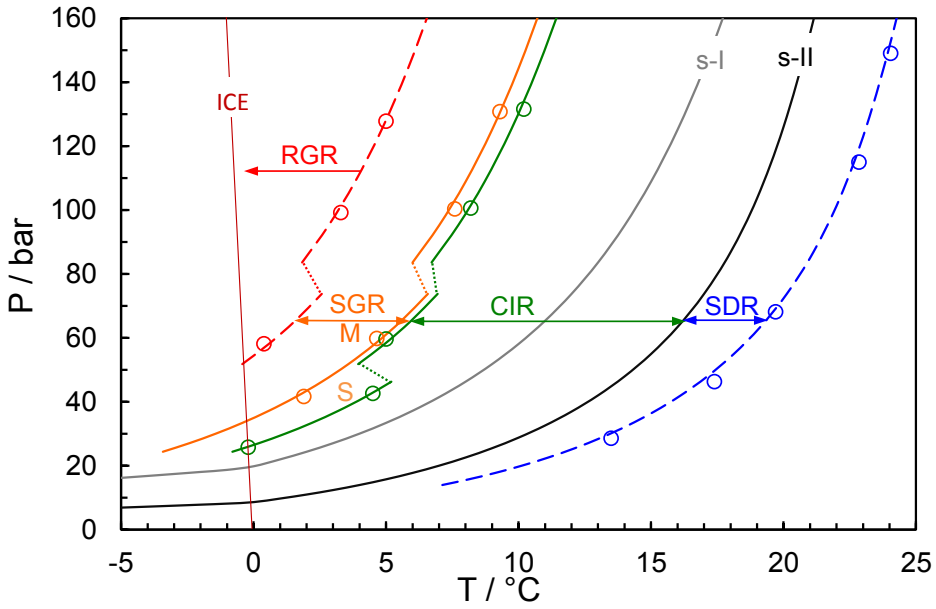

Figure 6.4 Experimentally determined points and interpolated CGI region boundaries for 0.5 mass% Luvicap-bio aqueous with natural gas.

This polymer induces complete inhibition (CIR) up to a subcooling of ~5.1 °C at low pressures (< 100 bar), ~6.3 °C at high pressures (>100 bar) and shows total crystal growth inhibition up to ~11.3 °C subcoolings from the s-I boundary at higher pressures. As shown in Figure 6.5 for pressures above ~60 bar, Luvicap Bio showed good performance with natural gas; while not as powerful as PVCap, it did offer very good inhibition up to ~11 °C subcooling. At below ~40 bar however, a further significant step reduction in performance is observed in addition to the one seen below ~70-80 bar; for

the former the CIR is reduced from around 5.1 °C to 2.8 °C subcooling. While a similar step reduction in CGI performance at ~70-80 bar is seen for PVCap, the additional step reduction below 40 bar seen for Luvicap-bio is not observed with PVCap. Compared to data for methane (Figure 6.5), this bio-polymer performed much better in the natural gas case (all CGI regions larger in extent relative to the s-I boundary), which is also consistent with previous findings for PVCap (Mozaffar, 2013).

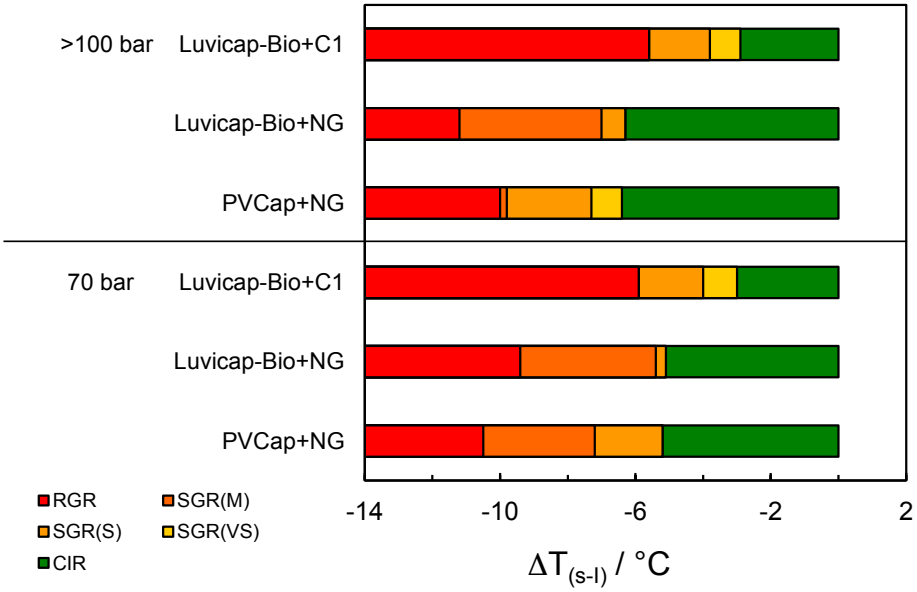

Figure 6.5 Comparison of subcooling extents of CGI regions from s-I phase boundary for 0.5 mass% Luvicap-bio aqueous with methane (Mozaffar, 2013), with natural gas and 0.5 mass% PVCap with natural gas (Mozaffar, 2013).

The origins of the reduction in KHI performance at lower pressures remains unclear, however, based on work to date, it is believed gas composition/cage occupancy plays an important role, notably CO_2 content. Clearly the nature of the polymer is also important – speculatively its adsorption strength on hydrate surfaces being the major factor – although the general rule of thumb that the ~70-80 bar region KHI performance can change significantly in natural gas systems.

In addition to the above, Inhibex Bio-800 was another biodegradable KHI tested with natural gas. This KHI is supplied at a concentration of 30 mass% in ethylene glycol butyl ether (EGBE / 2-butoxyethanol) from Ashland (kindly provided by Champion Technologies). In hydrate nucleation tests with natural gas by Daraboina et al. (2015), this polymer reduced hydrate nucleation temperature even more than Luvicap-bio.

Figures 6.6 shows experimentally determined CGI region boundaries for the system (data points are reported in Appendix A Table A.3).

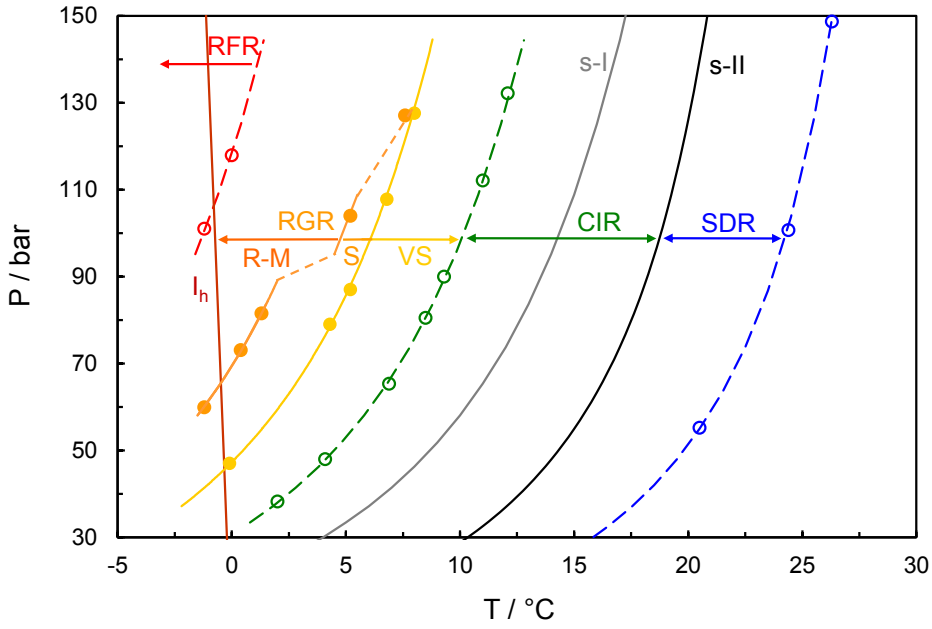

Figure 6.6 Experimentally determined points and interpolated CGI region boundaries for 0.5 mass% Bio 800 aqueous (1.2 mass% EGBE solvent) with natural gas.

Bio-800 overall shows good CGI performance with natural gas, although at higher pressures (>100 bar), inhibition strength becomes significantly reduced; changes across this pressure range being common in natural gas systems. However this is in contrast with Luvicap-bio and PVCap where performance was reduced at lower pressures.

The CIR for Bio-800 appears relatively constant at ~4.3 °C from the s-I boundary, and, depending on the pressure, can extend to up to 10 °C subcooling from the s-II boundary. For the complete pressure range studied, this follows a SGR(VS) region up to subcoolings of ~8.1 °C from the s-I boundary (up to 14 °C from s-II depending on pressure). Beyond this, a SGR(S) region is present, although this diminishes in extent from $\Delta T_{s\text{-}I} \approx -11.5$ °C at pressures below 90 bar to $\Delta T_{s\text{-}I} \approx -8.5$ °C by 130 bar where it appears to end. Finally, an SGR(M) region where performance is poor yet the KHI is still active extends to a subcooling of 15.6 °C from the s-I boundary where rapid growth invariably occurs.

One potential issue with Bio-800 was noted with respect to the CIR. While step cooling runs were generally clear, for a number of runs a phenomenon whereby a small fraction (< 0.5% of water) of hydrate would form and then stop growing within the CIR was sometimes observed (Figure 6.7). When first investigating the existence of CIR regions (Heriot-Watt Institute of Petroleum Engineering, 2012), this was sometimes observed and was eventually revealed that it was caused by hydrate finding a small dead volume in the cell where a crystal could grow without being splashed by the KHI-containing aqueous phase. When contact with the aqueous phase did occur, the growth stopped (or reversed) immediately.

For some KHIs, notably commercial formulations, this is rarely, if ever observed, most likely as it would result in a 'failure' under conservative testing conditions where the formation of any hydrate is typically considered a "fail". For Bio-800 it has been flagged up as it occurred not uncommonly and was not confined to one test cell, rather was observed in all 3 different cells used for testing. In all cases, the growth was tiny (< 0.5% of water phase) and, as noted, invariably stopped, commonly with no further growth observed in the following steps until conditions entered the SGR region. Whether or not these small 'hiccups' are, as for PVCap sometimes, associated with growth from the vapour phase in small areas of dead volume (the cells were in vertical orientation which has not proven an issue long term) or not is unclear. Certainly, the KHI was clearly still fully inhibiting the bulk of the system. However, it should be noted that this may present an issue with Bio-800 in NG systems, if only with respect to conservative 'no hydrate should form' lab scale field evaluations.

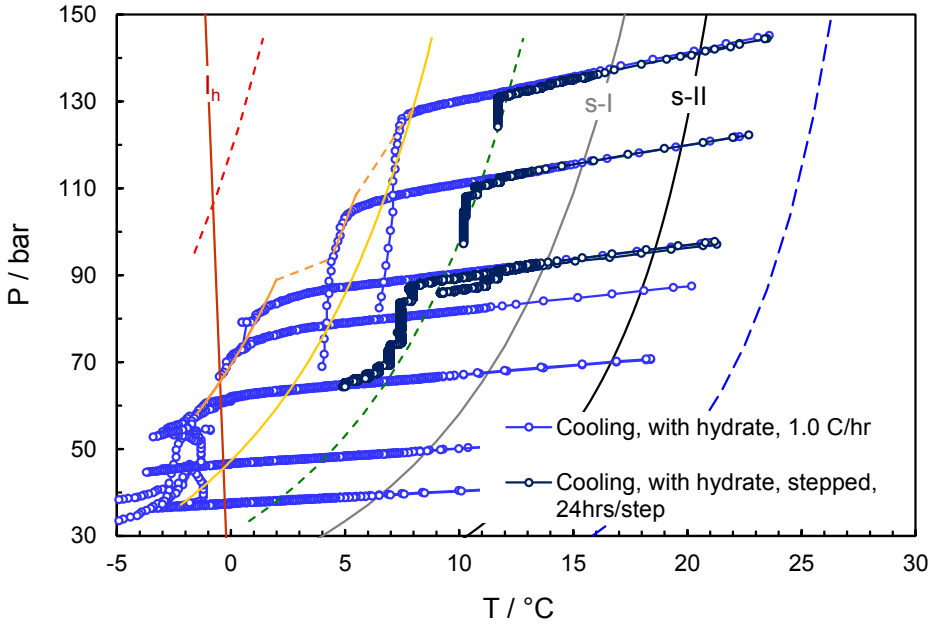

Figure 6.7 Example CGI method cooling curves for 0.5 mass% Bio-800 aqueous with natural gas showing step-cooling with hydrate runs where small (< 0.5% of water phase) fractions of hydrate could form apparently within the CIR, but then stop growing.

Figure 6.8 shows a comparison of subcooling extents of CGI regions (from the s-I phase boundary) for 0.5 mass% Bio-800, Luvicap Bio and PVCap aqueous with natural gas for a range of pressures. At the lowest pressure, the ability to determine the extent of regions beyond the ice point (where they are metastable in the absence of ice nucleation) depended on whether or not ice nucleated and grew.

As can be seen, for the lowest pressure of 30 bar, Bio-800 shows comparable performance with PVCap; while the CIR is slightly smaller by ~ 1 °C, SGR(VS) conditions extend beyond the ice point. Luvicap-bio has the poorest performance of the three at this pressure; the CIR extending only to 2.8 °C subcooling from the s-I boundary before SGR(S) conditions occur.

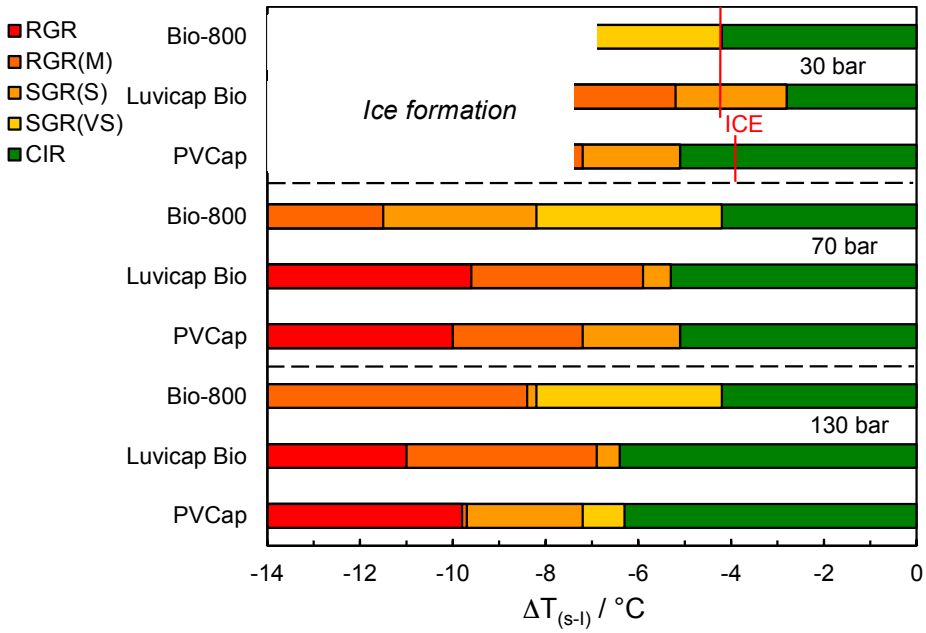

Figure 6.8 Comparison of subcooling extents of CGI regions from the s-I phase boundary for 0.5 mass% Bio 800, Luvicap-bio and PVCap (Mozaffar, 2013) with natural gas at various pressures. Those boundaries below the ice point are metastable projections (the presence of hydrate does not automatically trigger ice nucleation/growth).

At 70 bar, Bio-800 is arguably the best performing in terms of total extend of CIR + SGR(VS) regions; these extending up 8.2 °C subcoolings from the s-I phase boundary. PVCap has a slightly larger CIR, but this is followed by SGR(S) conditions. Luvicap-bio performs the most poorly at this pressure. Finally, at the highest pressures (130 bar), PVCap is the best performing, with Bio-800 CGI extents significantly reduced, although it still out-performs Luvicap-bio for this natural gas in terms of total CIR + SGR(VS+S) region extents.

6.4 KHI Removal/Recovery and Novel KHI Design

As mentioned earlier in this chapter, another option to address problems associated with kinetic hydrate inhibitors could be removal of the active polymer from produced water to avoid fouling problems as well as environmental concerns. Solvent extraction by using fatty alcohols, which are largely immiscible with water and have high affinity to KHI polymers, is a promising option in this regard (discussed in detail in Chapter 4 of this thesis). This simple extraction method has shown up to 100% effectiveness for PVCap –one of the most effective and widely used KHI polymers – alone and in the presence of other pipeline chemicals such as corrosion/scale inhibitors, thermodynamic

hydrate inhibitors and low concentrations of liquid hydrocarbons. The removal technique has also shown a high degree of effectiveness for other commercial KHIs (Anderson et al., 2014). Following the success achieved in removal properties of fatty alcohols they were also examined as an immiscible solvent for PVCap to see the performance in hydrate inhibition. Despite the fact that KHIs are generally formulated to be soluble in water, tests on TC-PVCap 'immiscible' KHIs in different gas-aqueous systems have shown performance comparable with aqueous PVCap (Chapter 5). These findings open up a new area in terms of KHI recovery. As shown in chapter 4, treatment chemicals have the ability of extracting up to 100% of PVCap from produced water. Thus implementing conventional separation method such as gravity settling, centrifuge and coalescing, PVCap+TC combination could be recovered from the water phase and applied directly as an immiscible KHI. This could be of particular interest in dry gas systems, where the separated TC+KHI could be directly recycled/reused. The envisaged benefits of the polymer removal/recovery method are:

- KHIs can be deployed more widely as disposal / water treatment issues are resolved (e.g. polymer fouling during reservoir re-injection or THI regeneration is avoided)
- KHIs can replace THIs wholly or partly, reducing THI purchase/regeneration costs, regeneration equipment footprints and inhibitor pumping requirements
- KHI application costs may be reduced due to recovery of most of the active polymer
- Used KHI disposal costs eliminated with environmental issues lessened
- Higher water cuts can be handled increasing the economical life of a reservoir

While PVCap is the most widely used polymer due to the good performance, there are still concerns about its performance in more challenging conditions such as high temperature and salinity. Polymer clouding and drop-out at high temperature and salt concentration, leaving the system with lower concentrations of polymer could cause serious risk in terms of hydrate formation and plugging. In light of this, the industry is working toward development of new polymers with high cloud point. Reasonable biodegradability is another challenge that industry is facing to comply with environmental regulations. However considering KHI removal/ recovery as a new option, designing polymers with higher recovery factor can open another area with respect to research on novel polymer design. With such an approach polymer could

either be reused as immiscible KHI combined with solvent or separated from solvent and disposed. In the latter case, developing techniques to recover solvent is inevitable.

As mentioned above, the polymer solvent extraction method (presented in chapter 4) has been mostly tested for PVCap and shown a high degree of effectiveness. However when it comes to other commercial KHIs there is still room for further investigations, this includes:

- Finding new solvent with high affinity for polymers other than PVCap
- Optimum solvent formulation by combining effective solvents to achieve higher affinity to polymer and easier/faster separation from water phase
- Improving removal effectiveness by applying better solvent injection techniques (seems to have considerable impact on effectiveness), separation method, etc.

A most likely scenario will be that oil companies consider removal/recovery efficiency as an important parameter in selecting KHI formulations.

6.5 Conclusions

KHIs are being highly used as hydrate inhibitors; however poor understanding of their inhibition mechanism can somehow limit their application. Detailed CGI studies for aqueous PVCap with methane strongly support that CGI regions are closely related to existing underlying crystal growth patterns as a function of subcooling upon which the polymer is acting by adsorption on faces favoured for growth, whereby preventing or significantly inhibiting crystal growth. As evident from the results, PVCap inhibition is not progressive as a function of increasing concentration, meaning small variations in the latter can induce abrupt changes in performance (which can be an important factor with respect to dosage selection for field operations).

Stoichiometric investigations of hydrate formation in a PVCap-methane system reveal that crystal growth in PVCap-inhibited systems, even at high hydrate fractions (up to 50% water as hydrate) is remarkably ordered and data provide quite compelling evidence for a PVCap to water stoichiometric ratio. As hydrate fraction increases, data strongly imply PVCap concentration being reduced in the remnant aqueous phase as it is adsorbed on growing hydrate crystals (or polymer-hydrate complexes).

Environmental restrictions has led industry to seek for some environmentally friendly hydrate inhibition strategies such as biodegradable KHIs, but there has been always a trade-off between achieving good inhibition performance and a reasonable biodegradability. CGI studies of the biodegradable polymer Luvicap Bio (from BASF) with natural gas shows a good crystal growth inhibition up to subcoolings of 10.8 °C, making it comparable or better than some existing commercial KHI formulations in performance. At higher pressures Luivicap-Bio performs quite comparably to PVCap. Bio-800 (Ashland) as another biodegradable KHI also shows good crystal growth inhibition performance in natural gas systems which is comparable with PVCap, particularly at lower pressures (< 100 bar). CGI performance however reduces at higher pressures (although it still out-performs Luvicap-bio in terms of total CIR + SGR(VS+S) at 130 bar). The reduced CGI regions observed at higher pressures with Bio-800 - while contrasting PVCap and Luvicap-bio which show the opposite - is still consistent with significant changes in polymer performance in the 70-100 bar pressure range that are believed to be a result of changing cage occupancy patterns / gas composition, with CO_2 playing an important role.

KHI removal / recovery could also be considered as an alternative way to comply with environmental regulations in some countries. This also can be beneficial in terms of lowering the cost of hydrate inhibition by introducing new opportunities in KHI applications. By eliminating concerns about polymer deposition in MEG regeneration unit, KHI removal can increase implementing of KHI+THI hybrid strategies, thus massive operating and capital cost saving.

CHAPTER 7 – CONCLUSIONS AND RECOMMENDATIONS FOR FUTURE WORK

7.1 Conclusions

Gas hydrate formation has been one of the major problems in the oil and gas industry for years, posing a high risk for pipeline blockage. Different hydrate prevention methods have been researched and applied in real fields. One of the relatively new methods in this regard is injection of kinetic hydrate inhibitors (KHI). Despite the extensive work on new KHI polymer/ formulation development (Kelland, 2006; Perrin et al., 2013), one particular issue which may limit their application is poor understanding of the inhibition mechanism. In this thesis the crystal growth inhibition method (Anderson et al., 2011) has been used to investigate different parameters affecting KHI performance and gain insight into the mechanisms involved. Another issue with the application of KHIs can be the risk of polymer drop-out and fouling at certain conditions. To address this, a solvent extraction method for the removal of KHI polymers from produced water streams has also been investigated.

7.1.1 Fundamental controls on KHI performance

In this work the CGI method has been utilized to examine in detail the fundamentals of KHI inhibition mechanisms as a function of various parameters. These parameters include gas and aqueous phase compositions, pressure, polymer type and presence of other pipeline chemicals such as thermodynamic inhibitors.

In Chapter 2, by using CGI method, the effect of sour and acid gas systems on KHI performance was evaluated. Tests on different gas mixture containing different concentrations of CO_2 showed particular changes in PVCap performance form low (< 70 bar) to high (> 100 bar) pressures. Although these particular changes were seen in all CO_2 containing systems, the effect depends on concentration of CO_2 and other gases present in the system.

The first tested gas system was a mixture of C_1, C_2, C_3 and 1.6 mol% CO_2. In another work by Mozaffar (2013) a natural gas containing the same concentration of carbon dioxide showed a reduction in PVCap performance at lower pressures (< 100 bar) which was also the case for this gas mixture. The fact that such an effect was not seen for the

C_1-C_2-C_3 mixture (Mozaffar, 2013), suggest that CO_2 is likely responsible for the reduced performance. However increasing CO_2 content to 10 mol% in a mixture with methane showed the reverse effect by having better performance at lower pressures. The data for 10 mol% CO_2 also contrasts that for 15 mol% CO_2 (Mozaffar, 2013), suggesting a reversal in effect between 10 and 15 mol%.

Therefore to see the effect of higher level of CO_2 in a multicomponent system, more carbon dioxide was added to the natural gas reaching concentration of 12 mol%. At this concentration results were consistent with 10 mol% CO_2 with methane and PVCap performance was improved at lower pressures. However presence of 12 mol% CO_2 in natural gas, reduced the total extents of CGI regions compared to 1.6% CO_2 (Mozaffar, 2013), supporting a generally negative effect.

Moreover in this chapter, the effects of different concentrations of hydrogen sulphide with methane was tested and showed markedly negative effects on PVCap performance especially while pressure increases up to 80 bar although after this point, performance appears to be constant. Consistent with the 10 mol% CO_2 and methane mixture, in the presence of H_2S, the extent of CGI region decreases by pressure. Such an effect was also seen for a ternary mixture of CO_2-H_2S-CH_4.

The reason for H_2S and CO_2 behaviour remains elusive while hydrate cage occupancy, solubility, and acidity could play a role. Results of modelling studies (Anderson, 2013, 2014) showed that at lower pressures H_2S probably stabilises hydrate-polymer complexes and thus improves PVCap performance, while by increasing pressure methane dominates cages and this effect is lost but the reason for negative effect remains unclear. Modelling studies of gas solubility in the presence of hydrate vs subcooling and pressure (Anderson, 2013, 2014) (and immiscible KHI results in Chapter 5) as well as tests on the effect of pH (moderate acidity) do not show these being a problem for KHIs. Thus, cage occupancy patterns - and presumably how that affects the strength of polymer adsorption on hydrate crystal surfaces / stability of polymer-hydrate complexes – is the most probable factor affecting PVCap performance.

Hybrid hydrate inhibition strategy by applying combination of KHIs and THIs was investigated in chapter 3. The most common thermodynamic inhibitors such as ethylene

glycol, methanol and ethanol at different concentrations were combined with KHI polymers and tested in multicomponent natural gas system.

Methanol, as a thermodynamic inhibitor appeared to have apositive effect when combined with 0.5 mass% PVCap at concentrations of 2.5 and 5.0 mass% for the natural gas system. However, increasing methanol content to 25.0 mass% caused a negative effect and reduced CGI regions compared to PVCap alone. This negative effect was also the case for the methanol+PVCap combination in a single component methane system. The contrasting behaviour of methanol between low and high concentrations in natural gas system as well as with lower concentrations in methane system strongly suggest that methanol may be involved in hydrate nucleation and/or growth. Because of its small molecular diameter, methanol can enter gas hydrate cavities and potentially compete with polymer pendant groups to occupy open cages and encourage hydrate growth. This can possibly be the reason for negative effect at higher concentrations with natural gas or in methane system.

Ethanol was the second thermodynamic inhibitor tested in combination with PVCap and in the presence of natural gas as hydrate former. Three concentrations were tested and all confirmed the negative effect of ethanol in a single component methane system. None of the 5.0, 13.1 and 25.0 mass% ethanol systems showed a top-up effect on PVCap with the only exception of a slight increase in RGR region at 5.0 mass%. Ethanol is known to form hydrate at the conditions under study and the stoichiometric concentration for this would be equal to 13.1 mass% (Anderson et.al, 2009). But tests for the stoichiometric concentration of ethanol with natural gas do not show any clear change in CGI region extents, which suggest that the role of ethanol enclathration is subtle in this case. This stoichiometric concentration (5.56 mol%) was also tested with ethane as hydrate former and the result supported the negative effect of ethanol on PVCap performance. The generally greater negative effect of ethanol compared to methanol is consistent with the emerging picture that molecules occupying cages are a major factor affecting polymer performance.

MEG, as the most popular thermodynamic inhibitor has shown to have top-up effect on PVCap performance in the single component methane system (Mozaffar et al., 2014). Following this, results of this work on three concentrations of MEG with natural gas also support the general positive effect on PVCap; crystal growth inhibition regions are larger or equal to those for PVCap alone, at least up to concentrations of 20.0 mass%

MEG. Moreover, the combination of MEG + PVCap offers far better inhibition by mass/volume inhibitor than MEG alone. Increase in CGI region subcoolings as a result of the MEG+PVCap combination strongly suggest that presence of MEG could increase the strength of polymer adsorption on hydrate crystal surfaces.

Work to date has shown that results of PVCap tests are not necessarily directly applicable to other polymer types. In light of this T1441 co-polymer was another polymer tested with natural gas to evaluate the effect of thermodynamic inhibitors. Experiments on the effect of 5.0 mass% methanol on this co-polymer were contradictory to PVCap; all CGI regions were reduced and the only improvement was a slight shift in RGR boundary to higher subcoolings at lower pressures. Reduction in CGI regions extent was also confirmed for 25.0 mass% methanol and ethanol supporting general negative effect of both of these alcohols on T1441. However combination of this co-polymer with MEG shows a contrasting effect between low and high pressures. While low-pressure results indicate a top-up effect of MEG on T1441 in terms of CIR, by increasing pressure this effect is lost and CIR is smaller than the one for polymer alone with natural gas. Over all, data show T1441 to be less powerful than PVCap, with the benefit of having a higher cloud point.

Bio-800, as a biodegradable KHI also seems to work well in combination with 5.0 mass% MEG in a natural gas system, with MEG showing a top-up effect in the pressure range tested. At pressures below 80 bar, CIR is slightly larger than PVCap at same concentration of MEG. Increasing pressure however shows a negative effect – which was also seen for T1441 – making the Bio-800+MEG combination less well performing than PVCap+MEG at least in terms of CIR.

Top of line hydrate formation was another issue investigated for natural gas system inhibited by PVCap+MEG combination. Top of line hydrates were encouraged by positioning autoclave cells vertical and reducing the aqueous phase to 25 vol% of the cell. A slow cooling run with hydrate for this case showed up to 30% of water conversion to hydrate within the CIR and with step-cooling runs there was an indication of very slow hydrate growth in the region where only s-II hydrates are stable.

In Chapter 6 three major concerns affecting KHIs future application are discussed, including inconsistencies in performance, environmental issues and KHI containing produced water disposal/handling. These concerns could be addressed by better

understanding of inhibition mechanism, developing environmentally friendly Bio-KHIs and KHI removal form produced water with the potential of novel KHI design respectively.

While the KHI inhibition mechanisms are still subject of debate, the most favoured mechanism is adsorption of polymer on to the hydrate crystal surface thus restricting further growth. Based on this over the course of this project, it has been speculated that a polymer-hydrate complex will form in presence of KHI polymer. Therefore some experiments were conducted to figure out any potential stoichiometry of these complexes. Stoichiometric investigations have revealed that even in presence of high amount of hydrate, crystal growth in PVCap-inhibited systems are ordered and provide evidence for stoichiometric ratio between water and PVCap.

To assess how biodegradable KHIs will perform in a real multicomponent hydrate forming system two Bio-KHIs were investigated with natural gas. Luvicap-bio showed to have comparable performance to PVCap at higher pressure specifically in terms of CIR, at lower pressure however CIR reduces to less than what PVCap offers. Bio-8oo also shows good CGI performance with natural gas. In contrast to PVCap and Luvica-bio, increasing pressure has negative effect on this polymer.

Moreover in this chapter, KHI removal is considered as another option to address environmental concerns associated with KHIs as well as polymer precipitation at high temperature and salinity. KHI removal can increase application of KHI+MEG combination by elimination of polymer deposition issues in MEG regeneration unit. Novel immiscible KHI design (polymer + removal solvent) could also be considered as another solution for concerns over polymer dropout/precipitation.

7.1.2 KHI removal and immiscible KHIs

KHI polymer removal from produced water using solvent extraction technique is investigated in Chapter 4. This method uses fatty alcohols, mainly normal hexanol to octanol, as solvent and shows that a very low quantity of them is required to displace polymer from aqueous phase. This method has shown up to 100% removal for PVCap and high degree of effectiveness for some other commercial polymers. However for the polymers that removal effectiveness is not high enough, solvent chemistry could be adjusted to achieve better efficiency. Presence of different pipeline chemicals including

thermodynamic inhibitors, salt, corrosion/scale inhibitors and modest quantities of liquid hydrocarbons doesn't show significant effect on removal efficiency. Applying this technique could encourage industry toward KHI+MEG combination hydrate inhibition strategies as the risk of polymer precipitation in MEG regeneration units is eliminated.

The removal technique has also opened up new opportunities in designing a novel immiscible KHI which is basically a combination of polymer and removal solvent. Chapter 5 focused on examining the performance of this new formulation for different systems using CGI method. The results suggest that polymers may be mostly active at water/hydrocarbon interface rather than in aqueous phase. As evident from the tests on a 10 mol% CO_2/90 mol% CH_4 system, hydrate formation from dissolved gas doesn't seem to be a problem for such immiscible formulation. Presence of condensate (10 vol% relative to water) reduces the PVCap CGI inhibition although the most important CIR remains constant.

Implementing immiscible KHI formulation could help to address gunking problems associated with water re-injection and polymer dropout at highly saline systems. This also could provide a potential solution for the systems where thermodynamic inhibitors cannot be used because of high cost or salt deposition problems.

7.2 Recommendations

In-depth studies in this work using the CGI method have given a novel insight into KHI inhibition mechanisms, providing data for increased operator confidence. Work has highlighted the importance of gas composition (notably CO_2 and H_2S), hydrate structure and pressure on KHI performance, in addition to yielding robust data on the effects of polymer type, common pipeline chemicals (e.g. alcohols, MEG), gas solubility and pH. A novel solvent extraction method for KHI polymer removal (and potential recovery) from produced water has also been investigated and shown significant promise.

Studies have shown that KHI performance can significantly vary with gas composition and pressure changes. Currently the conclusion is that this relates to cage occupancy patterns; this being important in terms of the growth/stability of polymer-hydrate complexes, which are speculated to form in KHI inhibited systems. This work has shown that CO_2 and H_2S content of gases have a major influence on KHI CGI extents as a function of concentration and pressure. Based on this, further work on compositional / structure / pressure effects with particular focus on CO_2 and H_2S (e.g. in multicomponent gas mixtures with both CO_2 and H_2S present) would considerably help to understand the effect of acid and sour gas systems on KHI performance. This can ultimately be used to optimise inhibition strategies/formulation for specific gas systems.

Results of this work have shown that to reduce the required volume of THIs, one possible solution is combining KHIs with THIs. Results to date show that in general, both methanol and ethanol have a negative impact on KHI performance, particularly at higher concentrations where CGI inhibition is reduced markedly. In contrast, MEG tends to have a positive effect, acting as both a top-up inhibitor and as a synergist for KHIs, improving crystal growth inhibition properties. However, initial studies in this work suggest there may be issues with ‘top of line’ hydrates in KHI-MEG systems. Such behaviour could pose a risk to the systems, which are inhibited by KHI-MEG combination and inhibition relies on the KHI component. Therefore this issue could be more investigated potentially for different thermodynamic inhibitors.

Studies on PVCap CGI patterns in this work suggest that for small fractions of aqueous polymer (e.g. 0.5% PVCap), relatively large aqueous fractions of hydrate can still be strongly inhibited (up to more than 50% water converted without agglomeration / blockage), indicating some anti-agglomerant properties. Further investigation of these properties as a function of polymer type and concentration, gas composition, pressure

and presence of other pipeline chemicals such as MEG can help to assess implications for KHI inhibition in pipeline systems.

To address environmental issues associated with KHI polymers, CGI properties of Luvicap-Bio (BASF) and Bio 800 (Ashland) were studied and both showed good KHI characteristics. Given the increasing industry interest in this area due to tightening environmental restrictions, inhibition performance where high fractions of hydrate are present could be investigated for these polymers to see the effect of different polymer type. It was also noted that the issue of top of line hydrates could be the case for Bio-800, therefore studying this issue for bio KHIs, specifically in the presence of THIs could help to understand the impact of different factors on this.

Results of KHI polymer removal from produced water has shown a high degree of effectiveness for PVCap, however for other polymers further studies are required to find a solvent formulation with higher effectiveness. Besides chemistry, in the case of polymer recovery developing techniques to recover solvent is inevitable. For further development of removal process, kinetics data of the extraction process are needed.

Tests using KHI removal 'treatment chemicals' as polymer solvents have shown that these 'water-immiscible' KHIs, can be as effective as miscible KHIs. These have the advantage of being easily removable (e.g. ahead of produced water re-injection or MEG regeneration) and thus resolving fouling problems. In light of this, investigating inhibition performance for different gas systems, resistance to polymer drop-out / fouling (due to temperature and salinity), potential for topping up with THIs such MEG for these novel formulations will help to gain confidence in their application.

REFERENCES

Adham S., Gharfeh S., Hussain A., Minier-Matar J., Janson A., 2014, *Kinetic hydrate inhibitor removal by physical, chemical and biological processes*, Proceedings of the Offshore Technology Conference Asia, Kuala lumpur, Malaysia.

Al-Adel S., Cruz I., 2011, *Unconventional hydrate inhibition for an offshore sour lean gas production*, Proceedings of the 7th International Conference on Gas Hydrates, Edinburgh, UK.

Alapati R., Lee J., Beard D., 2008, *Two Field Studies Demonstrate that New AA LDHI Chemistry is Effective at High Water-cuts Without Impacting Oil/Water Quality*. Proceedings of the Offshore Technology Conference, Houston, U.S.A.

Allenson S.J., Scott A., 2010, *Evaluation and field optimisation of kinetic hydrate inhibitors for application within MEG recovery unite, gas condensate fields, mediterranean sea*, Proceedings of the North African Technical Conference and Exhibition, Cairo, Egypt.

Anderson B.J., Tester J.W., Borghi G.P., Trout B.L., 2005, *Properties of Inhibitors of Methane Hydrate Formation via Molecular Dynamics Simulations*, Journal of the American Chemical Society, **127**, 17852-17862.

Anderson R., 2013, *Evaluation of low dosage hydrate inhibitors 2012-2015 programme*, Joint Industrial Project Progress Report September 2013, Edinburgh, UK.

Anderson R., 2014, *Evaluation of low dosage hydrate inhibitors 2012-2015 programme*, Joint Industrial Project Progress Report March 2014, Edinburgh, UK.

Anderson R., Chapoy A., Haghighi H., Tohidi B., 2009, *Binary ethanol-methane clathrate hydrate formation in the system CH_4-C_2H_5OH-H_2O: phase equilibria and compositional analyses*, Journal of Physical Chemistry C, **113**, 12602-12607.

Anderson R., Mozaffar H., Tohidi B., 2011, *Development of a crystal growth inhibition based method for the evaluation of kinetic hydrate inhibitors*, Proceedings of the 7th International Conference on Gas Hydrates, Edinburgh, UK.

Anderson R., Vajari S. M., Tohidi B., 2013, *Water treatment*, International Patent No. WO 2013121217 A3.

Anderson R., Tohidi F., Mozaffar H., Tohidi B., 2014, *Kinetic hydrate inhibitor removal from produced waters by solvent extraction*, Proceedings of the 8th International Conference on Gas Hydrates, Beijing, China.

Anklam M.R., Firoozabadi A., 2005, *An interfacial energy mechanism for the complete inhibition of crystal growth by inhibitor adsorption*, **123**, 144708/1-144708/12.

Arjmandi M., Tohidi B., Danesh A., Todd A.C., 2005, *Is subcooling the right driving force for testing low dosage hydrate inhibitors*, Chemical Engineering Science, **60**, 1313-1321.

Budd D., Hurd D., Pakulski M., Schaffer T.D., 2004, *Enhanced hydrate inhibition in Alberta gas field*, Proceedings of the SPE Annual Technical Conference, Houston, USA.

Cha M., Shin K., Kim J., Chang D., Seo Y., Lee H., Kang S.P., 2013, *Thermodynamic and kinetic hydrate inhibition performance of aqueous ethylene glycol solutions for natural gas*, Chemical Engineering Science, **99**, 184-190.

Clark L.W., Anderson J., 2007, *Low dosage hydrate inhibitors (LDHI): further advances and development in flow assurance technology and applications concerning oil and gas production systems*, Proceedings of the International Petroleum Technology Conference, Dubai, U.A.E.

Claussen W.F., 1951a, *Suggested structures of water in inert gas hydrates*, The Journal of Chemical Physics, **19**, 259-260.

Claussen W.F., 1951b, *Erratum: suggested structures of water in inert gas hydrates*, The Journal of Chemical Physics, **19**, 662.

Claussen W.F., 1951c, *A second water structure for inert gas hydrates*, The Journal of Chemical Physics, **19**, 1425-1426.

Daraboina N., Linga P., Ripmeester J., Walker V.K., Englezos P., 2011a, *Natural gas hydrate formation and decomposition in the presence of kinetic inhibitors. 2. Stirred reactor experiments*, Energy & Fuels, **25**, 4384-4391.

Daraboina N., Ripmeester J., Walker V.K., Englezos P., 2011b, *Natural gas hydrate formation and decomposition in the presence of kinetic inhibitors. 3. Structural and compositional changes*, Energy & Fuels, **25**, 4398-4404.

Daraboina N., Malmos C., von Solms N., 2013a, *Investigation of kinetic hydrate inhibiton using a high pressure micro differential scanning calorimeter*, Energy & Fuels, **27**, 5779-5786.

Daraboina N., Malmos C., von Solms N., 2013b, *Synergistic kinetic inhibition of natural gas hydrate formation*, Fuel, **108**, 749-757.

Daraboina N., Ripmeester J., Walker V.K., Englezos P., 2013c, *Assessing the performance of commercial and biological gas hydrate inhibitors using nuclear magnetic resonance microscopy and a stirred autoclave*, Fuel, **105**, 630-635.

Daraboina N., Pachitsas S., von Solms N., 2015, *Experimental validation of kinetic inhibitor strength on natural gas hydrate nucleation*, Fuel, **139**, 554-560.

Deaton W.M., Frost E.M., 1946, *Gas hydrates and their relation to the operation of natural gas pipe lines*, US Bureau of Mines Monographs, **8**,101-108.

Duchateau C., Dicharry C., Peytavy J.L., Glénat P., Pou T.E., Hidaldo M., 2008, *Laboratory Evaluation of Kinetic Hydrate Inhibitors: a New Procedure for Improving the Reproducibility of Measurements*, Proceedings of the 6th International Conference on Gas hydrates, Vancouver, Canada.

Duchateau C., Peytavy J.L., Glénat P., Pou T.E., Hidalgo M., Dicharry C., 2009, *Laboratory Evaluation of Kinetic Hydrate Inhibitors: A Procedure for Enhancing the Repeatability of Test Results*, Energy and Fuels, **23**, 962-966.

Ducheteau C., Glénat P., Pou T-E., Hidalgo M., *Dicharry C.,* 2010*, hydrate precursor test method for the laboratory evaluation of kinetic hydrate inhibitors*, Energy & Fuels, **24**, 616-623.

Franks F., Darlington J., Schenz T., Mathias S.F., Slade L., Levine H., 1987, *Antifreeze activity of Antarctic fish glycoprotein and a synthetic polymer*, Nature, **325**, 146-147.

Fink J.K., 2011, *Petroleum Engineer's Guide to Oil Field Chemicals and Fluids*, first Ed., Gulf Professional Publishing, Waltham, USA.

Fu B., 2002, *The development of advanced kinetic hydrate inhibitors*, Chemistry in the Oil Industry VII: Performance in a Challenging Environment, the Royal Society of Chemistry, Cambridge, UK.

Glénat P., Anderson R., Mozaffar H.,Tohidi B., 2011, *Application of a new crystal growth inhibition based KHI evaluation method to commercial formulation assessment*, Proceedings of the 7th International Conference on Gas Hydrates, Edinburgh, UK.

Habetinova E., Lund A., Larsen R., 2002, *Hydrate dissociation under the influence of low-dosage kinetic inhibitors*, Proceedings of the 4th International Conference on Gas Hydrates, Yokohama, Japan.

Haghighi H., 2009, *Phase Equilibria Modelling of Petroleum Reservoir Fluids Containing Water, Hydrate Inhibitors and Electrolyte Solutions,* PhD thesis, Heriot-Watt University, UK.

He S., Oddo J.E., Tomson M.B., 1995, *The Nucleation Kinetics of Strontium Sulfate in NaCl Solutions up to 6* m *and 90°C with or without Inhibitors*, Journal of Colloid and Interface Science, **174**, 327-335

Heriot-Watt Institute of Petroleum Engineering, 2012, *Evaluation of low dosage hydrate inhibitors 2009-2012 programme*, Joint Industrial Project, Edinburgh, UK.

Heriot-Watt Institute of Petroleum Engineering, 2013, *Evaluation of low dosage hydrate inhibitors 2012-2015 programme*, Joint Industrial Project Progress Report April 2013, Edinburgh, UK.

Hussain A., Gharfeh S., Adham S., 2012, *Study of kinetic hydrate inhibitor removal efficiency by physical and chemical processes*, Proceedings of SPE International Production and Operations Conference & Exhibition, Doha, Qatar: SPE 157146.

Hutter J.L., King H.E., Lin M.Y., 2000, *Polymeric Hydrate-Inhibitor Adsorption Measured by Neutron Scattering*, Macromolecules, **33**, 2670-2679.

Jhaveri J., Robinson D.B., 1965, *Hydrates in the methane–nitrogen system*, Canadian Journal of Chemical Engineering, **43**, 75-78.

Kelland M.A., 2006, *History of the development of low dosage hydrate inhibitors*, Energy & Fuels, **20**, 825-847.

Kelland M., 2014, *Production Chemicals for the Oil and Gas Industry*, Second Ed., CRC Press, Boca Raton, USA.

Kihara T., 1953, *Virial coefficient and models of molecules in gases*, Reviews of Modern Physics, **25(4)**, 831– 843

King H.E., Hutter J.L., Lin M.Y., Sun T., 2000, *Polymer conformations of gas-hydrate kinetic inhibitors: a small-angle neutron scattering study*, The Journal of Chemical Physics, **112(5)**, 2523-2532

Koh C.A., Westacott, R.E., Xhang W., Hirachand K., Creek J.L., Soper A.K., 2002, *Mechanisms of gas hydrate formation and inhibition*, Fluid Phase Equilibria, **194-197**, 143-151

Kulkarni P., *Flow assurance: Hydrate inhibitors for deepwater flow assurance*, 2003, Offshore, **63**, Issue 3.

Kumar R., Linga P., Moudrakovski I., Ripmeester J., Englezos P., 2008, *Structure and kinetics of gas hydrates from methane/ethane/propane mixtures relevant to the design of natural gas hydrate storage and transport facilities*, AIChE Journal, **54(8)**, 2132-2144.

Kvamme B., Kuznetsova T., Aasoldsen K., 2005, *Molecular dynamics simulations for selection of kinetic hydrate inhibitors*, Journal of Molecular Graphics and Modelling, **23**, 524-536.

Larsen R., Knight C.A., Sloan E.D., 1998, *Clathrate hydrate growth and inhibition*, Fluid Phase Equilibria, **150-151**, 353-360.

Larsen R., Knight C.A., Rider K.T., Sloan E.D., 1999, *Melt growth and inhibition of ethylene oxide clathrate hydrate*, Journal of Crystal Growth, **204(3)**, 376-381.

Lederhos J.P., Long J.P., Sun A., Christiansen R.L., Sloan E.D., 1996, *Effective kinetic inhibitors for natural gas hydrates*, Chemical Engineering Science, **51**, 1221-1229.

Lone A., Kelland M.A., 2013, *Exploring kinetic hydrate inhibitor test methods and conditions using a multicell steel rocker rig*, Energy & Fuels, **27**, 2536-2547.

Makogon T.Y., Larsen R., Knight C.A., Sloan E.D., 1997, *Melt growth of tetrahydrofuran clathrate hydrate and its inhibition: method and first results*, Journal of Crystal Growth, **179**, 258-262.

McDonald A.W.R., Petrie M., Wylde J.J., Chalmers A.J., Arjmandi M., 2006, *Field Application of combined kinetic hydrate and corrosion inhibitors in the southern North sea: case studies*, Proceedings of SPE Gas Technology Symposium, Calgary, Canada.

Mcleod H.O., Campbell J.M., 1961, *Natural gas hydrates at pressures to 10,000 psia*, Journal of Petroleum Technology, **222**,590-595

Menendez C.M., Hughes B., Jardine J., Mok W.Y., Ramachandran S., Jovancicevic V., Bhattacharya A., 2014, *New Sour Gas Corrosion Inhibitor Compatible with Kinetic Hydrate Inhibitor*, Proceedings of International Petroleum Technology Conference, Doha, Qatar.

Mohammadi A.H., Anderson R., Tohidi B., 2005, *Carbon monoxide clathrate hydrates: equilibrium data and thermodynamic modelling*, AIChE Journal, **51**, 2825-2833.

Mozaffar H., 2013, *Development and application of a novel crystal growth inhibition (CGI) method for evaluation of kinetic hydrate inhibitors*, PhD thesis, Heriot-Watt University, UK.

Mozaffar H., Anderson R., Tohidi B., 2014, *Effect of ethylene glycol, ethanol and methanol on PVCap-induced hydrate crystal growth inhibition in methane systems*, Proceedings of the 8th International Conference on Gas hydrates, Beijing, China.

Musa O.M., Cuiyue L., 2010, *Polymers having n-vinyl amide and hydroxyl moieties*, International Patent No. WO 2010117660 A1.

Nakagawa R., Akihiro H., Shoji H., 2008, *Dissociation and specific heats of gas hydrates under submarine and sublacustrine environments*, Proceedings of the 6th International Conference on Gas hydrates, Vancouver, Canada.

Nazeri N., Tohidi B., Chapoy A., 2012, *An evaluation of risk of hydrate formation at the top of a pipeline*, Proceedings of SPE Asia Pacific Oil and Gas Conference and Exhibition, Perth, Australia: SPE 160404.

Pakulski M., *Development of superior hybrid gas hydrate inhibitors*, 2011, Proceedings of the Offshore Technology Conference, Houston, USA.

Palermo T., Sloan E.D., 2011, *Natural Gas Hydrates in Flow Assurance*, Chapter Five, Gulf Professional Publishing, Burlington, USA.

Patel Z.D., Russum J., 2010, *Flow assurance: Chemical inhibition of gas hydrates in deepwater production systems*, Offshore, **70**, Issue 6.

Pauling L., Marsh R.E., 1952, *The structure of chlorine hydrate*, Proceedings of National Academy of Sciences (USA), **38**, 112-118.

Perrin A., Musa O.M., Steed J.W., 2013, *The chemistry of low dosage clathrate hydrate inhibitors*, Chemical Society Reviews, **42**, 1996-2015.

Peytavy J.L., Glénat P., Bourg P., 2008, *Qualification of low dosage hydrate inhibitors (LDHIs): Field cases studies demonstrate the good reproducibility of the results obtained from flow loops*, Proceedings of the 6th International Conference on Gas Hydrates, Vancouver, Canada.

Ripmeester J.A., Tse J.A., Ratciffe C.I., Powell B.M., 1987, *A new clathrate hydrate structure*, Nature, **325**, 135-136.

Rithauddeen M.A., Al-Adel S., Anderson R., Tohidi B., 2014, *A new approach to evaluate KHI performance*, Proceedings of the 8th International Conference on Gas Hydrates, Beijing, China.

Rojas Y., Lou X., 2010. *Instrumental analysis of gas hydrates*, Asian Pacific Journal of Chemical Engineering, **5 (2)**, 310-323.

Rydzy M.B., Schicks J.M., Naumann R., Erzinger J., 2007, *Dissociation enthalpies of synthesized multicomponent gas hydrates with respect to the guest composition and cage occupancy*, Journal of Physical Chemistry, **111**, 9539-9545.

Shin K., Udachin K.A., Moudrakovski I.L., Leek D.M., Alavi S., Ratcliffe C.I., Ripmeester J.A., 2013, *Methanol incorporation in clathrate hydrates and the implications for oil and gas pipeline flow assurance and icy planetary bodies*, PNAS, **110(21)**, 8437-8442.

Sloan E.D., Subramanian S., Matthews P.N., Lederhos J.P., Khokhar A.A., 1998, *Quantifying hydrate formation and kinetic inhibition*, Industrial & Engineering Chemistry Research, **37**, 3124-3132.

Sloan E.D., 2003, *Fundamental principles and applications of natural gas hydrates*, Nature, **426**, 353-359.

Sloan E.D., Koh C.A., 2008, *Clathrate Hydrates of Natural Gases*, Third Ed., CRC Press, Boca Raton, USA.

Svartaas T.M., Gulbrandsen A.C., Huseboe S.B.R., Sandved O., 2008, *An experimental study on "un-normal" dissociation properties of structure II hydrates formed in presence of PVCAP at pressures in the region 30 to 175 bars – dissociation by temperature increase*. Proceedings of the 6th International Conference on Gas Hydrates, Vancouver, Canada.

Szymczak S., Sanders K., Pakulski M., Higgins T., 2006, *Chemical compromise: a thermodynamic and low-dosage hydrate-inhibitor solution for hydrate control in the Gulf of Mexico*, SPE Project, Facilities & Construction .

Tian J., Bailey C., 2011, *Precipitation prevention in produced water containing hydrate inhibitors injected downhole*, International Patent No. WO 2011123341 A2.

Tohidi B., Burgass R.W., Danesh A., Todd A.C., Østergaard K.K., 2000*, Improving the accuracy of gas hydrate dissociation point measurements*, Annals of the New York Academy of Sciences, **912**, 924-931.

Tohidi B., Anderson R., Mozaffar H., Tohidi F., 2014, *The return of kinetic hydrate inhibitors*, Proceedings of the 8th International Conference on Gas hydrates, Beijing, China.

van der Leeden M.C., Kashchiev D., van Rosmalen G.M., 1992, *Precipitation of barium sulfate: Induction time and the effect of an additive on nucleation and growth*, Journal of Colloid and Interface Science, **152**, 338-350.

van der Leeden M.C., Kashchiev D., van Rosmalen G.M., 1993, *Effect of additives on nucleation rate, crystal growth rate and induction time in precipitation*, Journal of Crystal Growth, **130**, 221-232.

van der Waals J.H., Platteeuw J.C., 1959, *Clathrate solutions*, Advances in Chemical Physiscs, **2**, 1-57.

von Stackelberg M., 1949, *Feste gas hydrate*, Naturwissenschaften, **36**, 327-333.

von Stackelberg M., 1949, Feste gas hydrate, Naturwissenschaften, **36**, 359-362.

von Stackelberg M., Muller H.R., 1954, *Feste gas hydrate II. struktur und saumchemie*, Zeitschrift für Elektrochemie, **58**, 25-39.

von Stackelberg M., 1956, *Die struktur der einschlussverbindungen des wassers (gashydrate) und des phenols*, Recueil des Travaux Chimiques des Pays-Bas, **75**, 902-905.

Wu M., Wang S., Liu H., 2007, *A study of inhibitors for the prevention of hydrate formation in gas transmission pipeline*, Journal of Natural Gas Chemistry, **16**, 81-85.

Yagasaki T., Matsumoto M., Tanaka H., 2015, *Adsorption Mechanism of Inhibitor and Guest Molecules on the Surface of Gas Hydrates*, Journal of the American Chemical Society, **137**, 12079-12085.

Yang J., Tohidi B., 2011, *Characterization of inhibition mechanisms of kinetic hydrate inhibitors using ultrasonic test technique*, Chemical Engineering Science, **66 (3)**, 278-283.

Yousif M., 1998, *Effect of under-inhibition with methanol and ethylene glycol on the hydrate-control process*, SPE Production & Facilities, **13**, 184-189.

Yu X., Somasundaran P., 1996, *Kinetics of polymer conformational changes and its role in flocculation*, Journal of Colloid and Interface Science, **178**, 770-774.

Zhang J.S., Lo C., Couzis A., Somasundaran P., Wu J., Lee J.W., 2009, *Adsorption of Kinetic Inhibitors on Clathrate Hydrates*, The Journal of Physical Chemistry C, **113**, 17418-17420.

APPENDIX A –CGI DATA GENERATED AS PART OF THIS WORK FOR DIFFERENT POLYMER/GAS SYSTEMS

Table A.1 Experimentally determined points on CGI region boundaries for natural gas with 0.5 mass% T1441 co-polymer aqueous.

CGR boundary	Growth rate	T / °C (± 0.5)	P / bar (± 0.2)	ΔT_{s-I} / °C (± 0.5)	ΔT_{s-II} / °C (± 0.5)
SDR	Slow dissociation	20.7	76.0	-	3.5
		22.9	111.5	-	3.6
		24.3	149.9	-	3.5
CIR-SGR(VS)	No growth	8.2	68.4	-3.2	-8.3
		11.2	101.1	-3.2	-7.6
		13.4	136.0	-3.2	-7.0
SGR(VS-S)	Very slow	3.9	67.2	-7.3	-12.5
		7.1	97.9	-7.1	-11.5
		9.8	131.8	-6.6	-10.4
SGR(S-M)	Slow	2.2	64.3	-8.7	-13.9
		6.2	97.2	-7.9	-12.4
		9.1	129.8	-7.2	-11.0
SGR(M)-RGR	Moderate	1.6	65.0	-9.4	-14.6
		3.1	94.3	-10.8	-15.3
		4.2	121.8	-11.6	-15.6

Table A.2 Experimentally determined points on CGI region boundaries for 0.5 mass% Luvicap-bio aqueous with natural gas.

CGR boundary	Growth rate	T / °C (± 0.5)	P / bar (± 0.2)	ΔT_{s-I} / °C (± 0.5)	ΔT_{s-II} / °C (± 0.5)
SDR	Slow dissociation	13.5	28.7	-	3.5
		17.4	46.8	-	3.5
		19.7	68.1	-	3.4
		22.9	115.0	-	3.1
		24.1	149.0	-	2.9
CIR-SGR(S)	No growth	-0.2	25.7	-2.8	-9.2
		4.5	42.6	-2.8	-8.6
		5.0	59.6	-5.1	-10.4
		8.2	100.6	-6.3	-10.7
		10.2	131.6	-6.3	-10.3
SGR(S-M)	Slow	1.9	41.6	-5.2	-11.0
		4.7	59.8	-5.4	-10.8
		7.6	100.4	-6.8	-11.3
		9.3	130.7	-7.2	-11.2
SGR(M)-RGR	Moderate	0.4	58.1	-9.4	-14.8
		3.3	99.1	-11.1	-15.5
		5.0	127.8	-11.3	-15.3

Table A.3 Experimentally determined points on CGI region boundaries for 0.5 mass% Bio 800 (+ 1.2 mass % EGBE solvent) aqueous with natural gas.

CGR boundary	Growth rate	T / °C (± 0.5)	P / bar (± 0.2)	ΔT_{s-I} / °C (± 0.5)	ΔT_{s-II} / °C (± 0.5)
SDR	Slow dissociation	20.5	55.2	-	5.5
		24.4	100.7	-	5.6
		26.3	148.7	-	5.5
CIR-SGR(VS)	No growth	2.0	38.2	-4.3	-10.3
		4.1	47.9	-4.2	-9.9
		6.9	65.3	-4.1	-9.2
		8.5	80.5	-4.2	-9.0
		9.3	90.1	-4.3	-8.8
		11.0	112.1	-4.2	-8.4
		12.1	132.2	-4.3	-8.1
SGR(VS-S)	Very slow	-0.1	47.1	-8.3	-14.0
		4.3	79.0	-8.2	-13.0
		5.2	87.0	-8.1	-12.7
		6.8	107.8	-8.1	-12.3
		8.0	127.6	-8.1	-12.1
SGR(S-M)	Slow	-1.2	59.9	-11.5	-16.8
		0.4	73.1	-11.5	-16.5
		1.3	81.5	-11.5	-16.2
		5.2	104.0	-9.4	-13.7
		7.6	127.1	-8.5	-12.4
SGR(M)-RGR	Moderate	-1.2	101.0	-15.6	-20.0
		0.0	117.9	-15.6	-19.6